

UNIVERSITY OF NOTTINGHAM  
DEPARTMENT OF MECHANICAL ENGINEERING

*The Application of Microwave Preheating in  
Resin Transfer Moulding*

by

Michael S. Johnson

*Thesis submitted to the University of Nottingham  
for the degree of Doctor of Philosophy  
July 1995*

# Contents

---

	<b>Page</b>
<b>Abstract</b>	i
<b>Acknowledgements</b>	iii
<b>Glossary</b>	iv
<b>Nomenclature</b>	xi
<b>Chapter 1 Introduction</b>	1
1.1 Fibre Reinforced Plastics for Automotive Applications	1
1.2 Liquid Composite Moulding Processes for Fibre Reinforced Plastics	3
1.3 The FRP Research Programme at the University of Nottingham	4
1.4 Theme of This Research Project	5
Figures	8
<b>Chapter 2 Microwave Heating Principles</b>	9
2.1 Introduction	9
2.2 Mechanisms of Microwave Heating	10
2.3 Microwave Heating of Dielectric Materials	10
2.4 Microwave Ovens	12
2.4.1 Multimode Microwave Ovens	12
2.4.2 Single Mode Microwave Ovens	13
2.5 Nomenclature for Single Mode Applicators	13
2.6 Rectangular Applicators	14
2.7 Cylindrical Applicators	15
2.7.1 Mode Excitation within $TM_{0mn}$ Cylindrical Applicators	15
2.7.2 Examples of $TM_{0m0}$ Mode Cylindrical Applicators	15
2.8 Characterisation of Single Mode Applicators	16
2.8.1 Determination of the Applicator Efficiency	16
2.8.2 Determination of the Quality Factor	17
2.8.3 Optimisation of a Single Mode Applicator	18
List of Figures	19
Figures	20
<b>Chapter 3 Literature Review</b>	30
3.1 Introduction	30
3.2 High Volume Manufacture of Fibre Reinforced Plastic Components	30
3.3 Injection Strategies for Resin Transfer Moulding	31
3.4 High Volume Resin Transfer Moulding	32
3.5 Cycle Time Reduction Techniques for Resin Transfer Moulding	33
3.5.1 Injection Gate Location	34
3.5.2 Injection Pressure	35
3.5.3 Preform Permeability	35

3.5.4	Resin Viscosity	36
3.5.5	Resin Reactivity	37
3.6	The Effect of Process Variables on Resin Transfer Moulded Laminates	38
3.6.1	Void Content	39
3.6.2	Fibre Reinforcement	39
3.6.3	Resin Formulation	40
3.7	Microwave Processing of Polymers	40
3.7.1	Microwave Cure	41
3.7.2	Microwave Preheating	42
3.7.3	In-Line Microwave Processing	43
3.7.4	Alternative Methods for Polymer Processing	44
3.8	Simulation Techniques for Microwave Applicator Design	45
3.9	Dielectric Property Data for Thermosetting Resins	47
3.10	Conclusion	47
	Figures	50
<b>Chapter 4 Experimental Techniques</b>		<b>51</b>
4.1	Introduction	51
4.2	The Experimental Resin Transfer Moulding Facility	51
4.2.1	RTM Equipment	52
4.2.2	Microwave Preheating Equipment	53
4.2.3	The Automatic Moulding Cycle	54
4.3	The Thermal Cycle During RTM	55
4.4	The Pressure Cycle During RTM	56
4.5	Standard Moulding Conditions	58
4.6	Material Property Testing	59
4.6.1	Mechanical Testing	59
4.6.2	Degree of Cure Testing	59
4.7	Tuning Methods for the Cylindrical Applicator	61
4.7.1	Primary Tuning of the Applicator	61
4.7.2	Fine Tuning of the Applicator	62
4.7.3	Mode Pattern Identification within the Applicator	62
4.8	Transmission-Line Modelling of the Cylindrical Applicator	63
4.9	Magnetron Characterisation Trials	63
4.9.1	Magnetron Calibration	64
4.9.2	Applicator Heating Efficiency Measurements with Regard to Variations in the Magnetron Output Frequency	64
4.10	Determination of Applicator Sensitivity	65
4.11	Dielectric Property Measurements	65
4.12	Conclusion	66
	List of Tables	67
	List of Figures	67
	Tables	68
	Figures	69
<b>Chapter 5 Evaluation of the Microwave Resin Preheating System</b>		<b>83</b>
5.1	Introduction	83

5.2	Background on the Microwave Resin Preheating System	83
5.2.1	Manual Control of the Microwave Resin Preheating System for Undershield Production	84
5.2.2	Limitations of the Microwave Resin Preheating System	85
5.3	Microwave Resin Preheating Using a Low Power Density System	85
5.4	Automatic Power Control Methods for the Microwave Resin Preheating System	86
5.4.1	ON-OFF Power Control	87
5.4.2	PID Power Control	88
5.5	Undershield Production Using the Adapted Microwave Resin Preheating System	91
5.6	Conclusion	92
	List of Tables	93
	List of Figures	93
	Tables	94
	Figures	95

<b>Chapter 6</b>	<b>RTM Processing Advantages through Microwave Resin Preheating</b>	102
6.1	Introduction	102
6.2	Constant Resin Temperature Injection	103
6.2.1	Constant Resin Temperature Injection into a 60°C Mould	104
6.2.2	Constant Resin Temperature Injection into a 90°C Mould	106
6.3	Discussion of Constant Resin Temperature Injection	108
6.4	Isothermal Impregnation in RTM	108
6.5	Ramped Resin Temperature Injection	109
6.6	Discussion of Ramped Resin Temperature Injection	110
6.7	The Effect of Pre-Exotherm Pressure on Component Thickness	111
6.8	Conclusion	112
	List of Tables	113
	List of Figures	113
	Tables	115
	Figures	116

<b>Chapter 7</b>	<b>The Effect of Microwave Resin Preheating on the Properties of RTM Laminates</b>	129
7.1	Introduction	129
7.2	Tensile Properties of RTM Laminates Produced by Constant Resin Temperature Injection	129
7.3	Tensile Properties of Laminates Produced by Constant Resin Temperature Injection Compared to Post-Cured Laminates	130
7.4	Determination of Residual Styrene Content by Gas Chromatography	131
7.5	Conclusion	132
	List of Tables	134
	List of Figures	134
	Tables	135
	Figures	136

<b>Chapter 8</b>	<b>Sensitivity Analysis of the Microwave Resin Preheating System</b>	140
8.1	Introduction	140
8.2	Dielectric Property Measurements	141
8.3	Applicator Heating Efficiency Trials	143
8.4	Sensitivity Analysis of the Cylindrical Applicator	144
8.5	Conclusion	145
	List of Tables	146
	List of Figures	146
	Tables	147
	Figures	148
<b>Chapter 9</b>	<b>Performance Aspects of the Cylindrical Applicator</b>	152
9.1	Introduction	152
9.2	Mode Superposition within the Cylindrical Applicator	152
9.3	Single Mode Isolation within the Cylindrical Applicator	153
9.4	Stability of the High Q Cylindrical Applicator	155
9.5	Calibration of the YJ1600 Magnetron	156
9.6	Methods to Improve Heating Stability for High Q Applicators	157
	9.6.1 Active On-Line Tuning	157
	9.6.2 Power Modulation Using a Constant Magnetron Output Frequency	158
	9.6.3 Frequency Tracking Magnetrons	159
9.7	Preheating Trials Using the High Q Cylindrical Applicator	159
9.8	Reconciliation of the Numerical Model by Hill	160
9.9	Transmission Line Modelling of the Cylindrical Applicator	161
9.10	Performance Improvements to the Cylindrical Applicator	163
9.11	Conclusion	165
	List of Tables	166
	List of Figures	166
	Tables	169
	Figures	170
<b>Chapter 10</b>	<b>Discussion</b>	193
10.1	Introduction	193
10.2	Microwave Preheating for Resin Transfer Moulding	193
	10.2.1 Batch Preheating for Low Volume Resin Transfer Moulding	193
	10.2.2 In-Line Resin Preheating for High Volume Resin Transfer Moulding	194
	10.2.3 Cycle Time Reductions Using In-Line Resin Preheating	195
10.3	CAE Design Approach for Microwave Heating Systems	196
10.4	Injection Strategies for In-Line Microwave Resin Preheating	197
	10.4.1 Single Stream Injection	197
	10.4.2 Twin Stream Injection	198
10.5	The Scope of Microwave Assisted RTM for High Volume Production	198
10.6	Alternative Applications for the Microwave Preheating System	199
10.7	Recommendations for Future Work	200

<b>Chapter 11</b>	<b>Conclusions</b>	202
	<b>References</b>	205
<b>Appendix 3.1</b>	<b>Dielectric Property Relationships for Two Part Mixtures</b>	217
<b>Appendix 4.1</b>	<b>Motorsport Lay-Up</b>	220
<b>Appendix 4.2</b>	<b>Dielectric Property Calculations</b>	221
<b>Appendix 5.1</b>	<b>Ziegler-Nichols Tuning Equations</b>	222
<b>Appendix 5.2</b>	<b>Determination of the PID Controller Constants Over a Temperature Range</b>	223
<b>Appendix 7.1</b>	<b>Estimation of Tensile Modulus Using the Model by Krenchel</b>	224

# Abstract

---

## **The Application of Microwave Preheating in Resin Transfer Moulding**

by

Michael S. Johnson

Fibre reinforced plastics (FRP) are of considerable interest to the automotive industry. Intelligent application of these materials could reduce vehicle weight for higher operating efficiency, at a reduced manufacturing cost. The principal use of FRP in high volume (greater than 100,000 parts per annum) has been restricted to non-structural body panels made from short fibre reinforcement. Long fibre reinforced composites are ideal for load bearing structures resulting from a high specific strength. However, a high volume technique to produce these components at a moderate cost has not been realised. One long fibre reinforcement process with the potential to meet the high volume demands of the automotive industry is resin transfer moulding (RTM).

Prolonged cycle times are an obstacle to high volume RTM. Cycle time is dictated by thermal quench near the injection gate from cold resin entering the hot mould. Heat recovery by the mould, and coincident heating of the resin to initiate cure is necessary to complete the cycle. Microwave preheating of the resin before injection reduces thermal quench. Since microwave heating is volumetric, low conductivity resins can be heated uniformly and efficiently. In-line resin preheating has been developed for its compatibility with high volume RTM.

The use of an in-line microwave resin preheating system to reduce cycle time was investigated. This system was incorporated into the automatic RTM cycle. The resin temperature could be held constant or profiled during injection using a proportional-integral-derivative (PID) power controller. Both injection techniques reduced cycle time, although temperature profiling enabled coincident resin cure across the mould for a maximum cycle time reduction. Resin

preheating had no adverse affects on the RTM process or laminates. This suggested that the microwave resin preheating system could be retrofitted within an existing RTM facility to reduce the component cycle time without damaging the mould or degrading component quality.

# Acknowledgements

---

The author lends effusive thanks to Ken Kendall, Richard Jeryan, and Carl Johnson (USA), along with Alan Harrison and Stephen Scarborough (UK) of the Ford Motor Company for their help in getting me here.

I owe my gratitude to Chris Rudd and Mike Owen for their supervision and continual efforts to keep me here.

John Hill deserves special praise for his fanatical dedication to my work as a supervisor, researcher, and friend.

I have benefitted greatly from the diverse knowledge of my colleagues. Patrick Blanchard, Linda Bulmer, Andrew Long, Julian Lowe, and Pete McGeehin have all suffered from my scholastic and cultural ignorance. I commend the tolerance of Kevin Lindsey, in addition to his appreciation of resin chemistry, single malt whiskies, and a good cupholder design.

Andrew Kingham has a mind as sharp as his resin chipping chisel. My thanks to him, Roger Smith, and Brian Foster for their expertise as technicians and machinists.

Finally, I would like to thank Louise. Only she knows how vital she has been.

All of you have made it worth the trip.

# Glossary

---

<b>Accelerator</b>	A chemical substance added to a resin to increase the cure reaction rate.
<b>Aperture</b>	A hole in the wall of a resonant applicator through which microwaves enter.
<b>Applicator</b>	A metallic enclosure in which dielectrics are heated by a resonating electric field.
<b>Binder</b>	A thermoplastic additive applied to reinforcement to permit preforming.
<b>BMC</b>	Bulk Moulding Compound. Chopped short fibres blended with resin and filler, used in compression and injection moulding.
<b>CFRM</b>	Continuous Filament Random Mat.
<b>Catalyst</b>	A chemical substance that breaks down to form free radicals that can be used to initiate polymerisation.
<b>Charge</b>	The quantity of BMC or SMC that is placed in the mould.
<b>Choke</b>	A structure added to the input and output of an applicator to limit the leakage of microwave radiation during continuous processing.
<b>Circulator</b>	A three port device that acts as a one-way valve. Incident energy is transmitted through the device, while reflected energy is directed to a water load connected to the third port.
<b>Coupling</b>	The transfer of energy from the waveguide into the applicator.
<b>Cure</b>	The phase change of a resin from a liquid to a solid state by polymerisation.
<b>DAC</b>	Digital to Analogue Converter.

<b>Derakane</b>	A range of commercial vinyl-ester resins made by Dow Chemical.
<b>Derivative Control</b>	A control that applies a correcting signal in proportion to the rate of change of the error signal.
<b>Dielectric</b>	A non-conducting material that is polarised by an electric field.
<b>Dielectric Constant</b>	The real component ( $\epsilon'$ ) of the complex dielectric constant of a material. A measurement of the amount of energy that can be stored in a material. A synonym for permittivity.
<b>Dipole</b>	Molecules of displaced positive and negative charges of equal magnitude.
<b>DMC</b>	Dough Moulding Compound. A synonym for BMC.
<b>Electroforming</b>	The process used to make shell moulds by electrolytically depositing metal onto a model of the component.
<b>Error Signal</b>	The difference between the desired and actual values of a process variable.
<b>Exotherm</b>	Heat liberation during the polymerisation reaction.
<b>Extender</b>	A type of filler used to increase the resin bulk so that less resin can be used to produce a moulding.
<b>Fibre Washing</b>	Movement of fibres in the mould under the action of resin flow.
<b>Filler</b>	An inert substance added to a resin to limit shrinkage, improve properties, and reduce cost.
<b>FDTD</b>	Finite Difference Time Domain. A numerical simulation technique.
<b>FE</b>	Finite Element. A numerical simulation technique.
<b>FETD</b>	Finite Element Time Domain. A numerical simulation technique.
<b>FRP</b>	Fibre Reinforced Plastics.
<b>Fundamental Mode</b>	The lowest order mode excited in a waveguide or applicator.

<b>Gas Chromatograph</b>	An instrument used to determine the percentage of individual molecules within a liquid mixture.
<b>Gate</b>	The port through which resin enters the mould.
<b>GRP</b>	Glass Reinforced Plastics.
<b>Impregnation</b>	The displacement of air and the penetration of a fibre preform by liquid resin.
<b>Integral Control</b>	A control action based on integration of the error signal.
<b>Laminate</b>	A stack of reinforcement plies that make up the composite. Also the final moulded component.
<b>LCM</b>	Liquid Composite Moulding.
<b>Loss Factor</b>	The imaginary component ( $\epsilon''$ ) of the complex dielectric constant of a material. A measurement of the amount energy the material can dissipate as heat.
<b>LPA</b>	Low Profile Additive. A filler used to limit resin shrinkage.
<b>Magnetron</b>	A thermionic device for generating microwave power.
<b>Microwave Heating</b>	Heating of a material by electromagnetic energy operating at the permissible frequencies of either 896 MHz (UK)/915 MHz (USA) or 2450 MHz.
<b>Mode</b>	A pattern of electromagnetic energy formed by two or more travelling waves that resonate upon interaction.
<b>Mode Stirrer</b>	A rotating metallic fan used to redistribute the modes within a multimode oven for more even heating.
<b>Monomer</b>	A molecule that can join with others to form a polymer.
<b>Multimode Applicator</b>	An applicator whose large volume allows several standing waves to be excited.
<b>Network Analyser</b>	An instrument for measuring the impedance and phase of an applicator over a swept frequency range.
<b>ON-OFF Control</b>	A simple control form where power is either fully on or fully off, in response to the process variable rising above or falling below the set point variable, respectively.
<b>Parasitic Mode</b>	Any electromagnetic field pattern other than the desired pattern within an applicator.

<b>PC</b>	Personal Computer.
<b>PCI</b>	Phased Catalyst Injection.
<b>Power Penetration Depth</b>	The distance from the surface of the dielectric where the field strength has been attenuated to 37% (1/e) of its strength at the surface.
<b>Perkadox 16</b>	Tertiary Butyl Peroxy Dicarboxylate. An organic peroxide catalyst for curing high temperature resins, provided by Akzo Nobel Chemicals Ltd.
<b>Permeability</b>	The property of a porous material that characterises the ease with which a fluid will flow under an applied pressure gradient.
<b>Permittivity</b>	A synonym for the Dielectric Constant.
<b>PFC</b>	Preform-Compound. CFRM impregnated with a thermoplastic resin to allow thermoforming.
<b>PID Control</b>	Proportional Integral Derivative Control. A three term controller that combines the proportional, integral, and derivative control actions.
<b>PLC</b>	Programmable Logic Controller. A microprocessor based control device with inputs and outputs that are switched according to conditions specified by the logic program.
<b>Polymerisation</b>	A chemical reaction in which monomers cross-link to produce a rigid network structure.
<b>Preform</b>	A semi-rigid reinforcement that has been cut and shaped to the component geometry.
<b>Proportional Control</b>	A control mode that applies a correcting signal in proportion to the error signal.
<b>PTFE</b>	Polytetrafluoroethylene. A thermoplastic material with a low loss factor for minimal absorption of microwave power.
<b>Q Factor</b>	Quality Factor. The ratio of energy stored in an applicator to the energy dissipated in that applicator. A high Q applicator has a sharp resonance, whereas a low Q applicator has a broad resonance.

<b>Reinforcement</b>	Fibres used to provide strength in FRP materials.
<b>r.f. Heating</b>	Heating of a material by electromagnetic energy operating at the permissible radio frequencies of either 13.56 MHz or 27.12 MHz.
<b>RIM</b>	Reaction Injection Moulding. A polymeric moulding technique characterised by impingement mixing of two reactants immediately before injection.
<b>RRIM</b>	Reinforced Reaction Injection Moulding. The addition of chopped fibres to one of the RIM reactants.
<b>RTM</b>	Resin Transfer Moulding.
<b>Shell Mould</b>	A thin, lightweight mould produced by electroforming and attached to a rigid backing frame.
<b>Size</b>	An emulsion applied to fibre surfaces for lubrication and protection during processing. The size binds the fibres into strands and provides a coupling agent between the fibre and resin matrix.
<b>SMC</b>	Sheet Moulding Compound. A mixture of resin, short fibre reinforcement, and fillers supplied as a charge in sheet form.
<b>SRIM</b>	Structural Reaction Injection Moulding. Similar to RIM but a fibre preform is placed in the mould before injection.
<b>Styrene</b>	A monomer used as a cross-linking agent in unsaturated polyester and vinyl-ester resins.
<b>Synolac</b>	A range of commercial polyester resins from Cray Valley Total Chemie.
<b>TBPEH</b>	Tertiary Butyl Peroxy 2-Ethyl Hexanoate. An organic peroxide catalyst for curing high temperature resins, provided by Interlox Chemicals Ltd.
<b>TBV</b>	Thermal Break Valve. An injection valve or vent that thermally isolates the hot mould from the cold resin within the valve body.

<b>TE</b>	Transverse Electric. Description of an electromagnetic wave whose electric field is oriented perpendicular to the direction of propagation.
<b>Thermoplastic</b>	A plastic material that is softened by heating and hardened by cooling in a reversible process.
<b>Thermoset</b>	A plastic material that is hardened by an irreversible chemical reaction.
<b>TLM</b>	Transmission-Line Modelling. A numerical simulation technique.
<b>TM</b>	Transverse Magnetic. Description of an electromagnetic wave whose magnetic field is oriented perpendicular to the direction of propagation.
<b>Trigonox 44B</b>	Acetyl Acetone Peroxide. An organic peroxide catalyst for curing high temperature resins, provided by Akzo Nobel Chemicals Ltd.
<b>Tuning</b>	Adjustment of the resonant frequency of the applicator to correspond with the output frequency of the magnetron.
<b>Turbo Pascal</b>	A high level computer programming language.
<b>Turntable</b>	A rotating platter placed within a multimode applicator onto which the product is located to provide more even heating.
<b>Unifilo</b>	A commercial brand of CFRM manufactured by Vetrotex (UK) Ltd.
<b>VARI</b>	Vacuum Assisted Resin Injection. A vacuum assisted variant of RTM.
<b>Vent</b>	The port through which air and resin leave the mould.
<b>Viscosity</b>	A measure of the resistance to flow that a fluid offers when subjected to a shear stress.
<b>VSWR</b>	Voltage Standing Wave Ratio.
<b>ULEV</b>	Ultra Low Emission Vehicles.
<b>Water Load</b>	A load attached to the circulator that absorbs the microwave energy reflected from the applicator.

<b>Waveguide</b>	A metallic duct used for the transmission of microwave radiation.
<b>Wet-Out</b>	Complete coating of the individual fibres by the liquid resin.
<b>Wet-Through</b>	Penetration of the resin through the preform, which must take place to permit wet-out.
<b>ZEV</b>	Zero Emission Vehicles.

# Nomenclature

---

## Upper Case

$A$	Area	$m^2$
$C_p$	Specific heat capacity	J/kgC
$D_p$	Power penetration depth	m
$E$	Electric field strength	V/m
$E_z(r)$	Electric field strength at radius r	V/m
$J_0$	Zero order Bessel function of the 1 <sup>st</sup> kind	
$K$	Permeability constant	
$K_p$	Proportionality constant	
$P$	Power	Watts
$Q$	Volumetric flow rate	$m^3/s$
$T$	Temperature	$^{\circ}C$
$T_d$	Derivative time constant	
$T_I$	Reset time constant	
$V$	Volume	$m^3$

## Lower Case

$f$	Frequency	Hz
$l$	Length	m
$m$	Mass	kg
$p$	Pressure	Pa
$dp/dx$	Pressure drop per unit length	Pa/m
$r$	Radius	m
$t$	Time	s

## Greek

$\alpha$	Degree of cure
$d\alpha/dt$	Rate of reaction

$\epsilon^*$	Relative complex permittivity	
$\epsilon'$	Relative dielectric constant	
$\epsilon''$	Relative loss factor	
$\lambda_0$	Free space wavelength ( $\lambda_0=C_0/f$ )	m
$\rho$	Density	kg/m <sup>3</sup>
$\mu$	Viscosity	PaS

### Constants

Dielectric permittivity of free space ( $\epsilon_0$ ) = $8.8542 \times 10^{-12}$	F/m
Velocity of light in free space ( $C_0$ ) = $2.9979 \times 10^8$	m/s

## Chapter 1

# Introduction

---

### 1.1 Fibre Reinforced Plastics for Automotive Applications

Government legislation prompted by public concern is forcing automobile manufacturers to produce more environmentally responsible vehicles. Automotive hydrocarbon emissions, consisting of low level ozone, produce urban smog. Pollution control regulations in southern California have mandated that 2% of all cars be ultra low emission vehicles by 1997, with a further 2% of sales on zero emission vehicles by 1998. The rest of the world is expected to follow suit [1].

Compressed natural gas and methanol powered transport are being developed as ultra low emission vehicles (ULEV), with zero emission vehicles (ZEV) utilising electric power. Batteries and fuel cells in zero emission vehicles can account for one-third of the overall weight, while ancillary hardware creates a weight penalty in ultra low emission vehicles. Weight reductions are necessary to maintain the efficiency gains of these automobiles [2].

The US automobile manufacturers are further affected by proposed increases in the corporate average fuel economy (CAFE) regulations. Traditionally, engine refinements have enabled manufacturers to meet fuel economy goals, however, Owen et al. [3] predicted that vehicle weight reductions will soon become necessary. It is in this area that fibre reinforced plastics (FRP) excel. The strength to weight ratio of FRP exceeds that of steel so that the overall weight of the automobile can be reduced without degrading structural performance.

FRP is not new to the automotive industry. The 1974 Lotus Elite was produced in a matched mould using a vacuum assisted resin injection technique (VARI) [4]. Manufacturers such as Alpha Romeo, BMW, and TVR have also used composites successfully in low volume, niche market applications (less than 10,000 units per annum). These producers justify the higher raw material costs of FRP compared to sheet steel, by component integration, lower tooling costs, and

reduced tooling lead times. Weight reduction, corrosion resistance, and perceived high quality are additional advantages [5].

High volume use of FRP (greater than 100,000 units per year) has been restricted to short fibre reinforcement processes due to the simplicity and maturity of these techniques. Sheet moulding compound (SMC) is used extensively in the United States. Ford, Pontiac (General Motors) and Chrysler have used SMC tailgate panels for their minivans. The tailgate for the Fiat Tipo was manufactured by injection of a dough moulding compound (DMC) which, according to Folonari and Bruno [6], provided fewer surface defects, faster cycle times, and lower labour costs compared to SMC. The disadvantage of these methods is that short fibre orientation is difficult to control during injection resulting in wide variations in the material properties. For this reason, components manufactured by short fibre processes are limited to non-structural applications.

Optimum material properties are obtained using long fibre reinforcements. Vosper Thornycroft use a mechanically assisted hand layup operation for making boat hulls. Continuous filament random mat (CFRM) and resin are laid down by a traversing gantry. Several weeks are required to produce a single hull [7]. High performance road cars such as the McLaren F1 are made with epoxy prepreg that is consolidated and cured in an autoclave. McLaren Cars produces these stressed monocoque structures at a rate of 2.5 vehicles per month [8]. Filament winding has been used to manufacture a composite driveshaft for the Renault Espace Quadra [9]. This process restricts the component shape since fibres must be applied to a rotating mandrel. Prolonged cycle times or geometric considerations limit the use of these long fibre composite techniques for high volume production. Liquid composite moulding (LCM) processes such as resin transfer moulding (RTM) and structural reaction injection moulding (SRIM) are alternative long fibre processes. The Ford Motor Company indicated that LCM processes offer the greatest potential to reduce cycle times, making high volume production of fully and semi-structural FRP components feasible [10].

## 1.2 Liquid Composite Moulding Processes for Fibre Reinforced Plastics

The liquid composite moulding process is illustrated in Figure 1.1. A heated matched tool is used to shape layers of fibre reinforcement into a semi-rigid preform. The preform is trimmed and placed into a heated mould. Resin is injected into the closed mould and flows through the preform to peripheral vents, purging air in the process. The component is removed after the resin has cured. Finishing operations are performed as necessary. Separation of the preforming and impregnation stages is an important advantage of liquid composite moulding processes.

Isolation of the preforming stage allows tailoring of the reinforcement to meet design load conditions. Foam cores and metallic inserts can be used and regions of localised reinforcement can be incorporated due to controlled fibre placement.

Although RTM and SRIM share the same preform design stage, they involve different resin injection strategies. SRIM resin systems begin to polymerise when the resin components are mixed. Typically, the reaction proceeds rapidly, leaving only a short period for air purging and fibre wet-out within the mould. SRIM requires high pressure (significantly greater than 10 bar) to mix the resin components, then to drive the initiated resin through the mould. These pressures are contained using robust steel tooling. High volume RTM normally employs resin systems that are initiated at elevated temperature. Ambient temperature resin is injected and heated by the mould to the activation temperature, permitting a longer impregnation time for improved fibre wet-out and air purging, without the risk of premature cure. Lower injection pressures (less than 10 bar) are possible so that less rigid tooling can be used, reducing equipment costs. Compared to SRIM, RTM cycle times typically are longer, as a consequence of the resin heating phase.

Process selection of RTM or SRIM is made on the basis of cost effectiveness. Parts consolidation with both processes reduces the number of tools needed for parts manufacture when compared to equivalent steel or aluminium components. However, high pressure bearing SRIM tooling is costly, making it more viable at high production volumes. Lower pressure RTM tooling is less

expensive and enables manufacturers to compete more aggressively in the medium to high volume niche market.

Johnson [11] observed in his comparison of SRIM and RTM that these techniques are converging to become a single process known as high speed resin transfer moulding (HSRTM). SRIM is slowing down to realise the benefits of long impregnation times, while RTM is speeding up with the advent of fast curing resins and improved process control.

### **1.3 The FRP Research Programme at the University of Nottingham**

High volume manufacture of FRP components has been a research priority at the University of Nottingham since 1985. The programme objective is to develop an automated, cost effective technique for high volume production of FRP components without sacrificing quality. The RTM process has been selected by virtue of its cost advantages to the manufacturer. Three fundamental aspects of the RTM process have been studied.

The first topic was introduced in a PhD thesis by Scott [12] and concerned the selection of materials compatible with high speed RTM processing. Scott determined that polyester resins incorporate the flow and kinetic properties suitable for the process at a lower cost than vinyl-ester or epoxy resins. Revill [13] demonstrated that high speed processing has an effect on the material properties of the laminate. Lindsey [14] supplied additional processing information by relating laminate properties to the interface formed between the resin matrix and reinforcement. Void formation as a result of high speed processing was shown to have an adverse effect on laminate quality as determined by Lowe [15].

Rudd [16] proposed a second area of research in preform development. His work on preform fabrication and resin flow through a preform was detailed in a PhD thesis. Rudd found reinforcement permeability to be an important factor in predictive flow modelling. The complex aspects of permeability were described by Bulmer [17] who ultimately proposed a standard permeability measurement technique. Production of net shaped preforms to reduce waste and increase efficiency has been investigated by McGeehin [18].

The third research subject was initiated by Hutcheon [19] in a M. Phil thesis. Hutcheon demonstrated that the RTM process could be automated for high volume production. Process automation was furthered by Kendall [20] who characterised the process variables and developed a technique for lightweight tool design. Additional work was done by Blanchard [21] who developed a low cost cure sensing technique that provided a signal to open the mould. A means of increasing production speed was investigated by Hill [22] who used an in-line microwave oven to preheat the resin as it entered the mould. Introducing preheated resin into the hot mould reduced quenching and decreased component cycle time.

A computer aided engineering (CAE) approach for RTM has been developed from this experimental basis providing an up front mould design strategy. Rice [23] developed a model for mould design analysis, and optimisation of injection gate placement. Reinforcement deformation during preforming was modelled by Long [24] so that near net shaped preforms with the desired properties could be specified for components.

#### **1.4 Theme of This Research Project**

A principal disadvantage of RTM is long component cycle times. Substantial reductions in cycle time have been made using zone heated moulds and high temperature activated resin systems. Kendall observed that cycle time was dictated by thermal quench [20]. Using a mould instrumented with thermocouples, he identified a large temperature drop near the injection gate as cold resin entered the hot mould. A means of reducing thermal quench by preheating the resin before it entered the mould was investigated. This technique had the compound effect of decreasing the amount of heat required to initiate cure, while reducing resin viscosity for improved flow characteristics. Kendall recorded a 30% reduction in cycle time by batch preheating catalysed resin in a domestic microwave oven prior to injection. Despite a reduction in cycle time, the risk of premature cure caused by storing catalysed resin at elevated temperatures made bulk resin preheating impractical for high volume manufacture.

Hill [22] implemented an in-line resin preheating system to avoid the problem of bulk resin storage at elevated temperatures. In-line preheating allowed small amounts of resin to be heated during injection. Bulk quantities of the catalysed resin could be kept at a lower temperature, thereby increasing storage life. The low thermal conductivity of resin makes conduction heating difficult. A large thermal gradient at the heat transfer surface leads to premature cure of the catalysed resin in that area. Microwave preheating was pursued due to the volumetric nature of dielectric heating. Rapid heat up rates and stable temperature control culminated in a 35% reduction in cycle time.

The formation of cured resin lobes within the microwave applicator during operation hindered the performance of the system. The cylindrical applicator was designed to resonate in the  $TM_{020}$  mode. Ideally, this applicator produces a heating pattern within the axially positioned injection pipe such that maximum heating occurs along the pipe axis with zero heating at the pipe wall where a boundary layer forms. Disturbances to the  $TM_{020}$  mode led to excessive heating at the stagnant boundary layer so that lobes of cured resin accumulated within the applicator. Ultimately, the cured resin lobes would block the injection system.

The objective of this thesis was to demonstrate maximum cycle times reductions using an in-line microwave resin preheating system. The preheating system was integrated into the fully automatic RTM cycle to simulate a production facility. The effect of microwave resin preheating on the degree of cure, and the mechanical properties of RTM laminates was investigated. The deficiencies in the applicator were identified and suggestions to improve the performance of the system have been made.

Limitations of the microwave resin preheating system designed by Hill were identified. A non-parabolic heating profile produced localised hot spots within the microwave applicator leading to premature resin cure. The system was adapted to avoid premature resin cure by limiting the amount of power being delivered to undesirable heating modes. A proportional-integral-derivative (PID) power controller was developed and incorporated into the automated RTM process software. This temperature based feedback control system provided stable resin temperature control regardless of variations in the resin flow rate.

The microwave resin preheating system was used to minimise the RTM cycle time. A series of mouldings was produced with resin injected at constant temperatures to quantify reductions in the impregnation and cycle times. Mouldings made by this technique maintained the traditional periphery to injection gate cure sequence preventing optimisation of the RTM process and led to high pre-exotherm pressures near the injection gate. A second series of mouldings was produced with resin injected according to a ramped temperature profile. This technique resulted in a controlled method for achieving cycle time reductions. The cure sequence was altered to provide simultaneous resin cure at the mould periphery and injection gate. Using this ramped injection method, the cycle time was minimised. In addition, the pre-exotherm pressure, identified as a limiting factor in mould design [20], was reduced significantly.

The effect of microwave resin preheating on laminate properties and the degree of cure was investigated. Mechanical properties for laminates produced with resin injected at various temperatures were measured. A comparison of mechanical properties was made between these laminates and equivalent post-cured examples. The degree of cure for a laminate produced with resin injected at elevated temperature was compared to one made with ambient temperature resin. The results of these experiments indicated that microwave resin preheating did not affect adversely the overall laminate properties.

The performance of the microwave system was characterised. The complex shape of the resonant peak within the applicator suggested a superposition of the desirable  $TM_{020}$  heating mode with a closely occurring parasitic mode. Identification of the parasitic mode as a form of the  $TM_{21n}$  mode was established by empirical techniques, and supported by a numerical simulation. An alternate applicator geometry was proposed for operation in a pure  $TM_{020}$  mode.

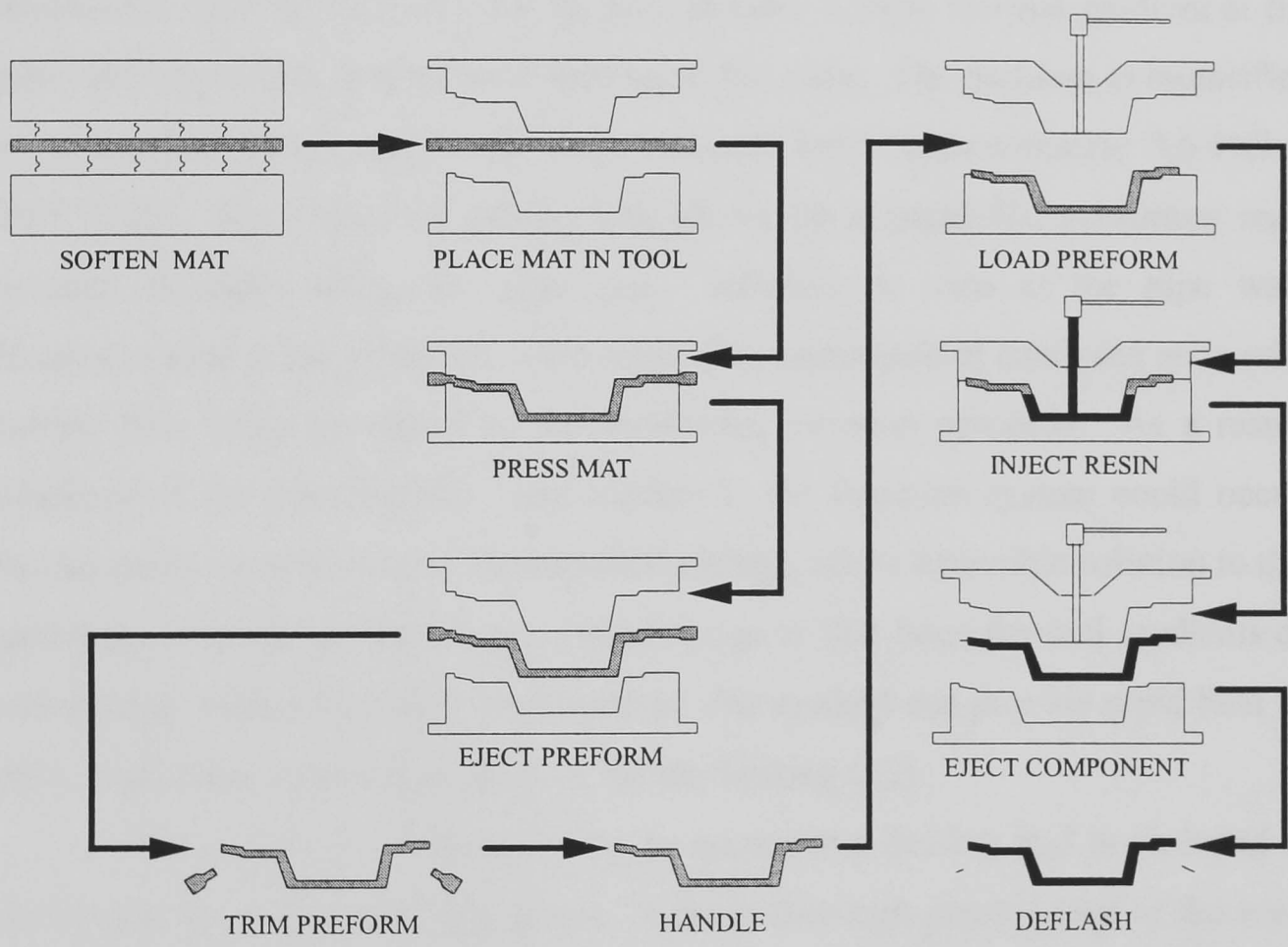


Figure 1.1 Schematic of the liquid composite moulding process

# Microwave Heating Principles

---

### 2.1 Introduction

The low thermal conductivity of polymer resins (approximately 0.3 W/mK [25]) makes in-line heating difficult by conventional means. Conduction based techniques, such as band or trace heaters, produce a large thermal gradient at the pipe wall promoting non-uniform heating of the resin. The problem is intensified by a laminar velocity profile for high viscosity resin (approximately 0.6 PaS at 20°C [22]). Since the flow profile through a pipe is parabolic, maximum resin velocity develops along the pipe axis, reducing to zero at the pipe wall. Excessive heat at the pipe wall could cause premature cure of catalysed resin with further heat being generated as the exothermic reaction proceeds. As a result, blockage of the injection line, and damage to the injection system could occur. In-line microwave heating of thermosetting resins, offers a possible solution to this problem. Microwave heating is non-contacting so that large thermal gradients do not develop within the resin. Furthermore, this method can provide rapid heat up rates, and stable temperature control during heating [22].

This chapter is an introduction to microwave heating and is included to further the development of this thesis. A more thorough presentation of the topic can be found in *Industrial Microwave Heating* by Metaxas and Meredith [26]. Mechanisms of heating dielectric materials using microwaves are examined. Microwave oven types, classified as multimode and single mode applicators, are discussed. Finally, a method to optimise the heating efficiency of a single mode applicator is explained.

## 2.2 Mechanisms of Microwave Heating

Microwave heating is based on the ability of an electric field to polarise the charges in a material, and the inability of this polarisation to follow rapid reversals of the electric field [26]. Dipoles are oriented randomly within a non-metallic material while it is in an equilibrium state as illustrated in Figure 2.1a. Application of an electric field forces a reorientation of the dipoles in a direction opposite to the field as shown in Figure 2.1b. The reorientation energy is retained by the dipoles as stored potential energy while the field is applied. Removing the electric field releases the stored energy as the dipoles relax to a new equilibrium position. This kinetic energy is transferred to the system in the form of heat. Reversing the polarity of the electric field compels the dipoles to rotate through an angle of 180°. Rotational interference with neighbouring molecules forces the dipole orientation to lag that of the electric field while generating heat within the sample (Figure 2.1c) [27].

The heating potential of a material is described by the complex dielectric constant ( $\epsilon^*$ ) expressed as:

$$\epsilon^* = \epsilon' - j\epsilon'' \quad \text{Equation 2.1}$$

The dielectric constant ( $\epsilon'$ ) influences the amount of energy that can be stored in a material in the form of electric fields, while the loss factor ( $\epsilon''$ ) is a measurement of how much energy the material can dissipate as heat. Material property tables often list the loss tangent ( $\tan\delta$ ) which is equivalent to the ratio  $\epsilon''/\epsilon'$ . Dielectric properties vary as a function of frequency and temperature. Tinga and Nelson [28] provide a lucid explanation of the dielectric heating process in the preface to their table of dielectric properties.

## 2.3 Microwave Heating of Dielectric Materials

Microwaves are a specific form of electromagnetic radiation occupying the 300 MHz to 30 GHz bandwidth of the spectrum. Electromagnetic energy is comprised of orthogonally related magnetic and electric field components that propagate as sinusoidally varying waves. It is the electric field component that is

important for microwave heating since it produces dipole reorientation that ultimately heats the dielectric material.

Exponential decay of the electric field occurs within a material according to its dielectric properties. The distance from the surface of the material to a point which the microwave power has been attenuated to 37% ( $1/e$ ) of its original value is termed the power penetration depth ( $D_p$ ), and can be calculated as [26]:

$$D_p = \frac{\lambda_o}{2\pi [2\epsilon'(\sqrt{1+\tan^2\delta})-1]^{1/2}} \quad \text{Equation 2.2}$$

where  $\lambda_o$  is the free space wavelength. A power penetration depth much greater than the sample dimensions is necessary to promote uniform heating throughout the material.

The magnitude of the electric field ( $E$ ) is related to the amount of microwave power ( $P$ ) that a volume of dielectric material ( $V$ ) can absorb, as illustrated by the following equation [26]:

$$P = 2\pi f E^2 \epsilon_0 \epsilon'' V \quad \text{Equation 2.3}$$

where  $f$  is the microwave frequency and  $\epsilon_0$  is the permittivity of free space. Microwave power can also be related to the temperature rise ( $\Delta T$ ) in a material for a given heating period ( $t$ ) as [26]:

$$P = \frac{m}{t} C_p \Delta T \quad \text{Equation 2.4}$$

where  $m$  is the mass and  $C_p$  is the specific heat capacity of the sample. Combining Equations 2.3 and 2.4 leads to an expression for a uniform temperature rise in a sample heated by an electric field:

$$\Delta T = \frac{2\pi f t E^2 \epsilon_0 \epsilon''}{\rho C_p} \quad \text{Equation 2.5}$$

where  $\rho$  is the material density. It is evident from Equation 2.5 that the dielectric loss factor ( $\epsilon''$ ) enables heating of a material, regardless of its thermal properties. Low conductivity materials, such as thermosetting resins, can be heated uniformly by microwaves avoiding large thermal gradients through the material. In addition,

the temperature rise within the sample is proportional to the oscillation frequency of the electric field. Legislation within the United Kingdom restricts the frequency of microwave heating to either  $896 \pm 10$  MHz or  $2450 \pm 50$  MHz [29].

## **2.4 Microwave Ovens**

Figure 2.2 shows a schematic of the components comprising the domestic microwave oven and is typical of all microwave heating systems. Mains power is converted to high voltage by a transformer then supplied to the magnetron. Normally, magnetrons are used to produce microwaves since they provide efficient high power output at a stable frequency, and are relatively inexpensive [30]. Power is extracted from the magnetron via an antenna and launched into a rectangular metallic waveguide for transmission. Microwave energy propagates along the waveguide to the oven, or applicator, where the product is heated. An applicator is a conductive metallic enclosure with a small aperture in one wall through which microwaves enter. Microwaves are reflected off the walls of the applicator, combining with incident microwaves to form a standing wave, termed a mode. The mode includes both electric and magnetic field components, however, only the electric field component contributes to the heating of a dielectric material as shown in Equation 2.5. For this reason, future reference to a mode will concern only the resonating electric field, which is equivalent to the heating profile within an applicator.

### **2.4.1 Multimode Microwave Ovens**

A domestic microwave oven (Figure 2.2) is referred to as multimode oven since its large volume supports several coincident modes. The mode shape determines the heating profile within the oven. Maximum heating occurs when the product is situated at a mode peak (antinode), with zero heating at a node. The heating profile within a domestic oven is non-uniform due to an uneven modal distribution. Localised hot and cold spots develop within such applicators in relation to the mode amplitude at a particular location. The product is often placed on a turntable and passed through a series of hot and cold spots to even out the heating. A mode stirrer provides another means of heating the product more

uniformly. This device consists of a rotating metallic fan that continuously disturbs the modes within the applicator.

#### **2.4.2 Single Mode Microwave Ovens**

Figure 2.3 is a schematic of a typical single mode heating system. The components of this system are similar to those in a domestic microwave oven (Figure 2.2), with the addition of a circulator. A circulator allows incident microwave power from the magnetron to pass through it. Reflected power is diverted by the circulator to a water load, protecting the magnetron and ensuring a more stable output frequency. Non-reflected microwave power enters the single mode applicator. Compared to multimode ovens, the volume of a single mode applicator is reduced so that a unique standing wave, or mode, is excited. Knowledge of the mode shape permits location of the product at the point of maximum heating (antinode). Since the balance of microwave power is directed into a single mode, heating is more concentrated than for multimode ovens. As a result, low loss factor dielectric materials can be heated rapidly within single mode applicators.

#### **2.5 Nomenclature for Single Mode Applicators**

An infinite number of mode profiles can be established within an applicator depending upon its geometry. Single mode applicators, or ovens, are typically rectangular or cylindrical. A notation representing a specific mode profile is used to distinguish between applicators operating in different modes. The notation defines the electric or magnetic field transverse to the direction of propagation within a waveguide, and has been extended to describe stationary fields within single mode applicators. Modes are classified as transverse electric (TE) or transverse magnetic (TM) and further specified using the subscripts  $l$ ,  $m$ , and  $n$ . A comprehensive description of the notation is given by Mariner [31].

Orthogonal coordinates are used to classify modes within rectangular applicators. The subscripts  $l$ ,  $m$ , and  $n$  are related to the number of half wavelengths in the  $x$ ,  $y$ , and  $z$  directions as defined in Figure 2.4. For example, the electric field profile within the  $TE_{102}$  mode rectangular applicator is

characterised by a single half wavelength along the width ( $x,l$ ) of the rectangular section. The heating rate is constant along the height of the applicator ( $y,m$ ) since no variation in the electric field occurs in that direction. Finally, two half wavelengths are produced along the length of the applicator ( $z,n$ ).

Mode profiles within cylindrical applicators are defined using cylindrical polar coordinates. The subscripts  $l$ ,  $m$ , and  $n$  are related to the  $\phi$ ,  $r$ , and  $z$  directions as defined in Figure 2.5. The  $l$  coordinate designates the number of full wavelengths in the electric field along the circumference ( $\phi$ ) of the applicator. The  $m$  coordinate specifies the number maximums and minimums occurring in the electric field between the axis and wall of the applicator. Variation in the electric field along the length of the applicator ( $z$ ) is denoted by the  $n$  subscript. For example, the  $TM_{020}$  mode is characterised by one maximum and one minimum along the radial direction ( $r$ ) so that  $m = 2$ . No circumferential or lengthwise variations are excited in the  $TM_{020}$  mode for even heating along these coordinates.

## 2.6 Rectangular Applicators

Figure 2.6 shows a  $TE_{101}$  mode rectangular applicator consisting of a metallic waveguide section with a moveable double plunge tuner at one end and an aperture at the other. The product is heated as it flows through a PTFE pipe oriented perpendicular to the applicator in a slotted choke. PTFE absorbs little microwave power due to its low loss factor ( $\epsilon''=0.0003$  [22]) so that the balance of the microwave energy is transferred to the product. The slotted choke is sized to prevent microwave radiation from leaking through the opening while enabling continuous processing of the product. Heating materials that have different dielectric properties shifts the resonant frequency of the mode within the applicator, and likewise, the heating profile. Adjusting the double plunge tuner realigns the resonant frequency with the magnetron output frequency, correcting the problem. The tuning capability of rectangular applicators permits a variety of materials with different dielectric properties to be heated effectively. The heating profile is virtually uniform across the pipe diameter making this system unsuitable for heating catalysed resins with laminar flow properties. Excessive heat at the pipe wall could cause premature resin cure within the PTFE pipe [22].

## 2.7 Cylindrical Applicators

Figure 2.7 shows a cylindrical applicator comprising a capped metallic cylinder with a rectangular aperture through the circumference. The product is heated as it flows through a PTFE pipe located concentrically along the applicator. The diameter of the applicator is calculated for resonance in a particular mode based on the dielectric properties of the product. As a result of its fixed geometry, heating within the cylindrical applicator is limited to materials with similar dielectric properties. The advantage of cylindrical applicators is that modes suitable for heating thermally sensitive materials, such as the  $TM_{020}$  mode, can be established.

### 2.7.1 Mode Excitation within $TM_{0mn}$ Cylindrical Applicators

The simplest cylindrical applicators operate within the  $TM_{0mn}$  family of modes, such as the  $TM_{020}$  mode cylindrical applicator shown in Figure 2.7. These applicators exhibit no circumferential variation in the electric field, since  $l=0$ . However, a vertically oriented electric field ( $E_z$ ) is established along a radial path ( $r$ ) described by the following equation [22]:

$$E_z(r) = E J_0 \left[ \frac{2\pi fr \sqrt{\epsilon'}}{C_o} \right] \quad \text{Equation 2.6}$$

where  $E$  is the electric field strength and  $C_o$  is the velocity of light. The shape of the electric field is described by  $J_0$ , the Bessel function of the first kind (order zero), with a maximum amplitude at the applicator axis and a zero value at the applicator wall. Rotating this electric field profile through a swept angle of  $360^\circ$  generates the three dimensional heating mode.

### 2.7.2 Examples of $TM_{0m0}$ Mode Cylindrical Applicators

Figure 2.8 shows a  $TM_{010}$  mode cylindrical applicator used for continuous processing. This is the lowest order mode that can be excited within the applicator, and is termed the fundamental mode. A vertically oriented electric field (Equation 2.6) is established within the applicator with no electric field components along its length or circumference. A maximum electric field occurs

at the centre of the PTFE pipe decaying to zero at the applicator wall according to the first root of the  $J_0$  Bessel function. The heating profile across the PTFE pipe is approximately uniform, similar to the  $TE_{101}$  mode rectangular applicator (Figure 2.6), and is not desirable for heating thermally sensitive fluids.

Figure 2.7 shows the  $TM_{020}$  mode cylindrical applicator used for heating thermally sensitive fluids. The  $TM_{020}$  mode is the second mode in the  $TM_{0m0}$  family and is produced by expanding the applicator diameter to correspond with the second root of the  $J_0$  Bessel function. This applicator can be used to heat catalysed resin since the electric field decays to zero at the wall of the PTFE pipe with a maximum electric field along the pipe axis where the resin velocity is greatest. The presence of three dielectric materials within the applicator (resin, PTFE, and air) must be considered when calculating the applicator diameter. An analytical treatment of this problem was developed by Hill in designing the  $TM_{020}$  mode cylindrical applicator used in this thesis [22].

## **2.8 Characterisation of Single Mode Applicators**

The heating performance of a single mode applicator is optimised by an iterative tuning and coupling procedure. Tuning involves matching the natural resonant frequency of the desired mode within the applicator to the magnetron output frequency. Coupling is performed to maximise the transferral of microwave energy from the waveguide into the applicator. A fully optimised applicator will resonate at the magnetron output frequency with all of the available microwave energy being directed into the applicator for heating. The extent of applicator tuning and coupling over a swept frequency range can be determined using a network analyser.

### **2.8.1 Determination of the Applicator Efficiency**

Figure 2.9 shows a typical set up for the optimisation of a single mode applicator. A network analyser is connected by a coaxial waveguide to a rectangular waveguide transition section. This transition piece distributes microwave energy to the applicator via a stub tuner and an aperture. The network analyser emits an energy pulse that travels towards the applicator, termed the forward power. A

portion of the forward power enters the applicator and resonates, while the remainder strikes the aperture and returns to the network analyser as reflected power. The forward and reflected power travel as waveforms, and combine to form a standing wave in the waveguide. A network analyser determines the ratio of maximum to minimum voltage in the standing wave, and displays it as the VSWR (voltage standing wave ratio) over a swept frequency. A VSWR of unity represents a perfectly coupled system having zero reflected power, while a VSWR of infinity corresponds to 100% reflected power. The VSWR can be related to applicator efficiency by the following equation [22]:

$$\text{Applicator Efficiency}(\%) = \left[ 1 - \left( \frac{\text{VSWR} - 1}{\text{VSWR} + 1} \right)^2 \right] \times 100 \quad \text{Equation 2.7}$$

This expression is illustrated graphically in Figure 2.10.

### 2.8.2 Determination of the Quality Factor

A VSWR trace also indicates the sharpness of response, or bandwidth, of a resonant mode. Ideally, a resonant mode is excited at a single frequency. In practice, the mode can be excited over a range of frequencies resulting from energy dissipation in the applicator walls and the dielectric load [26]. The bandwidth of the resonant frequency is quantified by the quality factor (Q) and is calculated as:

$$Q = \frac{f_0}{\Delta f} \quad \text{Equation 2.8}$$

where  $f_0$  is the resonant frequency and  $\Delta f$  is the frequency bandwidth at the half power points (defined as a VSWR of six [32]). Figure 2.11a shows a single mode applicator with a high quality factor ( $Q = 85$ ) resulting in a sharp response profile with a narrow bandwidth. The system illustrated in Figure 2.11b has a broad bandwidth for a low Q value of eight. A low Q system is desirable for microwave heating since a slight variation in the resonant frequency of an applicator due to a change in the dielectric properties of the product will not cause a large reduction in the VSWR and the heating efficiency.

### 2.8.3 Optimisation of a Single Mode Applicator

Optimisation of a single mode applicator for maximum heating is accomplished by an iterative technique. The system is attached to a network analyser (Figure 2.9) displaying a VSWR response trace for the non-optimised system. The applicator is tuned with a four stub tuner to match its natural resonant frequency with the magnetron output frequency (2.45 GHz). Adjusting the tuner equalises the impedance of the loaded applicator to the characteristic impedance of the magnetron and waveguide system. The size of the aperture is altered to increase applicator coupling, indicated by a reduction in the VSWR. As a result of coupling, the resonant frequency of the applicator can shift slightly. Further tuning and coupling are performed until a minimum VSWR is achieved at the desired resonant frequency (2.45 GHz). The response trace of a perfectly coupled applicator is shown in Figure 2.12. The applicator efficiency is 100% (VSWR equal to unity) at a magnetron output frequency of 2.45 GHz, representing a single mode applicator optimised for maximum heating performance. A disadvantage of this technique is that no information regarding the shape of the excited mode is available from the network analyser. Consequently, the heating profile within an applicator can not be determined exclusively by this technique.

## List of Figures

- Figure 2.1a Random dipole orientation in uncharged, equilibrium state
- Figure 2.1b Reorientation of dipoles by an applied electric field
- Figure 2.1c Dipole vibration due to an alternating electric field
- Figure 2.2 Schematic of the components comprising a domestic microwave oven
- Figure 2.3 Schematic of the components comprising a single mode microwave oven
- Figure 2.4 Electric field pattern within a  $TE_{102}$  mode rectangular applicator [22]
- Figure 2.5 Electric field pattern within a  $TM_{020}$  mode cylindrical applicator
- Figure 2.6  $TE_{101}$  mode rectangular applicator [22]
- Figure 2.7  $TM_{020}$  mode cylindrical applicator [22]
- Figure 2.8  $TM_{010}$  mode cylindrical applicator [22]
- Figure 2.9 Experimental set up for the optimisation of a single mode applicator [22]
- Figure 2.10 Applicator efficiency versus VSWR
- Figure 2.11a Typical VSWR response trace for a single mode applicator having a high Q
- Figure 2.11b Typical VSWR response trace for a single mode applicator having a low Q system
- Figure 2.12 VSWR response trace illustrating a perfectly coupled, single mode applicator tuned to 2.45 GHz

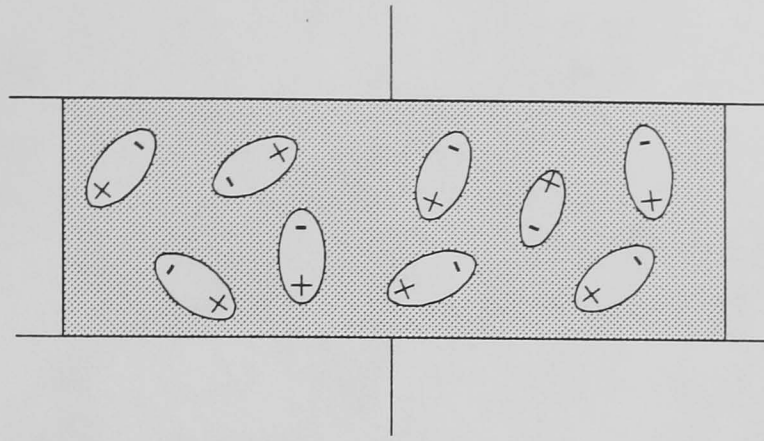


Figure 2.1a Random dipole orientation in uncharged, equilibrium state

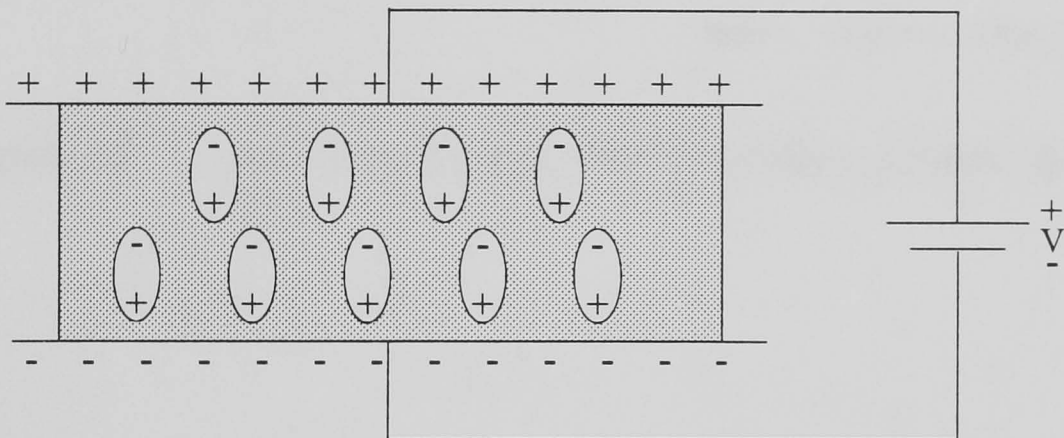


Figure 2.1b Reorientation of dipoles by an applied electric field

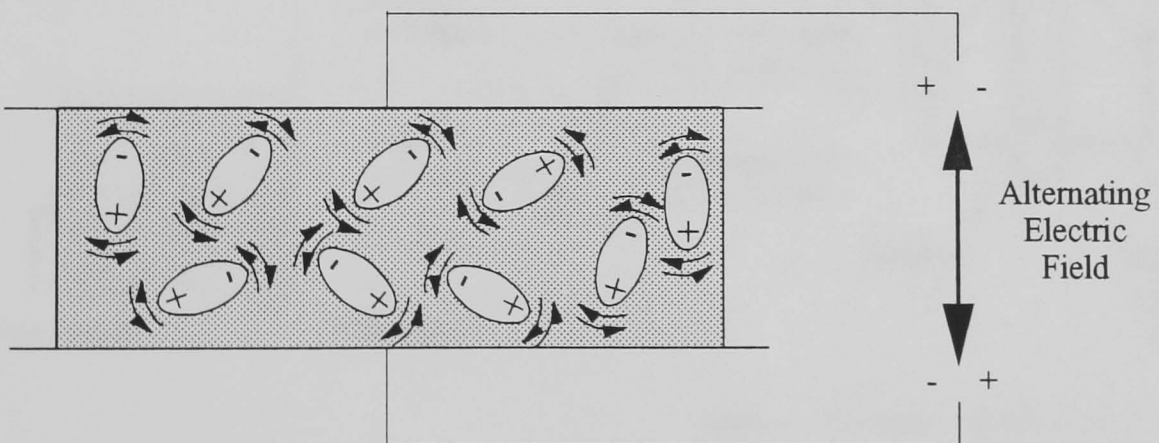


Figure 2.1c Dipole vibration due to an alternating electric field

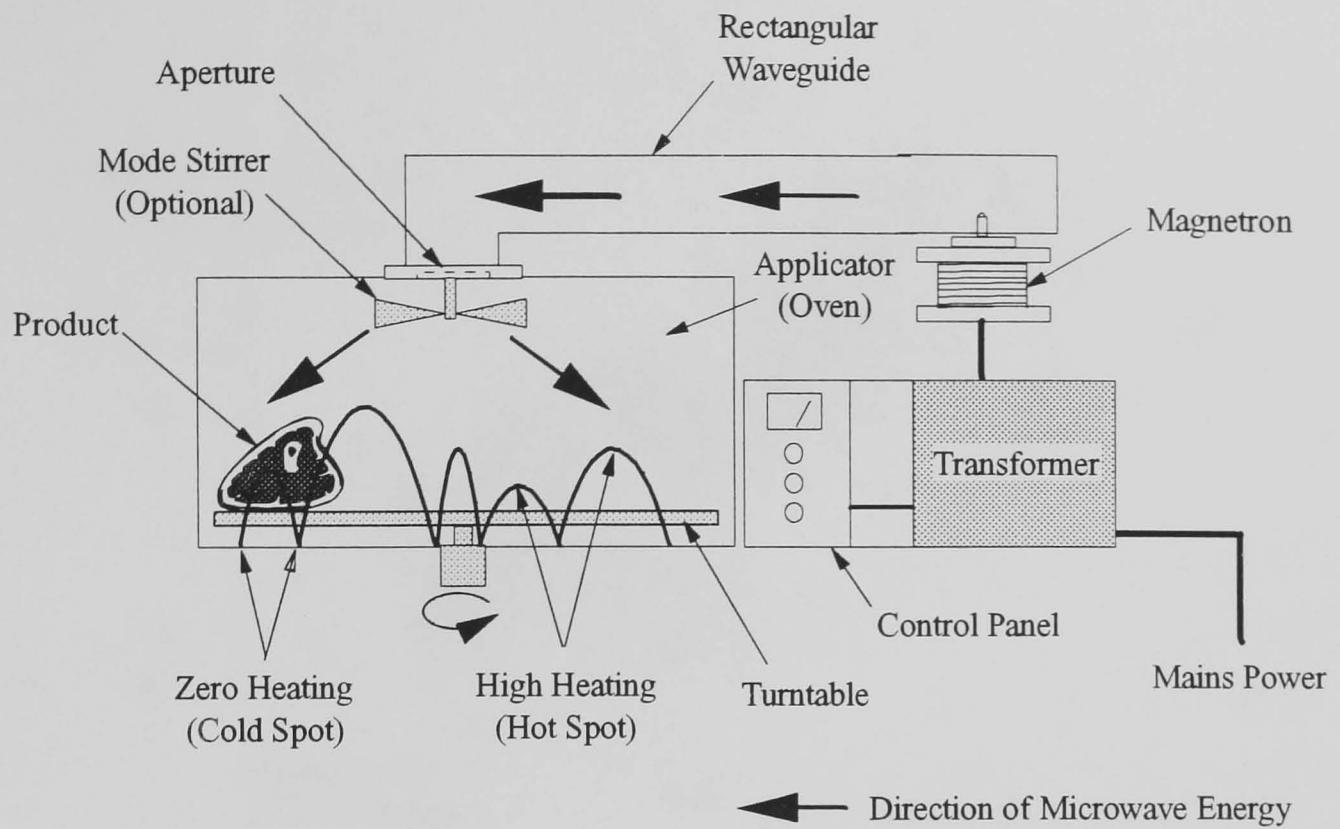


Figure 2.2 Schematic of components comprising a domestic microwave oven

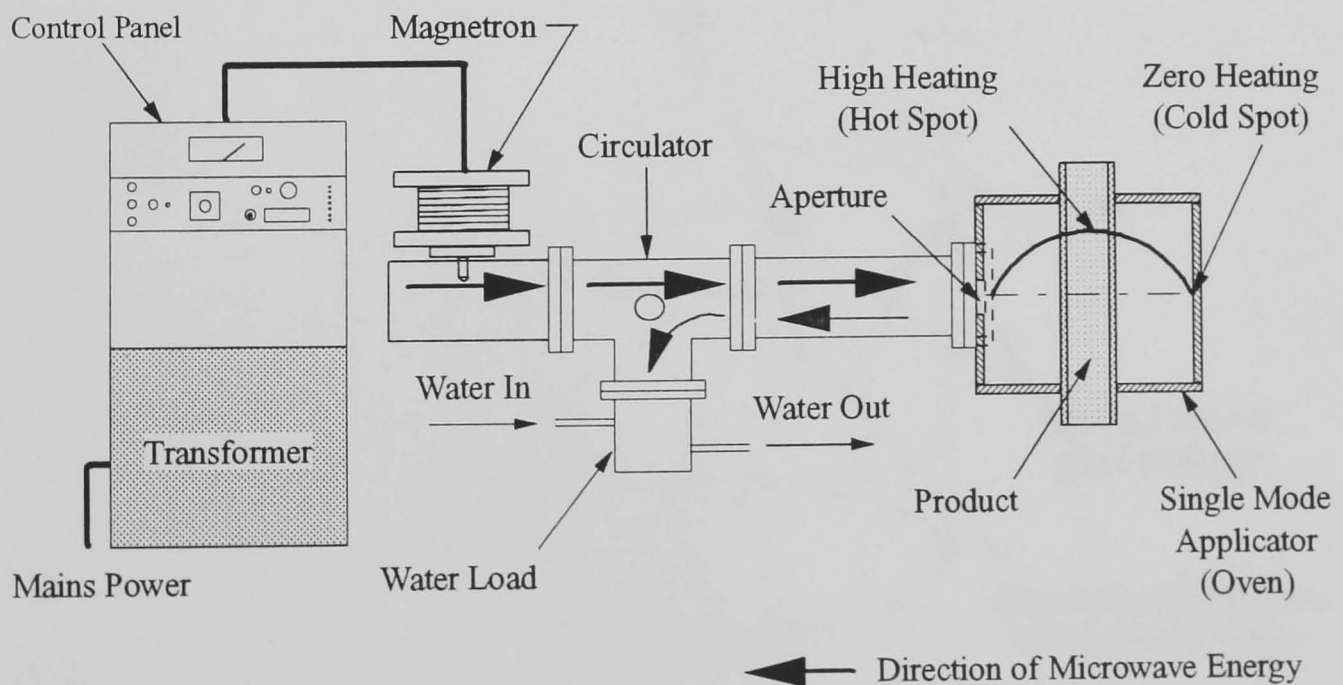


Figure 2.3 Schematic of components comprising a single mode microwave oven

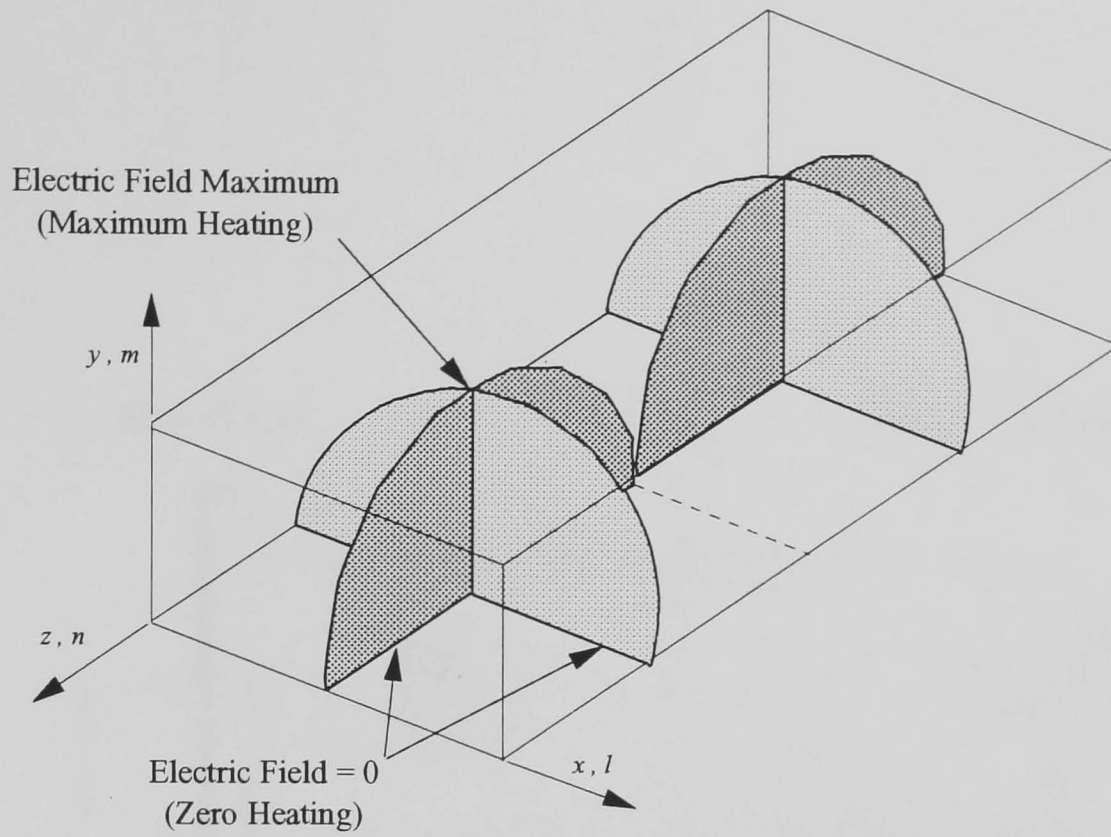


Figure 2.4 Electric field pattern within a  $TE_{102}$  mode rectangular applicator

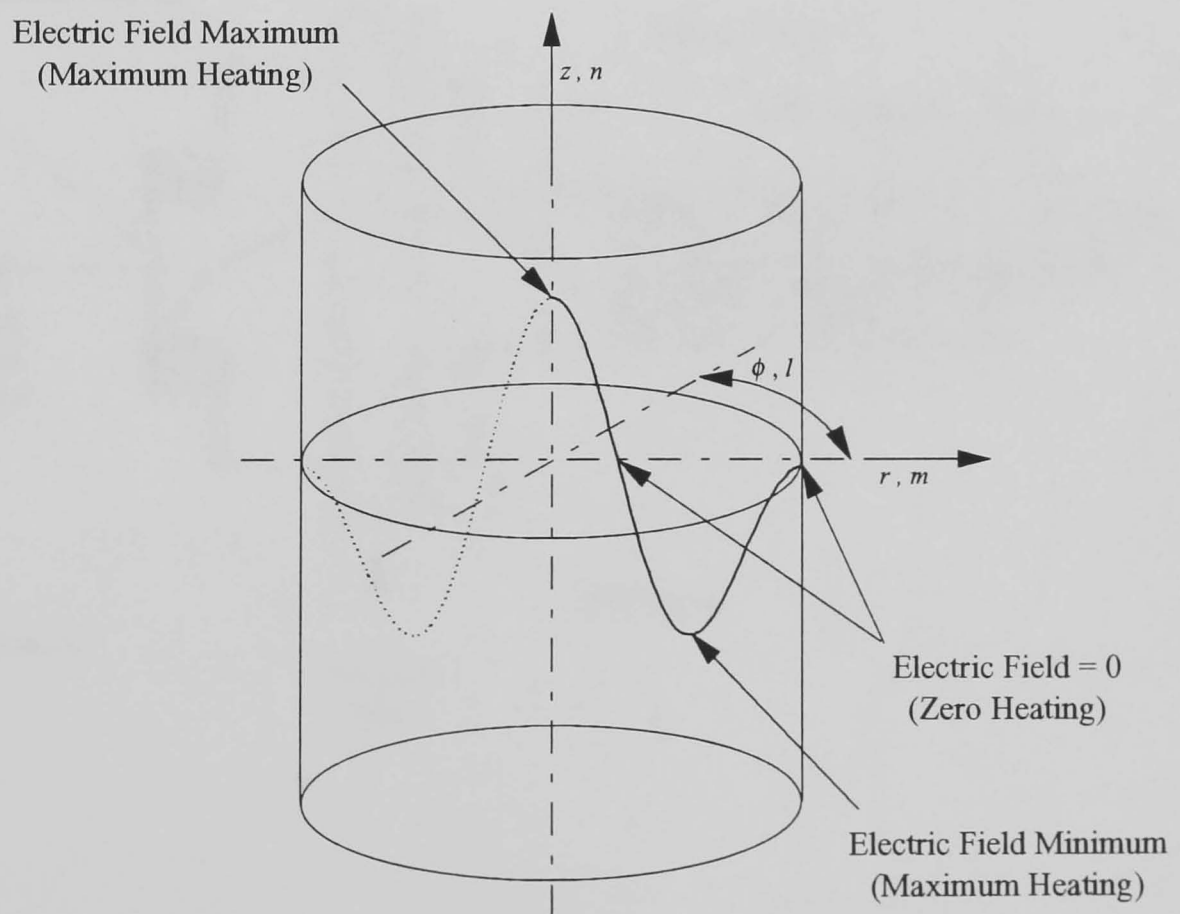


Figure 2.5 Electric field pattern within a  $TM_{020}$  mode cylindrical applicator

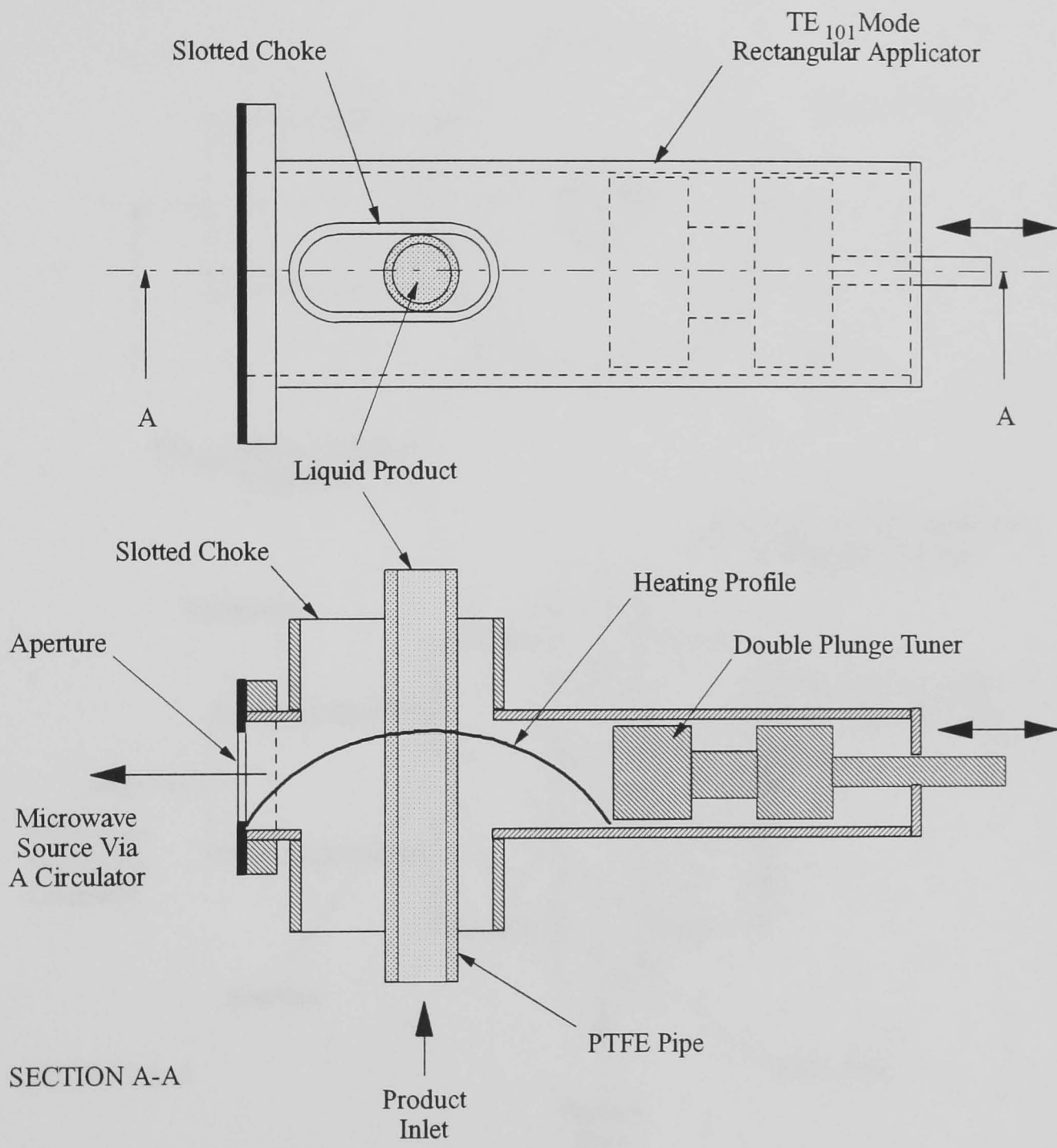


Figure 2.6  $TE_{101}$  mode rectangular applicator

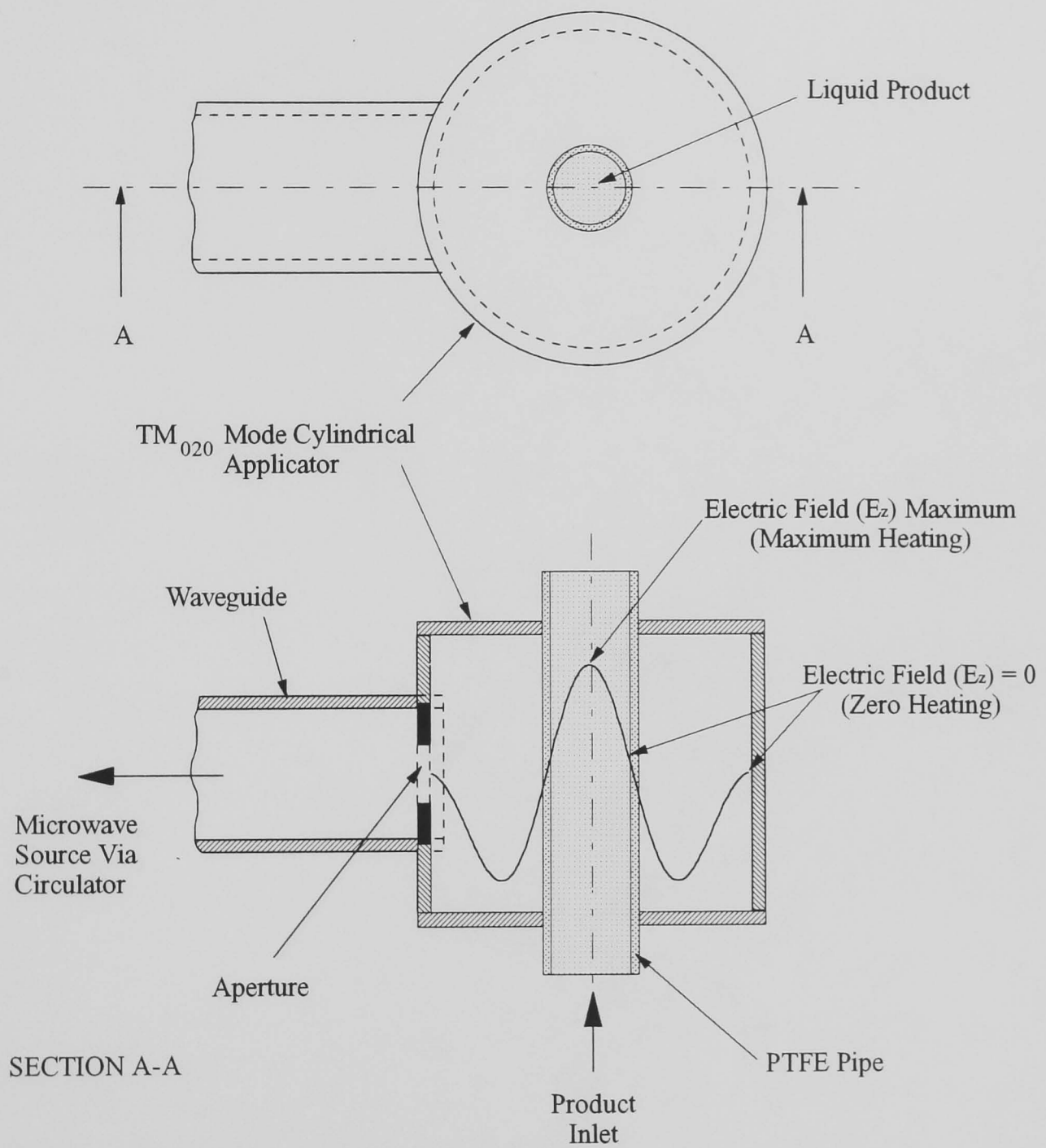


Figure 2.7  $TM_{020}$  mode cylindrical applicator

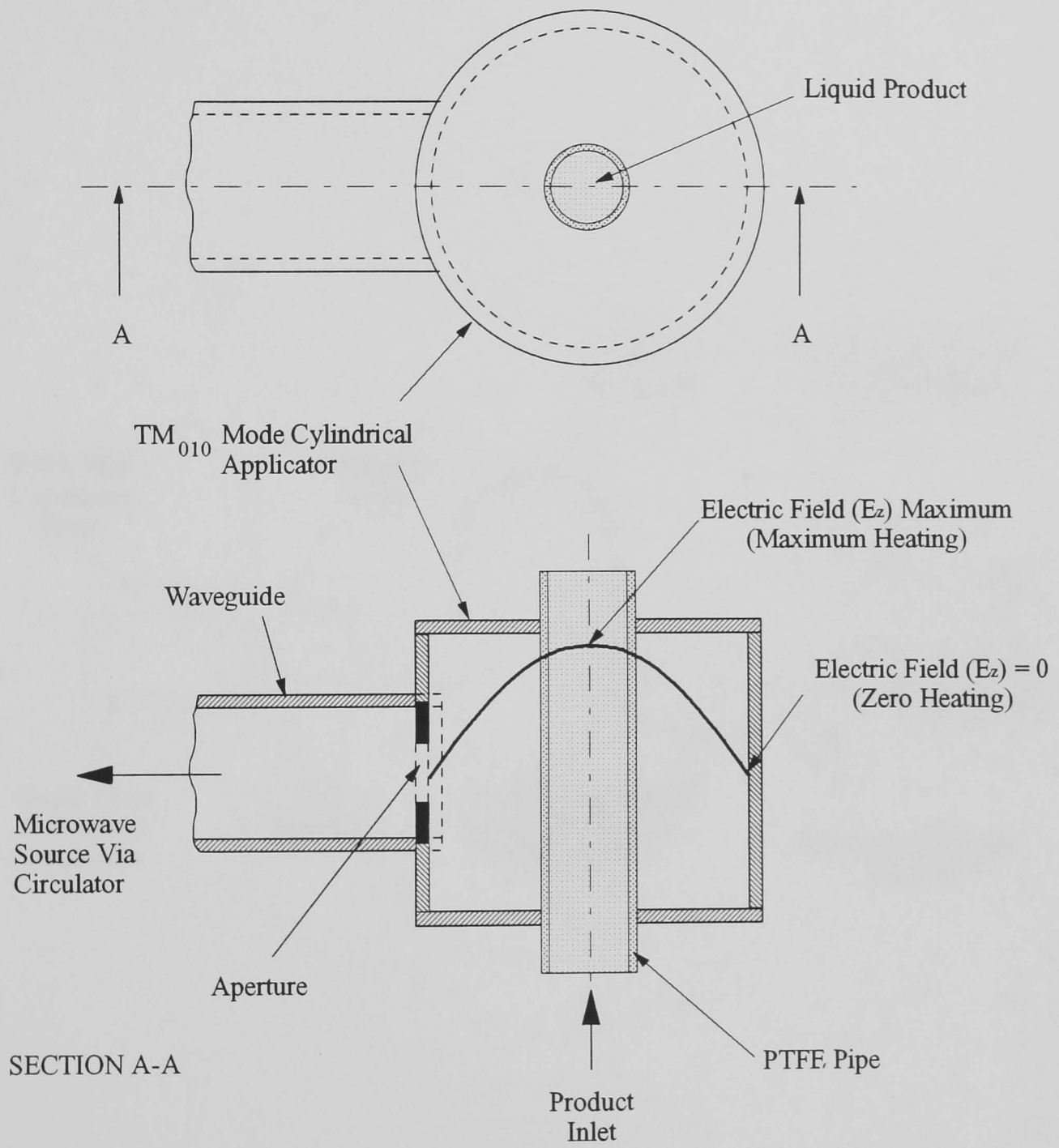


Figure 2.8  $TM_{010}$  Mode Cylindrical Applicator

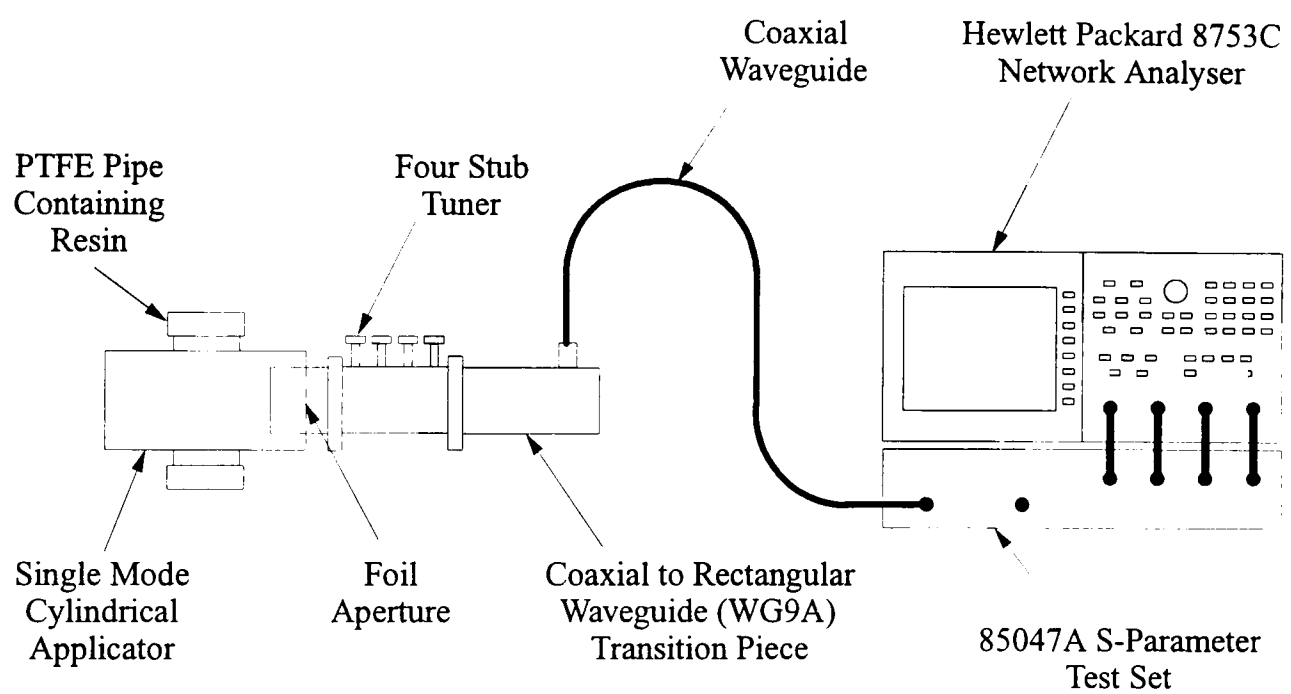


Figure 2.9 Experimental set up for the optimisation of a single mode applicator

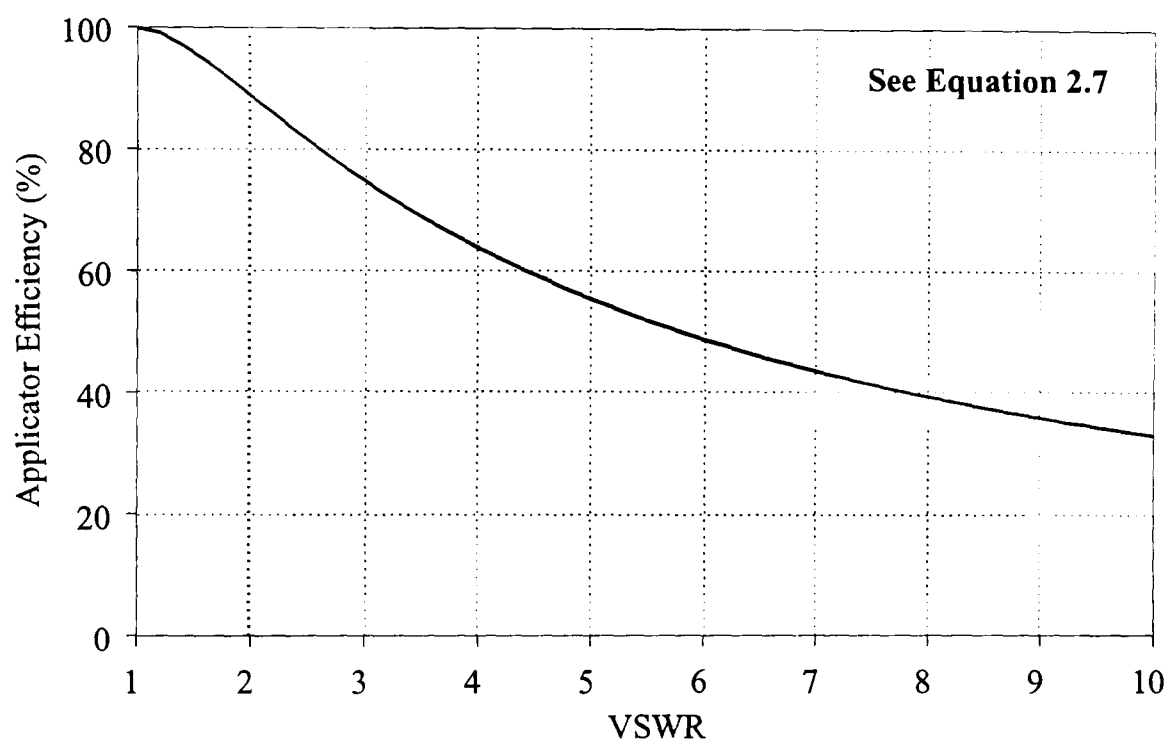


Figure 2.10 Applicator efficiency versus VSWR

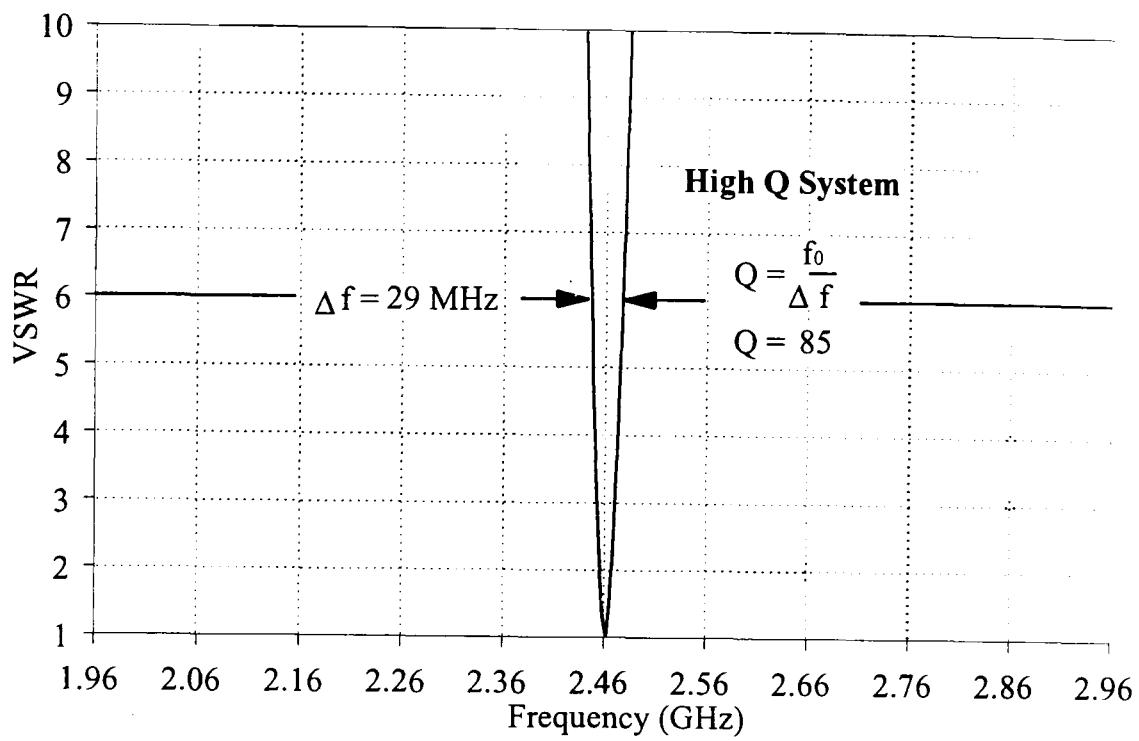


Figure 2.11a Typical VSWR response trace for a single mode applicator having a high Q

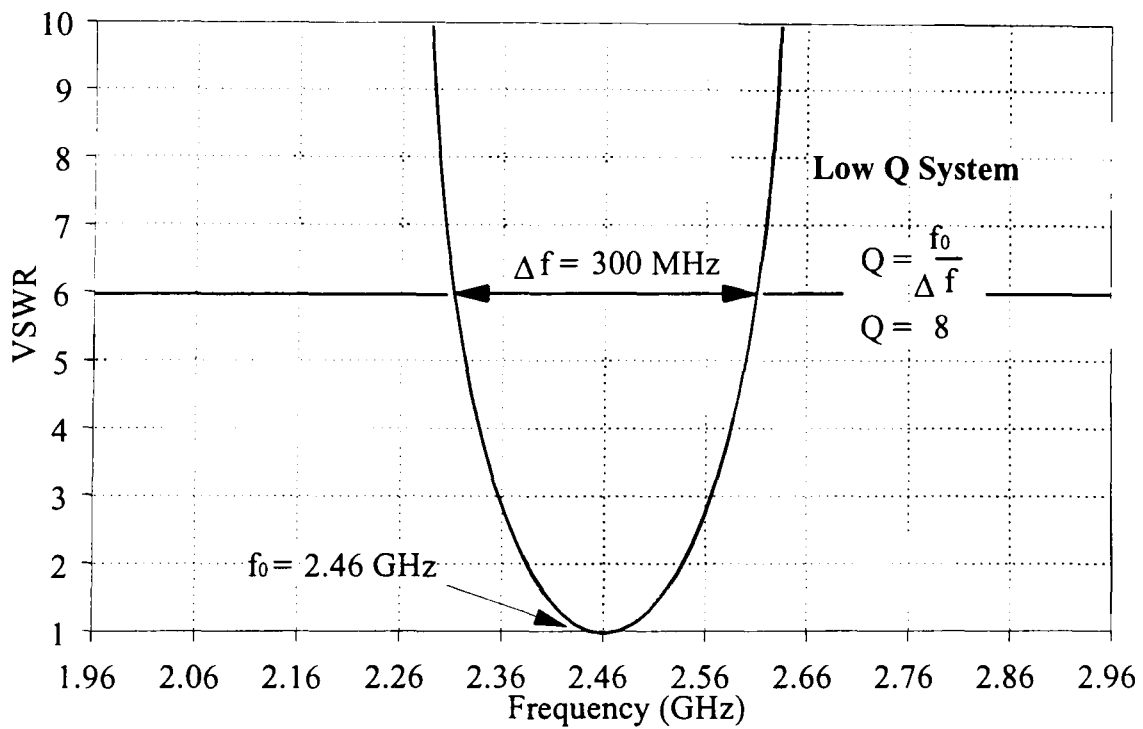


Figure 2.11b Typical VSWR response trace for a single mode applicator having a low Q

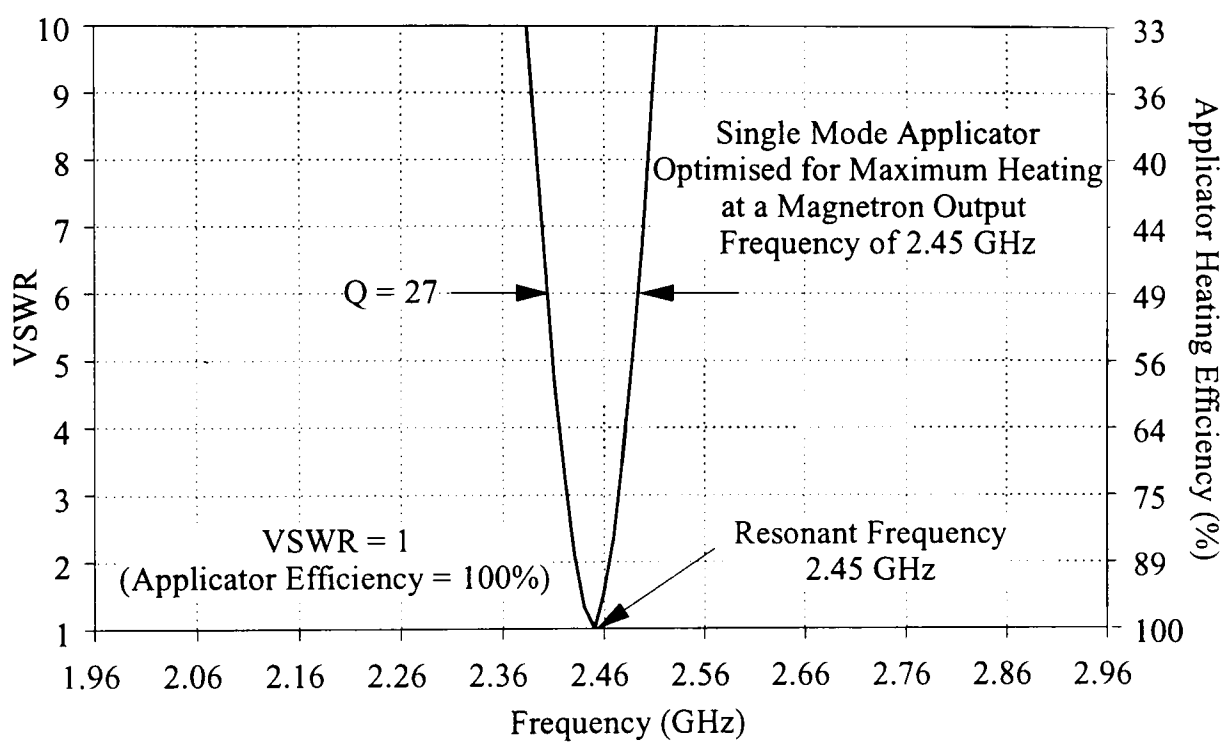


Figure 2.12 VSWR response trace illustrating a perfectly coupled, single mode applicator tuned to 2.45 GHz

# Literature Review

---

### 3.1 Introduction

A survey of the literature is presented in this chapter regarding cycle time reductions in RTM. The principal cause of extended RTM cycle times was identified as thermal quench at the injection gate as cold resin enters the hot mould. A number of cycle time reduction techniques were reviewed to assess the effect of each on the RTM process and component quality. Heating the resin using microwaves was found to be an effective means of reducing cycle times since thermal quench was decreased. A review was conducted to determine the extent of microwave heating applications used in polymer processing. Finally, computer aided design methods were considered for the efficient development of microwave heating systems.

### 3.2 High Volume Manufacture of Fibre Reinforced Plastic Components

A three minute cycle time has been targeted for production of FRP components at a rate of 100,000 parts per annum [3]. Manufacturing techniques, such as DMC, SMC, and RRIM, are used to meet current production requirements. However, components made using these short fibre techniques are unsuited for structural applications [33]. The shortcomings of these techniques have been acknowledged with ongoing industrial efforts to improve mechanical performance. For example, Ehnet [34] described a preform-compound (PFC) consisting of CFRM impregnated with a thermoplastic resin (80% fibre mass fraction) to allow thermoforming. The PFC was compressed with SMC to produce a reinforced component with improved mechanical properties.

Structural FRP components can be produced by oriented, long fibre techniques such as SRIM and RTM. Cycle times of one minute are feasible with SRIM due to rapid polymerisation of the resin [35]. The resin gels shortly after

mixing necessitating a costly, high pressure injection system to fill the mould cavity rapidly (over 1 kg/s) [36]. Robust steel tooling to contain the high injection pressures adds to the initial cost of an SRIM system. Despite the high investment costs, dedicated SRIM facilities do exist. Hufnagel [37] described a fully automated plant for the production of large SRIM components. Maximum preform sizes were quoted at 2200 mm × 2800 mm, although no mention of fibre fraction, or cycle time was made.

Traditionally, cycle times are longer for RTM than for SRIM due to heat activated, rather than chemically activated resin systems [36]. The increased gel times permit a longer impregnation phase for the production of large components and improved preform wet-out. Lower pressure injection enables less sophisticated metering systems and lightweight tooling to be used in RTM. As a result, the initial cost of an RTM production facility is typically less than for an equivalent SRIM unit. This suggests that both RTM and SRIM are viable for FRP component production, with SRIM becoming more cost efficient at higher volumes. However, the production of FRP components at volumes normally associated with SRIM, using a lower cost technique is the principal motivation for reducing RTM cycle times.

### **3.3 Injection Strategies for Resin Transfer Moulding**

Figure 3.1 illustrates the single stream and twin stream injection techniques typically used in liquid composite moulding processes. SRIM is constrained to twin stream injection by nature of the chemically reactive resin systems. The resin and hardener streams remain separate until impingement mixing near the injection gate. Most RTM resin systems are thermally activated making twin stream injection possible, but not essential. The principal advantage of a twin stream delivery system is that the resin and catalyst components are non-reactive, and therefore, insensitive to temperature until mixing at the injection gate. Preheating large volumes of each component to increase resin reactivity is possible using simple conduction heating devices, although precise temperature control would be difficult to achieve. Highly reactive resin systems can be used with the qualification that the mould is filled, and fibre wet-out is sufficient, before the

resin gels. Twin stream injection systems prevalent in industry for producing large components commonly are driven by reciprocating pumps. Pressure variations occur during the pump stroke using these systems. Karbhari et al. [38] showed that decreasing the length of the pump stroke reduced the pressure variations and improved the mechanical properties of the laminate. Pulsed delivery of the individual streams leads to inaccurate dosing and has prompted the following investigators to implement constant volume, lance driven injection systems. Parmar et al. [39] modified an existing RIM system for use with RTM, while Jander [40] described a sophisticated cam operated metering device on an RTM pump that could maintain a specific resin to catalyst ratio during injection.

Constant pressure, single stream injection systems have the advantage of non-pulsed resin delivery without the need for elaborate metering devices. As a result, these systems are simple and inexpensive compared to twin stream injection systems. Measured resin quantities can be mixed before moulding and stored in a pressure vessel. Delivery of the resin into the mould under constant pressure results in cavity pressures that are typically lower than for a reciprocating pump system [41]. The primary disadvantage of single stream injection is that the pre-mixed resin is thermally sensitive. Resins with low reactivity at ambient temperature must be used to prevent premature cure within the storage vessel before injection has been completed. Single stream systems are dependent upon heat to initiate the polymerisation reaction. Normally, heat is provided by the mould. Thermal quench at the injection gate due to cold resin entering the hot mould hinders the heat transfer capacity of the mould and extends cycle time. Preheating the resin to reduce mould quench is an obvious solution, however, the thermal sensitivity of the resin warrants special treatment to prevent premature cure within the injection system [22].

### **3.4 High Volume Resin Transfer Moulding**

High volume manufacture in the automotive industry is dominated by the production of steel components. Robust tool sets and sequential pressing operations are necessary to make a steel part by traditional methods. Parts integration is possible with RTM so that less operations are necessary to produce

an equivalent FRP component. As a result, production costs can be reduced. Further cost benefits can be realised using lightweight shell tooling since lead times are shorter, total material costs are less, and lower capacity manipulation equipment can be used, compared to steel tools [33].

RTM has been implemented successfully for low volume manufacture of automotive components (less than 10,000 parts per annum). However, high volume RTM is hindered by inefficient preform manufacturing, and long cycle times [42]. Jander [40] described an automated system that produced net shaped preforms of random and oriented fibre, ready for moulding. Development continues to produce engineered, net shaped preforms with compensated fibre angles to account for fibre slip and shear during preforming [24][18]. Parallel studies to reduce the moulding cycle time are cited below.

### **3.5 Cycle Time Reduction Techniques for Resin Transfer Moulding**

Several authors have identified the process variables that affect cycle time and have suggested techniques to reduce this time. The interaction between process parameters makes isolation of a single factor difficult. Karbhari et al. [38] performed a Taguchi study to quantify the interaction of several moulding parameters including reinforcement types, mould temperature, and injection strategies. They found that a short pump stroke had the greatest influence on the tensile, flexural, and shear properties of composites. From a broader standpoint, their work proposed a methodology to define a robust processing window for RTM. Other investigators have varied a single parameter then analysed the resulting changes to the process.

Cycle time comprises both the impregnation and cure phases. Most process models separate the phases into two separate events for simplicity [43]. Resin flow during impregnation has been described by the Darcy relationship:

$$Q = \frac{KA}{\mu} \frac{dp}{dx}$$

where the resin flow rate ( $Q$ ) is proportional to the preform permeability ( $K$ ), the flow area ( $A$ ), and the pressure gradient ( $dp/dx$ ), but inversely proportional to the

resin viscosity ( $\mu$ ). Typically, reductions in the impregnation time will promote overall cycle time reductions. The cure phase consists of heat transfer into the stationary resin at the end of impregnation, followed by heat generation from the exothermic polymerisation reaction. The rate of this reaction ( $d\alpha/dt$ ) is often expressed by the Kamal and Sourour expression [44]:

$$\frac{d\alpha}{dt} = (k_1 + k_2\alpha)^m (1 - \alpha)$$

where  $\alpha$  is the degree of cure and the kinetic constants are  $k_1$  and  $k_2$ . The end of the cure phase (and cycle time) can be defined as being equal to a pre-established percentage of conversion. Several RTM process variables that influence cycle time are discussed below.

### 3.5.1 Injection Gate Location

Gebart et al. [45] determined that the impregnation time was influenced strongly by the injection gate location. Three injection techniques were used to fill a square plaque mould including centre pin gate injection, edge, and peripheral gate injection. Peripheral injection was approximately three times faster than edge injection and ten times faster than centre injection as a result of a larger flow area for the resin. Lower impregnation times were assumed to result in proportional reductions in the cycle time. Rudd and Kendall [43] reported similar results for equivalent gating strategies. Peripheral and edge injection also reduced mould quench by increasing the area of the mould being subjected to cold incoming resin. Local cooling was limited, and the overall cycle time was reduced [46]. However, the authors concluded that the pressure on the mould was greatest during peripheral injection, and least for centre injection. Overfilling the mould increased the hydrostatic pressure and caused significantly higher in-mould pressures during exotherm. High pressure, particularly in shell moulds, could result in resin leakage, clamp damage, localised mould distortion, or part thickness variations. For these reasons, Kendall [20] stated that localised cure pressures within the mould should be considered as critical loads at the mould design stage rather than the hydrostatic load.

### **3.5.2 Injection Pressure**

Increasing the pressure of a constant pressure injection system reduces the impregnation time. This results from an increased forcing pressure gradient, but is countered by a higher resin viscosity as in-mould heating of the flowing resin is decreased. Rudd et al. [47] concluded that the injection pressure affected the impregnation time to a greater extent than the cycle time since thermal quench was distributed over a larger portion of the mould. One disadvantage of high injection pressure is mould deflections. Selection of injection pressures beneath the mould damage threshold has been controversial. Some manufacturers argued that a low injection pressure improves fibre wet-out, while others claimed high pressure is necessary to purge air from the mould [48].

### **3.5.3 Preform Permeability**

Preform permeability is governed by fibre architecture and volume fraction. Highly permeable preforms reduce the restriction of resin flow, lowering the impregnation time. Peterson and Robertson [49] determined that for a given fibre volume fraction, increasing the fibre diameter increased reinforcement permeability, reducing the impregnation time. Increasing fibre bundle diameter also increased the resin flow rate, but void formation was a dominant effect. Thermoplastic binders on preformable mats (approximately 10% by weight) reduce permeability and increase impregnation time [50]. Rudd et al. [47] demonstrated that reductions in impregnation time do not always translate to cycle time reductions. They showed a 50% reduction in impregnation time by reducing the fibre mass fraction of CFRM from 43% to 18%. However, the cycle time increased by 60% despite the lower impregnation time. The authors reasoned that although the fibre content restricted resin flow, it also acted as a heat source. Reducing the fibre fraction placed a greater demand on the mould to supply heat to the resin, and led to a longer cycle time. In addition, the fibre was displaced by resin, requiring more heat from the mould to activate the greater resin volume within the mould.

### **3.5.4 Resin Viscosity**

Reducing resin viscosity improves resin flow through the preform, in turn lowering the impregnation time for constant pressure injection systems. The dependence of resin viscosity on temperature was demonstrated by Scott [12] who reported a 60% reduction in viscosity for a polyester resin (Synolac 6345) by raising the temperature from ambient to 60°C. Resin viscosity has been reduced by several other means including mould temperature increases, preform preheating, and resin preheating. The influence of each of these parameters is described below.

#### **Mould Temperature**

Increasing the mould temperature heats the resin to a greater extent as it flows through the mould, reducing viscosity and shortening the impregnation phase. In addition, the cure phase can be reduced significantly by increasing the mould temperature since gel times across the mould are reduced.

Thermal quench occurs when cold resin enters the hot mould, cooling the preform and mould. Kendall [20] determined that the overall cycle time was dictated by thermal quench at the injection gate, and proposed the use of zone heating at that location to counteract heat losses, reducing the cycle time. Using this technique a 50% reduction in cycle time was demonstrated by Kendall and Rudd [46].

Perry et al. [51] investigated the relationship between mould material and cycle time. The use of high thermal conductivity moulds such as aluminium and chromed copper, shortened the cycle time compared to epoxy tooling, as a result of faster heat up after thermal quench, and a more even temperature distribution across the mould. In addition, peak exotherm temperatures were lower in the high conductivity moulds since heat could be removed more effectively from the mould surface.

#### **Preform Preheating**

Preheating the preform to the mould temperature (110°C) prior to injection under constant pressure was shown to reduce the impregnation time by 15% and the cycle time by 40% compared to moulding produced with a colder preform

(50°C) [47]. The warm preform lowered the resin viscosity for improved flow, contributing to a reduction in impregnation time. Furthermore, the temperature within the mould cavity at the end of impregnation was greater so that the time to heat the quenched laminate back to mould temperature was reduced.

### **Resin Preheating**

Preheating lowers the resin viscosity to facilitate flow, and reduces the amount of heat that must be supplied by the mould to initiate polymerisation. These factors promote reductions in both the impregnation and cure phases, resulting in an overall cycle time reduction. Several techniques have been used to preheat the resin. Rudd et al. [47] fitted a heater jacket to the resin storage vessel to raise the temperature from 20°C to 55°C. A moulding produced with preheated polyester resin reduced both the impregnation and cycle times by 20%. Hill [22] produced a similar result by preheating polyester resin in a domestic microwave oven to 60°C for a 50% reduction in cycle time. However, these cycle time reductions did not include the time required to heat the resin before injection or flushing of the injection system after moulding. Subsequently, Hill developed a sophisticated in-line microwave resin preheating system that yielded true cycle time reductions, since the resin was heated during injection. Using this microwave system, a 35% reduction in cycle time by preheating resin to approximately 46°C was demonstrated.

### **3.5.5 Resin Reactivity**

Increasing the resin reactivity produces shorter gel times at a given mould temperature, thus reducing cycle times. The penalty for using high reactivity resin is increased exotherm temperatures. Scott and Owen [52] suggested that high peak exotherm temperatures had an adverse affect on the surface finish of mouldings made from polyester resin. High resin reactivity increased the temperature gradients within the mould causing matrix cracking and promoted monomer boil at low internal mould pressures. They advocated using resin systems with mixed percentages of high and low reactivity catalysts to reduce the possibility of laminate degradation. The high reactivity catalyst would initiate gel, raising the

temperature and activating the low reactivity catalyst. The low concentration of high reactivity catalyst would be depleted rapidly, so that exotherm temperatures would not escalate.

This work was furthered by Blanchard [21] who developed a twin stream, phased catalyst injection (PCI) system. A medium reactivity resin system was stored in one pressure vessel, while a high reactivity system was contained in a second. The medium reactivity resin entered the mould first, before switching to the high reactivity resin at a predetermined time in the injection sequence. The high reactivity resin provided rapid, low temperature polymerisation, compensating for the heat lost at the injection gate through thermal quench. A 50% reduction in cycle time was demonstrated using this system. Jander [40] described a single stroke injection pump with three separate cylinders containing the resin, catalyst, and initiator. Delivery of the catalyst and initiator was based on a cam profile that allowed the concentrations of each to be phased during injection. He suggested that increasing the accelerator content during injection would reduce the cycle time, but provided no experimental evidence.

The introduction of fillers into the resin system further affects the cycle time. Calcium carbonate is a common filler used in the plastics industry principally as a low cost means of increasing the resin volume. Rudd et al. [53] showed that the addition of calcium carbonate increased resin viscosity and was expected to be the greatest factor in lengthening the impregnation time. The filler also modified the thermal properties of the resin system. The authors concluded that adding calcium carbonate in modest amounts (100 phr) reduced the exotherm temperatures by 26% without lengthening the cycle time.

### **3.6 The Effect of Process Variables on Resin Transfer Moulded Laminates**

The effect of high speed processing on the mechanical properties and surface finish of RTM laminates has been investigated by several authors. Void content, reinforcement properties, and resin formulations have been shown to affect the quality of the laminates.

### **3.6.1 Void Content**

Two mechanisms have been identified that promote void formation in composites [54]. Gas discharge into the resin due to the chemical reaction between the resin and catalyst is one cause of voids. Styrene boil at high mould temperatures, described by Scott and Owen (Section 3.5.5) is a common example. A second mechanism for void formation is the mechanical entrapment of air during mould filling. This situation occurs when the longitudinal resin flow front (macroflow) exceeds the lateral flow of resin into the fibre bundles (microflow). Macroflow is responsible for displacing the air within the reinforcement (wet-through), while microflow allows the resin to wet and bond with the individual fibres (wet-out). Peterson cited this effect when the fibre bundle size was increased (Section 3.5.3). Lundstrom and Gebart [54] stated that void content dropped significantly when a vacuum was drawn at injection, or pressure was applied during cure. These authors did not support their finding with mechanical property data. However, Hayward and Harris [55] determined that vacuum assisted injection increased the tensile strength of laminates, implying that reduced void content improved the mechanical properties of composites.

Patel et al. [56] showed that low injection pressures increased the tensile strength of unidirectionally reinforced polyurethane laminates. They attributed this result to improved microflow for better fibre wet-out during the longer impregnation phase. These researchers also recorded higher tensile strengths for high temperature mouldings as a result of enhanced wet-out due to lower viscosity, and greater chemical bonding between the fibre sizing and the resin. Lindsey [14] produced similar results with CFRM reinforced polyester laminates and reasoned that a higher mould temperature provided a greater degree of cure throughout the moulding.

### **3.6.2 Fibre Reinforcement**

Young and Tseng [48] related fibre configuration to the degree of fibre wetting. They concluded that large bundle sizes in bidirectional woven roving reinforcements created flow channels between the bundles. Low filling speeds were necessary to allow sufficient wet-out without rapid advancement of the flow

front down the channels. Fabrics with smaller fibre bundles could be filled faster with improved fibre wet-out. Revill [13] related wet-out time to the mechanical properties of CFRM reinforced laminates. He demonstrated an improvement in tensile modulus and strength of approximately 80% by extending the fibre wet-out time from 120 seconds to 24 hours. This work suggested that resins and reinforcement sizings currently used in RTM are not compatible with short cycle time production strategies. Lindsey [14] investigated the relationship between size formulation and the resin matrix. Mouldings produced with unsaturated polyester resin and CFRM reinforcement coated in an unsaturated polyester sizing agent, produced the highest strength laminates due to good bond formation at the interface.

### **3.6.3 Resin Formulation**

Lindsey [14] showed that increasing the catalyst concentration from 1% to 3% (by mass) in polyester resin not only reduced cycle times, but also improved the strength of CFRM reinforced laminates. Furthermore, the addition of calcium carbon filler to polyester resin was determined to affect laminate mechanical properties. Rudd et al. [53] showed that increasing the filler content up to 50 phr increased the laminate mechanical properties, with decreases in properties occurring at higher concentrations.

## **3.7 Microwave Processing of Polymers**

The time required to heat the stationary thermosetting resin at the injection gate to the activation temperature of the initiator dominates the cycle time [47]. Kendall [20] and Hill [22] have shown that this time can be reduced by microwave resin preheating, particularly in a continuous process.

Industrial acceptance of microwave processing over conventional heating methods is increasing since microwave heating features high power density applicators, improved thermal control, and reduced equipment size. Microwave processing is common in the rubber industry where extruded rubber is heated to the vulcanisation temperature in a microwave oven in a continuous process. The

food preparation industry has developed continuous microwave heating processes with the additional advantages of greater sanitation and pasteurisation capabilities [26]. Industrial microwave systems dedicated to FRP processing are less developed although research in the following areas has been reported.

### 3.7.1 Microwave Cure

An early application of microwave cure in the composites industry was presented by Strand [57] who showed a thirty-fold reduction in the cure time of an iron-oxide filled epoxy resin. Glass fibre reinforcement impregnated with the resin was placed in a microwave transparent mould. The mould was located in a multimode oven for curing. The dielectric loss factor of the epoxy mould was relatively low compared to uncured liquid epoxy resin so that it absorbed only a small amount of the microwave power. The uncured resin, however, readily absorbed the microwave power (Equation 2.3) and the cure time was reduced. Strand used the same technique to cure a polyester resin. A more recent application was described by Boey et al. [58] who modified an autoclave for microwave curing of glass reinforced epoxy components. Laminates were placed in a single-sided mould, vacuum bagged for consolidation, then placed in an autoclave that had been sealed to prevent microwave leakage. Microwaves were emitted from a horn directed towards the composite. A PC controlled stepper motor moved the horn along an X-Y plane over the surface of the component. Dosage levels were controlled by altering the microwave power or the traversing speed of the horn so that laminates of varying thickness could be cured more evenly.

Conductive fillers, such as carbon black and metallic flakes, have been added to resins with a low dielectric loss factor to make them more susceptible to microwave energy. Eddy currents develop on the surface of these inclusions and conduct heat into the resin matrix to initiate resin cure [59].

The addition of glass reinforcement into neat resin systems causes no microwave processing difficulties since most glasses are virtually transparent to microwave energy. However, use of carbon fibre reinforcement complicates microwave processing. Typically, the carbon fibres are longer than the microwave wavelength so that reflection occurs when the fibre are placed parallel to the

electric field, and absorption when the fibres are oriented perpendicularly. Lee and Springer [60] considered this to be a limitation for microwave processing of structural components since the carbon fibres would have a multidirectional orientation. Subsequently, Drzal et al. [61] determined that the heated carbon fibres initiated cure in the epoxy by thermal conduction, with the advantage of improved interfacial bonding.

The effects of microwave processing on laminate properties is disputed. Yue and Boey [62] measured a 50% increase in the tensile modulus of epoxy by microwave curing as opposed to conduction curing. Hawley et al. [63] claimed improved flexural properties for epoxy composites but did not quantify their results. Marand et al. [64] concluded that microwave processing led to a lower degree of cure and was expected to result in inferior mechanical properties. Lewis and Shaw [59] attempted to reconcile these contradictory findings by suggesting that the cure reaction rate is altered by microwave processing. Resins that contain a great number of microwave absorbing functional groups could produce a highly crosslinked laminate by microwave curing. These same reactive functional groups would not be affected by conventional conduction heating.

### **3.7.2 Microwave Preheating**

Thermoplastic materials that do not possess a dipolar structure normally can not absorb microwave power. However, thermoplastics such as polyethylene and polyphenylene sulfide, have been preheated by mixing a microwave absorbing additive (N-ethyl toluenesulfonamide) into the matrix. The additive promotes localised heating to allow processing of the thermoplastic without degrading its mechanical properties [65].

Costigan and Birley [66] batch preheated SMC in a multimode oven prior to compression moulding. The viscosity of the charge was reduced and flowed more readily, implying that a lower capacity press could be used. Furthermore, the temperature drop across the mould was reduced, lowering cycle times. The tensile strength of the laminate increased proportionally with the charge preheat temperature. The authors attributed this result to less fibre reorientation, more even cure, and reduced thermal stresses.

### 3.7.3 In-Line Microwave Processing

Cassagnau and Michel [67] used a single mode applicator ( $TE_{01n}$ ) to polymerise continuously blends of ethylene vinyl acetate (EVA) and ethylene methyl acrylate (EMA) in a microwave transparent polypropylene matrix. The mixed resin was fed through the microwave after extrusion. The authors claimed that the EVA/EMA crosslinked to a greater degree when the microwave residence time was increased. As a result, the morphology of the structure could be controlled to tailor the mechanical properties of the polypropylene.

Methven and Ghaffariyan [68] developed a  $TM_{010}$  mode cylindrical applicator to process glass FRP reinforcement bars for concrete by pultrusion. Heat was transferred efficiently to the resin so that the die length could be reduced with a corresponding decrease in frictional forces. As a result the glass fibre reinforcement could be pulled through the die more rapidly, and larger cross section parts could be produced, compared to the conventional system.

In-line preheating of thermally sensitive liquids is more complex. Under laminar flow conditions, maximum velocity is developed along the flow axis, decreasing to zero at the wall of the transporting pipe. Uniform heating across the pipe diameter would heat the boundary layers at the pipe wall excessively, with inadequate heating along the flow axis. Apart from the  $TM_{020}$  mode cylindrical applicator developed by Hill [22], no microwave preheating system for thermally sensitive resins has been discovered in the literature. Two systems for use in the food preparations industry are described below.

Risman [69] patented the design of a  $TM_{021}$  mode cylindrical applicator for continuous preheating of a thermally sensitive food. The product was pumped through a PTFE pipe, positioned concentrically within the applicator for maximum heating at the centre of the pipe, and minimum heating at the pipe wall. Using this applicator, the food could be heated without scorching the outer layer. The consolidated product was delivered horizontally through the applicator making this system unsuitable for processing liquid thermosetting resins. These materials must be processed vertically so that a parabolic flow profile is maintained with respect to the similarly shaped heating profile.

A sophisticated microwave system was developed by an EC cooperative group named Flair-Flow [70] for preheating thermally sensitive foods. The heater consisted of four identical cylindrical applicators, with the food being pumped vertically through an axially positioned tube. The applicator waveguide feeds were oriented at  $0^\circ$ ,  $90^\circ$ ,  $180^\circ$ , and  $270^\circ$  so that a superposition of the four modes produced a virtual  $TM_{020}$  mode heating profile. The authors claimed that a pipe diameter between 16 mm and 30 mm could be used to preheat thermally sensitive fluids without damage. The size and complexity of this system limits its use for preheating thermosetting resins. A large volume of resin would fill the four stage applicator during injection making precise temperature control difficult. Furthermore the system would need to be flushed after injection, producing waste and lengthening the overall cycle time.

#### **3.7.4 Alternative Methods for Polymer Processing**

Radio frequency (r.f.) heating, like microwave heating, relies upon dipole relaxation to generate heat in the product under an alternating electromagnetic field. Operating frequencies in the UK are restricted to  $13.56 \pm 0.07$  MHz and  $27.12 \pm 0.16$  MHz. The simplest r.f. heating systems consist of a product positioned between two flat metal plates across which an alternating electric field is established. Situating the product on a r.f. transparent conveyor belt enables continuous processing. The power from r.f. generators can be as high as 100 kW with an overall efficiency of approximately 50%. Magnetrons are limited to 15 kW (2.45 GHz) for single mode heating applications, although at higher microwave frequencies greater power can be dissipated into the product for a given electric field strength (Equation 2.3). As a result, a microwave plant can be approximately 1/30th the size of an r.f. plant operating at equivalent power levels. Furthermore, r. f. systems could not be used to heat thermally sensitive resins since the desired parabolic electric field profile could not be produced. A uniform heating profile would be established between parallel plates. Passing resin between the plates in a PTFE pipe would cause excessive heating at the pipe wall, promoting cure within the injection system.

Boey et al. [58] reviewed several other radiation heating techniques for processing polymers. Ultra-violet (UV) sources are limited by low penetration depth (approximately 0.4 mm for epoxies). However, stereolithography represents a recent application of UV cure, whereby thin layers of resin are cured consecutively to build-up a three dimensional model. X-ray systems would achieve greater penetration into the sample than UV radiation, although current systems are capable of delivering dosage rates between 500-5000 rad/hr. Efficient curing of composites would require dosages on the order of 2-19 Mrad/hr. Similarly low dosage rates are available from gamma ray generators with the additional concern of hazardous ionising radiation.

Singh et al. [71] described a 10 MeV electron beam accelerator for curing epoxy resins. The system was installed at Aerospatiale for curing filament wound rocket motor casings. Several advantages of the system were mentioned including, ambient temperature cure, reduced cycle times, and lower operating costs compared to thermal curing. Widespread industrial acceptance was hindered by the availability of electron curable resins, lack of a viable processing technique, and high initial costs.

### **3.8 Simulation Techniques for Microwave Applicator Design**

Accurate prediction of the heating profile within a loaded applicator is desirable to optimise the applicator geometry for efficient heating. Analytical solutions are possible for some single mode applicators with simple geometries. Hill [22] derived the conditional equation controlling resonance within an applicator containing three concentric dielectrics assuming excitation of the  $TM_{020}$  mode. Metaxas and Meredith [26] have provided solutions for other single mode applicators. However, determination of heating profiles within single mode applicators with complex shapes and multimode applicators requires numerical techniques. Simulations provide a computer aided engineering (CAE) approach to applicator development resulting in a more time and cost effective design process. Several techniques have been identified to simulate the microwave field structure within an applicator for subsequent characterisation of the heating profile.

Jia and Jolly [72] used the finite element method (FE) to model a loaded, multimode applicator. The model was validated by selecting a load that corresponded to a known analytical solution. Power and temperature profiles then were generated for various load configurations at a single frequency. A relatively coarse mesh (greater than 15 mm) was necessary to limit computing time and data storage.

Dibben and Metaxas [73] implemented a finite element time domain (FETD) technique to provide accurate simulations of a loaded, multimode applicator. The model was validated by comparing simulated thermal profiles to those measured using a thermal imaging camera. Results were available across a frequency spectrum and showed that the heating profile was sensitive to variations in the magnetron output frequency. This method, however, was not capable of modelling the effect of mode stirrers within the applicator, or a rotating product.

Iskander [74] summarised the finite difference time domain (FDTD) technique to model microwave structures within complex applicators. Like FETD, the method provided a solution over a frequency range. The author suggested that the simulation results could be adapted to a finite difference heat transfer routine to provide a clear understanding of the thermal distribution within the load during heating.

The transmission-line modelling (TLM) method is preferable to the FDTD technique in that fewer nodes can be used to model a structure without a loss of numerical accuracy at the boundaries [75]. Solutions can be obtained over a broad frequency bandwidth. TLM requires greater storage space to run simulations than FDTD since both the electric and magnetic field components are calculated. However, the simplicity of the calculations reduce overall run times.

Irrespective of the modelling technique, the numerical solutions are only as accurate as the data supplied. Therefore, it is imperative that reliable dielectric property data be used.

### **3.9 Dielectric Property Data for Thermosetting Resins**

Limited dielectric property data were found in the literature on thermosetting resins. Hill [22] measured the dielectric properties of four resin systems in catalysed and uncatalysed form: polyester (Cray Valley Total Chemie, Synolac 6345.001), low profile polyester (DSM, Synolite 40-7417), vinyl-ester (Dow, Derakane 8084), and methyl-methacrylate (ICI Chemicals, Modar). Measurements were made at room temperature over a 2-3 GHz frequency range. Hill showed that the addition of 1% catalyst to the base resins had a negligible effect on the dielectric properties, while adding 66 phr calcium carbonate to the low profile polyester produced a 26% increase in the dielectric constant. Large shifts in the dielectric constant alter the resonant frequency of a single mode applicator. As a result, heating efficiency can be reduced.

Several authors have derived dielectric property mixture equations so that measurements are not necessary to characterise the material due to alterations in the proportion of the constituent components. Nelson and You [76] provided a summary of the equations, and rated the accuracy of each with respect to two plastic materials: polyvinylidene fluoride (PVDF) and a styrene based thermoset. The dielectric properties for both materials were measured after being pulverised. Samples differed in the ratio of material to air content. Six mixture equations were evaluated as listed in Appendix 3.1. The Landau and Lifshitz, Looyenga equation were the most accurate with the Bottcher and refractive index mixture equations yielding similar values. The Bruggeman-Hanai, Rayleigh, and Lichtenecker mixture equations predicted the dielectric property values less accurately.

### **3.10 Conclusion**

Separation of the preforming and moulding stages enables production of oriented long fibre composites by RTM. The ability to fabricate niche market vehicles in a cost effective manner has made RTM desirable to automobile manufacturers. A major limitation to high volume RTM production is long cycle times. Several techniques to reduce the impregnation and cure phases that comprise the cycle time were found in the literature.

Variation of the injection gate location, and injection pressure are effective means of reducing the impregnation time. However, rapid injection of the resin does not reduce the cure phase which has the greatest influence on the cycle time. Furthermore, high speed injection can lead to high cavity pressures, fibre washing, and less control over the resin flow through the mould. Increasing the hydrostatic pressure in the mould was shown to increase the cavity pressures developed during resin exotherm. These high cavity pressures can cause damage to the mould and sacrifice component quality. No efforts to reduce these pressures were discovered in the literature.

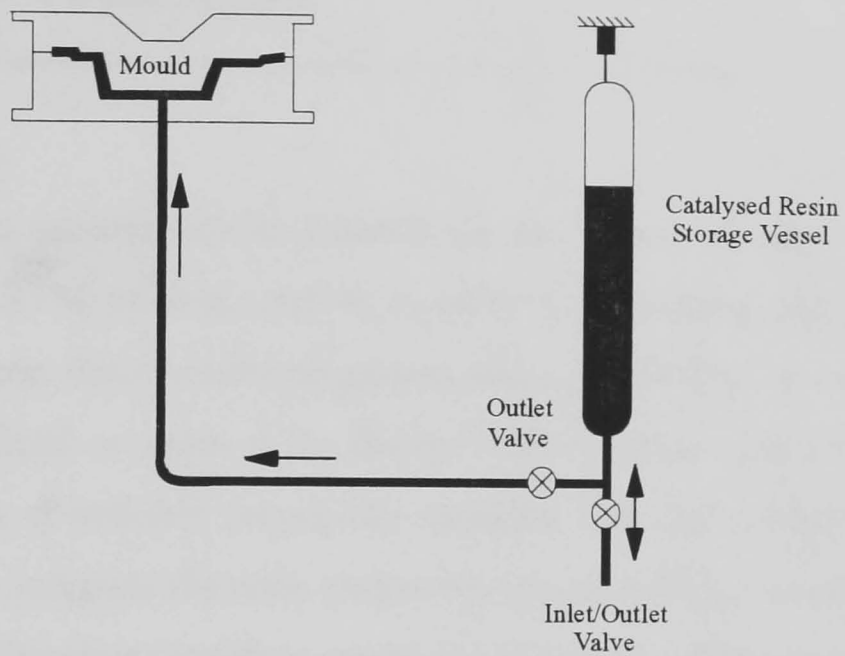
Thermal management strategies have been used to shorten the cure phase, and emphasized the need to reduce mould quench. Preform and batch resin preheating have been employed successfully, although the overall cycle time may increase when the preheating time is considered. Elevated mould temperatures and high reactivity resin systems increase peak exotherm temperatures and can cause monomer boil that degrades laminate quality. Zone heating provides location specific temperature control to compensate for quench at the injection gate. Temperature control is greatest using in-line microwave resin preheating making rapid temperature variations during impregnation possible. Investigations into resin temperature profiling for manipulation of the cure sequence was not discovered in the literature review.

Microwave radiation for processing thermosetting resins continues to develop. Most applications have focused on microwave curing to reduce cycle times. Microwave absorbing additives that allow faster processing of low loss factor resins could alleviate the need for higher powered microwave generators. Continuous microwave processing of thermally sensitive materials has been demonstrated in the food preparation industry using a  $TM_{0,21}$  mode cylindrical applicator. A similar applicator configuration was used by Hill to preheat a thermosetting resin in-line, however, no other research was discovered on the topic.

Microwave field simulation techniques can provide three dimensional renderings of the power and heating profiles within single mode and multimode applicators. The modelling techniques that calculate applicator response

characteristics over a range of frequencies enable variations in the applicator geometry, dielectric properties, and variations in the magnetron output frequency to be assessed at the design stage. These modelling methods are expected to reduce the development time and costs for microwave heating systems.

### Single Stream Injection System



### Twin Stream Injection System

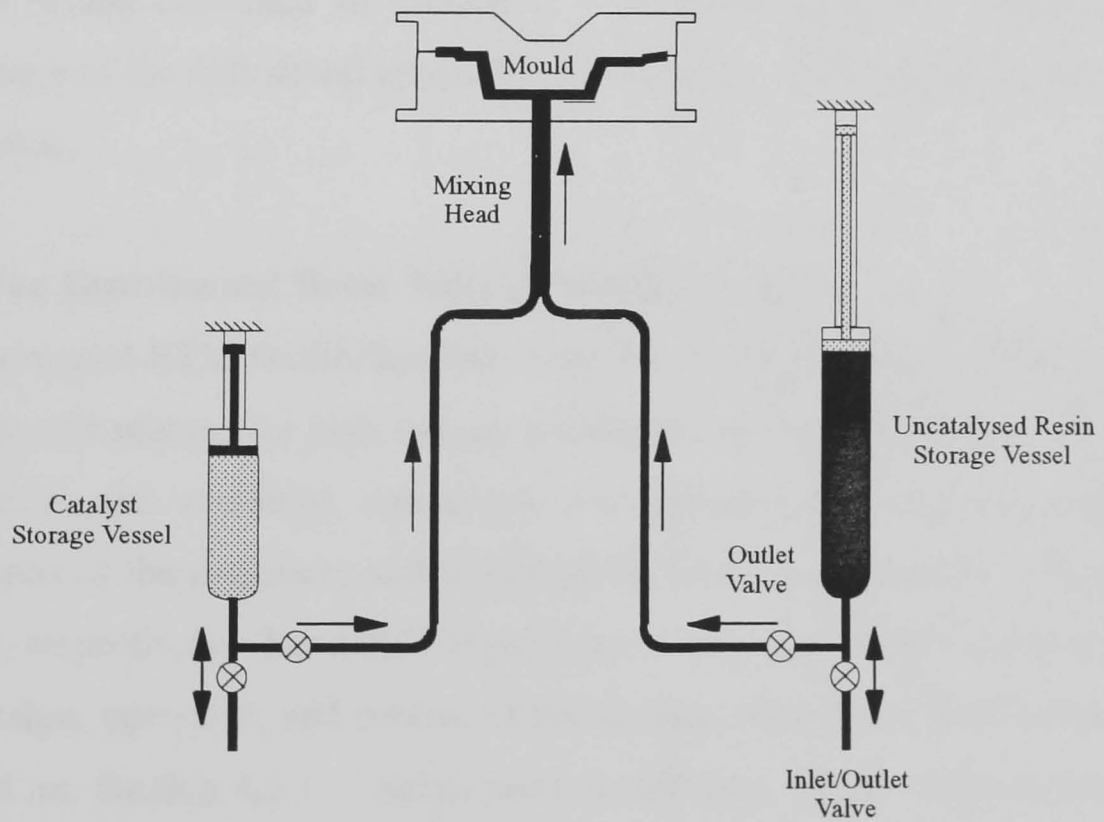


Figure 3.1 Schematic showing typical injection systems used in liquid composite moulding processes

# Experimental Techniques

---

### 4.1 Introduction

The purpose of this research was to characterise the effects of microwave resin preheating on the RTM process, and to quantify the resulting changes in the laminate. This chapter describes the equipment and methods used to complete the study. RTM is defined in terms of the thermal and pressure cycles to delineate between the effects of ordinary processing variables and resin preheating. The hardware utilised to integrate the resin preheating system into the automatic RTM cycle is described. Standard moulding conditions are listed and the results of these moulding experiments will be presented in Chapter 6. Resin preheating was expected to influence mechanical properties of the laminate. Tensile testing and degree of cure measurements were used to gain an understanding of these effects with the results contained in Chapter 7. The methods used to establish the performance of the cylindrical applicator and the magnetron are also presented in this chapter.

### 4.2 The Experimental Resin Transfer Moulding Facility

An experimental RTM facility has been installed at the University of Nottingham to evaluate the process for high volume production of FRP components. Preform manufacture and moulding operations are carried out within the facility. Photographs of the preformer and moulding hardware are shown in Figures 4.1a and 4.1b, respectively. Kendall [20] provides a more comprehensive description of the design, operation, and control of the facility, although a brief summary is presented in Section 4.2.1. Subsequent installation of the microwave resin preheating system is described in Section 4.2.2. Details of the original microwave hardware and control software are given by Hill [22]. A schematic plan of the experimental RTM facility is shown in Figure 4.2.

### 4.2.1 RTM Equipment

Lightweight shell tooling was used to make prototype engine undershield components within the RTM facility. The undershield mould, pictured in Figure 4.3, was made from electroformed nickel on a copper substrate each layer being 3 mm thick. Copper tubing was bonded to the back face of the shell moulds with an aluminium filled epoxy resin. Oil was passed through the tubing after being circulated through a 48 kW heater incorporating a 15 kW chiller unit to maintain a prescribed mould temperature.

The upper and lower shell moulds were attached to a cast aluminium support frame. Loads were transferred through the support frames to stiffeners that formed the mould manipulator. Synchronised jacks at each corner of the manipulator lowered the upper tool evenly onto the stationary bottom half. Ten peripheral clamps held the mould closed.

A constant pressure, single stream resin injection system was used. Catalysed resin was held in a 30 litre storage vessel pressurised by a laboratory air supply up to a maximum of 7 bar. The resin storage vessel was suspended from a load cell to monitor the resin quantity and flow rate during injection. A flexible injection line ran from the supply vessel, through the microwave applicator, and into the lower mould via a centrally located pin gate. Quick release connectors on the injection line allowed the microwave applicator to be bypassed when not in use. Two vents were located on either side of lower mould half. The mould was sealed with a closed cell silicone foam strip around the mould periphery. The injection gate and vent valves were isolated thermally from the hot mould. These thermal break valves (TBV) prevented catalysed resin from curing prematurely inside the valve body. A solvent system pressurised to 4 bar allowed the injection system to be flushed.

Instrumentation points on the undershield mould are shown in Figure 4.4. Nine K-type thermocouples in the upper mould half protruded into the mid-plane of the mould cavity (3 mm). A PTFE sleeve insulated these thermocouples from the heated mould. Pressure transducers were located opposite the thermocouples in the lower mould half and followed the same numbering scheme. The transducers were recess mounted to eliminate the effect of reinforcement

compaction pressure. A pressure history at the injection gate could be produced by removing the injection gate thermocouple (upper mould half) and replacing it with pressure transducer 7 from the lower mould half.

A data acquisition system (Burr-Brown PCI-20000) was installed within an Akhter 386, 25 MHz personal computer (PC). Thermocouples (14 maximum) and pressure transducers (16 maximum) were wired to external analog termination panels. Digital inputs and outputs (16 of each) were accessed via a Mitsubishi F2-40M/F2-40E programmable logic controller (PLC). The RTM process, including microwave preheating, was controlled automatically from the PC through a PLC interface.

#### **4.2.2 Microwave Preheating Equipment**

Resin was preheated in a cylindrical applicator attached to the magnetron by metallic waveguide (WG9A), a stub tuner, and circulator. The system layout for moulding experiments is shown in Figure 4.5. A circulator connected to a water load, diverted reflected power into a stream of water, isolating the magnetron from damage. The water load supply was then passed through a chiller unit to prevent overheating. A coupling probe was inserted into the circulator to measure reflected power, and was monitored during on-line tuning of the applicator. The Philips YJ1600 continuous wave magnetron generated microwaves over a 0.5-5 kW power range at a nominal output frequency of  $2.46 \pm 0.01$  GHz [77]. Distilled water to cool the magnetron was stored in a tank and circulated by an electric pump. Water from the chiller unit cooled the distilled water by passing through a copper coil in the tank *en route* to the water load. The magnetron, waveguide and applicator were fixed to a rigid chassis and suspended beneath the lower mould stiffener. The distance between the microwave applicator outlet and the injection gate (380 mm) was minimised to avoid significant heat loss to the resin through that section of the pipe.

The microwave preheating system could be operated either in manual or automatic mode by turning a key on the control unit. Applicator heating efficiency trials were conducted under manual control. The operator switched the microwave on and off at the control panel, while the power level was adjusted via

a potentiometer. Undershield mouldings were produced under automatic control. A digital to analog convertor (DAC) card was installed in the PC to switch the system on or off via the PLC, and to adjust the magnetron power output.

Instrumentation for automatic microwave control included four K-type thermocouples positioned at the inlet and outlet points of the applicator and the water load. A fifth thermocouple monitored the magnetron cooling water temperature. Three capacitive proximity sensors were used to track the resin flow path. One sensor was positioned at the injection gate, and the two remaining sensors were situated at the mould vents. The proximity sensors were wired to the PLC which activated digital inputs on the PC upon resin detection. Resin arrival at the injection proximity sensor, downstream of the cylindrical applicator, was necessary for the microwave to turn on.

Figure 4.6 shows the system layout for the applicator heating efficiency trials. Resin flowed into an open container resting on an electronic balance (Oertling UD31) instead of into the mould. Output from the balance was directed to the computer so that the resin mass flow rate, and consequently, the efficiency could be calculated during a trial. The PLC was not necessary since on/off switching and power adjustments were controlled by the operator, although data acquisition was still required.

A series of safety features were incorporated into the microwave preheating system. Hard wired electrical interlocks at the mains, control unit, and magnetron reduced the risk of electrical shock. Local fans within the control unit and magnetron created positive pressure ventilation whereby clean air was blown over the electric terminals preventing the build up, and potential ignition, of volatiles. Flow sensors within the magnetron cooling circuit and water load prevented the system from operating at insufficient flow rates. The emergency stop button on the control panel shut down the complete microwave system under both manual and automatic control.

### **4.2.3 The Automatic Moulding Cycle**

The automatic moulding cycle was controlled by the interfaced PC and PLC system. A preform was loaded manually into the mould and resin pre-mixed with

catalyst was drawn into the storage vessel. The sequence was initiated from the PC causing the mould to lower and remain closed by the action of ten peripheral clamps. The storage vessel was pressurised and injection began by opening the resin outlet valve, in addition to the injection valve and vent thermal break valves. Resin arrival at the injection proximity sensor signalled the microwave to be turned on. Microwave preheating continued until the injection thermal break valve closed, signalling the microwave to be switched off. Immediate flushing of the injection line, and valves with solvent prevented preheated resin from curing in the injection system. Modifications to the automatic moulding cycle could be made to reduce the frequency and extent of solvent flushing for industrial applications so that wastage would be limited. Thermal and pressure histories were displayed on the PC monitor throughout the moulding cycle. The mould opened after the resin had cured, completing the automatic cycle. A description of the PLC control sequence and cure sensing algorithm has been given by Blanchard [21].

### **4.3 The Thermal Cycle During RTM**

The moulding cycle can be described in terms of a thermal history as shown in Figure 4.7. Thermocouple locations correspond to a diagonal across the undershield mould (Figure 4.4). Several principal events in the moulding cycle are defined below [41].

#### **Impregnation Time**

The start of impregnation is distinguished by a drop in the laminate temperature at the injection gate (position 5) as cold resin enters the hot mould. A temperature reduction is exhibited at successive thermocouples, although less severely, since the resin is heated as it passes through the hot mould. Impregnation ends when the injection valve closes, indicated by a rise in resin temperature.

#### **Fibre Wet-Out Time**

The time available for fibre wet-out and interfacial bond formation is dictated by the resin at the mould periphery (position 2). Cure occurs first at that position since the resin has been exposed to elevated temperature for the longest period of

time. Fibre wet-out begins at the mould periphery when resin arrives at that location, signified by the end of impregnation. The end of fibre wet-out is marked by resin gel. It is convenient to define the end of fibre wet-out as the time when the resin temperature has raised to 5°C above the nominal mould temperature (65°C).

### **Cycle Time**

The cycle time begins at impregnation and ends with the completion of the exothermic cure reaction. The last exotherm occurs at the injection gate (position 5) where the resin has had the shortest residence time within the mould. Resin at the injection gate must heat up to mould temperature, and the mould must recover heat transferred to the passing resin during impregnation before the process is completed.

### **Thermal Quench**

Thermal quench is a general term used to describe a rapid temperature drop at either the mould surface or within the laminate. Cold resin contacting the hot mould surface causes a sharp temperature drop at that location. The effect is most pronounced at the injection gate. A low thermal mass makes shell moulds particularly susceptible to mould quench. Thermocouples in the undershield mould protruded 3 mm into the reinforcement so that laminate quench, rather than mould quench, was measured.

## **4.4 The Pressure Cycle During RTM**

Figures 4.8a and 4.8b show a characteristic pressure cycle that occurs in RTM analogous to the thermal history. A typical pressure history is described below with transducer locations corresponding to the undershield mould diagonal shown in Figure 4.4.

### **Impregnation Time**

Cold resin contacting the warm pressure transducer diaphragm at the injection gate (position 5) causes a thermal quench, producing a negative pressure readings that

signifies the start of impregnation. Pressure rises at the injection gate during impregnation as back pressure develops in the mould. Transducers further along the mould diagonal (positions 4, 3, and 2, respectively) also experience a rise in pressure as the resin front progresses. A subsequent pressure drop at the injection gate signifies the end of impregnation and the beginning of the hydrostatic phase.

### **Hydrostatic Phase**

The pressure across the mould reaches equilibrium after the mould is sealed by closure of the injection valve and vents. This would be exhibited by a levelling in the pressures across the mould to a unique value. However, Figure 4.8b demonstrates that transducer inaccuracies, and the onset of cure prevents the establishment of a single pressure.

### **Cure Phase**

As the resin begins to cure, shrinkage occurs and the pressure drops. Thermal expansion during the exothermic reaction leads to a pressure increase. This sequence is evident at the mould periphery (position 2). Closer to the mould centre (position 3), the pressure increases after the hydrostatic phase before resin shrinkage and the subsequent exothermic pressure rise. The increase in pressure before shrinkage occurs to a greater degree at positions 4 and 5 near the injection gate. This rise in pressure, termed the pre-exotherm pressure [20], is attributed to the thermal expansion of the liquid resin at positions adjacent to the injection gate. Resin at the mould periphery cures first creating a rigid mould seal. The cure front advances towards the centre of the mould and expands during the exothermic reaction. This pressure increase is transmitted through the liquid resin to transducers ahead of the cure front. The pressure becomes more extreme as the cure front advances towards the centre of the mould since the volume available for the resin expansion is reduced. The intensity of the pre-exotherm pressure near the injection gate overshadows the exothermic pressure rise making it imperceptible at positions 4 and 5. It is because of this effect that the local pre-exotherm pressures on the mould are critical design loads, rather than the hydrostatic pressure which is significantly lower.

## 4.5 Standard Moulding Conditions

Standard moulding conditions are listed in Table 4.1 with a schematic of the experimental set up shown in Figure 4.5. Moulding parameters were dictated by the choice of two resin injection techniques. Trials with resin injected at a constant preheated temperature were conducted with the mould heated to either 60°C or 90°C. The second technique involved ramping the resin temperature during injection, with the mould heated to 40°C.

### Resin Systems

A different resin system was used at each of the three moulding temperatures (40°C, 60°C, and 90°C). Cray Valley Total Chemie Synolac 6345.001, an orthophthalic, unsaturated polyester resin, was combined with the following catalysts:

- i. Perkadox 16, bis (t-butyl peroxy dicarbonate), from Akzo Nobel Chemicals Ltd.
- ii. TBPEH, t-butyl peroxy 2-ethyl hexanoate, from Interlox Chemicals Ltd.
- iii. Trigonox 44B, acetyl acetone peroxide, from Akzo Nobel Chemicals Ltd.

An accelerator, tradename NL49P (1% by mass cobalt carboxylate content in a phthalate plasticizer), by Downland Chemicals, was used to reduce the activation temperature of the resin so that mouldings could be produced at 40°C. The initiation time for each resin system at several temperatures is shown in Figure 4.9 where the initiation time was defined as the period required to raise a 10 g sample of catalysed resin to 5°C above the oil bath temperature.

### Standard Reinforcement

Continuous filament random mat (CFRM), Vetrotex (UK) Ltd. U750-450 and U754-450 was the standard reinforcement. Composition of the thermoplastic binder on the glass fibre varied between mats types, although the superficial density (450 g/m<sup>2</sup>) remained constant. Preform thickness was 8 mm in the swage areas, and 6 mm elsewhere for an average glass volume fraction of 15%.

## **Miscellaneous Materials**

Vinyl-ester resin (Dow Chemical, Derakane 8084) catalysed with Perkadox 16 (2% by mass) was used during the development of the PID power controller for the microwave resin preheating system (Chapter 5). Aside from demonstrating that this resin system could be preheated as easily as polyester resin, no significance was attached to its use in this thesis. A sophisticated reinforcement, termed the Motorsport lay-up, was employed in conjunction with the vinyl-ester resin system. The components of this reinforcement are listed in Appendix 4.1.

### **4.6 Material Property Testing**

An investigation into the influence of microwave resin preheating on laminate properties was carried out. Mechanical testing provided an overall assessment of material properties effects. A degree of cure measurement was employed as a higher resolution technique to form a clearer understanding of the relationship between resin preheating and material characteristics.

#### **4.6.1 Mechanical Testing**

The tensile modulus (E) and ultimate tensile strength (UTS) of five undershield components were measured. The mouldings were made at 60°C under standard conditions (Table 4.1) with a glass fibre volume fraction of 16%. Seven specimens were cut from each undershield (250 mm × 25 mm × 6 mm) along the weft direction of the glass mat as shown in Figure 4.10. The random reinforced laminates were tested to BS 2782:Part 10:Method 1003 on an Instron Universal Mechanical Tester Model 1195 having a 100 kN load cell. Longitudinal displacements were recorded by an extensometer at a crosshead speed of 5 mm/min.

#### **4.6.2 Degree of Cure Testing**

A polyester resin consists of an unsaturated resin molecule dissolved in a styrene monomer to form a homogeneous solution. Curing involves copolymerisation of the styrene and unsaturated resin. In principle, copolymerisation will cease automatically when all the styrene has reacted [78]. Based upon the homogeneous

nature of the resin, it is convenient to define the fully cured state as having 0% residual styrene and the uncured state as having 100% residual styrene. The amount of residual styrene in the polyester resin can be measured by gas chromatography.

Residual styrene content measurements were made on two undershields produced under standard conditions for a 60°C mould with resin injected at 20°C and 50°C (Table 4.1). Glass fibre blanks were removed from the preform at eight locations along the mould diagonal before injection to form pure resin samples at those locations as shown in Figure 4.11. Resin disks (19 mm diameter) were cut from the undershield directly after demoulding. The samples were prepared individually by weighing, then dissolving in a solution of chloroform, n-butylbenzene, and a trace of 4-methoxyphenol for approximately three days. The n-butylbenzene was used as an internal calibration standard while the 4-methoxyphenol was necessary to inhibit further styrene reaction when the sample had dissolved. The liquid resin specimens were filtered into volumetric flasks, topped up with a chloroform and n-butylbenzene standard solution, then decanted into vials for testing.

A Perkin-Elmer 8500 Gas Chromatograph was used to measure residual styrene content. The measurement technique was a modified version of BS 2782:Part 4:Method 453A. The liquid sample was drawn from the vial into a 1  $\mu$ l syringe and injected into the instrument. The sample was vaporised and carried through a heated, capillary column by an inert carrier gas (helium). Molecular size determined the retention time of the components in the column. A flame detector at the end of the column ionised the components producing a current. The magnitude of the current was correlated to the percentage of the component in the sample. The column was heated over a linear ramp between 60°C and 90°C to consolidate the elution times. Chloroform, styrene, and n-butylbenzene had approximate elution times of 0.33 minutes, 2.60 minutes, and 6.20 minutes respectively. A practical explanation of gas chromatography principles is given by Schupp [79].

Five calibration samples were prepared using a set amount of n-butylbenzene and known amounts of pure styrene. The relative amount of styrene

in each calibration sample was determined using gas chromatography and then plotted. The free styrene content in the resin samples (Figure 4.11) were then related the calibration plot and expressed as a percentage of the original styrene content (100%).

#### **4.7 Tuning Methods for the Cylindrical Applicator**

Tuning of the cylindrical applicator was carried out in two phases. Primary tuning was performed on a network analyser, then fine tuning was undertaken on-line to maximise applicator efficiency.

##### **4.7.1 Primary Tuning of the Applicator**

An iterative approach to coupling and tuning resonant applicators was mentioned in Section 2.8, with a schematic of the experimental set up shown in Figure 2.9. A response trace for the cylindrical applicator was produced using a Hewlett Packard 8753C Network Analyser and 85047-A S-Parameter Test Set. Polyester resin (Synolac 6345) was sealed in the applicator then this unit was attached to a stub tuner and waveguide transition piece. A coaxial transmission-line joined the waveguide transition piece to the network analyser. The network analyser was calibrated over two frequency ranges. A wide bandwidth (1.96 GHz to 2.96 GHz) revealed modes in close proximity to the  $TM_{020}$  mode, while a narrow frequency band (2.45 GHz to 2.47 GHz) enabled applicator tuning within the operating frequency range of the magnetron ( $2.46 \pm 0.01$  GHz).

Broad band tuning was achieved by adjusting the screw stubs on the tuner so that the applicator resonated near 2.46 GHz. Aperture width was crucial to microwave power coupling, and this dimension was altered to minimise the VSWR. A VSWR of less than 1.92 was desirable for a coupling efficiency greater than 90% [26]. The narrow frequency band was selected for precise tuning and coupling at 2.46 GHz.

### **4.7.2 Fine Tuning of the Applicator**

The applicator and stub tuner were attached to the remainder of the system for on-line tuning as shown in Figure 4.6. Uncatalysed polyester resin (Synolac 6345) was passed through the applicator then into an open container resting on a balance. Microwave power was fixed at 500 W and switched on. The system was checked for microwave leakage using a Simpson 380M hand held detector. Operation of the microwave resin preheating system was halted if the emissions were above  $0.5 \text{ mW/mm}^2$  at 50 mm. Applicator heating efficiency was computed in real time and displayed on the monitor. Reflected power was measured via a probe in the waveguide section of the water load. This signal was converted to a DC voltage by connecting a diode in series. The tuning stubs were adjusted to minimise the reflected voltage so that the applicator heating efficiency was maximised. Full power (5000 W) efficiency measurements were made after the tuning stub locking nuts had been secured to prevent microwave leakage. The VSWR response trace for this system is shown in Figures 4.12a and 4.12b. The flatness of the VSWR response trace over the magnetron operating frequency range (2.45-2.47 GHz) suggested that a shift in the resonant frequency within this bandwidth would not reduce the heating efficiency below 96% (Figure 4.12b). Variations in the resonant frequency could occur due to changes in dielectric properties of the load and a power related drift in the magnetron output frequency.

### **4.7.3 Mode Pattern Identification within the Applicator**

The network analyser provided no information on the mode shape associated with the VSWR response trace, and hence the heating profile within the applicator. This temperature profile was measured for a stationary volume of resin within the PTFE pipe by inserting a circular array of sixty-nine thermocouples. A data logger was used to scan the thermocouples every 1.5 seconds and save the data to file. The amount of power and heating duration were specified before the experiment commenced. A temperature rise in the resin was determined by measuring the resin temperature before and after heating. A strip of Unifilo U750-450 was placed inside the resin to reduce vertical convection currents in the heated resin. Figure 4.13 shows a thermal plot of the temperature rise across the

diameter of the PTFE pipe generated by a linear interpolation between the thermocouple positions. Maximum heating occurred at the centre of the PTFE pipe, with three additional high temperature regions near the periphery of the pipe. Hill provides a complete description of the hardware, control software, and experimental technique [22].

#### **4.8 Transmission-Line Modelling of the Cylindrical Applicator**

Transmission-line modelling (TLM) is a numerical technique used to simulate electromagnetic wave propagation in a three dimensional space. Position is defined in the space by nodes connected with transmission-lines. An electromagnetic pulse travels along the transmission-line to a node where it is scattered to the other transmission-lines associated with that node. The scattered pulses travel to adjacent nodes where the process is repeated. Electromagnetic wave propagation, and mode shapes are simulated across a mesh of nodes in this way. The nodes can be arranged to represent a complex applicator geometry with each node having metallic or dielectric properties associated with it. TLM is a time domain method, so that a broadband frequency response can be obtained from a single pulse excitation.

The transmission-line modelling method was used to simulate the cylindrical applicator. The modelling work was carried out by the Department of Electrical and Electronic Engineering at the University of Nottingham. The objective of this simulation was to provide a response trace for the applicator over the 1.96-2.96 GHz frequency range. Post-processing routines were used to develop the mode shapes at the resonant peaks within that frequency range.

#### **4.9 Magnetron Characterisation Trials**

Experiments were carried out to determine the shift in magnetron output frequency over the 0.5-5 kW power range. A quantitative reduction in applicator efficiency was measured based on the magnetron frequency shift. A layout of the system is shown in Figure 4.14.

#### **4.9.1 Magnetron Calibration**

The magnetron was calibrated using a Hewlett Packard 8592A Portable Microwave Spectrum Analyser. A 50 dB directional coupler was positioned between the magnetron and the circulator with a fixed, high power load attached to one end and a waveguide to coaxial transition section at the other. The spectrum analyser was connected to the transition piece by a coaxial transmission-line. Locating the coupler between the magnetron and circulator ensured that the response trace on the spectrum analyser comprised only a forward travelling wave since the reflected power from the applicator was diverted to the water load. The 50 dB coupler reduced the maximum microwave power (5000 W) to 0.05 W so that in-line measurements could be made without damaging the spectrum analyser. The coupler was loaned by the Department of Engineering at the University of Cambridge and the spectrum analyser was supplied by Unilever Research.

Polyester resin (Synolac 6345) was passed through the cylindrical applicator at minimum power (500 W) and the resonant peak was recorded from the spectrum analyser. The procedure was repeated at 1000 W, then at 1000 W intervals up to full power (5000 W). The resonant frequency was plotted against microwave power to generate a calibration curve.

#### **4.9.2 Applicator Heating Efficiency Measurements with Regard to Variations in the Magnetron Output Frequency**

The cylindrical applicator was configured as a high Q system, characterised by a sharp response peak, to emphasise the effect of frequency drift on the applicator efficiency. Decreasing the axial length of the applicator was shown to increase the quality factor. The system was fine tuned for an applicator efficiency of 95% at 500 W as described in Section 4.7.2.

Efficiency measurements were based on heating resin to a prescribed temperature to maintain constant dielectric properties in the load. Initially, the resin flow rate was set to preheat the polyester resin (Synolac 6345) to 43°C using 1000 W of power. The applicator heating efficiency was recorded in addition to the magnetron output frequency. The resin flow rate was adjusted subsequently to heat the resin to 44°C using 3000 W of power. Again, the efficiency and

microwave frequency were monitored. Changes in the applicator heating efficiency then could be attributed directly to a shift in resonant frequency.

#### **4.10 Determination of Applicator Sensitivity**

The sensitivity of the cylindrical applicator was characterised with regard to efficiency measurements for a filled, low profile resin system. Calcium carbonate ( $\text{CaCO}_3$ ) filler was added to the polyester resin (Synolac 6345) in concentrations of 25 phr, 50 phr, and 100 phr. Efficiency measurements were made at each increment according to the technique described in Section 4.9.2. The series of experiments was repeated after a low profiling agent (Synolite 1080-M-1 provided by DSM Resins UK Ltd.) had been added to the resin system.

#### **4.11 Dielectric Property Measurements**

The dielectric properties of Synolac 6345 loaded with calcium carbonate filler (0 phr, 50 phr, and 100 phr) were measured by the cavity perturbation technique. Measurements were made at ambient temperature, 50°C, and 70°C representing a typical resin preheating range. A  $\text{TM}_{030}$  mode cylindrical applicator resonating at 2.13 GHz was positioned directly below a temperature controlled oven. The applicator was excited via a coupling probe that was connected to a Hewlett Packard 8753C Network Analyser and 85047-A S-Parameter Test Set with a coaxial transmission-line. Resin samples were heated in a quartz tube (5 mm bore) sealed at each end. The sample was moved automatically from the oven to the applicator by a PC based control system. Testing equipment was provided by the Department of Electrical and Electronic Engineering at the University of Nottingham.

The resonance and quality factor were measured for the empty applicator, then again when the applicator was loaded with an empty quartz tube. Applicator resonance and the quality factor were affected by the insertion of the resin sample at ambient temperature. The sample was moved into the 50°C oven and heated for 10 minutes before performing a second measurement. Testing concluded after a similar measurement was made at 70°C. The method used to calculate the dielectric constant and loss factor is presented in Appendix 4.2.

#### **4.12 Conclusion**

The microwave resin preheating system was integrated into the automatic RTM cycle. Automation lends itself to consistent, and repeatable results so that accurate conclusions regarding the contribution of microwave resin preheating to RTM can be drawn. Experimental mouldings were produced using either constant resin temperature injection or ramped resin temperature injection. The results of this study concerning the RTM process is the subject of Chapter 6. Methods to evaluate the quality and the mechanical properties of the laminates produced in the moulding experiments have been described. The outcome of these tests are presented in Chapter 7. Several techniques to improve the performance of the microwave resin preheating system have been described. These include methods to measure the temperature distribution within the applicator, and a computational technique to simulate the heating profile within the applicator. Performance improvements to the microwave resin preheating system are discussed in Chapter 9.

## List of Tables

Table 4.1 Standard conditions for moulding trials

## List of Figures

Figure 4.1a Preformer

Figure 4.1b Mould manipulator

Figure 4.2 Schematic of the experimental RTM facility

Figure 4.3 Undershield mould

Figure 4.4 Instrumentation positions on the undershield mould

Figure 4.5 Layout of the microwave resin preheating system for moulding experiments

Figure 4.6 Layout of the microwave resin preheating system for applicator heating efficiency trials

Figure 4.7 Thermal history of the moulding cycle showing principal events

Figure 4.8a Pressure history of the full moulding cycle

Figure 4.8b Pressure history during the first 600 seconds of the moulding cycle showing principal events

Figure 4.9 Initiation time versus temperature for the experimental resin systems

Figure 4.10 Orientation of tensile test specimens on the undershield component

Figure 4.11 Location of disk specimens on the undershield component for the degree of cure investigation

Figure 4.12a Broad band VSWR response trace for the tuned cylindrical applicator

Figure 4.12b Narrow band VSWR response trace for the tuned cylindrical applicator

Figure 4.13 Typical temperature distribution within the PTFE pipe of the cylindrical applicator

Figure 4.14 Layout of the microwave resin preheating system for magnetron calibration

**Table 4.1 Standard Conditions for Moulding Trials**

<b>INJECTION TYPE</b>	<b>CONSTANT TEMPERATURE</b>	<b>CONSTANT TEMPERATURE</b>	<b>ISOTHERMAL AND RAMPED TEMPERATURE</b>
<b>MOULD TEMPERATURE (°C)</b>	60	90	40
<b>INJECTION PRESSURE (bar)</b>	2	2	2
<b>RESIN FORMULATION NUMBER</b>	II	III	I
<b>RESIN</b>	Synolac 6345	Synolac 6345	Synolac 6345
<b>CATALYST</b>	Perkadox 16 2% by mass	TBPEH 1% by mass	Trigonox 44B 2% by mass
<b>ACCELERATOR</b>	None	None	NL49P 0.5% by mass
<b>REINFORCEMENT</b>	Unifilo U750-450	Unifilo U754-450	Unifilo U750-450

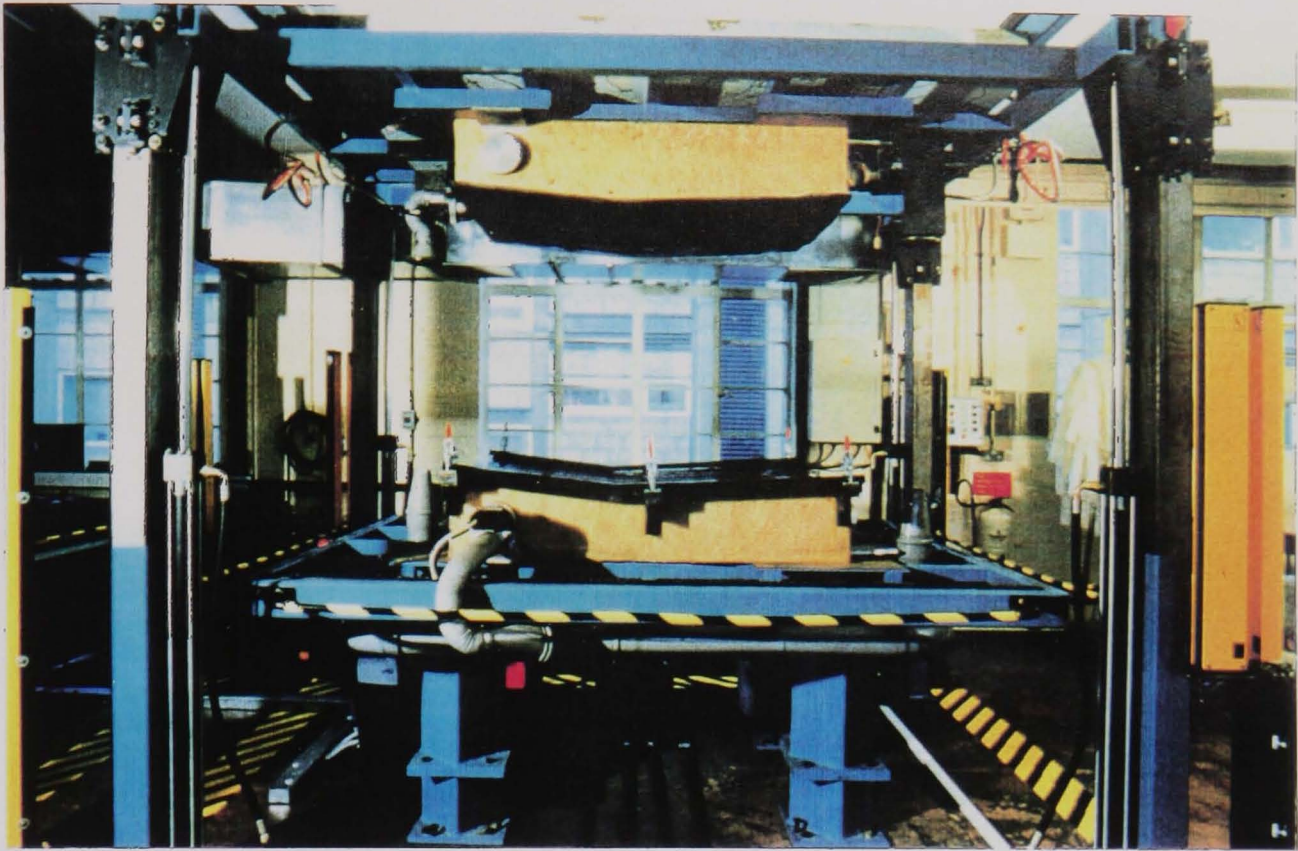


Figure 4.1a      Preformer

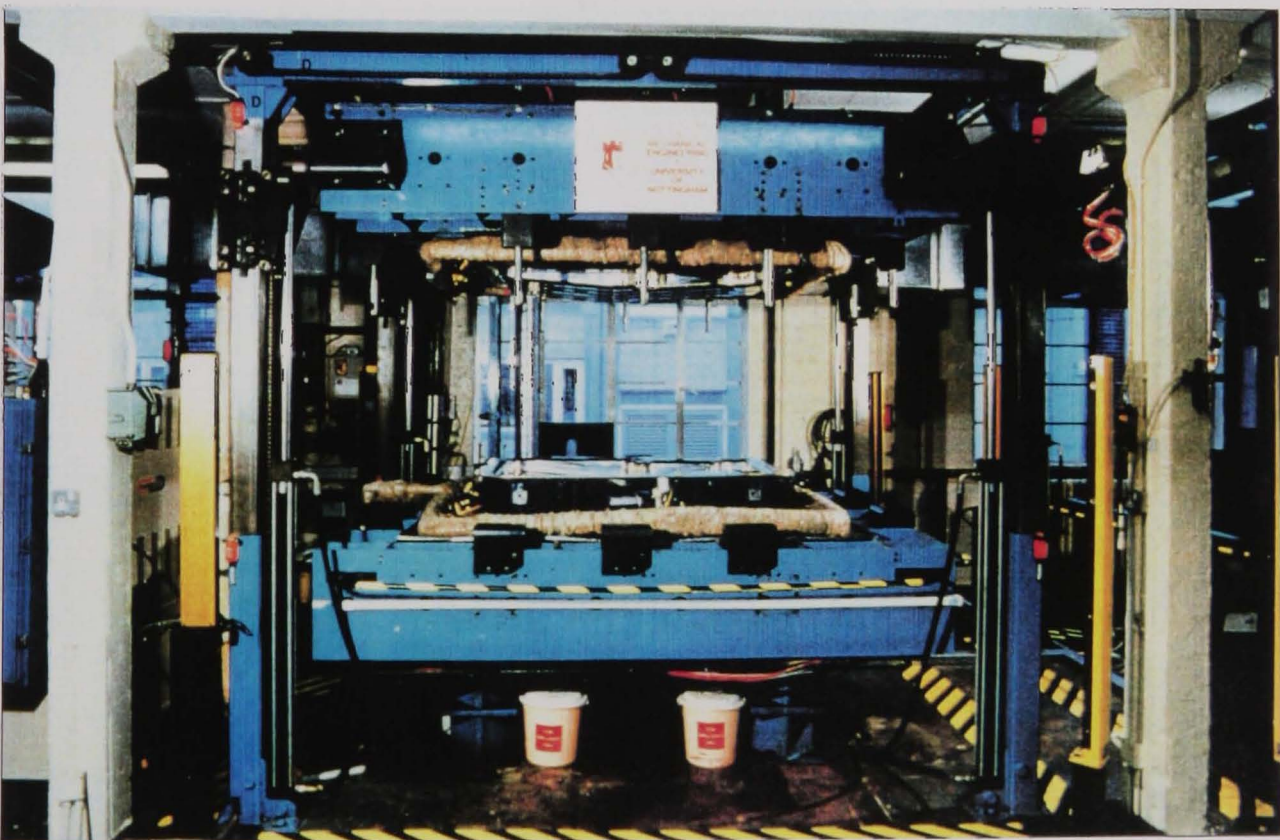
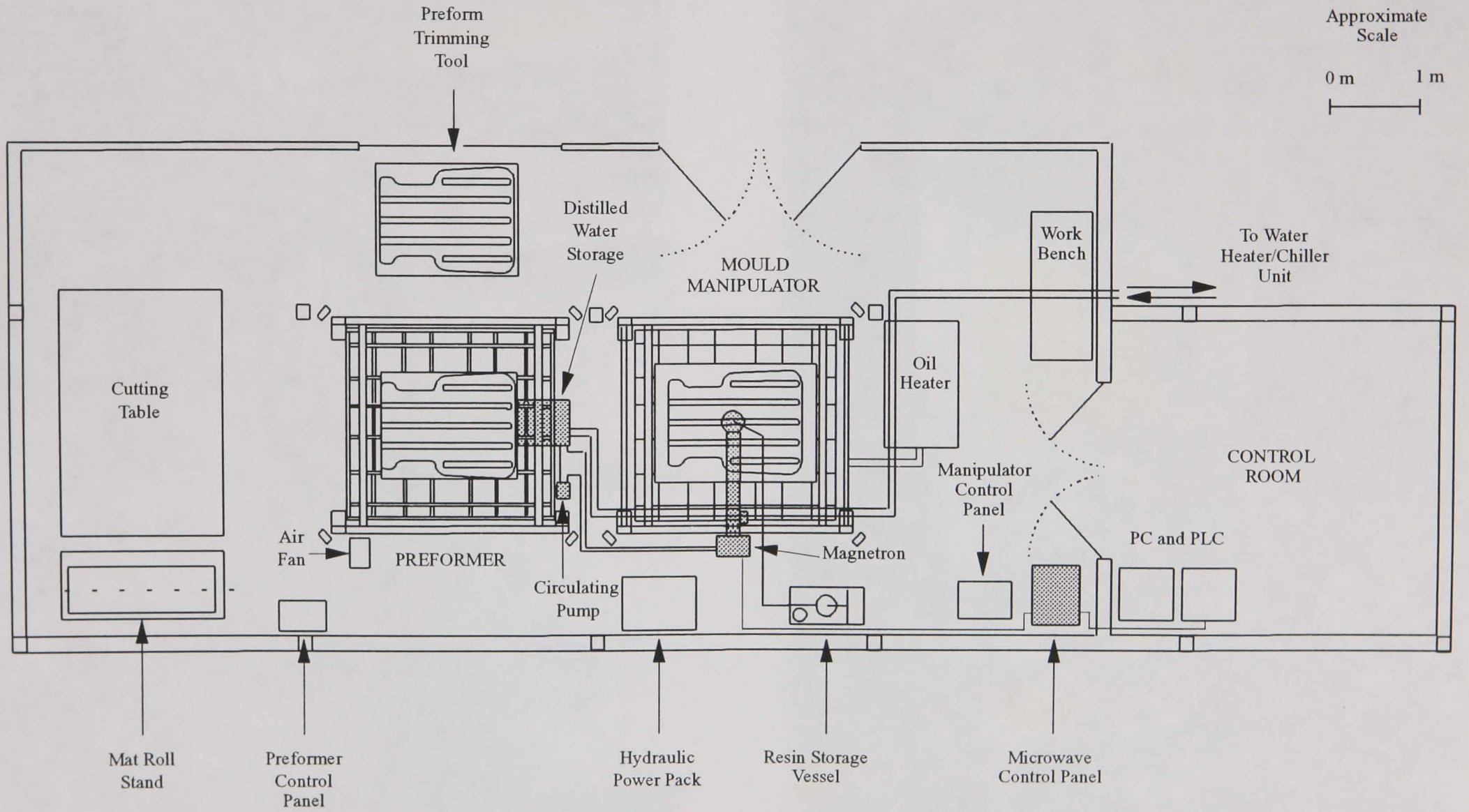


Figure 4.1b      Mould manipulator

Figure 4.2

Schematic of the experimental RTM facility



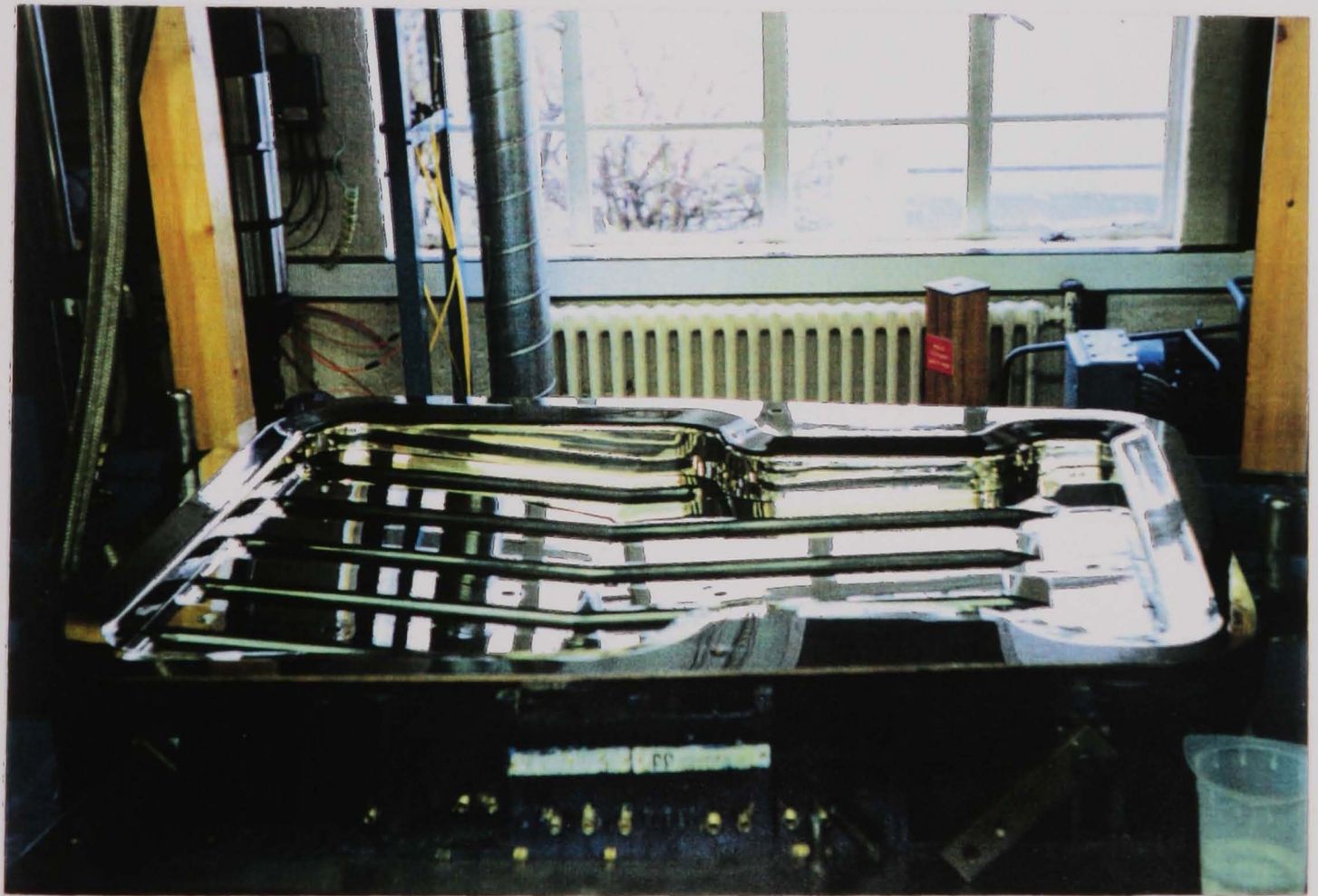
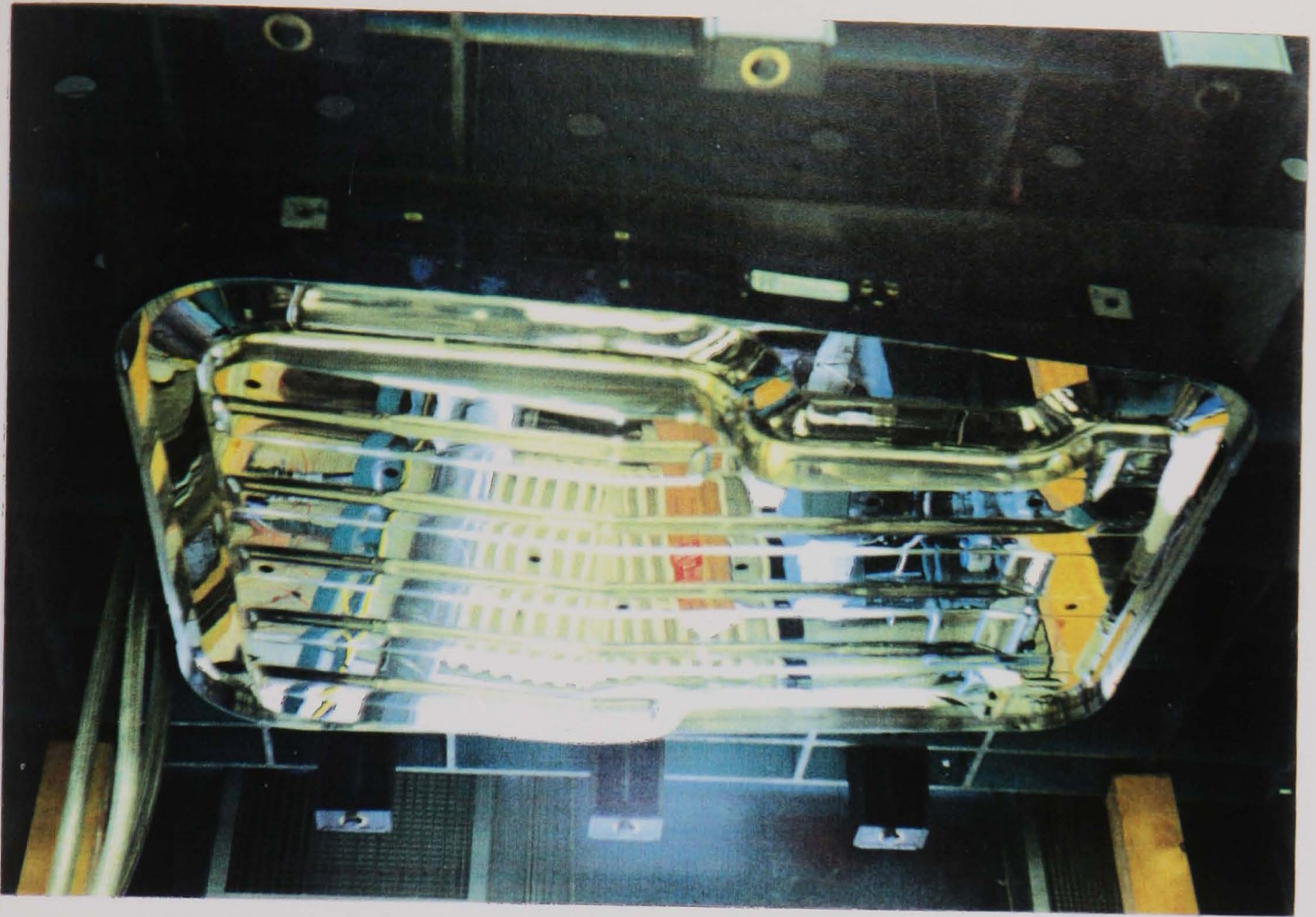


Figure 4.3 Undershield mould

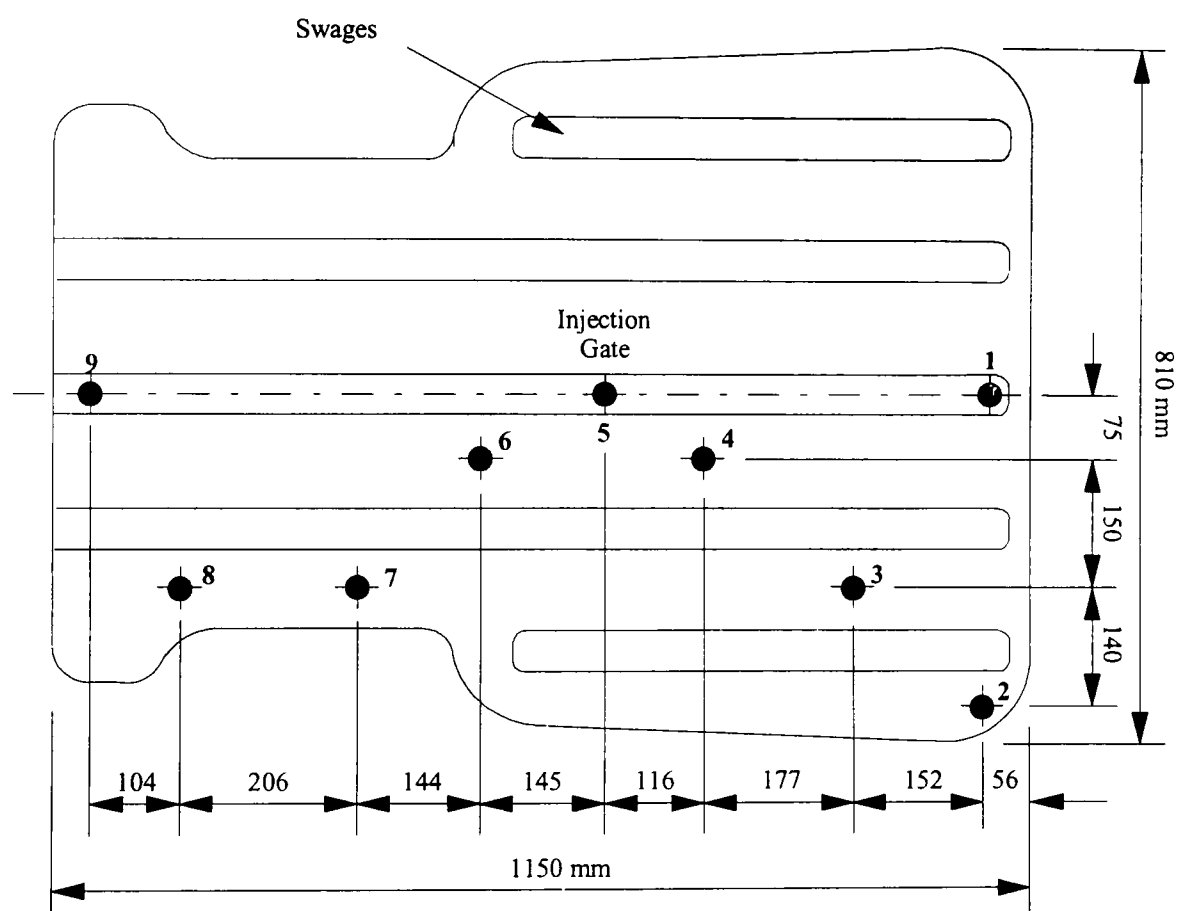


Figure 4.4 Instrumentation positions on the undershield mould

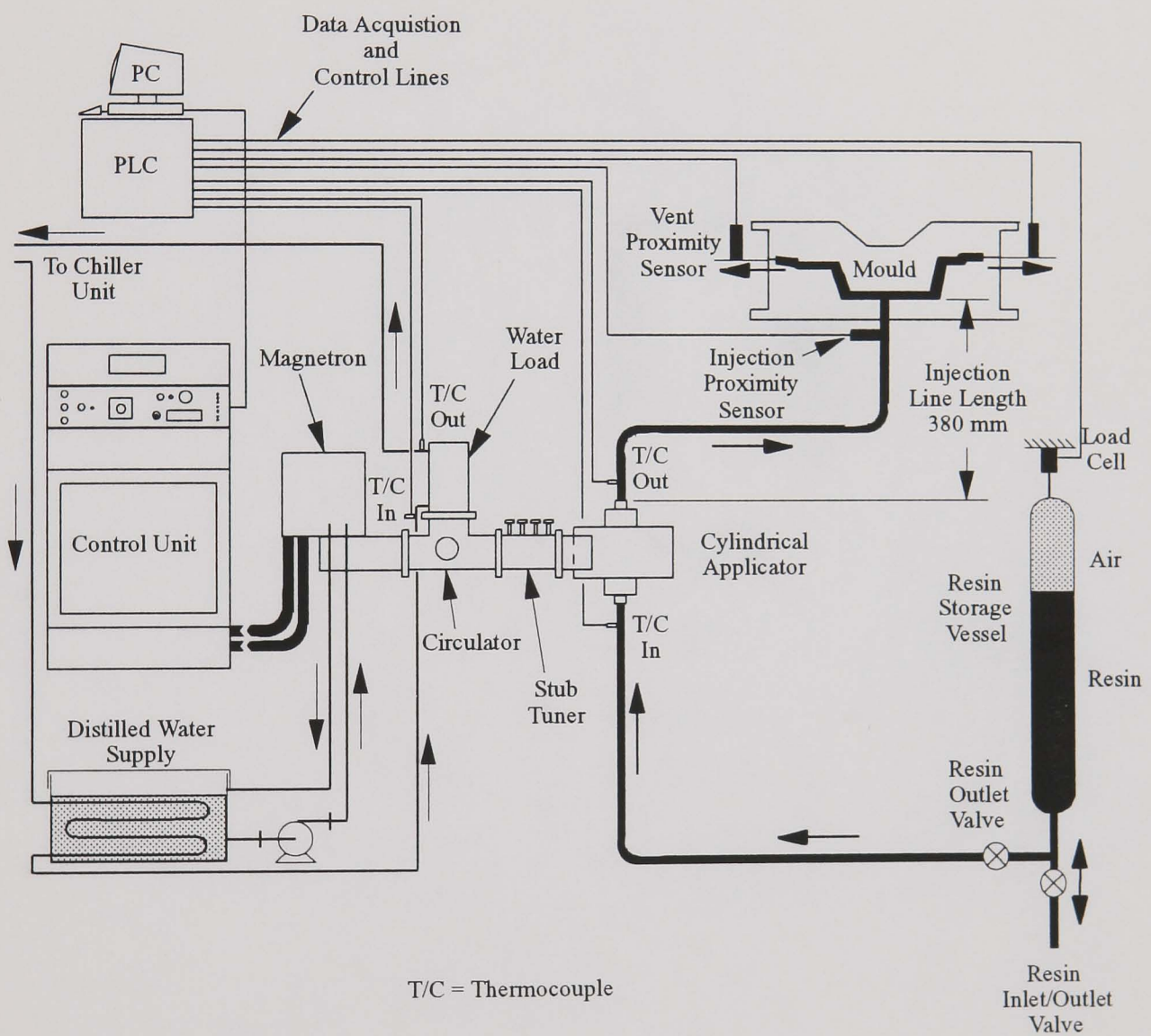


Figure 4.5 Layout of the microwave resin preheating system for moulding experiments



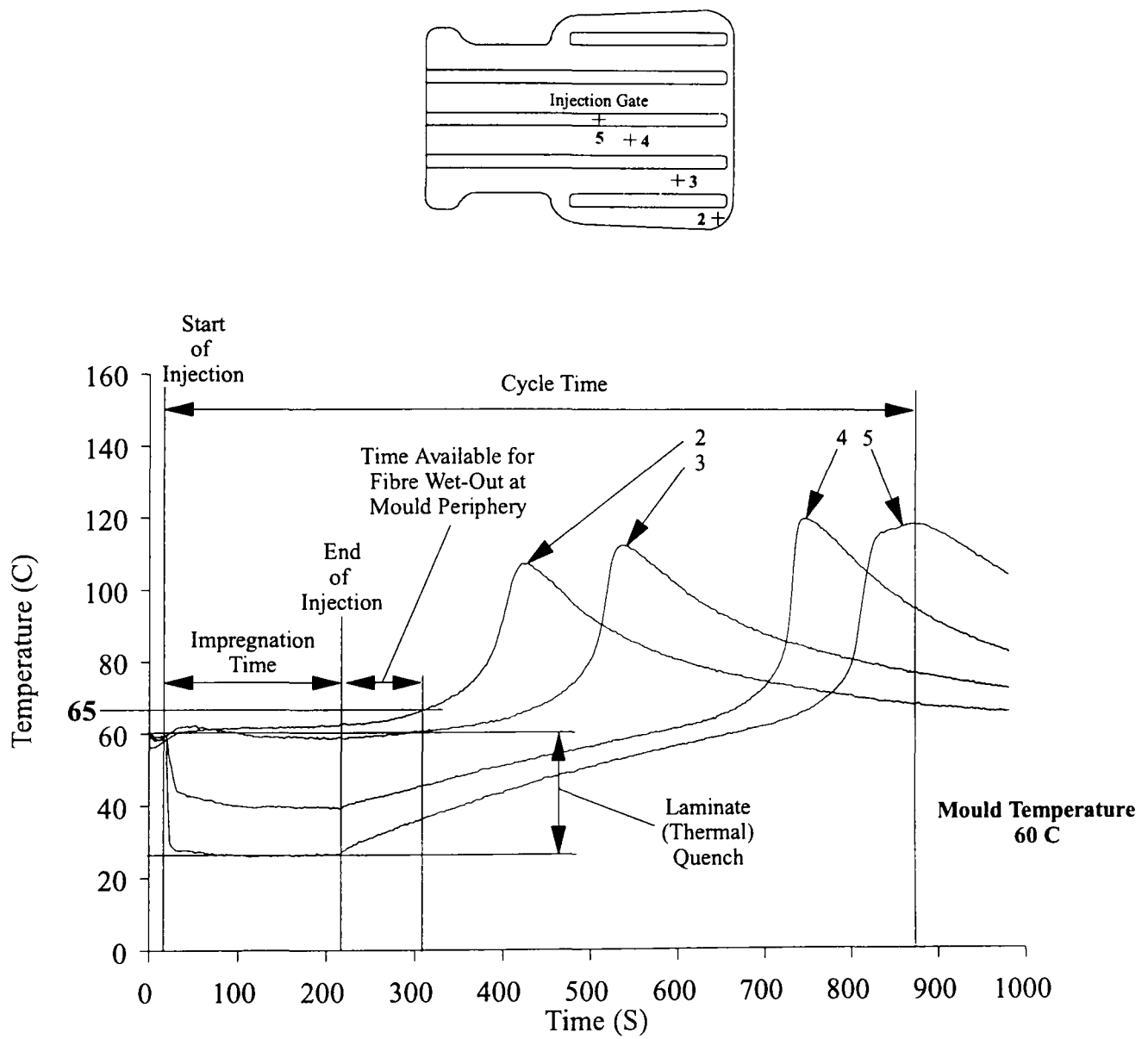


Figure 4.7 Thermal history of the moulding cycle showing principal events

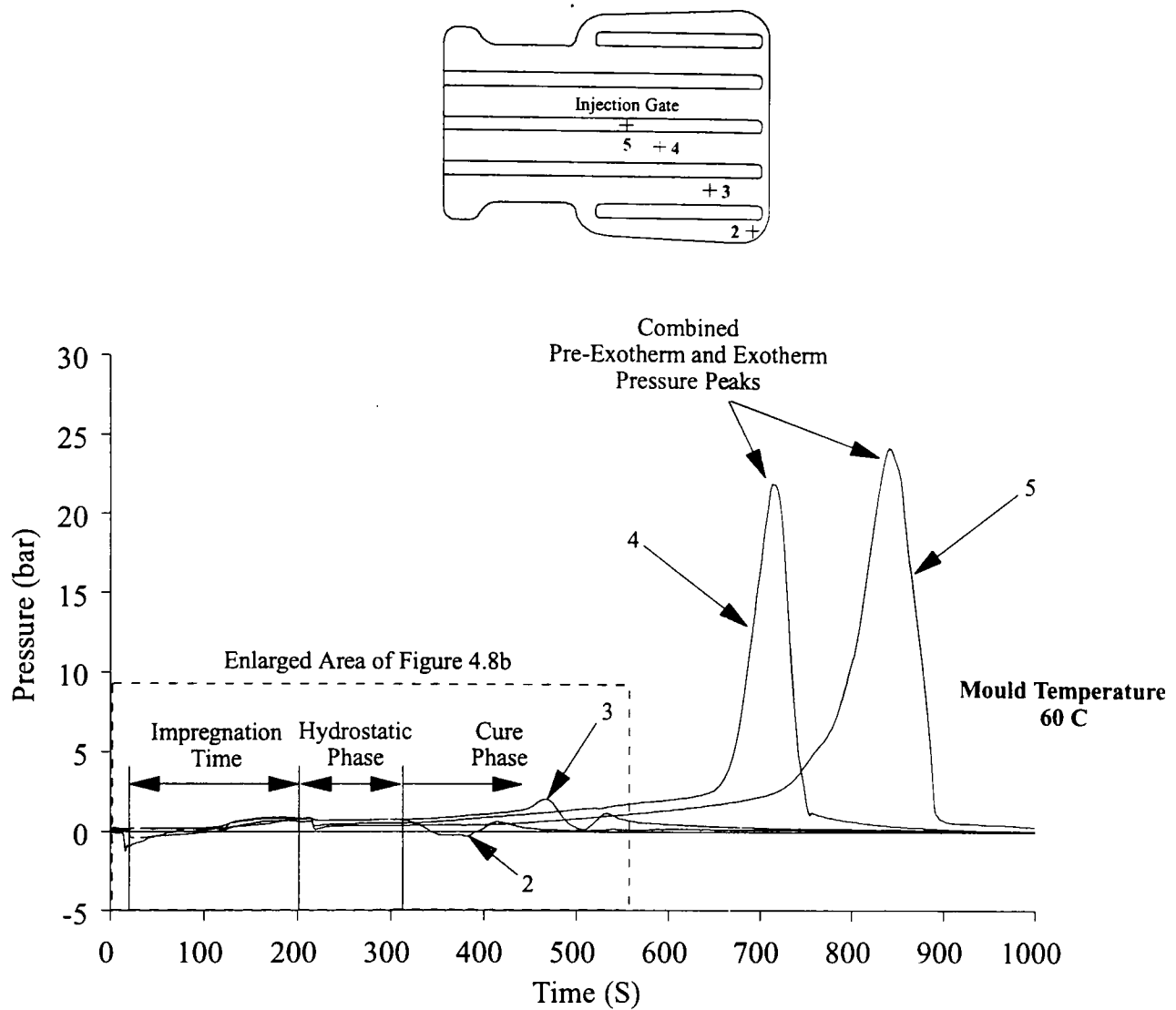


Figure 4.8a Pressure history of the full moulding cycle.

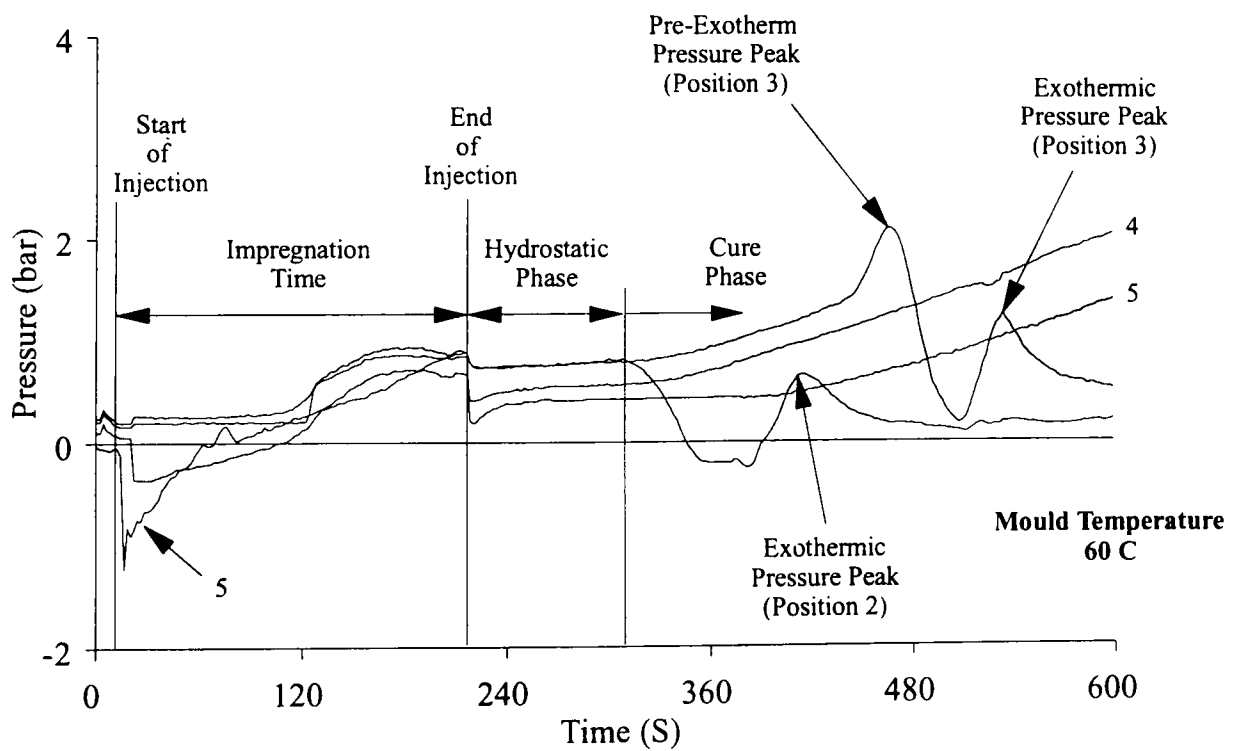
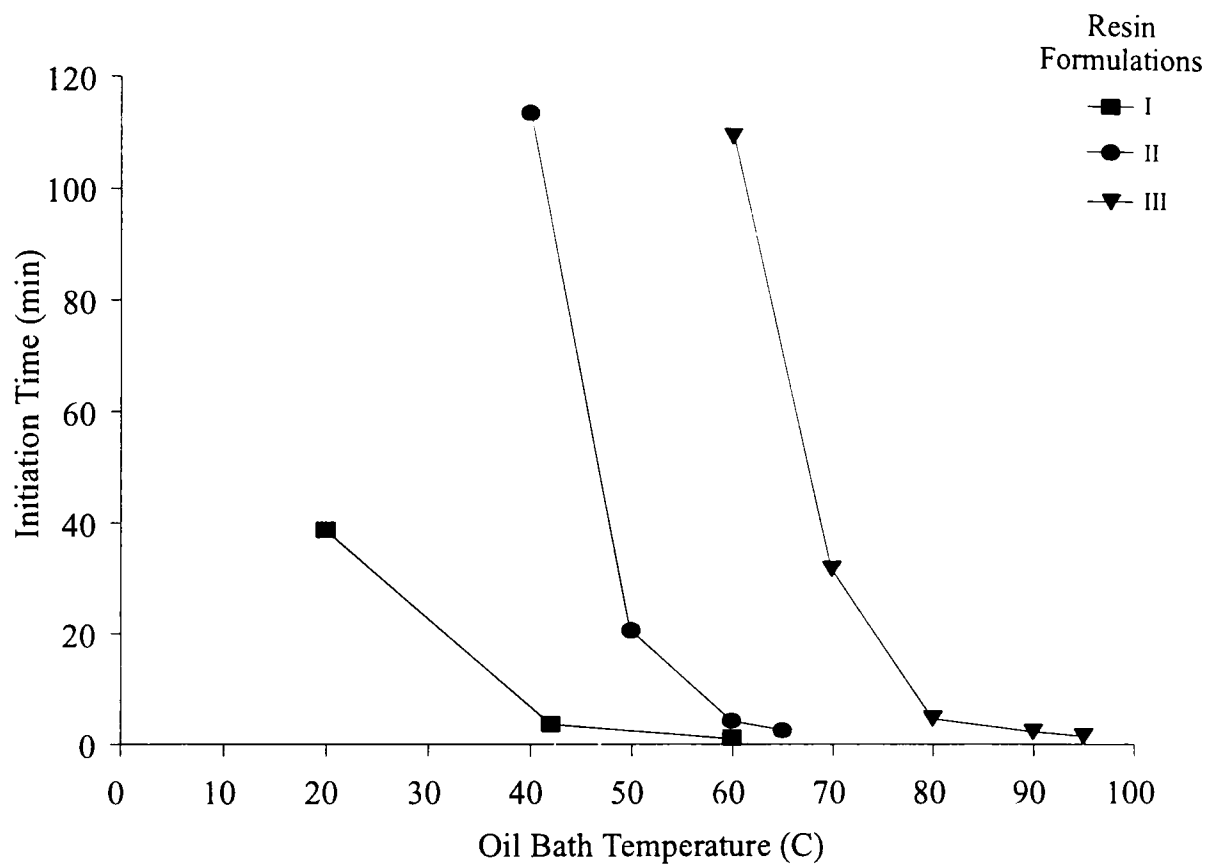


Figure 4.8b Pressure history during the first 600 seconds of the moulding cycle showing principal events



Key to Resin Formulations:

- I CVP 6345 + 2% Trigonox 44B + 0.5% NL49P
- II CVP 6345 + 2% Perkadox 16
- III CVP 6345 + 1% TBPEH

Figure 4.9 Initiation time versus temperature for the experimental resin systems

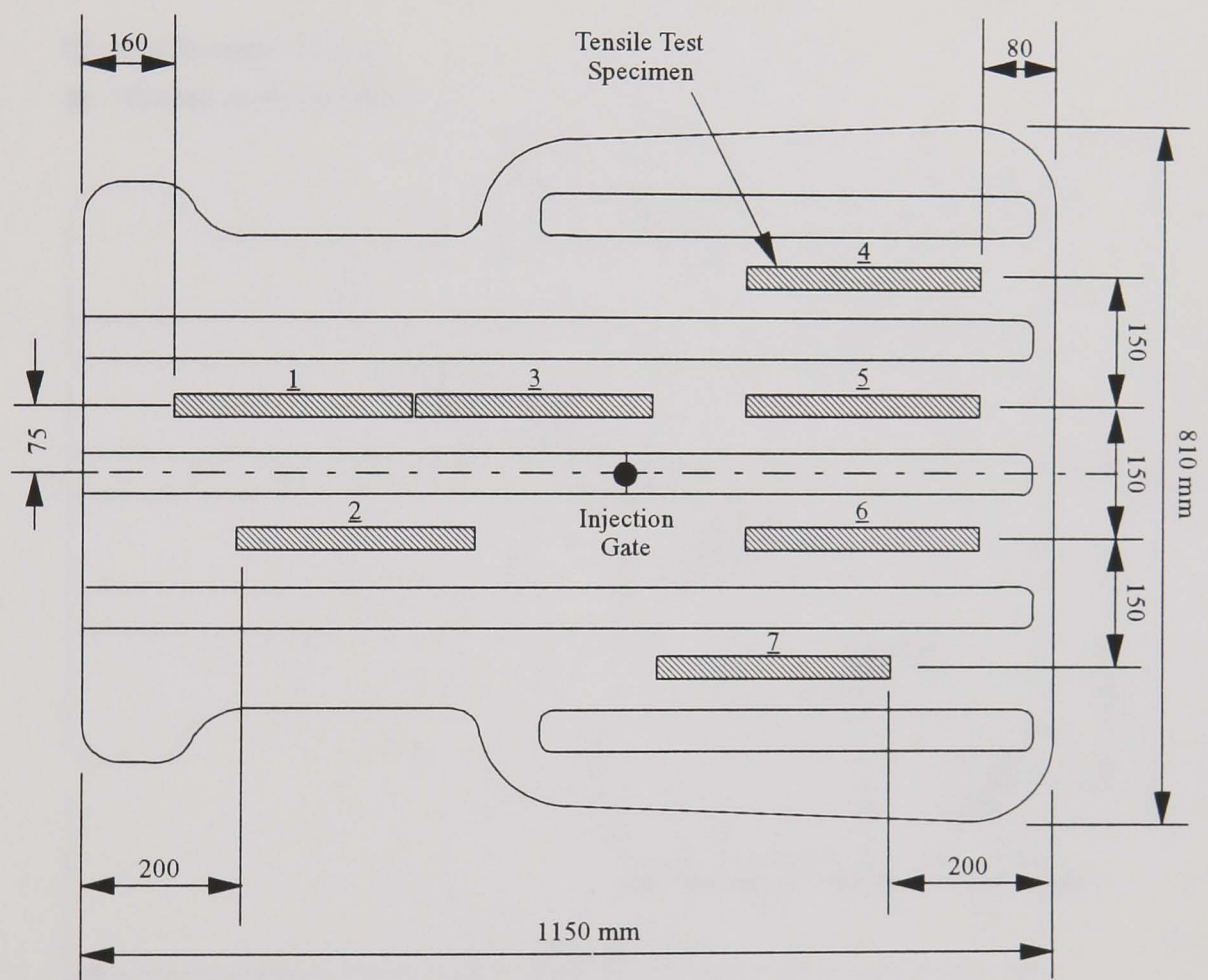


Figure 4.10 Orientation of tensile test specimens on the undershield component

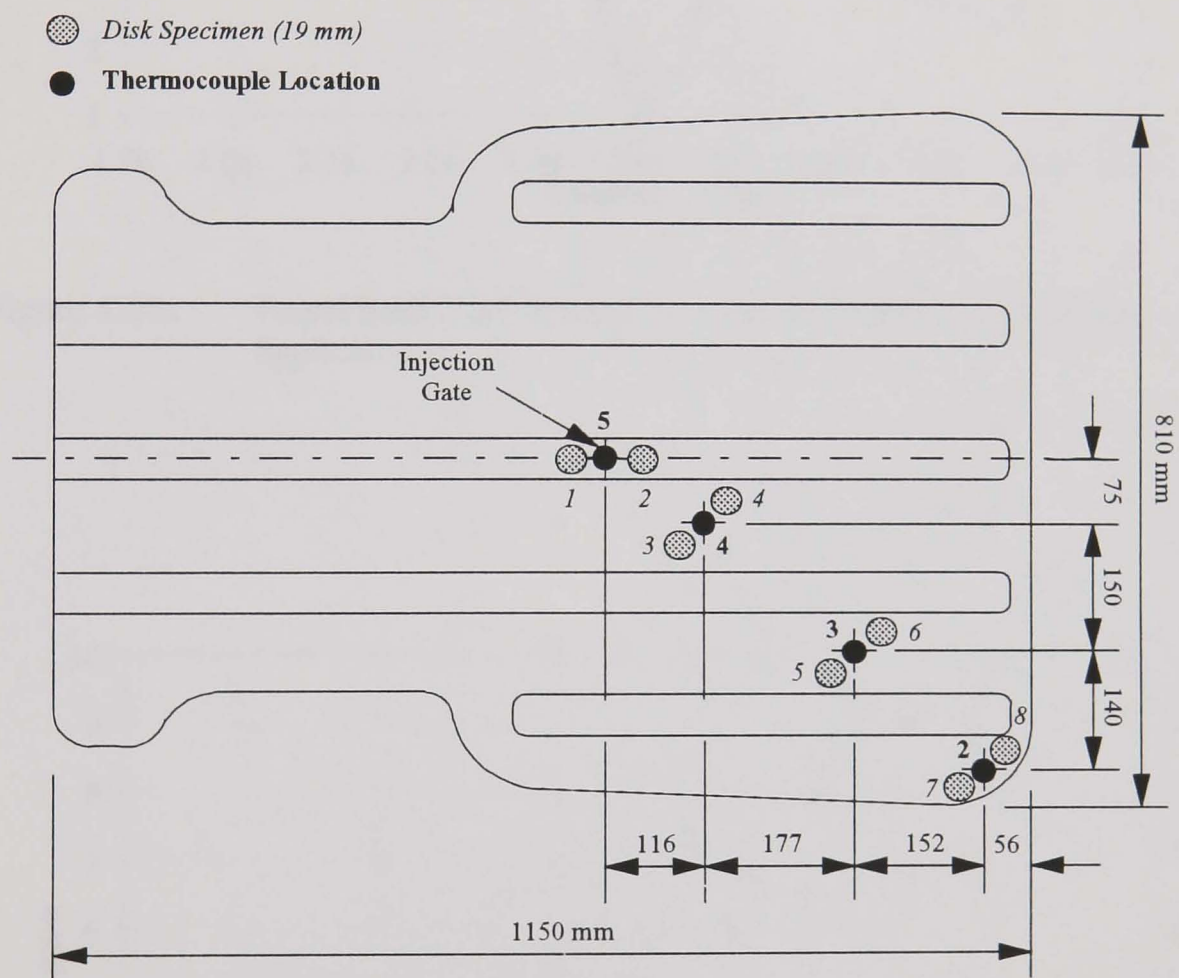


Figure 4.11 Location of disk specimens on the undershield component for the degree of cure investigation

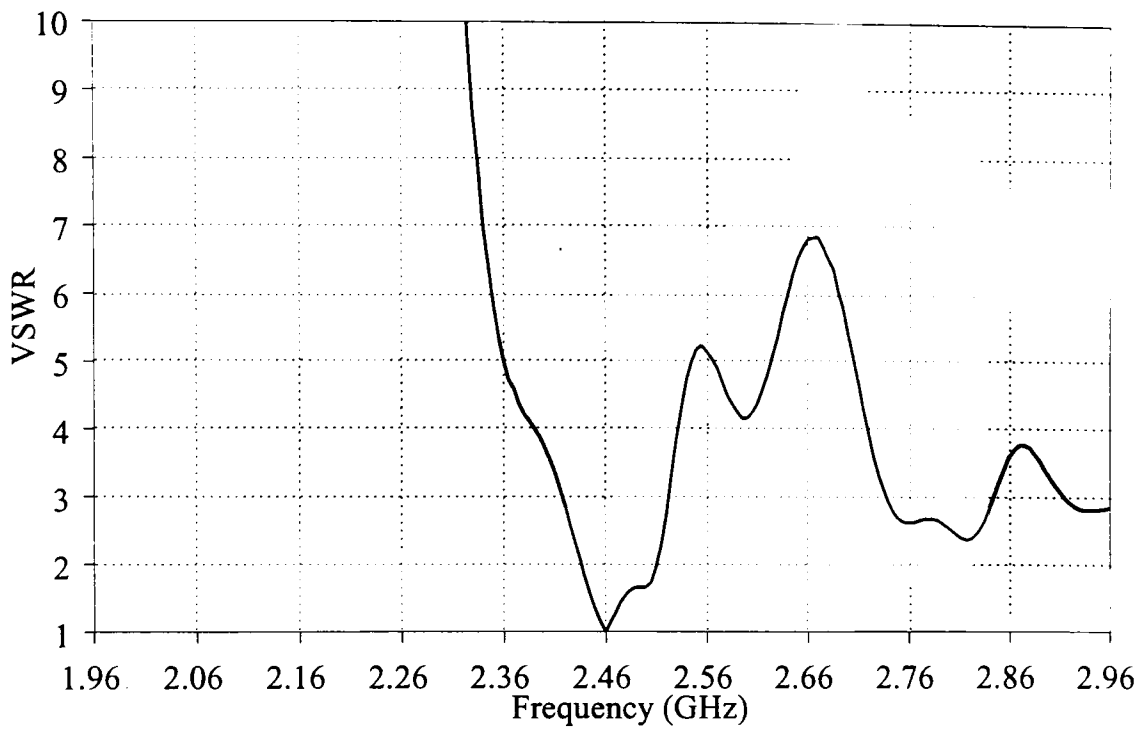


Figure 4.12a Broad band VSWR response trace for the tuned cylindrical applicator

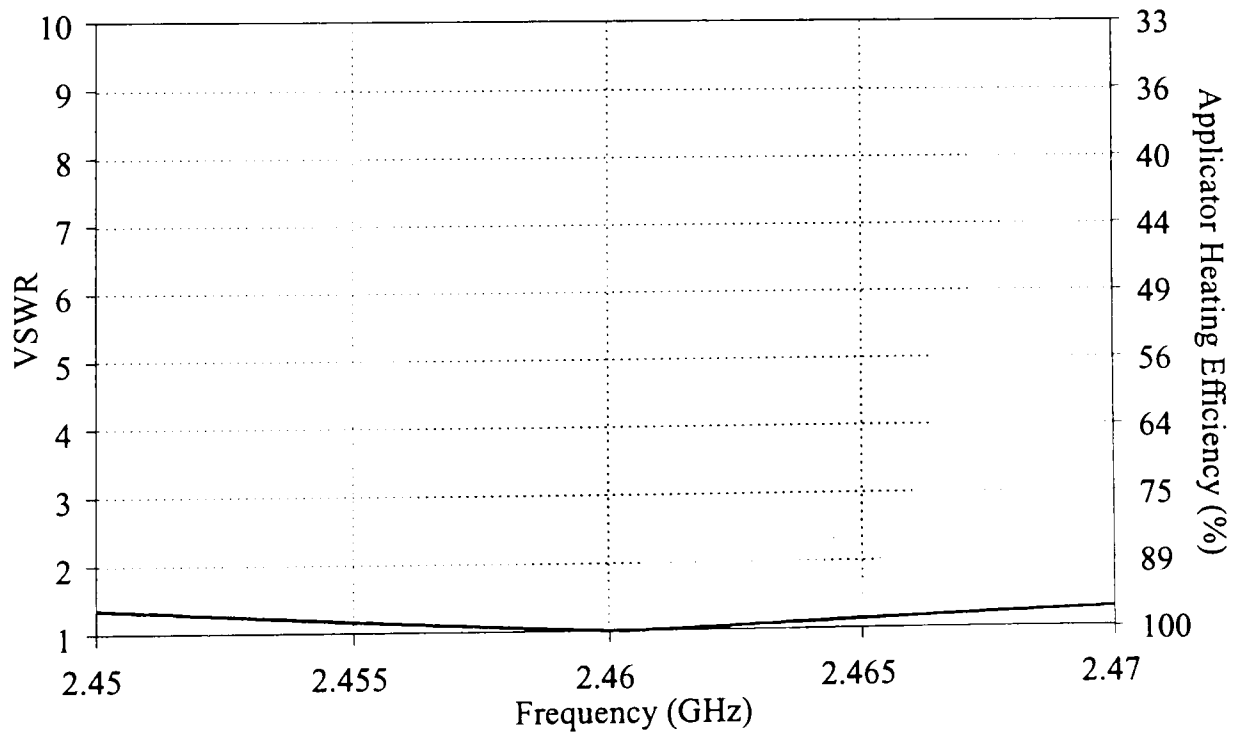


Figure 4.12b Narrow band VSWR response trace for the tuned cylindrical applicator

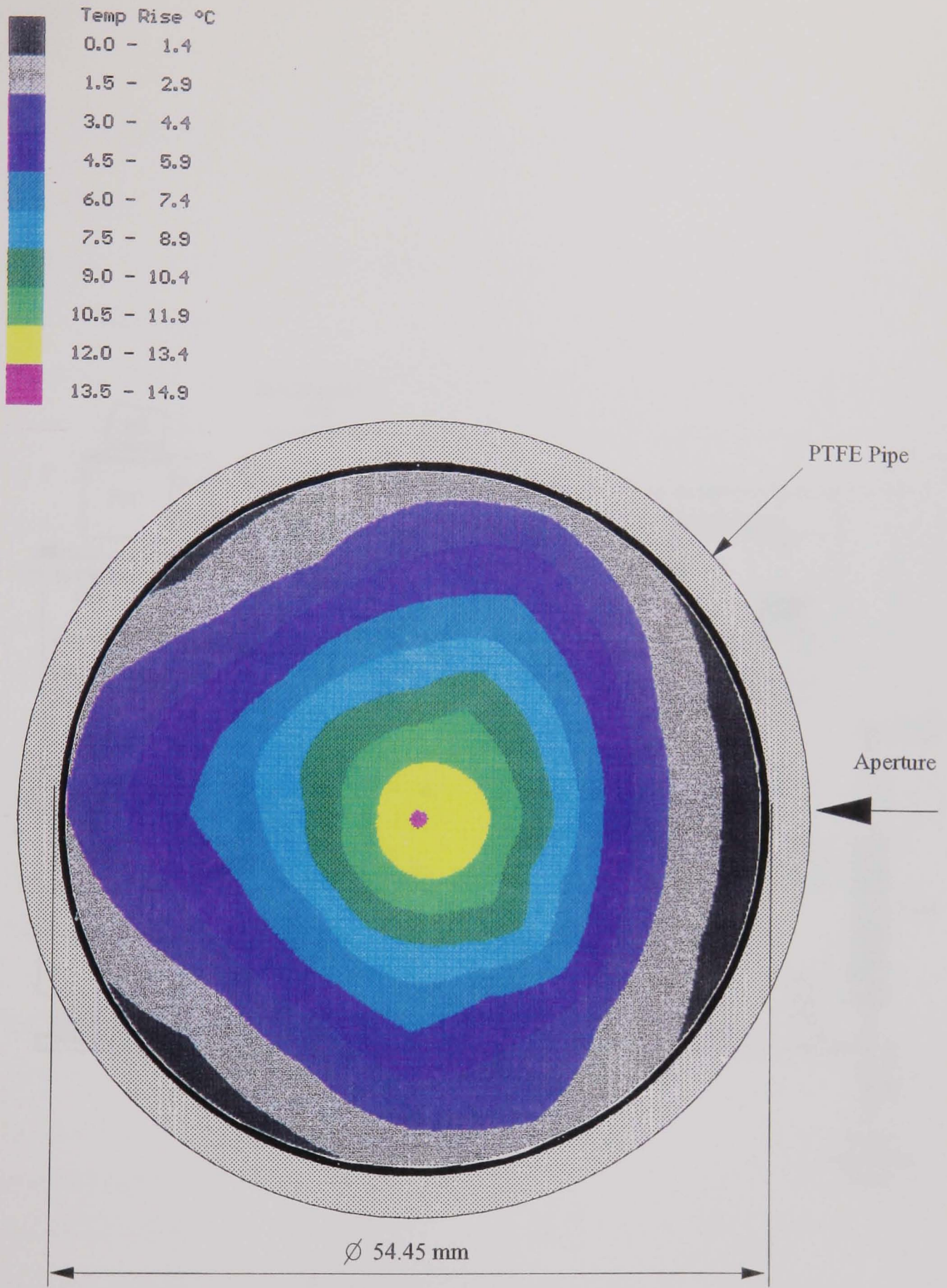


Figure Not To Scale

Figure 4.13 Typical temperature distribution within the PTFE pipe of the cylindrical applicator

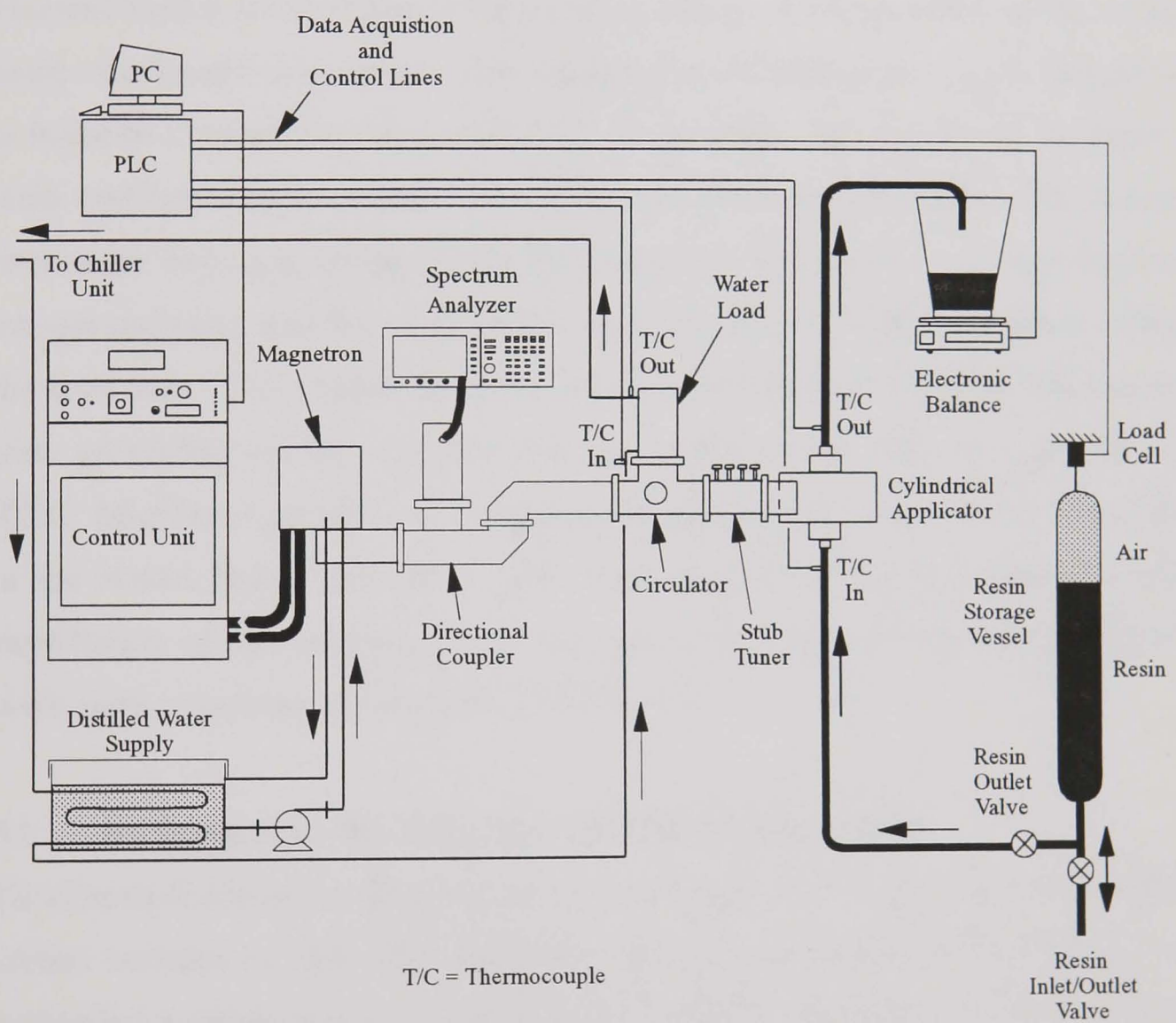


Figure 4.14 Layout of microwave resin preheating system for magnetron calibration

## Evaluation of the Microwave Resin Preheating System

---

### 5.1 Introduction

Thermal quench in the region of the injection gate has been identified as the major cause of extended cycle times. Hill showed that preheating the resin in-line prior to injection reduced thermal quench [22]. In addition, the viscosity of the heated resin was lower for improved flow through the preform and mould. The in-line microwave resin preheating system developed for this purpose was restricted to manual operation and its use resulted in the formation of cured resin lobes within the applicator. This chapter establishes the limitations of the original microwave resin preheating system, and describes the modifications made to it for use in RTM. Microwave power control was incorporated to facilitate automatic operation of the system and to provide a stable resin temperature during injection. Full exploitation of this adapted microwave resin preheating system with regard to cycle time reductions are presented in Chapter 6.

### 5.2 Background on the Microwave Resin Preheating System

This thesis furthers the development of an in-line microwave resin preheating system initiated by Hill who designed a  $TM_{020}$  mode cylindrical applicator for preheating a single stream of catalysed resin [22]. Application of this original system to RTM was limited to a single undershield moulding produced under manual control. This work demonstrated the potential of microwave resin preheating to increase RTM productivity by reducing cycle time.

### 5.2.1 Manual Control of the Microwave Resin Preheating System for Undersield Production

Figure 5.1 shows the thermal history of a benchmark undersield moulding produced by Hill [22]. Catalysed polyester resin was injected at 4.8 bar into a CFRM glass preform (volume fraction 19%). The mould was heated to 90°C with the resin at ambient temperature (17°C). The impregnation phase lasted for 151 seconds, and the cycle time (904 seconds) was dictated by cure at the injection gate (position 5).

Figure 5.2a shows the thermal history of a second undersield component produced by Hill under the same moulding conditions except that the in-line microwave resin preheating system was used. The system was operated manually, being turned on after resin arrival at the injection gate, indicated by a sudden drop in temperature at that location (position 5). Resin was heated under maximum power (5000 W) during impregnation, and switched off when the injection valve was closed. The resin temperature at the microwave outlet stabilised at 46.2°C after an initial overshoot, then rose by 8.8°C to 55°C by the end of injection (Figure 5.2b). This gradual rise in temperature suggested that the resin flow rate had decreased towards the end of injection causing the resin to be heated for a longer period within the applicator. A decrease in the resin flow rate near the end of impregnation is typical for constant pressure injection systems as no compensation is made for increasing back pressure in the mould.

Comparison of the thermal histories in Figures 5.1 and 5.2 shows that in-line preheating to an average temperature of 46.2°C reduced both the impregnation and cycle times by 35%. These savings can be attributed to the combined effect of reduced resin viscosity, a reduction in thermal quench, and a decrease in the amount of additional heat required to initiate resin cure.

In-line resin preheating enables small quantities of resin to be heated during injection so that the catalysed resin can be maintained in the supply vessel at a lower temperature, lengthening its storage life. The ability to reduce the cycle time using in-line microwave resin preheating was demonstrated by the moulding trial, however, limitations of the system also became apparent.

### **5.2.2 Limitations of the Microwave Resin Preheating System**

Application of the original microwave resin preheating system to high volume RTM was limited by several factors. First, manual operation was difficult to control. Switching the system on and off at the appropriate times required constant attention to the otherwise automatic moulding cycle. Additionally, no mechanism was available for precise resin temperature control. Constant power heating was the most tractable means of maintaining a stable resin temperature during injection. However, a reduction in the resin flow rate near the end of impregnation resulted in a temperature rise at the fixed microwave power level (Figure 5.2b). A second drawback of the original system was the generation of high solvent and resin waste, resulting from immediate flushing of the injection system at the end of impregnation. Under automatic control, flushing could be eliminated by switching the microwave off just before the end of injection so that no preheated resin remained within the injection line. Less resin and solvent would be wasted to reduce production costs, and lower volatile emissions could provide a health and safety benefit. Finally, the original system was limited by the formation of three cured resin lobes (65 mm × 13 mm) within the applicator as shown in Figure 5.3. It was assumed that continued use of the system would have produced additional cured resin lobes, ultimately blocking the injection system.

A technique to eliminate the formation of cured resin within the applicator is presented in Section 5.3, and the development of an automated power controller for the original microwave resin preheating system is detailed in Section 5.4. An undershield moulding was produced under automatic control to demonstrate the benefits of this adapted microwave resin preheating system compared to the original system operated under manual control (Figure 5.2). The results of this moulding are presented in Section 5.5

### **5.3 Microwave Resin Preheating Using a Low Power Density System**

The lobes of cured resin found within the cylindrical applicator (Figure 5.3) were attributed to localised high power density regions that produced hot spots. Hill suggested that the hot spots were generated by superposition of parasitic modes

on the dominant  $TM_{020}$  mode [22]. Microwave power within the applicator was distributed between these modes. Sufficient power was supplied to the parasitic modes at high microwave power to produce hot spots, resulting in the cured resin lobes. Positioning of the hot spots near the PTFE pipe wall, where the resin flow velocity was minimal, intensified the problem. The hot spots created localised regions of high temperature resin within the applicator. The resin temperature is related to the microwave power ( $P$ ), and the resin mass flow rate ( $\dot{m}$ ) by the following expression:

$$T_{set\ point} - T_{ambient} = \frac{P}{\dot{m} C_p} \quad \text{Equation 5.1}$$

where  $T_{set\ point}$  is the resin preheat temperature,  $T_{ambient}$  is the bulk resin storage temperature, and  $C_p$  is the specific heat capacity of the resin.

Operating the system at low power was found to limit the effect of parasitic modes and prevent cured resin from forming within the applicator. It is evident from Equation 5.1 that a given resin preheat temperature can be maintained at lower power levels only if the resin mass flow rate is also reduced. Decreasing the injection pressure reduces the resin flow rate so that resin residence time within the applicator is increased and less power is required to attain the preheat temperature. Normally, reducing the injection pressure increases the impregnation time. However, at elevated temperatures the resin viscosity is lower for improved flow to counter this effect. This low power density approach was adapted to enable characterisation of the RTM process described in Chapter 6.

#### **5.4 Automatic Power Control Methods for the Microwave Resin Preheating System**

Operation of the microwave resin preheating system under manual control is impractical for industrial applications. Production efficiency, component quality, and safety issues demand system automation. Ideally, the operator would specify a resin preheat temperature before initiating the automatic moulding cycle. The microwave would turn on automatically at the beginning of injection, operate at

the set point temperature during impregnation, and switch off just before the end of injection so that no preheated resin remained in the injection line, thus eliminating the need for solvent flushing between mouldings. A method to switch the microwave system on and off automatically has been mentioned in Section 4.2.3. Power modulation is necessary to maintain a specified resin temperature during impregnation. Fine power control is desired so that catalysed resin can be preheated just below its activation temperature for maximum reductions in thermal quench and viscosity without the onset of premature cure. Two power control strategies were investigated to enable precise resin temperature control. Both strategies relied upon temperature feedback at the outlet of the cylindrical applicator (Figure 4.5). A simple ON-OFF power controller, described in Section 5.4.1 offered poor control of the resin outlet temperature and ultimately was dismissed. Instead, a three term, proportional-integral-derivative (PID) controller was developed (Section 5.4.2) to provide more accurate resin temperature control during injection.

#### **5.4.1 ON-OFF Power Control**

ON-OFF power control is the simplest type of power control algorithm that can be implemented on a PC [80]. This technique is based upon a neutral heating zone consisting of upper and lower temperature bounds, centred around a resin set point temperature. The microwave remained on when the resin outlet temperature was within the neutral heating zone. This temperature band was intended to prevent on/off cycling of the system since heating at an exact set point temperature was not necessary.

#### **Demonstration of the ON-OFF Power Controller for Undersield Component Production**

A catalysed vinyl-ester resin was preheated during injection using ON-OFF power control to produce an undersield moulding. A temperature history of the impregnation phase is shown in Figure 5.4. Microwave power was set to 4500 W prior to injection. A resin set point temperature of 50°C was specified with a neutral control zone of  $\pm 3^\circ\text{C}$ . ON-OFF power control resulted in an oscillatory

resin temperature profile at the applicator outlet. The resin temperature rose above the upper bound of the neutral control zone (53°C) switching off the microwave. This heated resin was delivered to the mould, followed by unheated resin (22°C) that reduced the resin outlet temperature below 47°C, turning the microwave back on. A rapid heating and quenching cycle continued throughout impregnation. However, cycling of the microwave power did not appear to destabilise the laminate temperature at the injection gate (position 5) where an average value of 45°C was measured. Cycling of the power did affect the thermal history of the resin. Consequently, discrete volumes of resin heated above the set point temperature could cure prematurely either in the mould creating dry patches, or in the applicator blocking the injection system.

Cycling and overshooting of the set point temperature is typical of ON-OFF control systems. The main drawback of this type of controller is that the difference between the resin set point temperature and the resin outlet temperature is not taken into account. A PID controller was developed to provide finer resin temperature control, reducing the risk of premature cure.

#### **5.4.2 PID Power Control**

Compared to an ON-OFF controller, the PID controller is a more sophisticated device [80]. The proportional control component calculates a power level in proportion to the difference, or error, between the resin set point temperature and the resin outlet temperature. The larger the error, the more power applied to reduce that error. Proportional control generally stabilises at a temperature above the set point temperature, termed an offset error, and is compensated for by the integral component. Integral control specifies power with regard to an error history during the control period. Power is applied gradually until the resin set point temperature is reached. Integral control can result in temperature overshoot and oscillatory temperature response if not tuned correctly. Derivative control stabilises the system by reacting to a time rate of change of the error signal. The greater the rate of change in the error, the more power applied in reaction to that error.

The PID control algorithm was written in Borland International Turbo Pascal Version 6.0 on the PC. A discrete form of this algorithm is given by the following expression [80]:

$$P = K_p \left[ \Delta T_n + \frac{1}{T_I} \sum_{i=1}^n \Delta T_i (\Delta t) + T_d \frac{(\Delta T_n - \Delta T_{n-1})}{\Delta t} \right] \quad \text{Equation 5.2}$$

where

$P$	Power
$K_p$	Proportionality Constant
$T_I$	Reset Time Constant
$T_d$	Derivative Time Constant
$\Delta t$	Sampling Interval
$\Delta T_n$	$n^{\text{th}}$ Error Value
$\Delta T_{n-1}$	$(n-1)^{\text{th}}$ Error Value
$\Delta T_i$	$i^{\text{th}}$ Error Value

A continuous control loop is established whereby the resin outlet temperature is measured and conveyed to the PID controller which in turn adjusts the microwave power. The  $n^{\text{th}}$  term specifies the loop number while the  $i^{\text{th}}$  term is a sum of the passes through the loop. The error value is the difference between the resin outlet temperature and the set point temperature. Values for the constants  $K_p$ ,  $T_I$ ,  $T_d$ , and the time step,  $\Delta t$ , must be selected to tune the controller and ensure that oscillations, instabilities, and offset errors are minimised. A well known technique for establishing the PID control parameters is the Ziegler-Nichols tuning method.

### Ziegler-Nichols Tuning of the PID Controller

The Ziegler-Nichols stability boundary tuning method was adopted to determine the PID controller constants [81]. Figure 4.6 shows the experimental set up used for the tuning trials. Microwave power was modulated by proportional control only. A resin set point temperature of 40°C was specified with a sampling interval ( $\Delta t$ ) of unity and an arbitrary initial gain,  $K_p$ . The gain was increased to a critical value ( $K_u=80$ ) where the temperature response became oscillatory and the critical response period ( $P_u=7$  seconds) was determined based upon the results as shown in Figure 5.5a. The constants for the tuned PID controller ( $K_p$ ,  $T_I$ , and  $T_d$ ) were calculated according to the Ziegler-Nichols equations as described in Appendix 5.1 and are listed in Table 5.1. A heating trial was performed under PID control using

these constants to verify the stability of the system. A gradual increase to the set point temperature (40°C) occurred with a maximum overshoot of 1.7°C as shown in Figure 5.5b. The resin temperature stabilised to 41.0°C after 14 seconds of heating. The result of this trial suggested that the PID power controller was tuned correctly for heating resin at 40°C.

Heating resin to temperatures significantly above 40°C was found to require additional tuning of the PID controller. Stabilisation times at higher temperatures were excessive using the 40°C parameters. The Ziegler-Nichols tuning procedure was repeated at set point temperatures of 50°C and 60°C. Table 5.1 summarises the resulting parameters used to tune the PID controller at these temperatures. Expressions to calculate the values for the constants  $K_p$ ,  $T_I$ , and  $T_d$ , at any temperature within the 40°C-60°C range are listed in Appendix 5.2. These expressions could be programmed into the controller software so that the appropriate controller constants would be determined automatically for a user defined resin preheat temperature.

### **Demonstration of the PID Power Controller for Undersield Component Production**

The undershield moulding trial using ON-OFF power control (Figure 5.4) was repeated using PID power control to demonstrate the stability of the resin outlet temperature during impregnation. Figure 5.6 shows the thermal history of the moulding during the impregnation phase. A resin set point temperature of 50°C was specified before initiating the moulding sequence. An 8°C overshoot occurred at the start of heating, although the system did not become unstable. Action of the controller reduced the resin outlet temperature to an average of 50.2°C after 35 seconds of heating. Temperature at the injection gate (position 5) stabilised at 53.6°C after thermal quench at the start of injection (28 seconds). The thermal quench was preceded by an initial temperature drop of 5°C at the 10 second mark as the mould was closed onto the cold preform.

Compared to the ON-OFF power controller (Figure 5.4), the resin temperature at the applicator outlet was more stable using the PID power controller. As a result, the risk of premature cure while preheating near the resin

gel point temperature was reduced, although the initial temperature overshoot suggested that it was not eliminated completely. The PID power controller was used on all of the subsequent moulding trials.

### **5.5 Undershiield Production Using the Adapted Microwave Resin Preheating System**

The manually controlled moulding trial by Hill (Figure 5.2) was repeated using the adapted microwave resin preheating system. Fully automatic control was employed, including on/off switching and PID power control. A low power density system was established by reducing the injection pressure to 1.8 bar (from 4.7 bar) to prevent premature cure within the applicator. A thermal history of the moulding trial is shown in Figures 5.7a and 5.7b. An insignificant rise in impregnation time to 104 seconds (from 98 seconds) was recorded and a marginal cycle time reduction from 588 seconds to 570 seconds occurred under automatic control. However, this represented a 37% reduction in cycle time over the benchmark moulding (Figure 5.1). A resin set point temperature of 50°C was specified prior to moulding, and the PID controller provided an average resin outlet temperature of 50.7°C during impregnation after a 36 second stabilisation period. The reduced resin flow rate caused by increased back pressure in the mould at the end of injection did not alter the resin outlet temperature. Unlike the moulding produced under manual control (Figure 5.2), no trace of cured resin lobes were found within the applicator at the end of the moulding cycle.

The potential of the automated microwave resin preheating system to reduce cycle times becomes apparent when compared to the results provided by Hill. Using an injection pressure of 4.7 bar, Hill demonstrated a 35% reduction in cycle time (Figure 5.2) under manual control at 5000 W power. However, a similar cycle time reduction (37%) was measured under automatic control using an injection pressure of only 1.8 bar (Figure 5.7), and less power. A lower injection pressure was necessary to preheat the resin at a lower power level, thus preventing premature cure within the applicator. If the microwave power was not restricted, it is expected that even greater cycle time reductions could be achieved using the automated microwave resin preheating system. Higher injection

pressures would produce more rapid impregnation and proportionally lower cycle times.

## **5.6 Conclusion**

The original microwave resin preheating system was limited by manual operation and the generation of cured resin lobes within the applicator during injection. The lobes were formed by hot spots within the applicator. These regions of high temperature resulted from excitation of parasitic heating modes, coincident with the desired  $TM_{020}$  mode. The effect of the parasitic modes was emphasised under prolonged high microwave power conditions. A low power density heating approach was established by reducing the injection pressure, hence the resin flow rate through the applicator. This technique limited the effect of the parasitic modes allowing resin to be preheated without the formation of cured resin lobes. A PID power controller was used to automate the microwave resin preheating system within the RTM cycle. This controller restricted initial resin temperature overshoot, prevented a temperature rise at the end of injection due to increased back pressure within the mould, and permitted heating near the resin gel point with reduced risk of resin cure. These adaptations to the original microwave resin preheating system have allowed maximum cycle time reductions to be realised as described in Chapter 6.

## List of Tables

Table 5.1	PID control parameters determined by the Ziegler-Nichols tuning method at several set point temperatures
-----------	--

## List of Figures

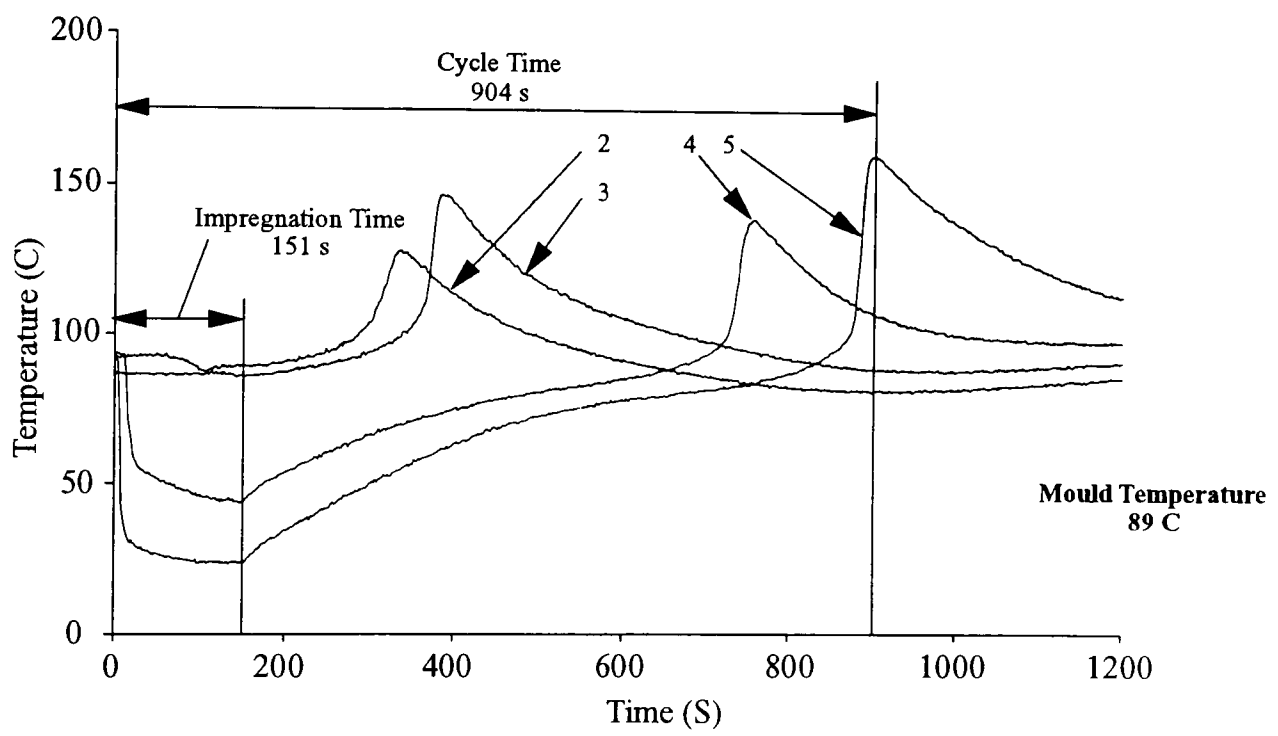
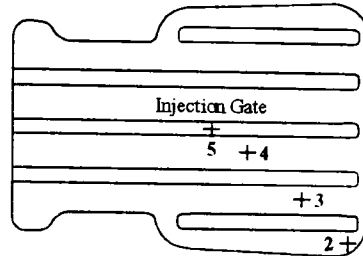
Figure 5.1	Thermal history of the benchmark undershield moulding by Hill [22]
Figure 5.2a	Thermal history of undershield moulding produced under manual control by Hill [22]
Figure 5.2b	Resin thermal history at the microwave applicator during impregnation of undershield moulding 5176
Figure 5.3	Cured resin lobes found within the cylindrical applicator after production of undershield component 5176
Figure 5.4	Thermal history of an undershield moulding to demonstrate the temperature control characteristics of an ON-OFF power controller
Figure 5.5a	Temperature response for a marginally stable system at a set point temperature of 40°C using the Ziegler-Nichols tuning method
Figure 5.5b	Temperature response of the microwave resin preheating system using PID power control tuned at a set point temperature of 40°C
Figure 5.6	Thermal history of an undershield moulding to demonstrate the temperature control characteristics of the PID power controller
Figure 5.7a	Thermal history of undershield moulding produced by automatic operation of the adapted resin preheating system under PID control
Figure 5.7b	Resin thermal history at the microwave applicator during impregnation of undershield moulding 5463

**Table 5.1 PID Control Parameters Determined by the Ziegler-Nichols Tuning Method at Several Set Point Temperatures**

	40°C	50°C	60°C
$K_u$ (W/°C)	80	110	130
$P_u$ (s)	7.0	6.2	5.9
$K_p$ (W/°C)	48	66	78
$T_i$ (°C s/W)	3.50	3.10	2.95
$T_d$ (W s/°C)	0.88	0.78	0.74

See Appendix 5.1

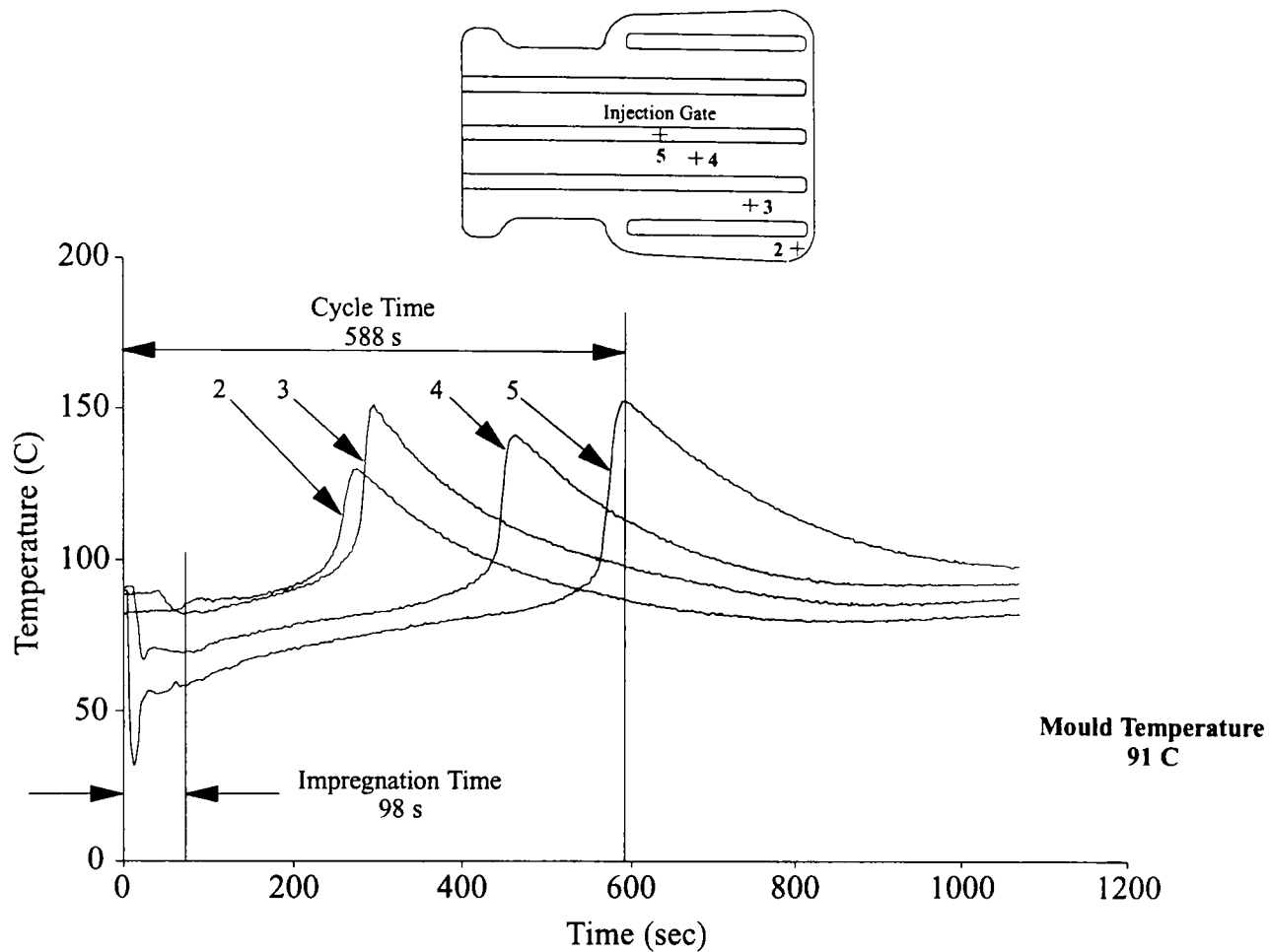
**Result Presented by Hill [22]**



Moulding No.	5174	Fibre Volume Fraction	19%
Resin	Synolac 6345	Mould Temperature	89 C
Catalyst	1% TBPEH	Resin Temperature	17 C
Reinforcement	U750-300	Supply Pressure	<b>4.8 bar</b>

Figure 5.1 Thermal history of the benchmark undershield moulding by Hill [22]

Result Presented by Hill [22]



Moulding No.	5176	Fibre Volume Fraction	19%
Resin	Synolac 6345	Mould Temperature	91 C
Catalyst	1% TBPEH	Resin Temperature	46.2 C
Reinforcement	U750-300	Supply Pressure	<b>4.7 bar</b>

Figure 5.2a Thermal history of undershield moulding produced under manual control by Hill [22]

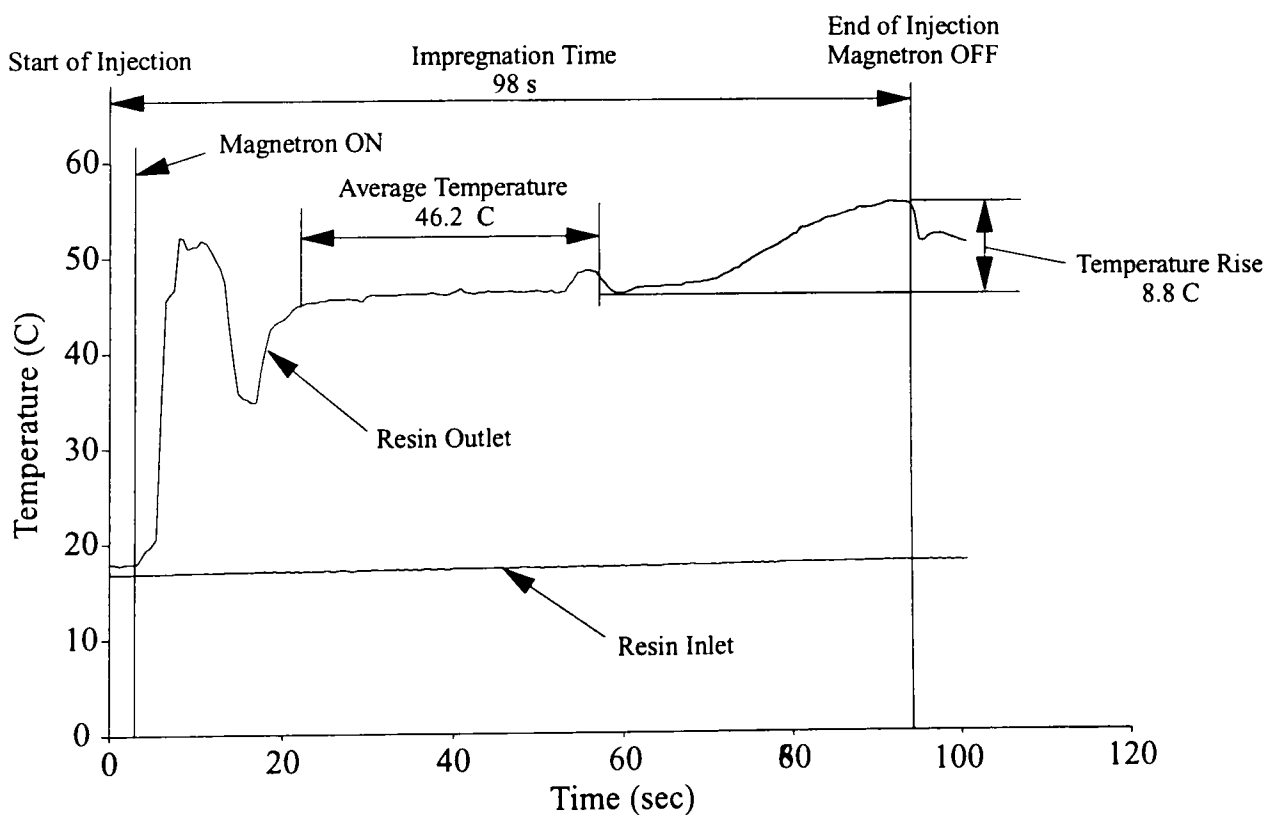


Figure 5.2b Resin thermal history at the microwave applicator during impregnation of undershield moulding 5176

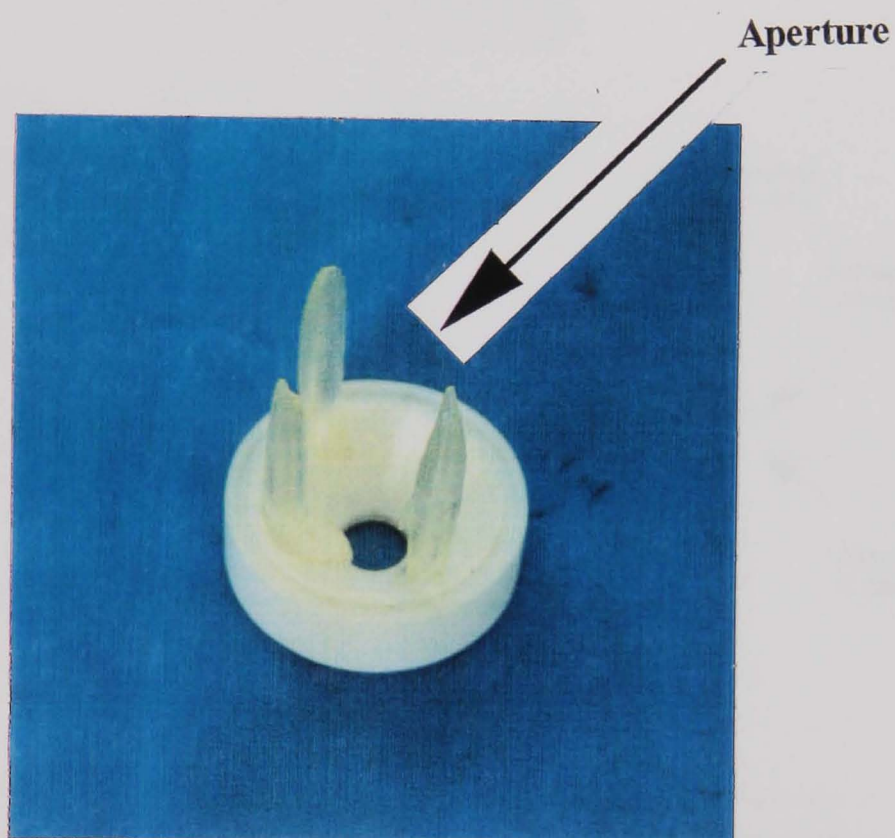
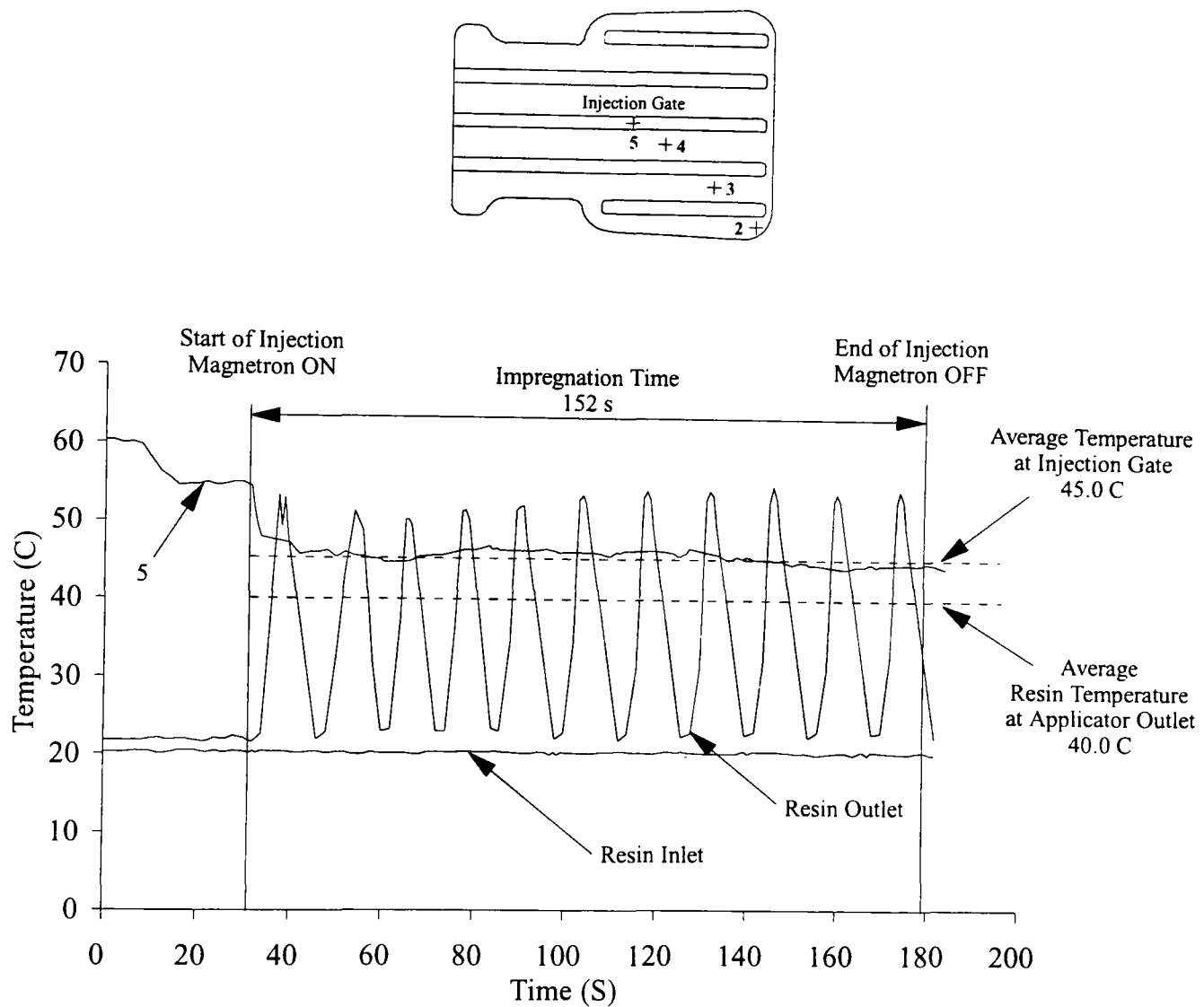
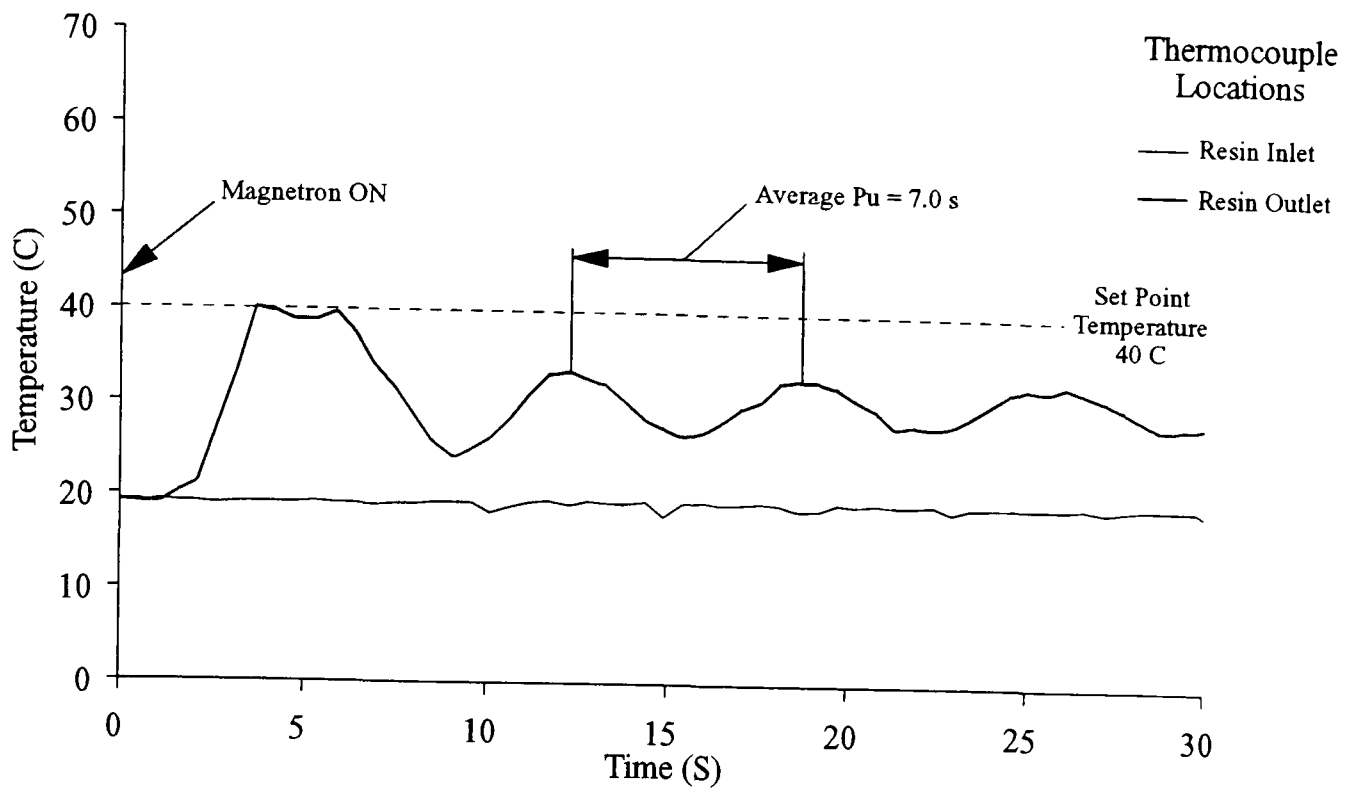


Figure 5.3 Cured resin lobes found within the cylindrical applicator after production of undershield component 5176



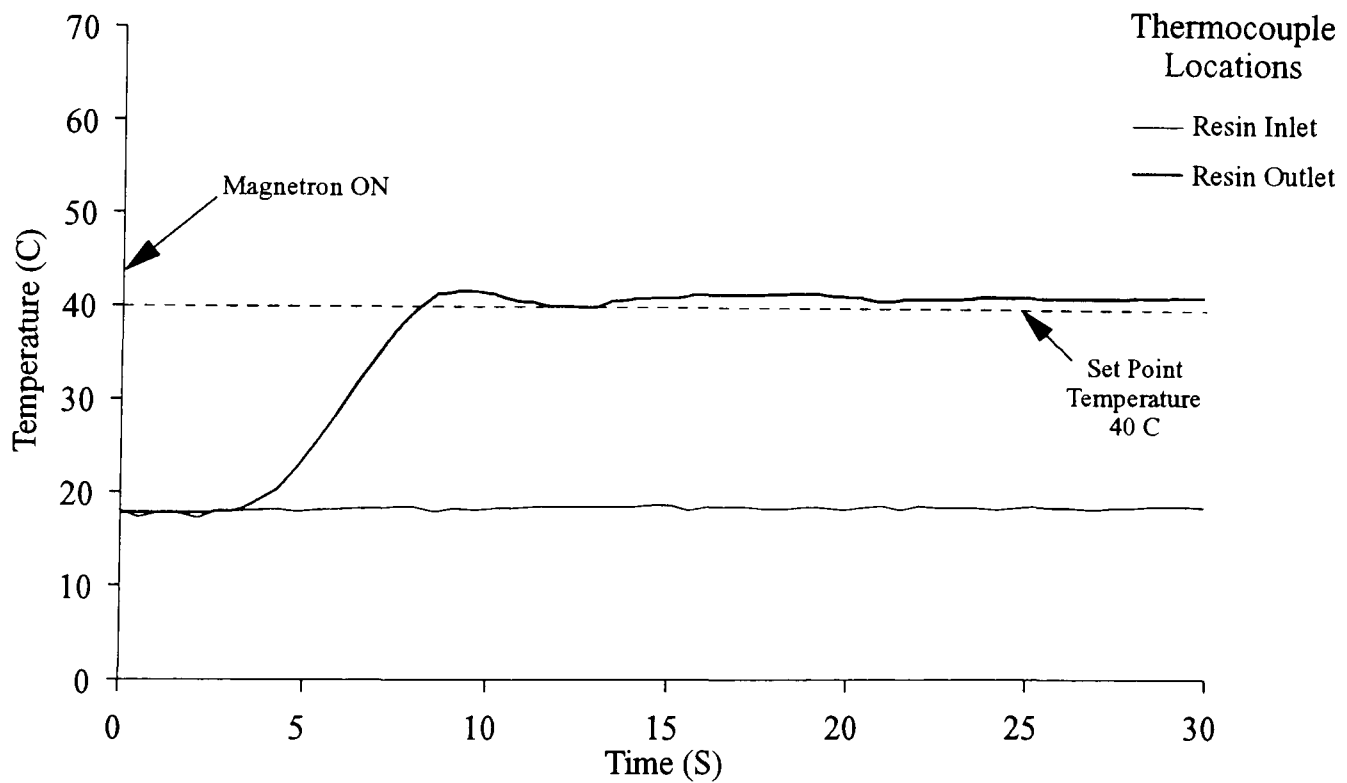
Moulding No.	5333A	Supply Pressure	1.8 bar
Resin	Derakane 8084	Mould Temperature	60 C
Catalyst	2% Perkadox 16	Set Point Temperature	50 ± 3 C
Reinforcement	Motorsport Layup	Avg Resin Temperature	40.0 C
Fibre Volume Fraction	Approx. 18%	Microwave Power	4500 W

Figure 5.4 Thermal history of an undershield moulding to demonstrate the temperature control characteristics of an ON-OFF power controller



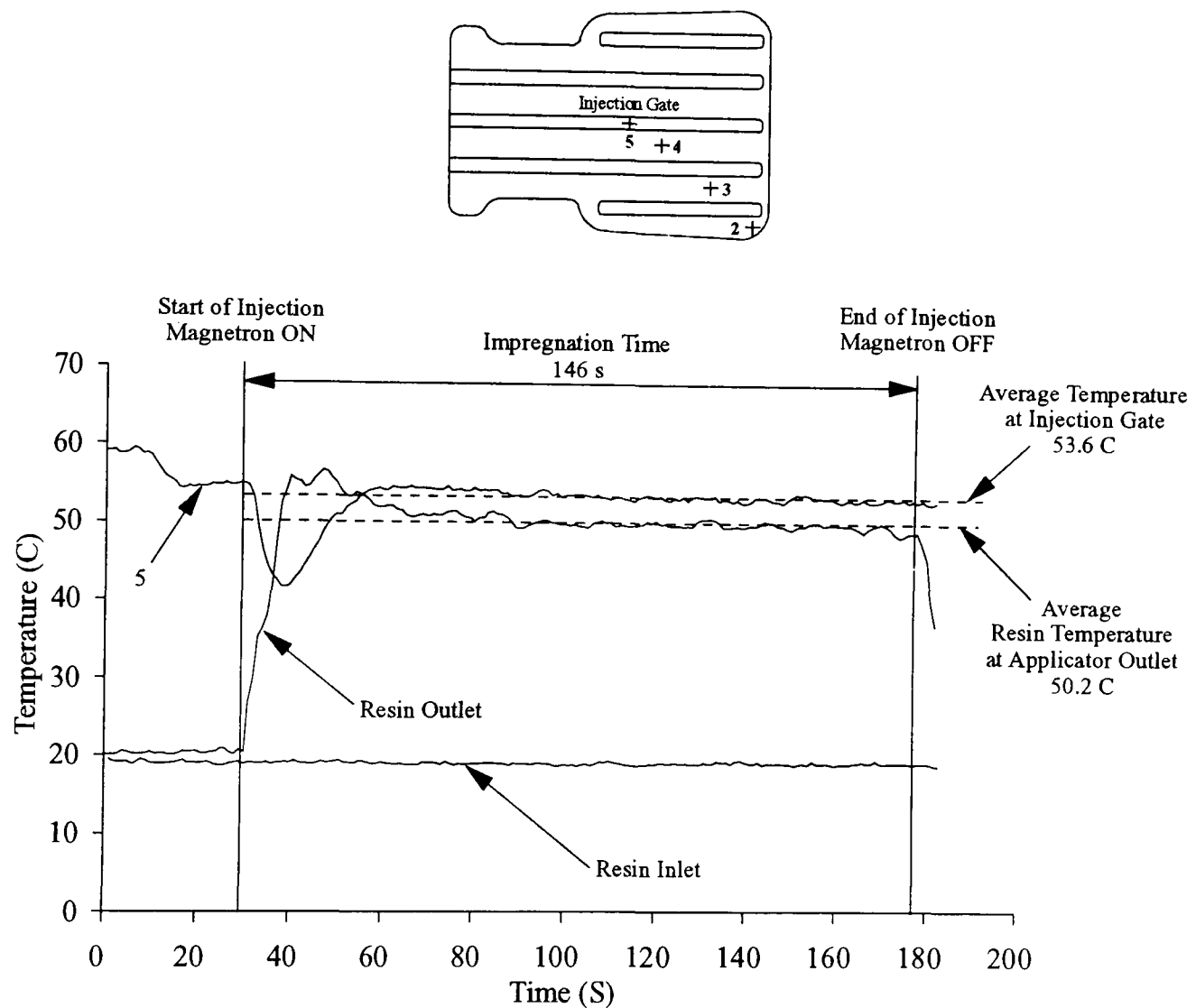
Trial No.	Tune022	Set Point Temperature	40 C	<b>Ku</b>	<b>80.0</b>
Resin	Synolac 6345	Resin Temperature	NA	<b>Pu</b>	<b>7.0</b>
Catalyst	NA	Supply Pressure	1.3 bar		

Figure 5.5a Temperature response for a marginally stable system at a set point temperature of 40 C using the Ziegler-Nichols tuning method



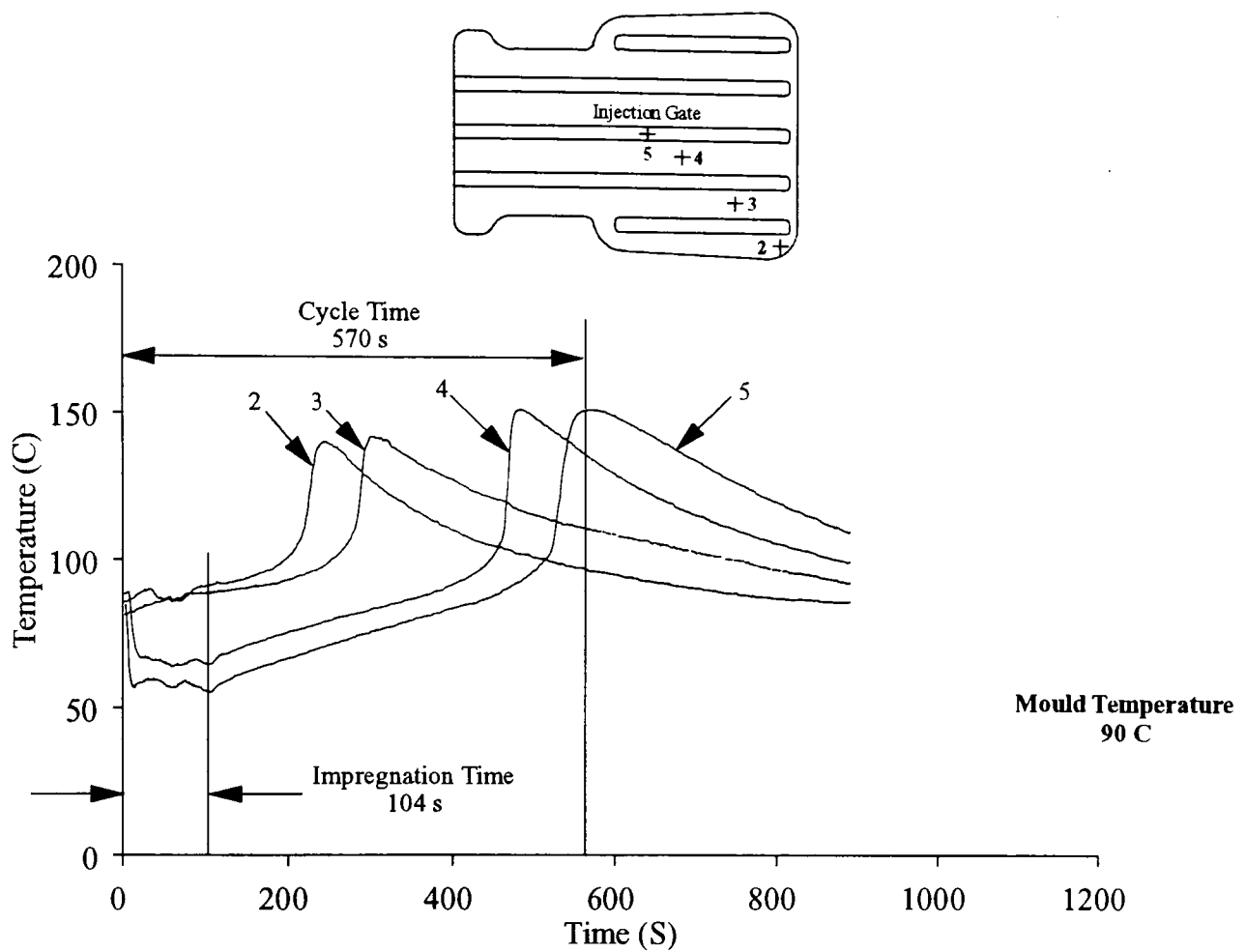
Trial No.	Tune027	Set Point Temperature	40 C	<b>Kp</b>	<b>48</b>
Resin	Synolac 6345	Resin Temperature	41.0 C	<b>T<sub>I</sub></b>	<b>3.50</b>
Catalyst	NA	Supply Pressure	1.3 bar	<b>T<sub>D</sub></b>	<b>0.88</b>

Figure 5.5b Temperature response of the microwave resin preheating system using PID power control tuned at a set point temperature of 40 C



Moulding No.	5368	Supply Pressure	2.0 bar
Resin	Derakane 8084	Mould Temperature	60 C
Catalyst	2% Perkadox 16	Set Point Temperature	50 C
Reinforcement	Motorsport Layup	Avg Resin Temperature	50.2 C
Fibre Volume Fraction	Approx. 18%	Microwave Power	Variable

Figure 5.6 Thermal history of an undershield moulding to demonstrate the temperature control characteristics of the PID power controller



Moulding No.	5463	Fibre Volume Fraction	16%
Resin	Synolac 6345	Mould Temperature	90 C
Catalyst	1% TBPEH	Resin Temperature	50.7 C
Reinforcement	U754-450	Supply Pressure	<b>1.8 bar</b>

Figure 5.7a Thermal history of undershield moulding produced by automatic operation of the adapted resin preheating system under PID control

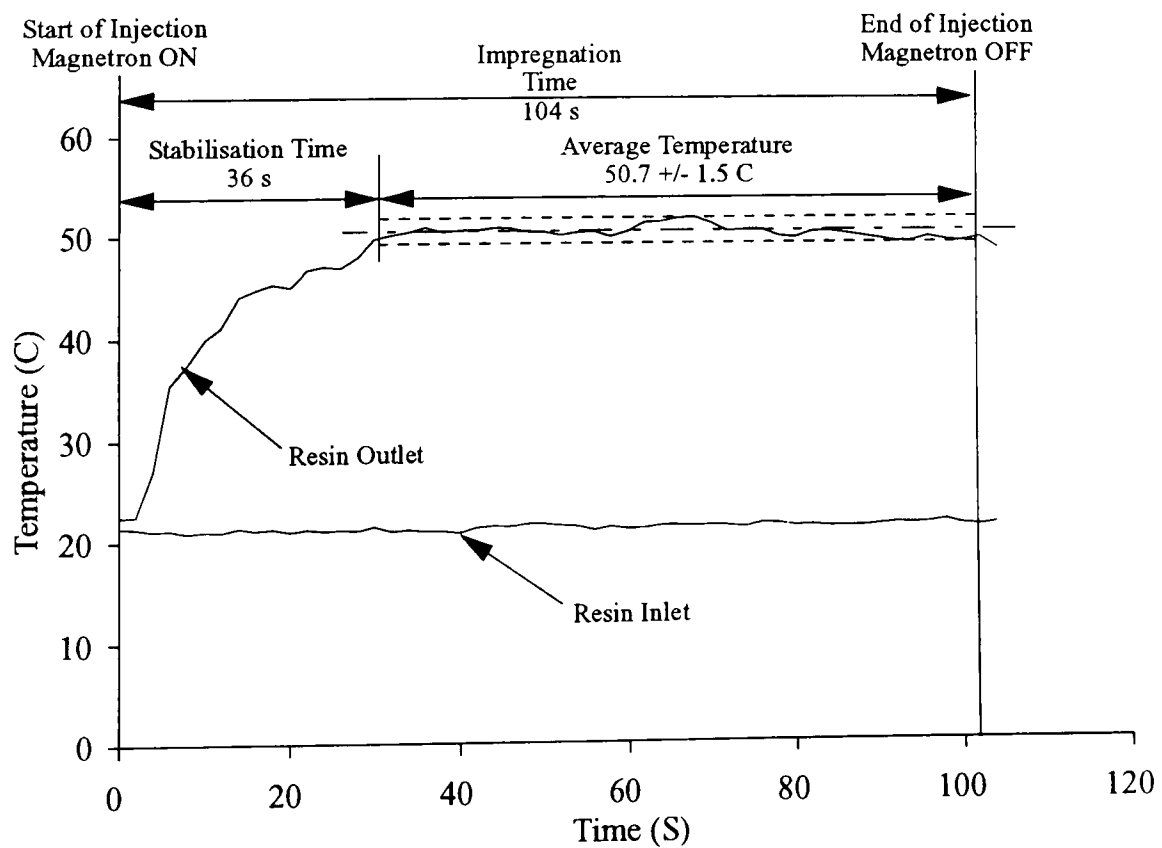


Figure 5.7b Resin thermal history at the microwave applicator during impregnation of undershield moulding 5463

## RTM Processing Advantages through Microwave Resin Preheating

---

### 6.1 Introduction

Modifications made to the in-line microwave resin preheating system to permit operation in the automatic RTM cycle were described in Chapter 5. Using this adapted system a 37% reduction in cycle time was demonstrated compared to conventional RTM. However, further investigation was necessary to establish the effect of microwave resin preheating on RTM to minimise cycle times.

This chapter is concerned principally with cycle time reduction strategies involving the adapted microwave resin preheating system. Moulding trials were conducted with resin injected at constant temperature. Like conventional resin injection at ambient temperature, cycle time was dictated by cure at the injection gate. Furthermore, significant pressure developed within the mould at that location during the cure phase. Kendall [20] determined that this pre-exotherm pressure could exceed the injection pressure, making it an important consideration in mould design. A second technique to ramp the resin temperature during injection was developed, resulting in maximum cycle time reductions. The resin cure sequence could be controlled to promote coincident cure across the mould. Thus, cycle time was no longer restricted by cure at the injection gate. In addition, the pre-exotherm pressure was reduced significantly by this technique, suggesting that mould deflections would be reduced for a more uniform laminate thickness. An analysis of the variation in undershield thickness was conducted to confirm this hypothesis. A more complete investigation into the effect of microwave resin preheating on RTM laminates is present in Chapter 7.

## 6.2 Constant Resin Temperature Injection

Conventional RTM is a non-isothermal process whereby resin is injected at constant ambient temperature into a heated mould, in turn reducing the temperature near the injection gate. Figure 6.1 shows a thermal history of the process using a centre pin injection gate. The first portion of resin flows from the centre of the mould to the periphery, and is heated by the mould in the process. This resin has the longest flow path and is exposed to elevated temperatures for the longest period of time. It is, therefore, the first to cure as indicated by the exotherm peak (position 2). Subsequent resin entering the mould travels a shorter distance and has a reduced residence time, so that it cures after the resin at the periphery. The last portion of resin injected remains stationary at the injection gate (position 5), and has the shortest residence time. Furthermore, the temperature of the preform and mould at this location has been quenched by the preceding resin so that thermal recovery by the system is necessary before the resin will reach its activation temperature. Resin cures last at the injection gate for these reasons, and therefore determines the cycle time.

The cycle time could be reduced by decreasing the thermal quench near the injection gate. The mould would then lose less heat to the flowing resin so that its temperature would be greater at the end of impregnation. As a result, the time to heat the last portion of resin at the injection gate to the activation temperature would be reduced. A series of undershield mouldings were produced with resin injected at a constant elevated temperature to determine the effect on the RTM cycle. The first series of mouldings was produced at a mould temperature of 60°C and is presented in Section 6.2.1. The mould was heated to 90°C for the second series of undershield components produced in Section 6.2.2. A different resin system was used at each mould temperature preventing a direct comparison between the two studies, but a qualitative analysis could be performed based upon the established trends. Resin formulations are listed in Section 4.5 with a comparison between the systems shown in Figure 4.9.

### **6.2.1 Constant Resin Temperature Injection into a 60°C Mould**

Undersheild mouldings were produced using the adapted in-line microwave resin preheating system at a mould temperature of 60°C. A benchmark moulding was made with resin injected at ambient temperature (22°C) followed by mouldings made with resin preheated to 30°C, 40°C, 45°C, and 50°C. Successive increases in the resin temperature were expected to reduce the impregnation and cycle times. Since the resin preheat temperature was always less than the mould temperature, thermal quench occurred in every case.

#### **Impregnation and Cycle Time Effects**

Figure 6.2a shows the relationship between impregnation time and resin preheat temperature. Impregnation time was reduced by 41% by raising the resin temperature from 22°C to 40°C. Increasing the resin temperature to 45°C did not reduce the impregnation time further. However, injecting the resin at 50°C increased the impregnation time by 14 seconds as a result of premature gel within the mould prior to the end of injection, as indicated by the flow of gelled resin from the mould vents.

Figure 6.2b shows that increasing the resin temperature from 22°C to 40°C reduced the cycle time by 24%. Further reductions in cycle time were not realised by increasing the preheat temperature from 40°C to 50°C as demonstrated by a levelling of the curve.

These results suggested that for the resin system and moulding parameters used in this series of mouldings, the optimum resin preheat temperature was 40°C. Preheating the resin above this temperature did not reduce the impregnation or cycle times further. The interaction of two factors, resin viscosity and resin gel, were expected to produce this result. Figure 6.3 shows the relationship between viscosity and temperature for Synolac 6345 resin. Increasing the resin temperature from 20°C to 40°C lowers the viscosity by 70%, but only a 40% reduction occurs between 40°C and 50°C. This large reduction in viscosity between 20°C and 40°C was expected to improve resin flow through the mould and preform resulting in reduced impregnation and cycle times. This effect, however, was diminished over the 40°C to 50°C temperature range. Figure 4.9 shows that by increasing the resin

(II) temperature from 40°C to 50°C significantly reduces the initiation time. Premature gel within the mould occurred prior to the end of injection at a resin preheat temperature of 50°C which impeded resin flow, countering the effect of a lower resin viscosity. As a result, the impregnation time increased by 12% at that temperature.

### **Thermal Effects**

Figure 6.4 shows the peak exotherm temperatures along the mould diagonal (positions 2-5) at the five different resin preheat temperatures. The conventional RTM process was represented by injecting resin at ambient temperature (22°C). Peak exotherm temperatures varied from 106°C at the mould periphery (position 2) to 119°C at the injection gate (position 5) for this moulding. Injecting resin at 50°C did not increase peak exotherm temperatures significantly, suggesting that the kinetics of the cure reactions were not altered by resin preheating. Further evidence of this is presented in Figure 6.5 showing thermal histories at the injection gate for undershield components produced with resin at 22°C and 50°C. Increasing the resin temperature to 50°C reduced thermal quench by 23°C. Therefore, the temperature at the injection gate was greater at the end of impregnation (50°C), and initiation of the resin occurred in a shorter period resulting in a 24% reduction in cycle time. However, resin cure proceeded at approximately the same rate as indicated by the similarity in shape of the two thermal histories above the mould temperature (60°C). This result implied that conventional RTM moulds designed to operate below a thermal damage threshold, such as GRP or epoxy backed moulds, could use resin preheating safely to reduce cycle times.

### **Pressure Effects**

Figure 6.6 shows the peak pressures measured within the mould along the diagonal (positions 2-5) at the five different resin preheat temperatures. Two additional mouldings were manufactured at 23°C and 50°C. A pressure history was recorded at the injection gate for these two mouldings by replacing the thermocouple at that location with a pressure transducer as described in Section 4.2.1. An extreme

pressure variation was measured across the mould diagonal ranging from 1 bar at the mould periphery (position 2) to 26 bar at the injection gate (position 5). This high pressure peak was identified by Kendall [20] as a characteristic of centre gate injection (Section 4.4). Resin cured first at the mould periphery creating a rigid seal, entrapping a pool of uncured liquid resin within the mould. The resin temperature increased through mould heating and the exothermic cure reaction. As a result, thermal expansion of the resin occurred, generating a pressure that was transferred inward to the liquid resin pool. The cure front advanced inward and this pressure, termed the pre-exotherm pressure, became more extreme as the volume of liquid resin was reduced. Thus, the intensity of the pre-exotherm pressure was greatest at the injection gate. Kendall [20] recorded pre-exotherm pressures five times greater than the injection pressure, concluding that they were a vital consideration in mould design. The pre-exotherm pressure is derived from an inward advancing cure front. Constant temperature resin injection had no effect on the cure sequence so that high pre-exotherm pressures were measured at all elevated resin temperatures. However, the peak pressures did not differ significantly from those produced during conventional RTM, suggesting that microwave resin preheating could be used without causing additional mould damage.

### **6.2.2 Constant Resin Temperature Injection into a 90°C Mould**

A second series of undershield components was produced using the adapted in-line microwave resin preheating system at a mould temperature of 90°C (Section 4.5). A benchmark moulding was made with resin injected at ambient temperature (20°C) followed by four others at 30°C, 40°C, 50°C, and 55°C. A qualitative comparison of the trends established at both moulding temperatures (60°C and 90°C) was expected to provide a general understanding of constant resin temperature injection on the RTM process.

### **Impregnation and Cycle Time Effects**

Figures 6.7a and 6.7b show the effect of resin preheat temperature on the impregnation and cycle times for these mouldings. Increasing the resin

temperature from 20°C to 55°C reduced the impregnation time by 50% and the cycle time by 29%. Unlike the results obtained at a 60°C mould temperature (Figures 6.2b), the cycle time continued to decrease with increased resin temperature. Impregnation time tended towards further reductions with increased temperature, although at a decreased rate. Referring to Figure 4.9, this result suggested that at 55°C the resin system (III) was far removed from its gel temperature so that slight viscosity reductions continued to reduce the impregnation and cycle times. It was predicted that these values would plateau when the resin temperature reached an initiation time near 20 minutes (75°C) as occurred at the 60°C mould temperature (Figures 6.2a and 6.2b). However, raising the resin temperature required additional microwave power, which in turn increased the likelihood of premature cure within the cylindrical applicator. For this reason, the optimum resin preheat temperature could not be specified for this series of mouldings.

#### **Thermal and Pressure Effects**

Figures 6.8a and 6.8b show the peak exotherm temperatures and the peak mould pressures along the mould diagonal (positions 2-5) at the five different resin temperatures. The conventional RTM process was represented by injecting resin at ambient temperature (20°C). The trends illustrated in these figures are similar to those in Figures 6.4 and 6.6 produced at a 60°C mould temperature, although, a quantitative comparison cannot be made since equivalent resin systems were not used. Peak exotherm temperatures (Figure 6.8a) did not increase with increasing resin injection temperature. This result suggested the relationship between the peak exotherm temperature and the resin preheat temperature was independent of the resin formulation. Development of high pressures at the injection gate (Figures 6.6 and 6.8b) was demonstrated at both mould temperatures (60°C and 90°C). This result was anticipated since high pre-exotherm pressures were associated with the inward advancing cure front.

### **6.3 Discussion of Constant Resin Temperature Injection**

Numerous benefits of in-line resin preheating at constant temperature have been demonstrated. Impregnation and cycle times were decreased as a result of reduced resin viscosity and thermal quench. Average cycle time reductions of 27% were realised without increases in the peak temperatures or pressures within the mould during the cure phase. These results seemed to occur independently of the resin formulation. In addition, resin preheating was not expected to alter the cure kinetics of the resin system. The implication of these results was that a constant temperature resin injection system could be retrofitted in a conventional RTM facility to reduced cycle times without damaging the mould. Eliminating thermal quench by establishing an isothermal impregnation phase would further reduce cycle times. Preheating the resin to the same temperature as the mould is one means of eradicating thermal quench.

### **6.4 Isothermal Impregnation in RTM**

An undershield moulding was produced under isothermal impregnation conditions to demonstrate the relationship between resin residence time within the mould and cycle time. Figure 6.9 shows the thermal histories at the mould periphery (position 2) and the injection gate (position 5). The mould and preform temperature stabilised at 42°C prior to injection. The microwave was turned on after resin reached the injection gate proximity sensor, downstream of the microwave applicator, thus a small volume of resin that initially entered the mould was not preheated. As a result, the laminate temperature dropped to 34°C (position 5) before stabilising at 40°C after 12 seconds of heating. Cure occurred first at the mould periphery after 402 seconds, and last at the injection gate for a cycle time of 580 seconds.

Neglecting initial thermal quench, the first resin into the mould travelled to the periphery at a constant temperature of 40°C. The residence time for the last resin to enter the mould (40°C) at the injection gate commenced with the end of injection. The difference in resin residence time at the mould periphery compared to resin at the injection gate equalled the impregnation time (164 seconds). The time difference between the peak exotherm at each location (178 seconds) should

have equalled the impregnation time. Initial quench may have delayed the onset of cure at the mould periphery, accounting for the slight variation.

Excessive RTM cycle times have been attributed to thermal quench near the injection gate, as both the mould and resin must be reheated to the nominal mould temperature before the onset of cure. As a result, resin always cures last at the injection gate, since the cure front advances from the periphery towards the centre of the mould. However, this same cure sequence was generated under isothermal conditions in the absence of thermal quench, with the cycle time still being dictated by cure at the injection gate. This result occurred due to a difference in the resin residence time within the mould at elevated temperatures. Resin positioned at the mould periphery had the longest residence time and cured first, whereas resin cured last at the injection gate as its residence time within the mould was shortest. Ramping the resin temperature during injection was investigated to minimise the cycle time by altering the cure sequence.

### **6.5 Ramped Resin Temperature Injection**

A series of undershield mouldings were produced by ramping the resin temperature during injection to alter the cure sequence. A benchmark moulding, representing the conventional RTM process, was made by injecting resin at ambient temperature (24°C) into a mould heated to 40°C (Section 4.5). Four additional mouldings were produced by ramping the resin temperature as follows: 40-45°C, 40-50°C, 40-55°C, and 40-60°C. The preheating sequence was based upon a linear ramping of the resin set point temperature as a function of the total mass of resin injected. The set point temperature was initialised to 40°C at the start of injection (0 kg injected), and increased to the maximum temperature by the end of injection (9 kg injected).

#### **Thermal and Pressure Effects**

The effect of resin temperature ramping on the moulding thermal histories is shown in Figures 6.10a and 6.10b. Insignificant changes in the time to peak exotherm temperature resulted at the mould periphery (435 seconds on average) as shown in Figure 6.10a. Resin at that position was preheated to 40°C, and

experienced isothermal conditions. These results agreed closely with the isothermal moulding shown in Figure 6.9 which had a peak exotherm time of 402 seconds at the mould periphery. The time to peak exotherm at the injection gate (position 5) decreased with successive increases in the resin temperature ramping gradient. Like the constant resin temperature mouldings, ramping the resin temperature did not increase the value of the peak exotherm temperature significantly as can be seen in Figure 6.10b.

Figure 6.11 illustrates that the magnitude of the pre-exotherm pressures decreased as the ramping rate increased. Subsequent pre-exotherm pressure values were measured at the injection gate (22°C and 40-50°C) to illustrate the trend at that location.

## **6.6 Discussion of Ramped Resin Temperature Injection**

Ramped resin temperature injection allowed the cure sequence across the mould to be controlled by varying the ramping rate. The conventional RTM process was represented by injecting resin at ambient temperature (24°C), demonstrating the typical cure sequence, from the periphery to the centre of the mould. Separation between the first and last peak exotherm temperatures for the conventional moulding was 268 seconds as shown in Figure 6.12a. Ramping the resin temperature from 40-45°C during injection reduced the separation to 68 seconds. Applying a temperature ramp from 40-50°C led to coincident resin cure across the mould surface with a 36% reduction in cycle time over the moulding produced by conventional RTM as shown in Figure 6.12b. Virtually no separation (13 seconds) existed between the injection gate and mould periphery exotherm peaks. Increasing the temperature ramp further reduced the time to peak exotherm at the injection gate, and led to a reversed cure sequence from the centre to the periphery of the mould as shown in Figure 6.12c. However, since the time to peak exotherm at the mould periphery remained unchanged (435 seconds on average), no further reduction in cycle time was realised (Figure 6.10a). The condition of coincident cure resulted in the lowest cycle time possible for the specific resin system and moulding parameters.

## 6.7 The Effect of Pre-Exotherm Pressure on Component Thickness

Pressure increases along the diagonal from the mould periphery to the injection gate for mouldings with a typical cure sequence. As the cure front advances towards the centre of the mould, resin expansion during exotherm transmits a pressure to a volume of liquid resin centred at the injection gate, resulting in a high pressure in that region. Ramping the resin temperature to promote coincident cure reduced this pre-exotherm pressure near the injection gate to the hydrostatic level as no entrapment of the liquid resin pool occurred.

Disadvantages of a high pre-exotherm pressure have been identified by Kendall [20]. Damage could occur to moulds not designed to prevent pressure induced deflections. In addition, these deflections could result in part thickness variations. Kendall produced a series of plaque mouldings with pre-exotherm pressures ranging from 0 bar to 28 bar. The thickness of the laminate increased by an average of 10.2% at 28 bar leading him to conclude that high pre-exotherm pressures appreciably influenced component quality.

A study was performed to determine whether high pre-exotherm pressures at the injection gate affected the thickness of the undershield component. Disks (19 mm in diameter) were cut from four undershields near the mould periphery (position 2) and the injection gate (position 5). Two mouldings exhibited a typical cure sequence from the periphery to the centre of the mould and had high pre-exotherm pressures at the injection gate (between 17 bar and 25 bar). The remaining mouldings were produced under a coincident cure sequence and had low pre-exotherm pressures at the injection gate (approximately 1 bar). Variation in thickness of the disks between the mould periphery and injection gate was determined with the results being presented in Tables 6.1a and 6.1b.

The thickness across the mouldings with a high pre-exotherm pressure increased on average by 8.8% from the mould periphery to the injection gate. The average increase was reduced substantially to 4.1% for mouldings produced with a low pre-exotherm pressure. These results confirmed the findings by Kendall, and suggested that component quality is related directly to the pre-exotherm pressure.

## 6.8 Conclusion

Non-isothermal moulding conditions resulted in thermal quench at the injection gate, dictating component cycle time. Preheating resin to a constant temperature below the mould temperature decreased this thermal quench and resin viscosity leading to reduced cycle times. Isothermal moulding conditions eliminated this thermal quench entirely. However, cure at the injection gate continued to govern the cycle time due to a minimum resin residence time at that location. A typical cure sequence commencing at the mould periphery and advancing toward the injection gate characterised these mouldings. As a result of this cure sequence, high pre-exotherm pressures developed at the injection gate.

Ramped resin temperature injection was demonstrated resulting in coincident resin cure across the mould. Resin at the injection gate was preheated above the mould temperature to initiate cure more rapidly, and compensate for the minimal residence time. Coincident resin cure reduced the cycle time by 36%, and since the resin cured evenly, high pre-exotherm pressures did not develop at the injection gate. Preheating resin at a higher rate further reduced the cure time at the injection gate, but did not decrease the cycle time. Resin at the mould periphery cured more slowly than at the injection gate, dictating cycle time.

High pre-exotherm pressures produced an 8.8% variation in the mould thickness from the mould periphery to the injection gate. This variation was reduced to 4.1% by profiling the resin temperature to produce coincident resin cure. Injection by this technique reduced the pre-exotherm pressure to the hydrostatic level, and implied that mould deflections were minimised. This suggested that lighter and more thermally responsive shell moulds could be employed.

## **List of Tables**

- Table 6.1a Variation in thickness for mouldings with a high pre-exotherm pressure
- Table 6.1b Variation in thickness for mouldings with a low pre-exotherm pressure

## **List of Figures**

- Figure 6.1 Thermal history of the conventional RTM process using a centre pin injection gate
- Figure 6.2a Effect of resin preheat temperature on impregnation time for undershield components produced at a mould temperature of 60°C
- Figure 6.2b Effect of resin preheat temperature on cycle time for undershield components produced at a mould temperature of 60°C
- Figure 6.3 Viscosity versus temperature for Synolac 6345 polyester resin
- Figure 6.4 Effect of resin preheat temperature on the peak exotherm temperatures across the diagonal of the undershield component
- Figure 6.5 Thermal histories at the injection gate to demonstrate the similarities in the resin cure kinetics between mouldings made with and without in-line microwave resin preheating
- Figure 6.6 Effect of resin preheat temperature on the peak pressures across the diagonal of the undershield component
- Figure 6.7a Effect of resin preheat temperature on impregnation time for undershield components produced at a mould temperature of 90°C
- Figure 6.7b Effect of resin preheat temperature on cycle time for undershield components produced at a mould temperature of 90°C
- Figure 6.8a Effect of resin preheat temperature on the peak exotherm temperatures across the diagonal of the undershield component
- Figure 6.8b Effect of resin preheat temperature on the peak pressures across the diagonal of the undershield component
- Figure 6.9 Thermal history at the injection gate and mould periphery for an undershield moulding produced under isothermal conditions

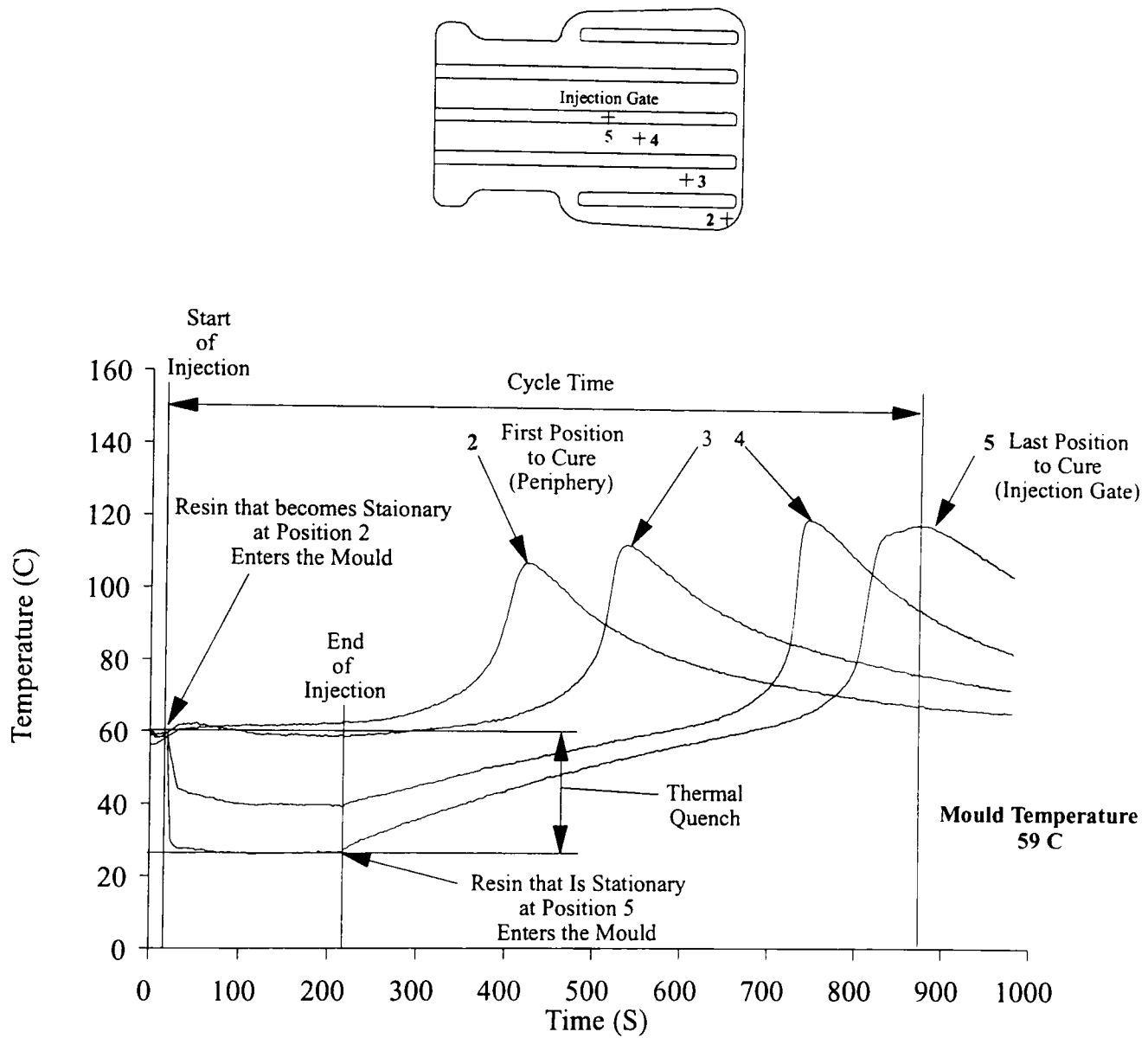
- Figure 6.10a Effect of ramped resin temperature on the time to peak exotherm across the diagonal of the undershield component
- Figure 6.10b Effect of ramped resin temperature on the peak exotherm temperatures across the diagonal of the undershield component
- Figure 6.11 Effect of ramped resin temperature on the peak pressures across the mould diagonal of the undershield component
- Figure 6.12a Thermal history for benchmark moulding at 40°C
- Figure 6.12b Thermal history for moulding produced with the resin temperature ramped from 40-50°C during injection
- Figure 6.12c Thermal history for moulding produced with the resin temperature ramped from 40-60°C during injection

**Table 6.1a Variation in Thickness for Mouldings with a High Pre-Exotherm Pressure**

Reference No.	Moulding Thickness (mm)		Increase in Thickness (%)
	Position 2	Position 5	
5456	7.84	8.51	8.5
5454	7.48	8.16	9.1
Average Values	7.66	8.34	8.8

**Table 6.1a Variation in Thickness for Mouldings with a Low Pre-Exotherm Pressure**

Reference No.	Moulding Thickness (mm)		Increase in Thickness (%)
	Position 2	Position 5	
5437	9.26	9.59	3.6
5435	9.10	9.51	4.5
Average Values	9.18	9.55	4.1



Moulding No.	5449	Supply Pressure	1.8 bar
Resin	Synolac 6345	Mould Temperature	59 C
Catalyst	2% Perkadox 16	Set Point Temperature	n/a
Reinforcement	U750-450	Avg Resin Temperature	<b>22 C</b>
Fibre Volume Fraction	16%	Power Control	n/a

Figure 6.1 Thermal history of the conventional RTM process using a centre pin injection gate

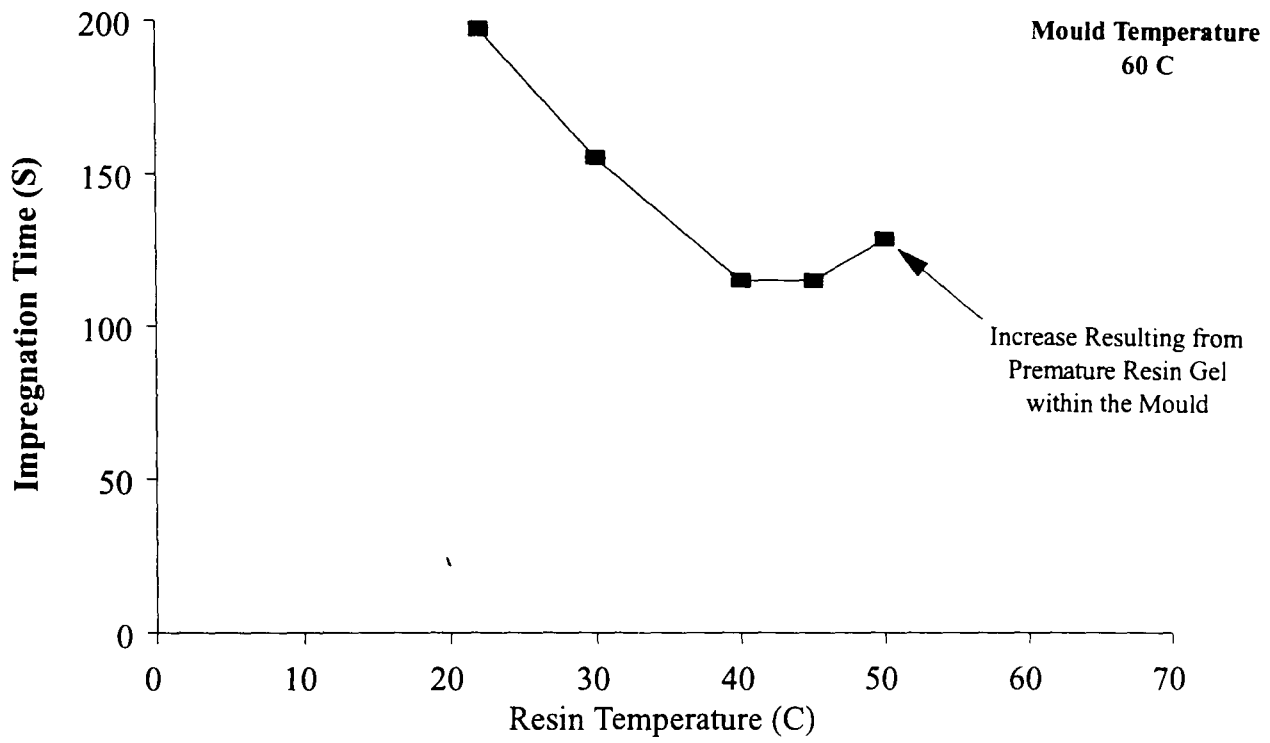


Figure 6.2a Effect of resin temperature on impregnation time for undershield components produced at a mould temperature of 60 C

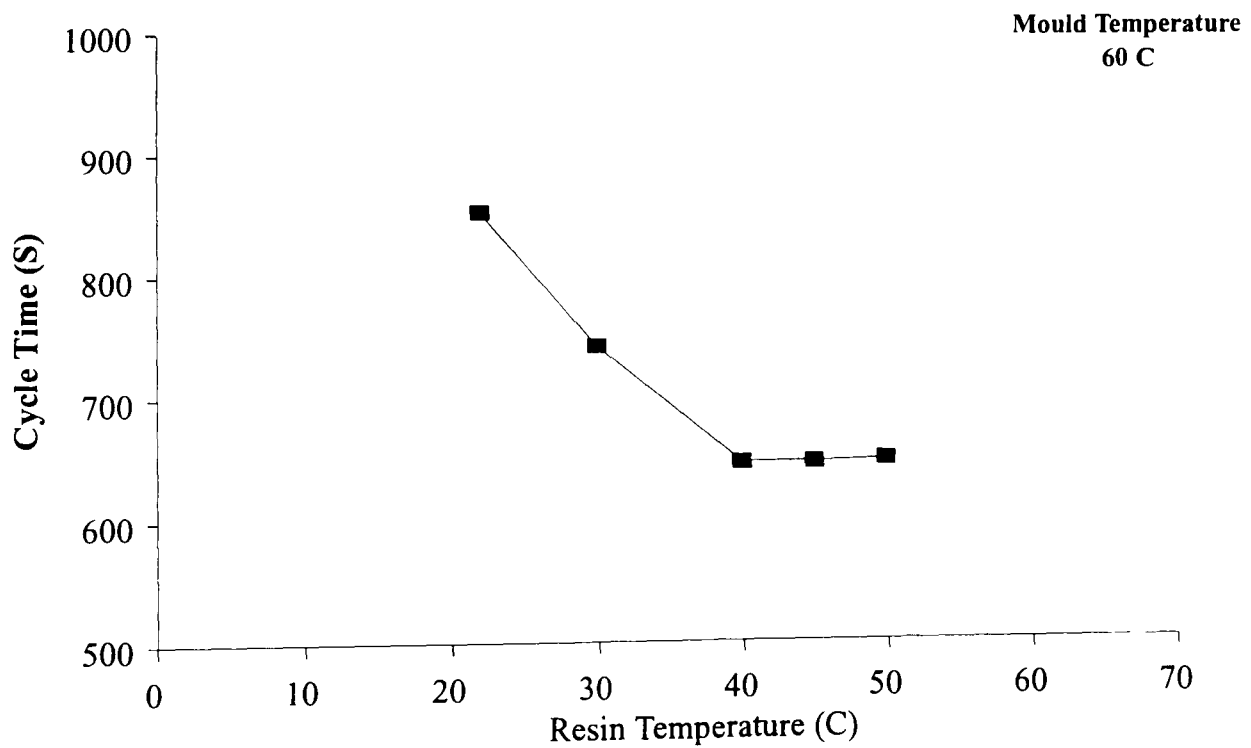


Figure 6.2b Effect of resin temperature on cycle time for undershield components produced at a mould temperature of 60 C

Data Presented by Hill [22]

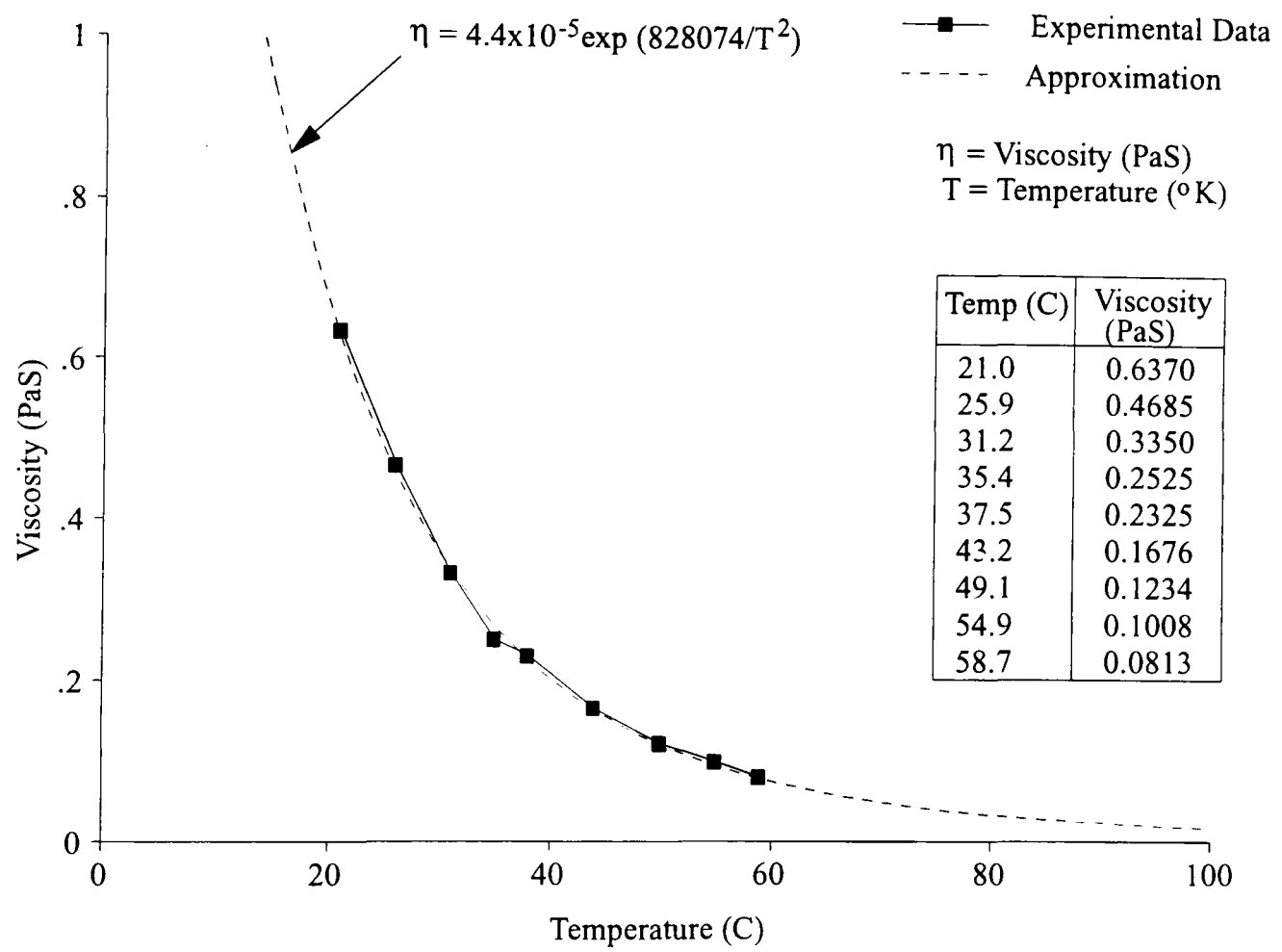


Figure 6.3 Viscosity versus temperature of Synolac 6345 polyester resin

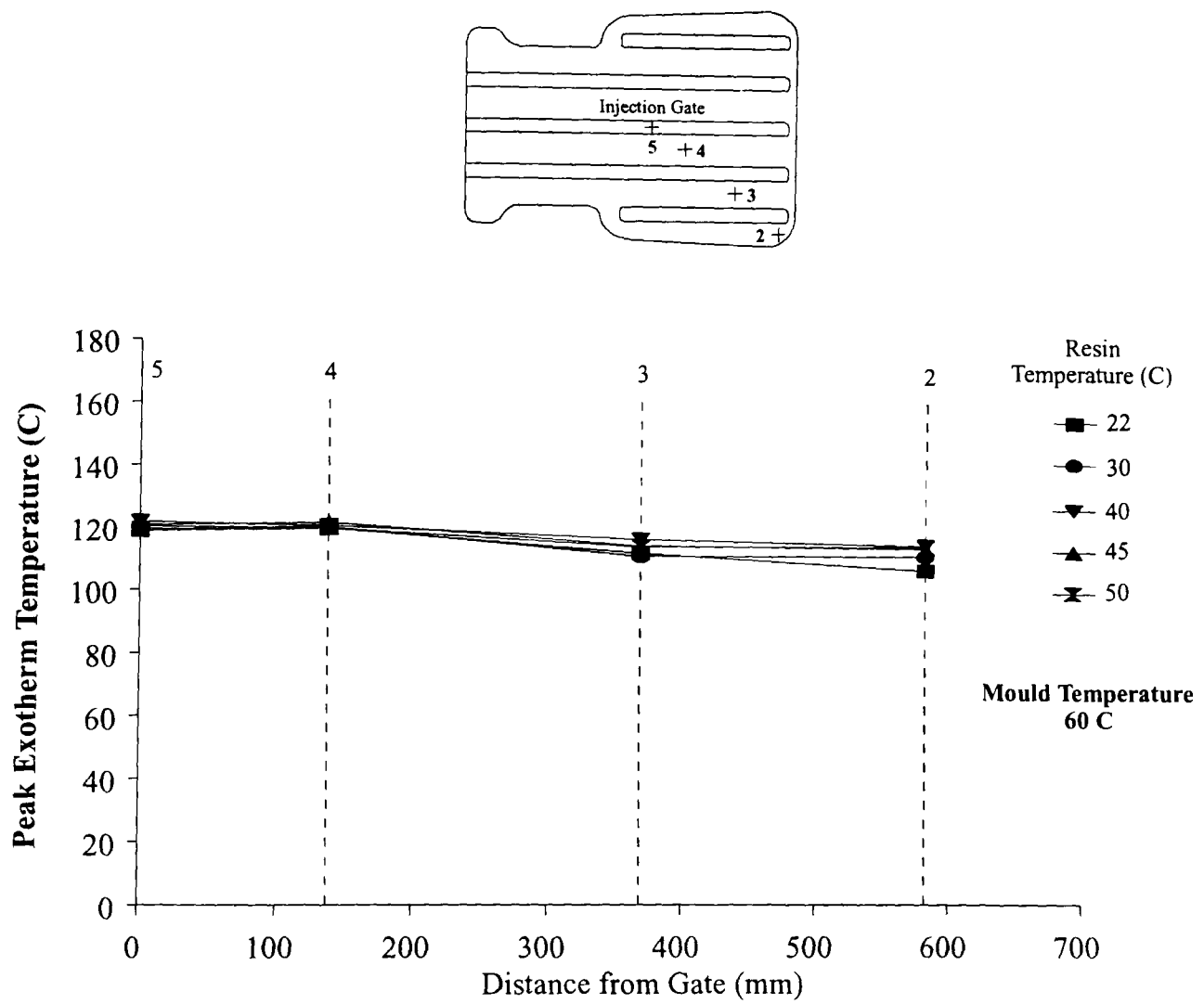
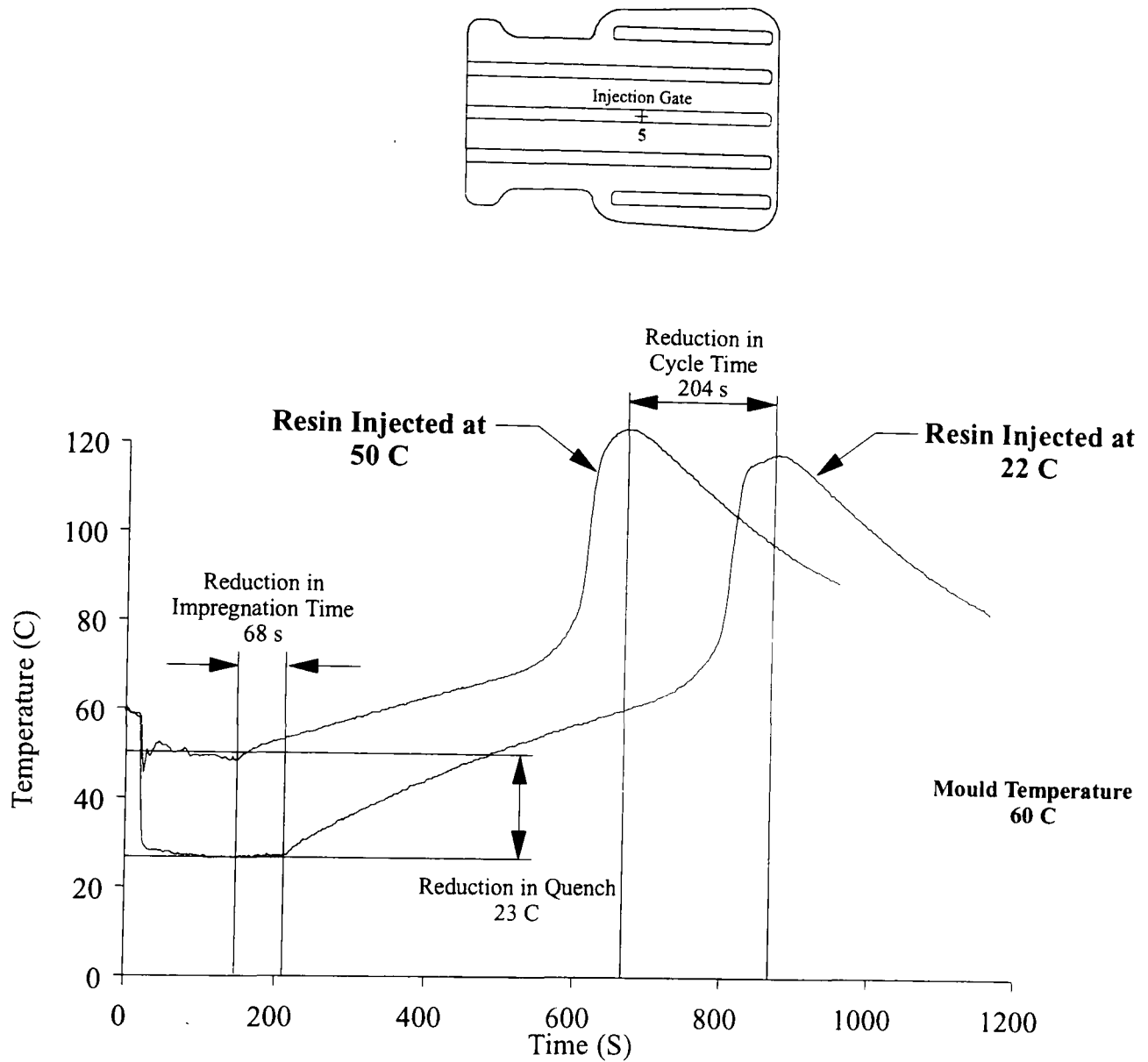


Figure 6.4 Effect of resin temperature on the peak exotherm temperatures across the diagonal of the undershield component



Moulding No.	5449	Supply Pressure	1.8 bar
Resin	Synolac 6345	Mould Temperature	59 C
Catalyst	2% Perkadox 16	Set Point Temperature	n/a
Reinforcement	U750-450	Avg Resin Temperature	<b>22 C</b>
Fibre Volume Fraction	16%	Power Control	n/a

Moulding No.	5446	Supply Pressure	1.8 bar
Resin	Synolac 6345	Mould Temperature	58 C
Catalyst	2% Perkadox 16	Set Point Temperature	50 C
Reinforcement	U750-450	Avg Resin Temperature	<b>50 C</b>
Fibre Volume Fraction	16%	Power Control	PID

Figure 6.5 Thermal histories at the injection gate to demonstrate the similarities in the resin cure kinetics between mouldings made with and without in-line microwave resin preheating

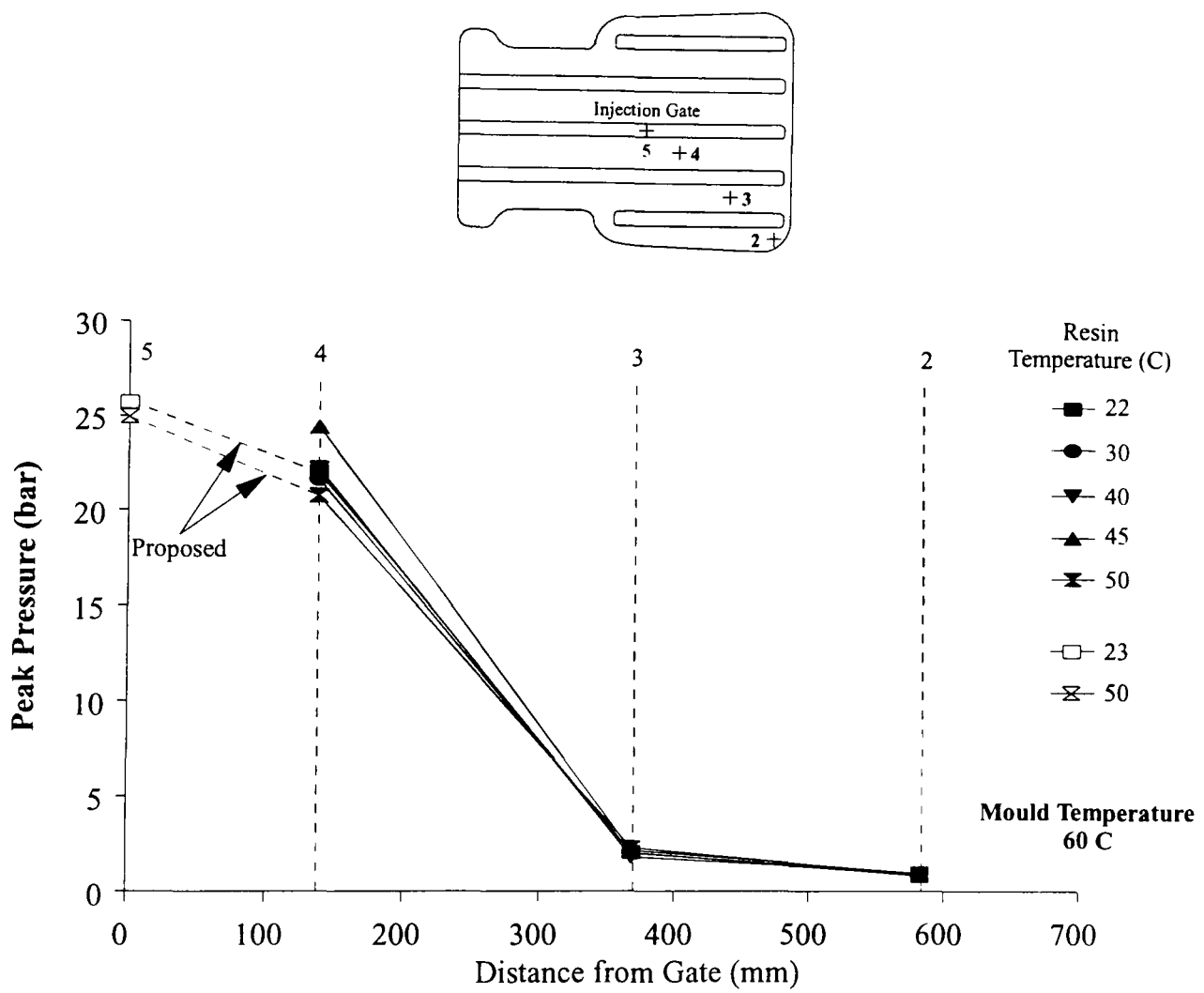


Figure 6.6 Effect of resin temperature on the peak pressures across the diagonal of the undershield component

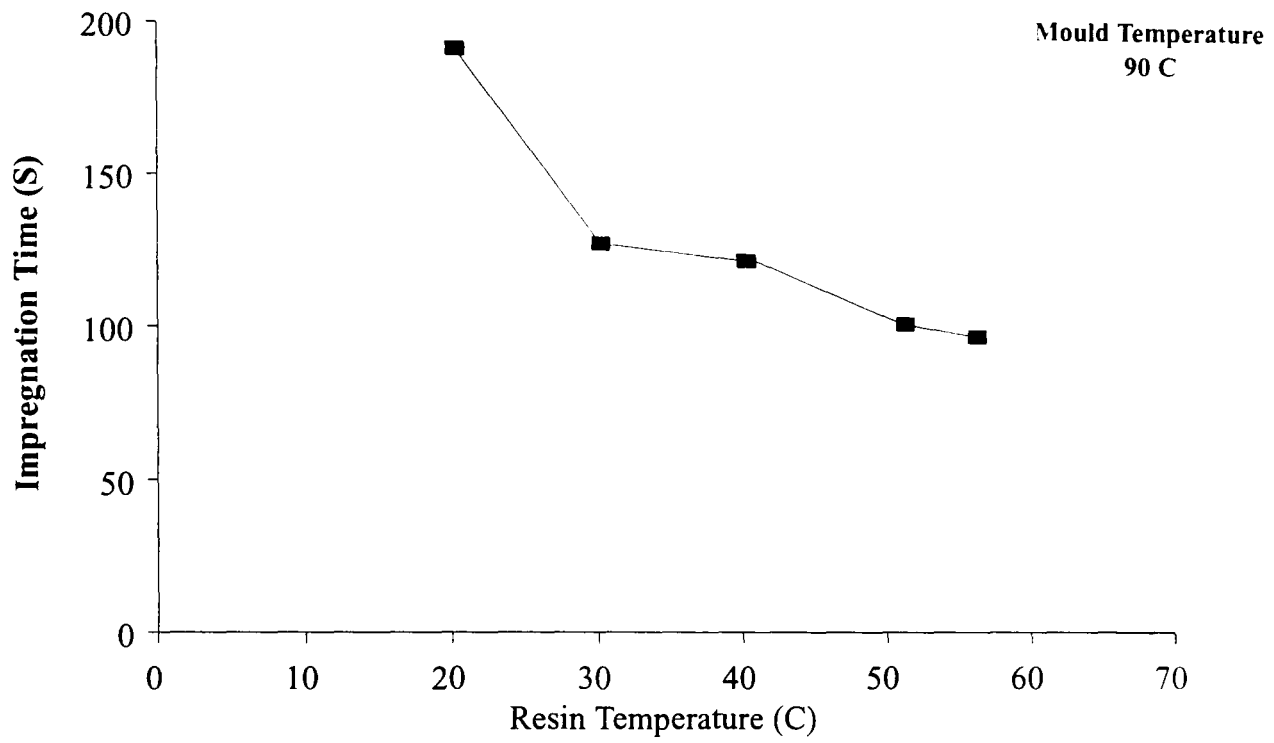


Figure 6.7a Effect of resin temperature on impregnation time for undershield components produced at a mould temperature of 90 C

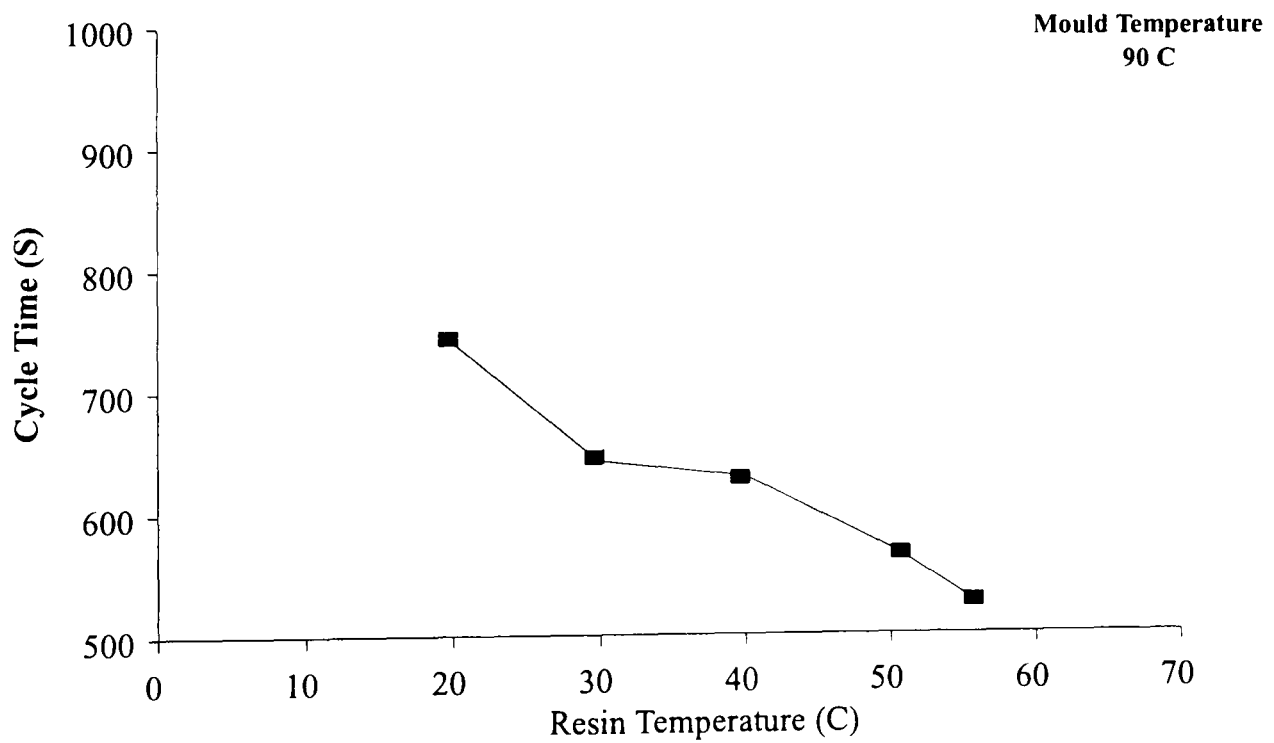


Figure 6.7b Effect of resin temperature on cycle time for undershield components produced at a mould temperature of 90 C

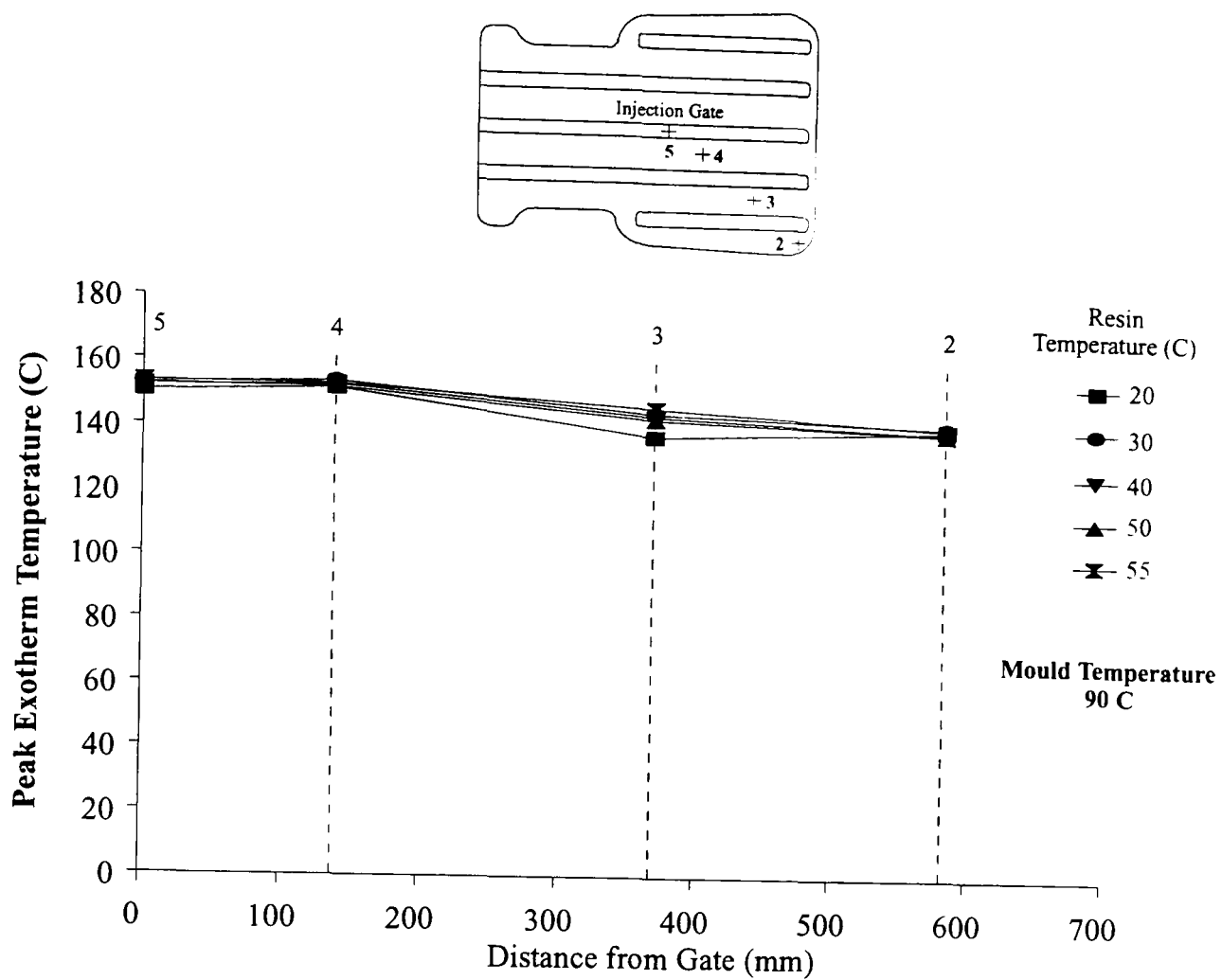


Figure 6.8a Effect of resin temperature on the peak exotherm temperatures across the diagonal of the undershield component

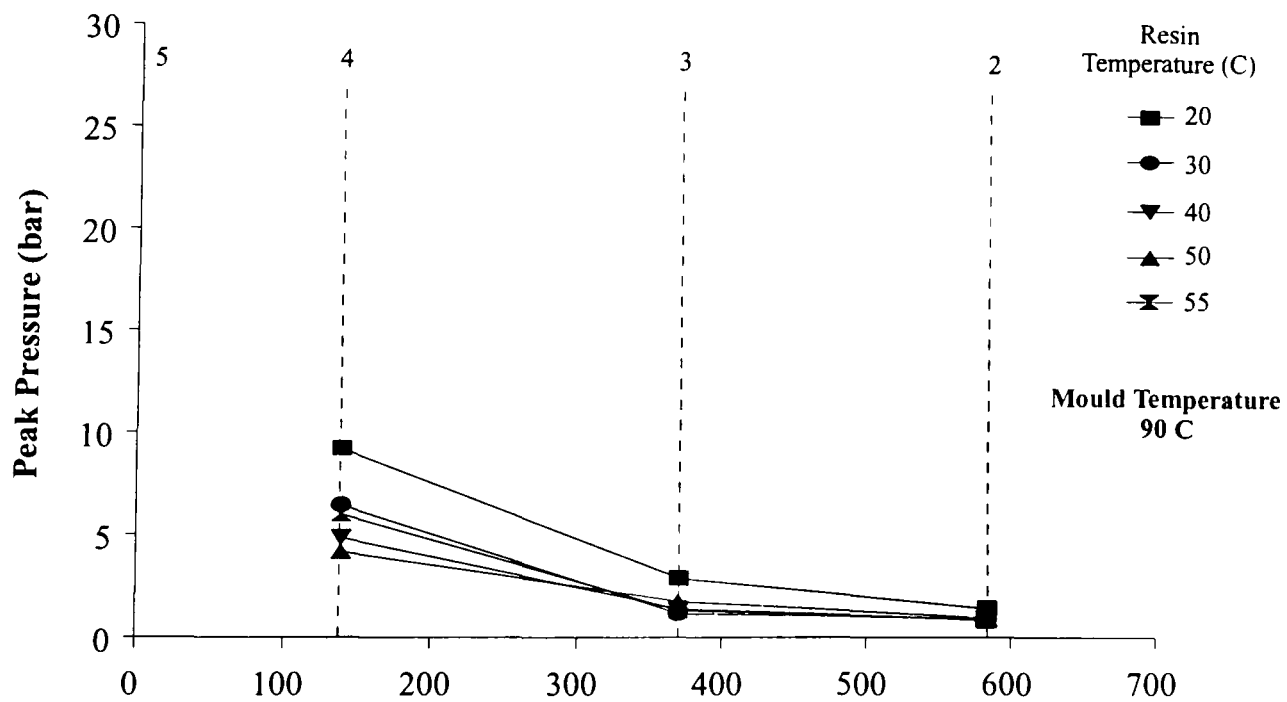
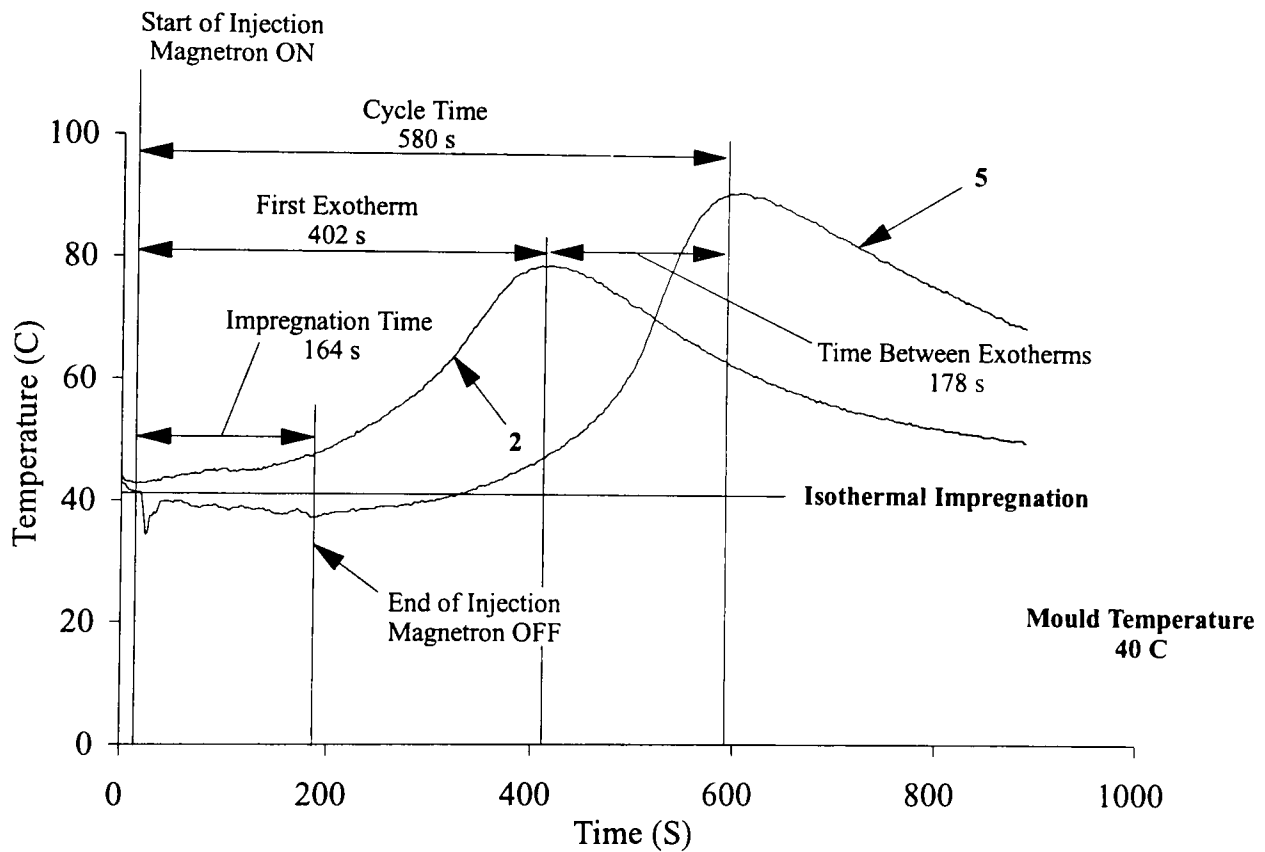
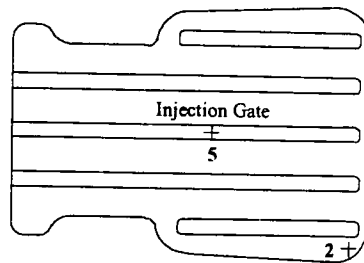


Figure 6.8b Effect of resin temperature on the peak pressures across the diagonal of the undershield component



Moulding No.	5433	Supply Pressure	1.8 bar
Resin	Synolac 6345	Mould Temperature	42 C
Catalyst	2% Trig 44B/0.5% NL49P	Set Point Temperature	40 C
Reinforcement	U750-450	Avg Resin Temperature	40 C
Fibre Volume Fraction	15%	Power Control	PID

Figure 6.9 Thermal history at the injection gate and mould periphery for an undershield moulding produced under isothermal conditions.

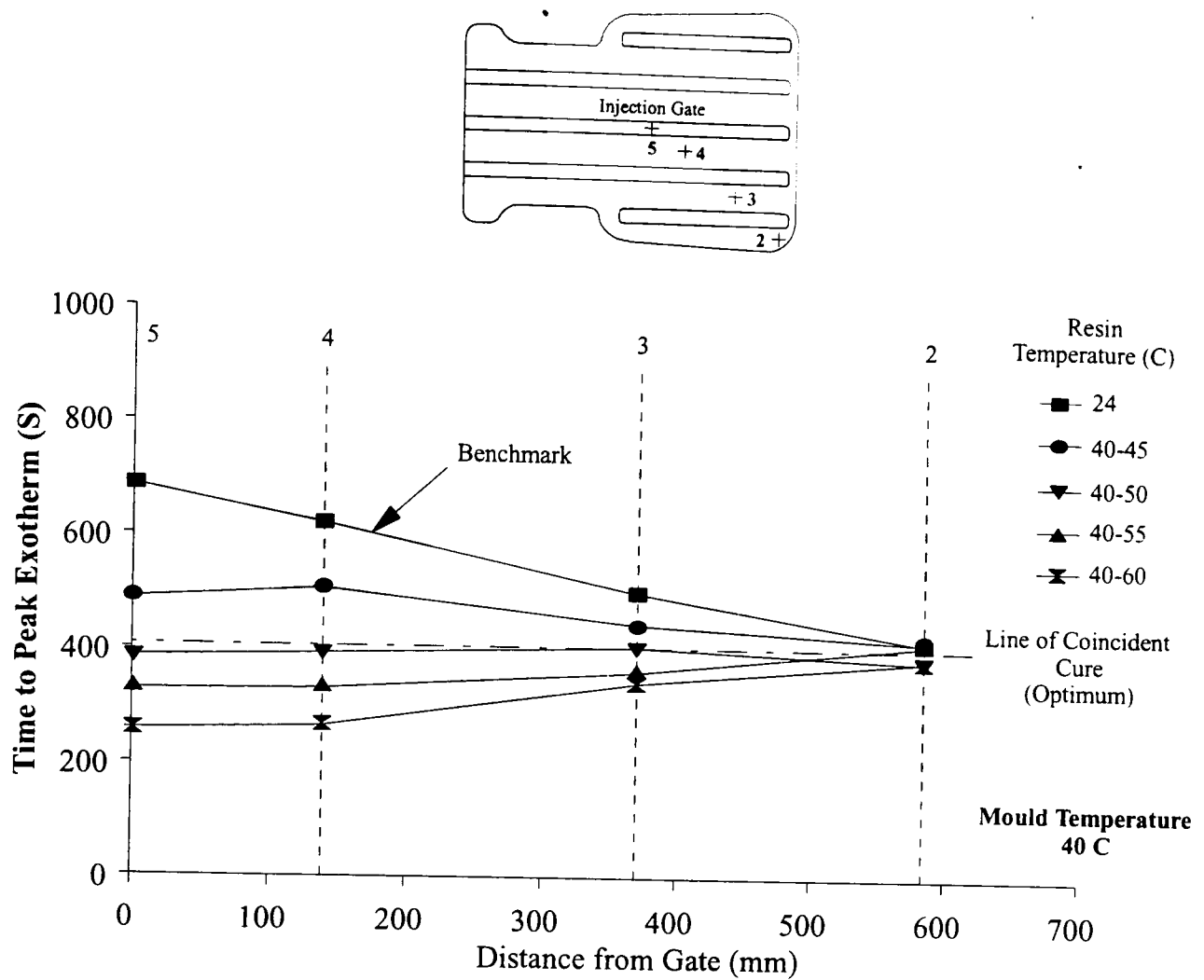


Figure 6.10a Effect of ramped resin temperature on the time to peak exotherm across the diagonal of the undershield component

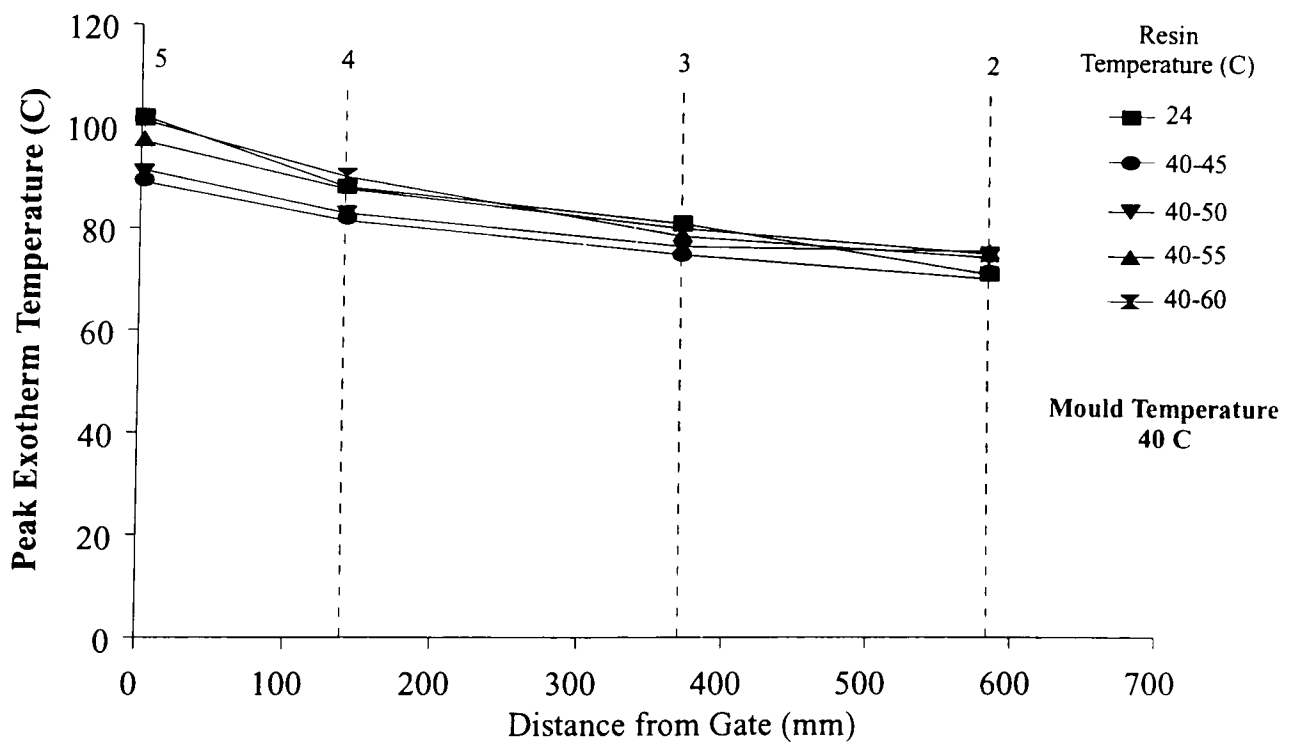


Figure 6.10b Effect of ramped resin temperature on the peak exotherm temperature across the diagonal of the undershield component

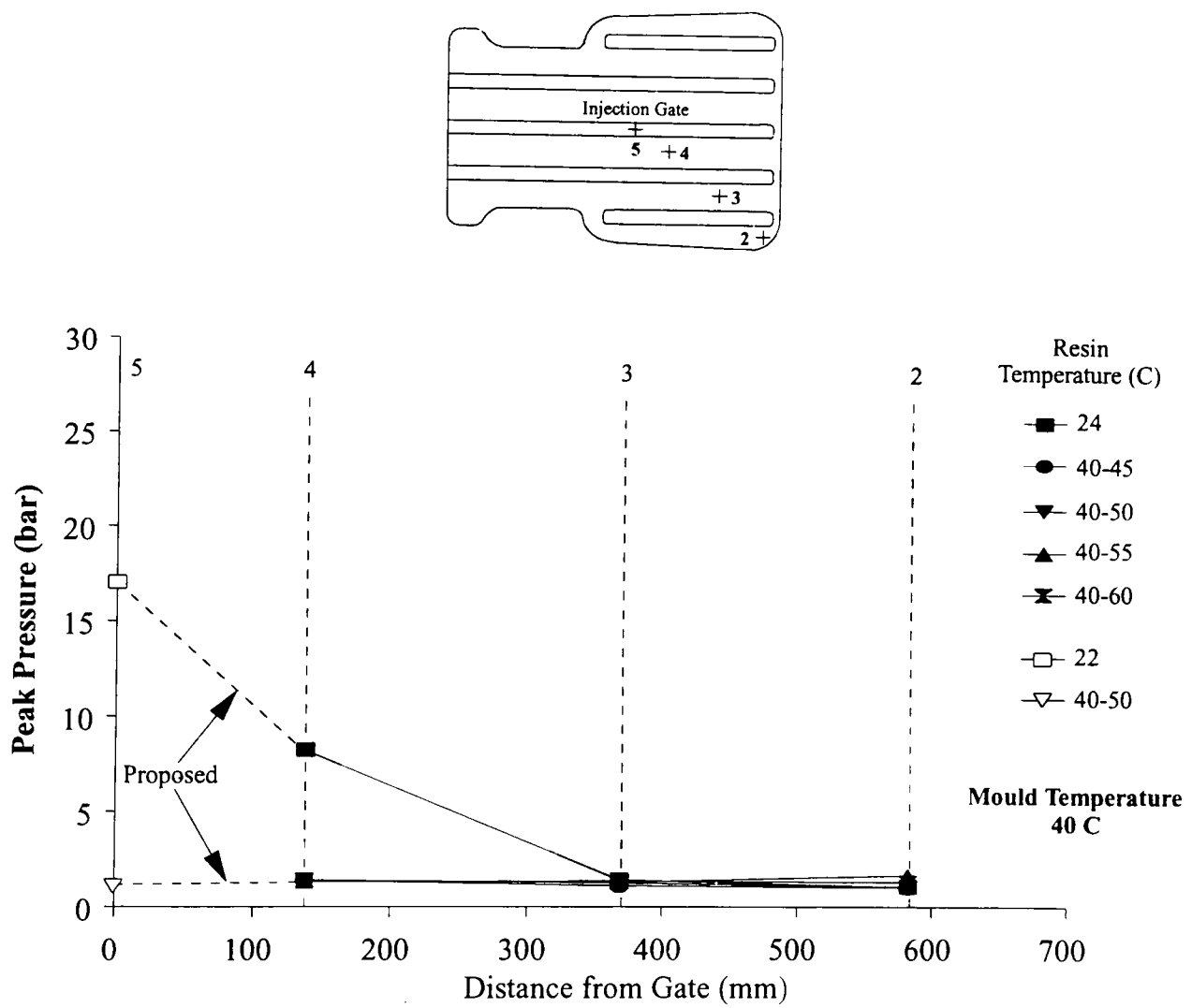


Figure 6.11 Effect of ramped resin temperature on the peak pressures across the diagonal of the undershield component

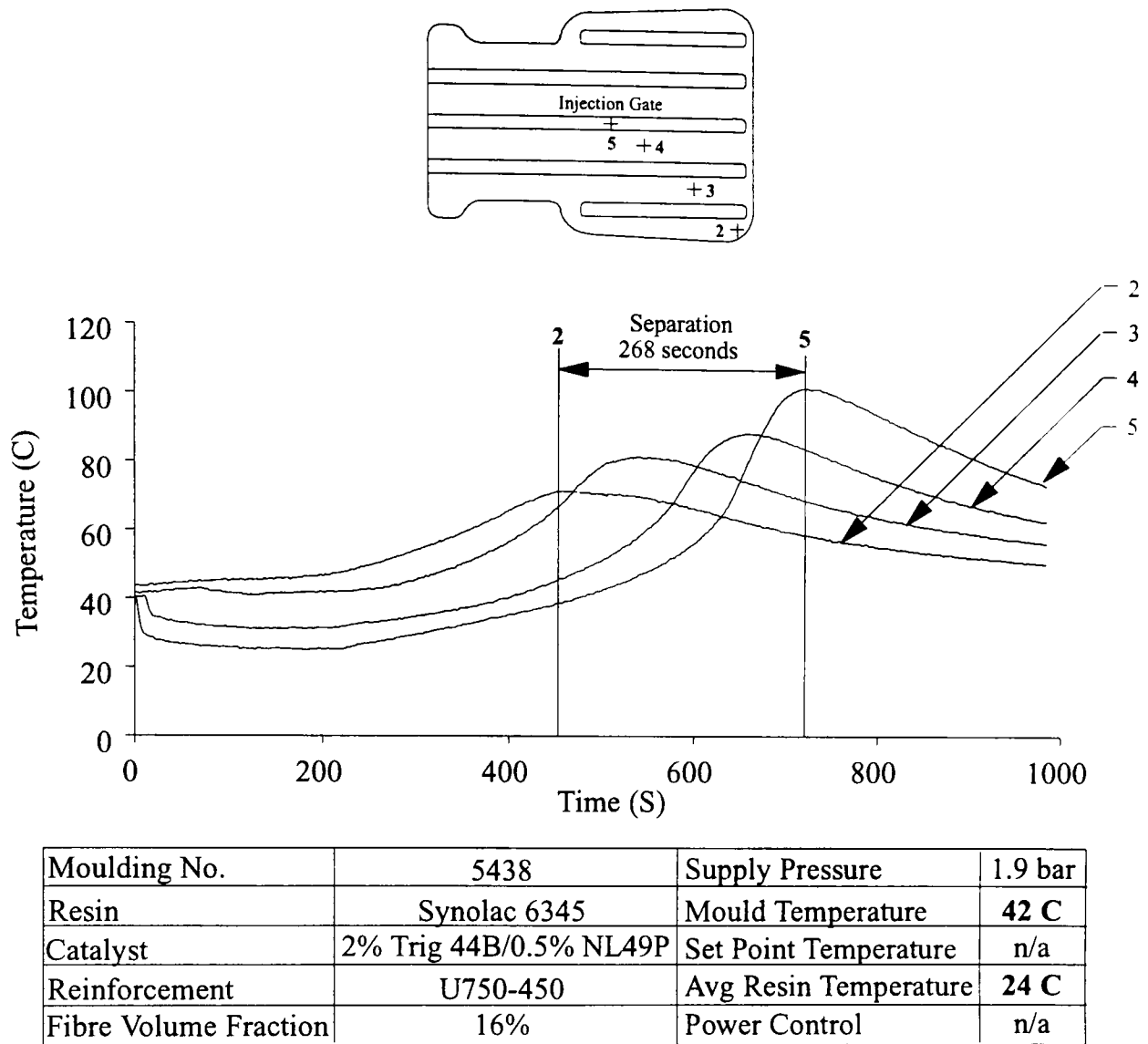


Figure 6.12a Thermal history for benchmark moulding at 40 C

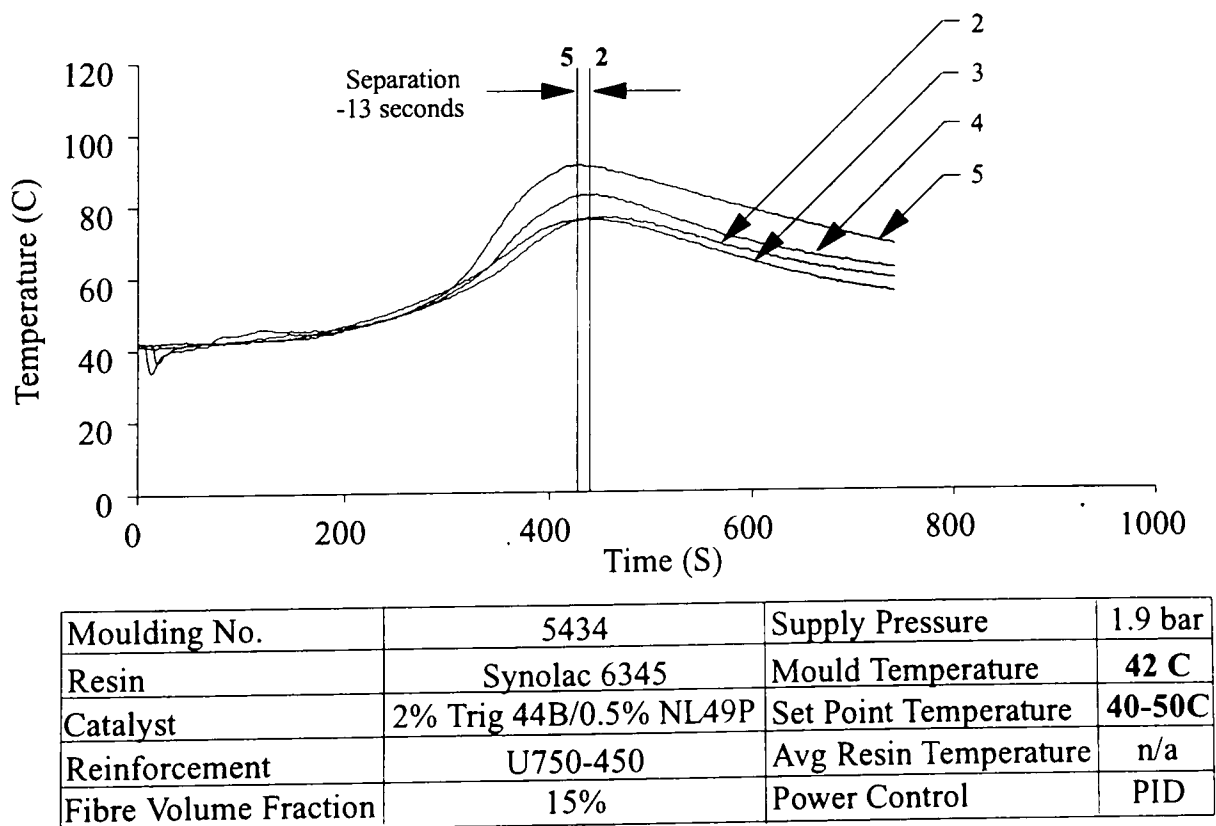
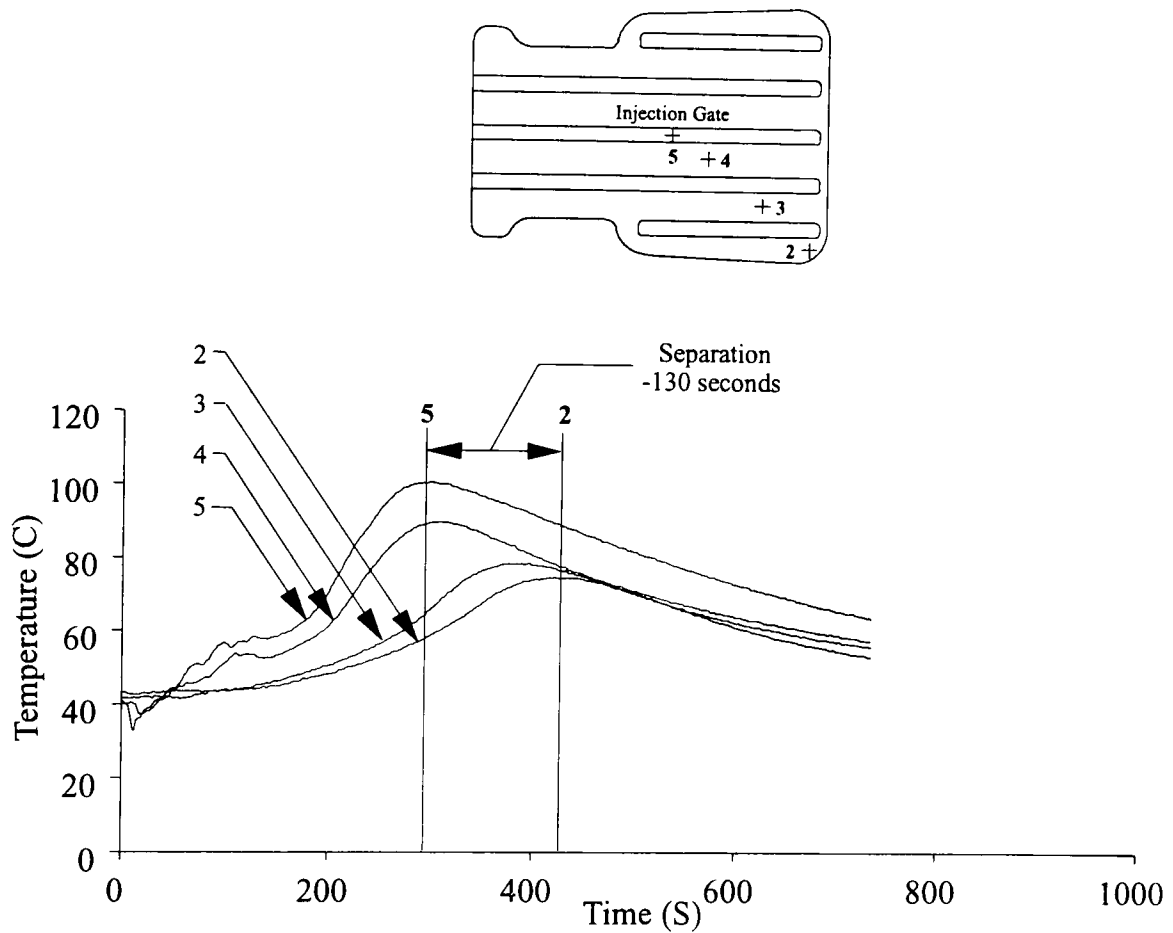


Figure 6.12b Thermal history for moulding produced with the resin temperature ramped from 40-50 C during injection



Moulding No.	5435	Supply Pressure	1.9 bar
Resin	Synolac 6345	Mould Temperature	41 C
Catalyst	2% Trig 44B/0.5%NL49P	Set Point Temperature	40-60 C
Reinforcement	U750-450	Avg Resin Temperature	n/a
Fibre Volume Fraction	15%	Power Control	PID

Figure 6.12c Thermal history for moulding produced with the resin temperature ramped from 40-60 C during injection

## The Effect of Microwave Resin Preheating on the Properties of RTM Laminates

---

### 7.1 Introduction

Use of the adapted microwave resin preheating system to reduce the moulding cycle time was demonstrated in Chapter 6. Increasing the resin temperature decreased thermal quench at the injection gate compared to conventional RTM. As a result, the cure reaction was initiated more rapidly and the cycle time was reduced. Furthermore, preheating the resin lowered its viscosity for less restricted flow through the preform, decreasing impregnation times. Lowering the resin viscosity was expected to enhance wet-out of the fibre bundles, improving the mechanical properties of RTM laminates. Tensile tests were conducted on mouldings produced at a series of resin preheat temperatures to investigate this possible effect. It was also suggested that preheating the resin would alter its thermal history, potentially resulting in a more highly crosslinked matrix structure. Degree of cure measurements were performed on laminates injected with resin at ambient temperature and preheated to 50°C to resolve this issue.

### 7.2 Tensile Properties of RTM Laminates Produced by Constant Resin Temperature Injection

Rudd and Revill [82] demonstrated that the tensile properties of RTM laminates were sensitive to cycle time. Decreasing the cycle time reduced the period available for fibre wet-out, prompting a decrease in the tensile modulus and strength of CFRM laminates. Reducing the resin viscosity was expected to promote better flow through the preform and enhance fibre wet-out, for improved tensile properties. Hayward and Harris [83] showed that lowering resin viscosity by increasing the mould temperature produced no difference in the shear strength or modulus of moulded components. Preheating the resin at constant temperature

was investigated to determine if this viscosity reduction had an effect on the tensile properties of RTM laminates.

Five undershields components were produced with resin at 22°C, 30°C, 40°C, 45°C, and 50°C in a mould heated to 60°C (Section 4.5). Cycle time reductions of up to 24% were recorded during the manufacturing of these mouldings (Figure 6.2b). Specimens were cut from the undershield components at the locations shown in Figure 4.10 and tested as described in Section 4.6.1.

Figure 7.1a shows the variation in modulus as a function of the resin preheat temperature with the values listed in Table 7.1. Average modulus values ranged from 5.5 GPa to 7.0 GPa, although no statistically significant difference was measured. Figure 7.1b shows similar results for the laminate tensile strength as a function of resin preheat temperature. Variation in average strength values were negligible ranging from 112 MPa at 40°C and 126 MPa at 22°C. These results suggested that preheating the resin to a constant temperature during injection had no effect on the tensile properties of RTM laminates.

### **7.3 Tensile Properties of Laminates Produced by Constant Resin Temperature Injection Compared to Post-Cured Laminates**

The effect of post-cure time on tensile properties was demonstrated by Lindsey [14] who produced laminates with an equivalent resin system and reinforcement type to those made by constant resin temperature injection (Section 7.2). However, the resin was injected at ambient temperature into a 60°C mould, with a fibre volume fraction of 30% instead of 16% as in the present case. Tensile specimens were produced by Lindsey from these laminates and tested along the weft direction of the glass mat according to BS2782:Part 10:Method 1003. One group of specimens were tested directly after de-moulding, termed the as-moulded state, while additional sample groups were post-cured at 115°C by increments up to 24 hours before being tested.

The modulus values plotted in Figure 7.1a, and listed in Table 7.1, were compared to those for the post-cured mouldings. Krenchel's [84] modified rule of mixtures expression was used to scale the modulus values at 16% volume fraction to 30% volume fraction so that a comparison could be made with the samples

prepared by Lindsey (Appendix 7.1). The scaled values are listed in Table 7.1, and the range of moduli have been superimposed on Lindsey's values in Figure 7.2. Lindsey showed that the modulus increased by 69% to 12.7 GPa after one hour post cure, then fell 20% to 10.1 GPa after a 24 hour post-cure. The overall increase in modulus after post-cure was attributed to more complete curing of the resin (from 92% to 97% conversion) [14]. Laminates made with resin injected at constant temperature produced moduli between the as-moulded and 1 hour post-cure values. However, variations in the constant resin temperature mouldings were insignificant as mentioned in Section 7.2. These results suggested that preheating the resin prior to injection did not have a post-cure effect on the RTM laminates.

Analysis of tensile properties provided information on the overall effect of resin preheating on fibre reinforced laminates. However, further investigation was necessary to determine its effect on the resin system.

#### **7.4 Determination of Residual Styrene Content by Gas Chromatography**

Compared to resin injected at ambient temperature, resin injected at a constant elevated temperature experiences a different thermal history. As a result, the properties of the laminate matrix could be altered. Preheated resin would be nearer to its activation temperature at the end of injection, so that the polymerisation reaction may be initiated preferentially, resulting in a more highly crosslinked structure. Tensile tests on the laminates (Section 7.2) did not confirm this hypothesis. However, the strength of the fibre reinforcement, and the fibre to matrix interface was expected to dominate these results. A measurement of the degree of cure was necessary to understand the effect of resin preheating on RTM laminates.

The amount of residual styrene in the matrix can be related to degree of cure. A polyester resin consists of an unsaturated resin molecule dissolved in a styrene monomer to form a homogeneous solution. Curing is accomplished by copolymerisation of the styrene and unsaturated resin. In principle, copolymerisation will cease automatically when all the styrene has reacted. Based on the homogeneous nature of the resin, it is convenient to define the fully cured

state as having 0% residual styrene and the completely uncured state as having 100% residual styrene. Residual styrene content can be measured by gas chromatography.

The residual styrene content of two undershield mouldings was measured using the gas chromatography technique as described in Section 4.6.2. The first moulding was produced by injecting resin at ambient temperature (20°C) into the heated mould (60°C). The second moulding was produced under the same conditions with the resin being preheated to 50°C during injection. The amount of residual styrene at locations along the mould diagonal (positions 2-5) is shown in Figure 7.3. Insignificant variations in residual styrene levels were measured between the two mouldings. The majority of the undershield components (positions 2-4) were cured to approximately 93%. A higher degree of cure (97%) was measured at the injection gate for both undershield components. The reason for a higher degree of cure at the injection gate was not clear, however, a higher peak exotherm temperature has been related to a greater degree of cure [14].

An examination of the exotherm temperatures across the mould diagonal (positions 2-5) for the moulding produced with resin at ambient temperature is shown in Figure 7.4. The exotherm temperature at the mould periphery was 17°C lower than at the injection gate (103°C compared to 120°C). This would seem to explain the higher degree of cure at the injection gate (97% compared to 93%). However, the exotherm temperature at position 4 was only 1°C lower than at the injection gate, yet the degree of cure at that location was 92% compared to 97% at the injection gate.

## **7.5 Conclusion**

Resin preheated to a constant temperature had an insignificant effect on the tensile properties of RTM laminates. Tensile tests on laminates produced at a series of resin temperatures substantiated this result. Changes in the modulus and strength of the specimens as a function of the resin preheat temperature were negligible. This implied that preheating the resin to lower its viscosity did not improve fibre wet-out. However, since impregnation times were reduced, this suggested that the equivalent fibre wet-out had occurred over a shorter interval.

Preheating resin was determined to have no effect on the degree of cure for the laminates. This result suggested that while resin preheating altered the thermal history of the resin, it did not change the kinetics of the cure reactions. Figure 6.5 provides further evidence to support this claim. Preheating the resin to 50°C reduced the amount of thermal quench at the injection gate compared to the moulding produced with resin at 22°C. However, the similarity in shape of the thermal histories above the mould temperature (60°C) suggests that the cure reaction proceeded at the same rate for both mouldings.

The tensile properties of components produced using resin preheated to a constant temperature were not improved. However, no degradation in performance was demonstrated either. This implied that resin preheating could be used to reduce cycle times without lowering the structural integrity of RTM components.

## **List of Tables**

- Table 7.1      Laminate moduli for constant temperature mouldings at a fibre volume fraction of 16% and scaled to a fibre volume fraction of 30%

## **List of Figures**

- Figure 7.1a    Average modulus values for undershield mouldings produced under constant resin temperature injection
- Figure 7.1b    Average Ultimate Tensile Strength (UTS) values for undershield mouldings produced under constant resin temperature injection
- Figure 7.2      Variation in modulus due to post-cure by Lindsey [14] including a range of moduli for mouldings made under constant resin temperature injection
- Figure 7.3      Degree of cure along the undershield diagonal for mouldings produced with resin at 20°C and 50°C
- Figure 7.4      Thermal history along the undershield mould diagonal illustrating the relationship between peak exotherm temperature and degree of cure

**Table 7.1      Laminate Moduli for Constant Temperature Mouldings at a Fibre Volume Fraction of 16% and Scaled to a Fibre Volume Fraction of 30%**

<b>RESIN TEMPERATURE (C)</b>	<b>20</b>	<b>30</b>	<b>40</b>	<b>45</b>	<b>50</b>
<b>E (GPa)* 16% VF</b>	6.9 ± 0.6	7.0 ± 0.5	5.5 ± 0.6	5.9 ± 0.9	6.5 ± 0.9
<b>E (GPa)' 30% VF</b>	10.2	10.3	7.5	8.3	9.4

\* Refer to Figure 7.1a

' Refer to Figure 7.2

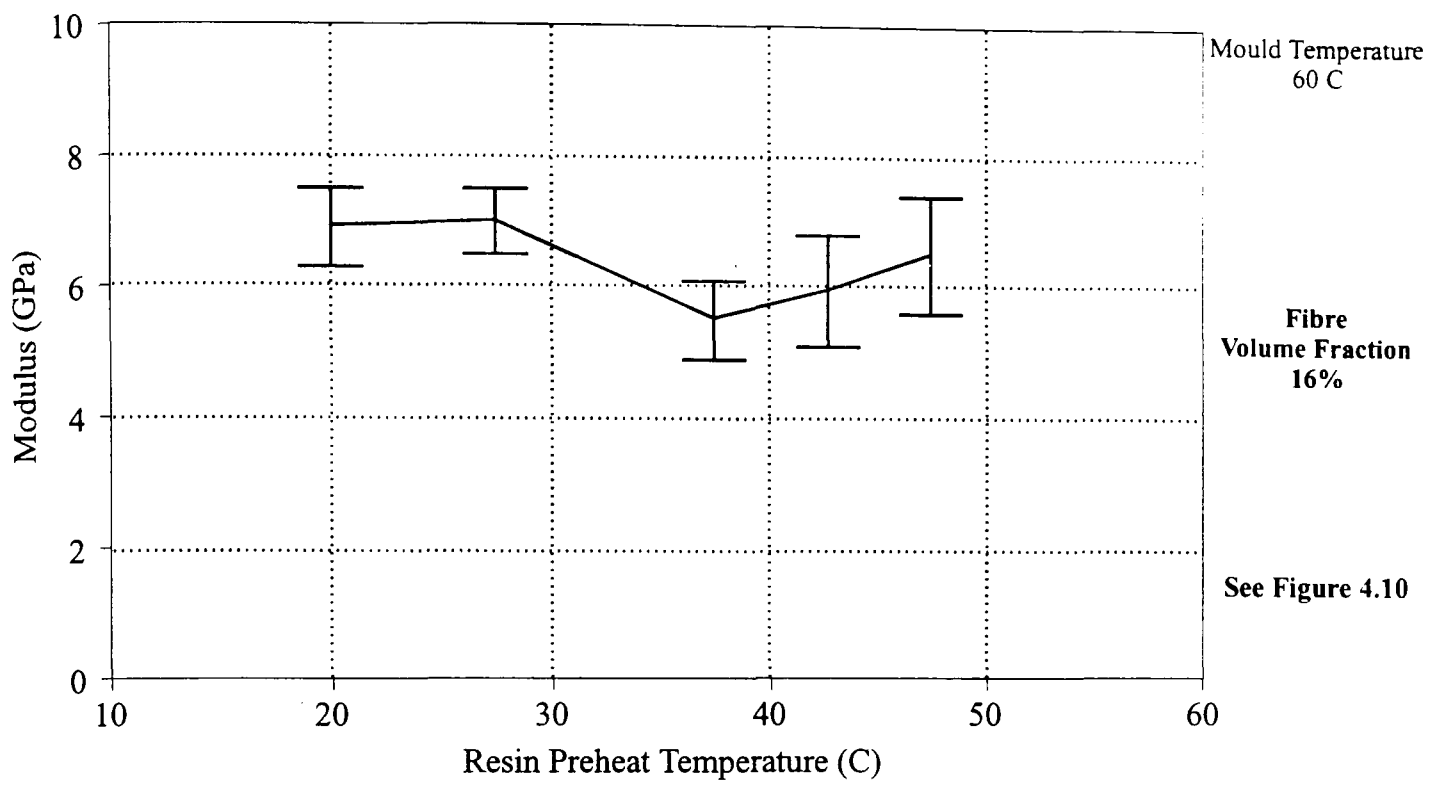


Figure 7.1a Average modulus values for undershield mouldings produced under constant resin temperature injection

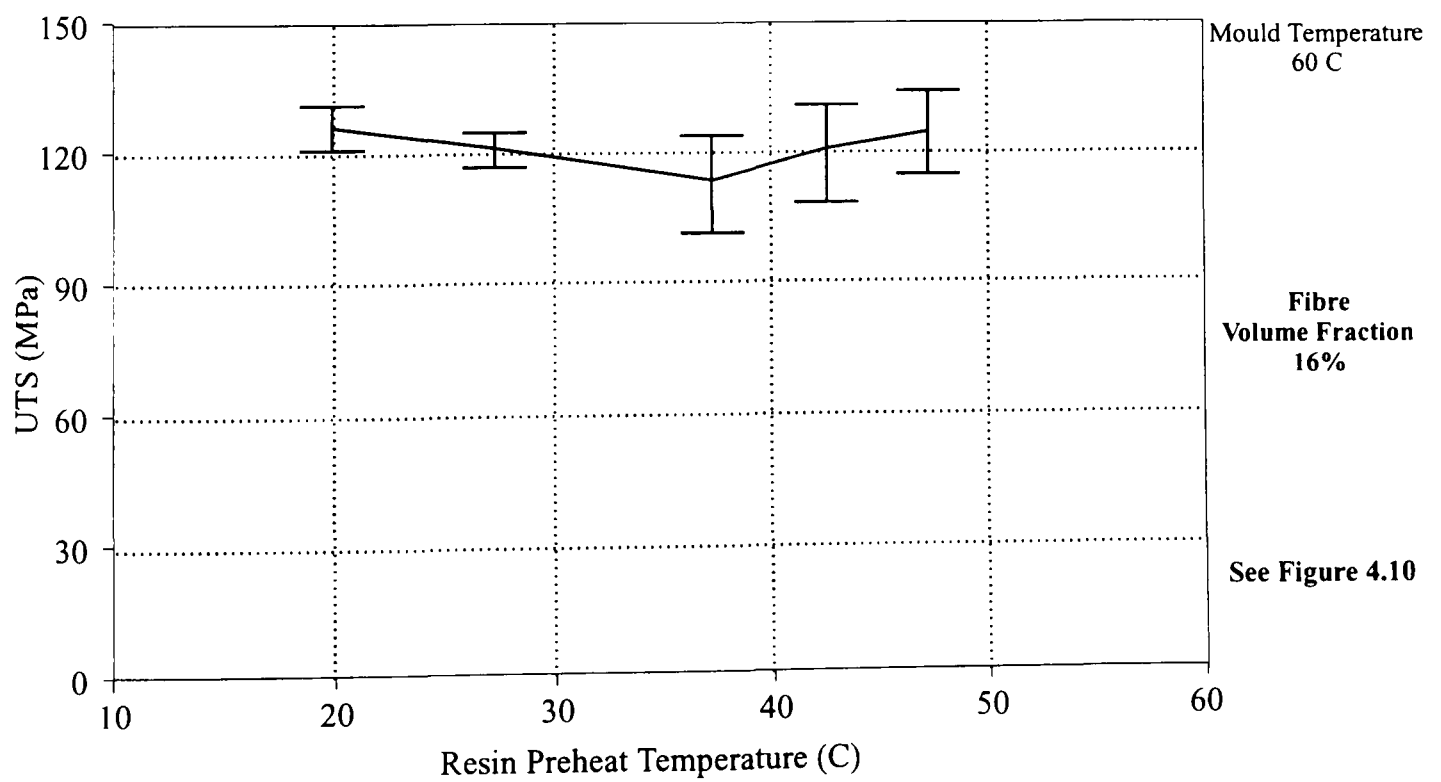


Figure 7.1b Average Ultimate Tensile Strength (UTS) values for undershield mouldings produced under constant resin temperature injection

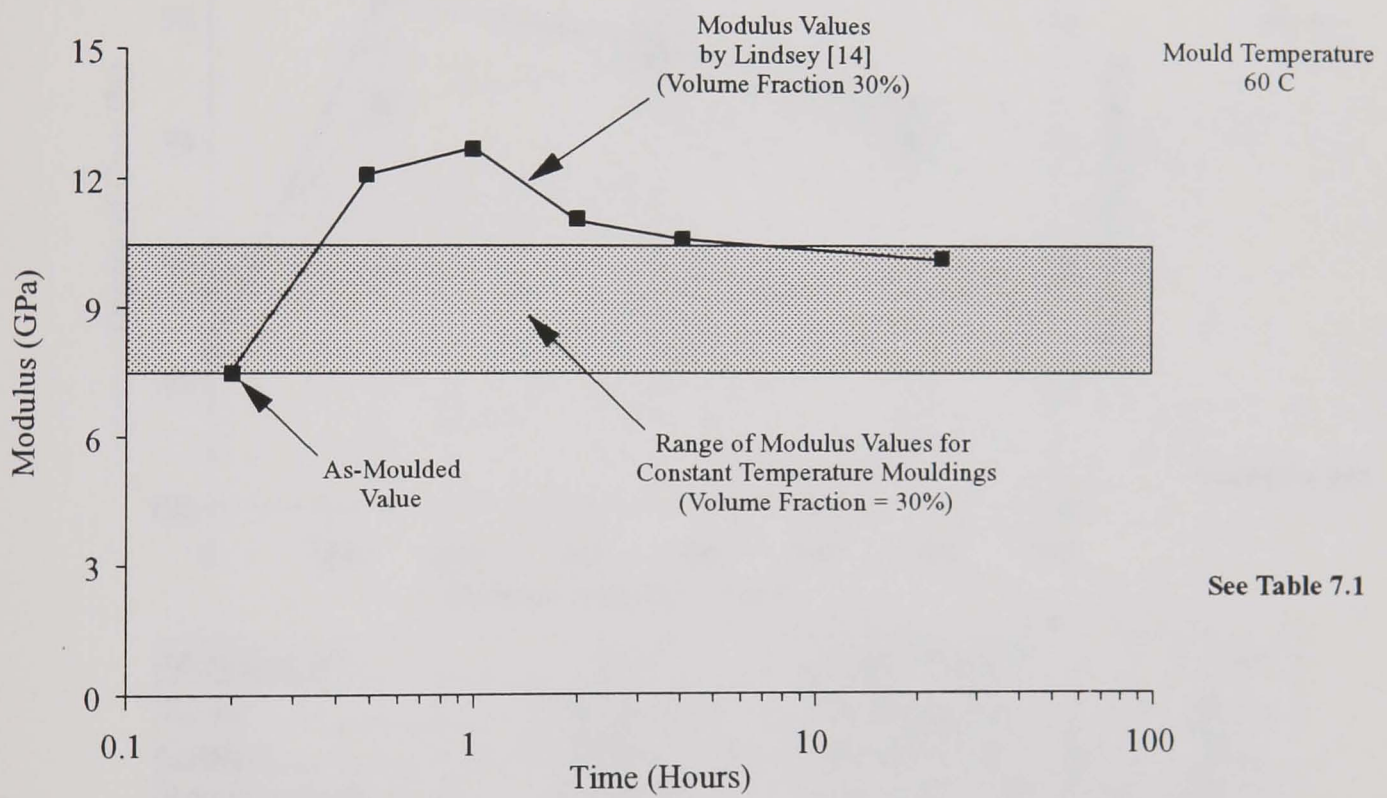
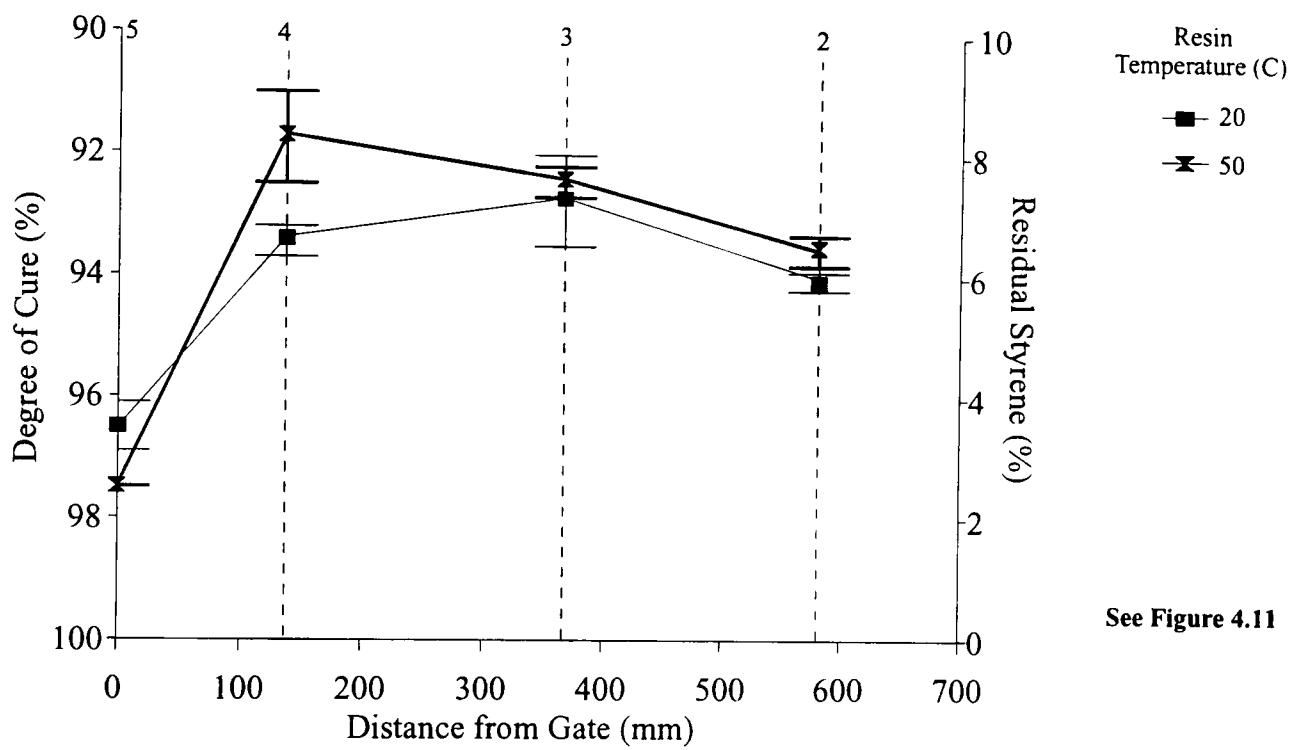
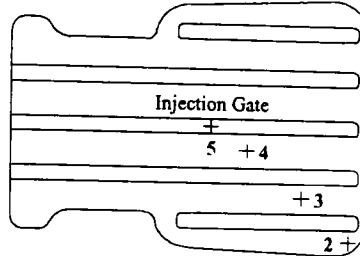


Figure 7.2 Variation in modulus due to post-cure by Lindsey [14] including a range of moduli for mouldings made under constant resin temperature injection

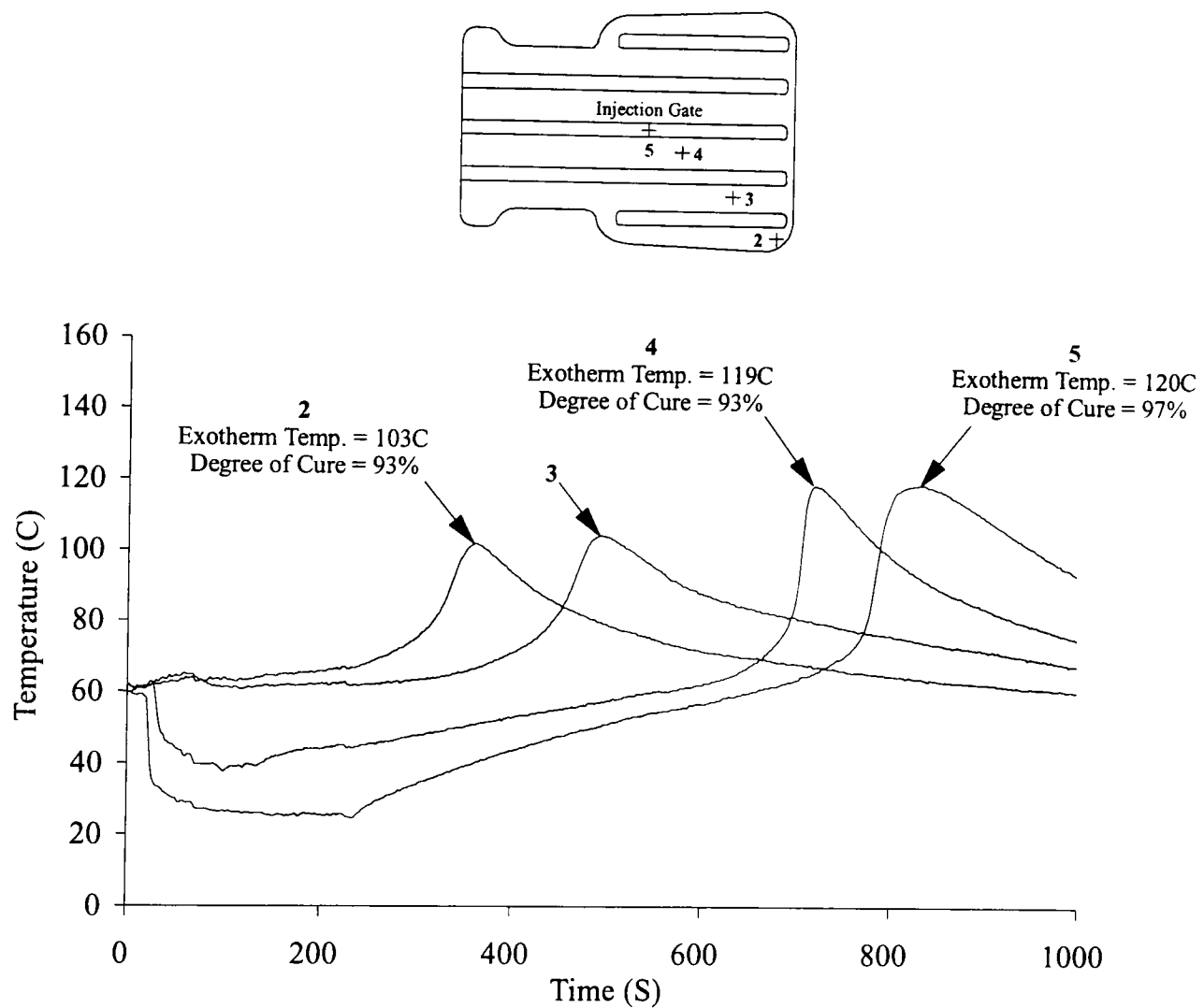


See Figure 4.11

Moulding No.	5467	Supply Pressure	2.0 bar
Resin	Synolac 6345	Mould Temperature	61 C
Catalyst	2% Perkadox 16	Set Point Temperature	n/a
Reinforcement	U754-450	Avg Resin Temperature	<b>20 C</b>
Fibre Mass Fraction	n/a	Power Control	n/a

Moulding No.	5466	Supply Pressure	1.9 bar
Resin	Synolac 6345	Mould Temperature	61 C
Catalyst	2% Perkadox 16	Set Point Temperature	50 C
Reinforcement	U754-450	Avg Resin Temperature	<b>50 C</b>
Fibre Mass Fraction	n/a	Power Control	PID

Figure 7.3 Degree of cure along the undershield diagonal for mouldings produced with resin at 20 C and 50 C



Moulding No.	5467	Supply Pressure	2.0 bar
Resin	Synolac 6345	Mould Temperature	61 C
Catalyst	2% Perkadox 16	Set Point Temperature	n/a
Reinforcement	U754-450	Avg Resin Temperature	<b>20 C</b>
Fibre Mass Fraction	n/a	Power Control	n/a

Figure 7.4 Thermal history along the undershield mould diagonal illustrating the relationship between peak exotherm temperature and degree of cure

# Sensitivity Analysis of the Microwave Resin Preheating System

---

### 8.1 Introduction

Cycle time reductions up of to 36% were demonstrated in Chapter 6 using the adapted microwave resin preheating system. This work was restricted to preheating polyester resin (Synolac 6345), although Hill [22] demonstrated that a vinyl-ester resin (Derakane 8084) with similar dielectric properties could be heated with equal efficiency. A robust preheating system capable of processing a wide variety of resins is desirable for RTM. However, efficient heating within cylindrical applicators, such as the one used in this thesis, is dependent upon the dielectric constant ( $\epsilon'$ ) of the resin. Consequently, establishment of the applicator sensitivity to variations in resin formulations or dielectric properties is required.

The cylindrical applicator was designed to resonate in the  $TM_{020}$  mode at the nominal magnetron output frequency of 2.46 GHz. Apart from the diameter of the dielectric load, resonance is also affected by the dielectric constant ( $\epsilon'$ ) of the material inside the applicator. The design of the cylindrical applicator was based upon a polyester resin (Synolac 6345) with a dielectric constant of 3.12 at 2.46 GHz. Out of the three dielectrics present within the applicator (air, the PTFE pipe, and the resin) only the resin system is likely to be altered for RTM applications. Base resins (polyester, vinyl-ester, or epoxy) are modified by the introduction of additives to reduce shrinkage (low profiling additives), add bulk (extenders), enhance laminate properties, or improve processing characteristics. These modifications can change the dielectric properties of the resin, and affect the applicator heating efficiency.

This chapter demonstrates the sensitivity of the cylindrical applicator to changes in the dielectric constant of polyester resin filled with calcium carbonate ( $CaCO_3$ ). Dielectric properties were measured for Synolac 6345 resin loaded with

this extender in varying amounts. The resins were heated in the cylindrical applicator and changes in applicator efficiency were monitored. Results of these trials were used to perform a simple sensitivity analysis on the applicator so that estimates of applicator heating efficiency could be made based upon the dielectric constant of the resin system. The robustness of the microwave resin preheating system for RTM was specified in this manner.

## 8.2 Dielectric Property Measurements

A limited amount of data has been presented in the literature on the dielectric properties of resin systems. Hill determined the dielectric properties of Synolac 6345 resin in addition to several specific resins by the coaxial transmission/reflection measurement technique [22]. This work demonstrated that by adding 66 parts per hundred resin (phr) of calcium carbonate filler to DSM Synolite 40-7417 low profile resin produced a 26% increase in the dielectric constant (from 3.27 to 4.12).

Dielectric properties of Synolac 6345 polyester resin were measured in pure form and with the addition of calcium carbonate filler in concentrations of 50 phr and 100 phr using the cavity perturbation technique (Section 4.11). The measurements were performed at 25°C, 50°C, and 70°C. Figures 8.1a and 8.1b show the results of the measurements including the dielectric properties for pure Synolac 6345 determined by Hill. Calcium carbonate filler was chosen for the sensitivity analysis since it changes the dielectric properties significantly and is a standard resin extender used in industry. A dielectric constant ( $\epsilon'$ ) of 2.69 was recorded for pure Synolac 6345 resin compared to 3.12 measured by Hill for the same system. Similarly, the loss factor ( $\epsilon''$ ) was 27% lower than that measured by Hill (0.16 compared to 0.22, respectively). Methven [85] measured the dielectric properties of the same resin ( $\epsilon'=2.81$ , and  $\epsilon''=0.18$ ) and was in close agreement with those made by the cavity perturbation technique. Discrepancies in the dielectric properties could have resulted from variations in the measurement techniques as well as differences in the frequency and temperature conditions. However, the tolerance on the cavity perturbation technique ( $\pm 0.5\%$  for  $\epsilon'$  and

$\pm 10\%$  for  $\epsilon''$  [86]), and the agreement with the results by Methven suggest that these dielectric properties are more accurate than those measured by Hill.

Filler concentration affected the dielectric constant considerably. A 36% increase in the dielectric constant was measured at 25°C (from 2.69 to 3.67) for an increase in filler content from 0 phr to 100 phr, however, variation in the loss factor was negligible under the same conditions. The dielectric constant increased by 9% between 25°C and 70°C for pure Synolac 6345, and an average increase of 13% was measured for the filled resins over the same temperature range. Changes in the loss factor with temperature were more extreme ranging from a 131% increase for the pure Synolac 6345 to a 194% increase in the resin filled with calcium carbonate (100 phr). The loss factor has no effect on applicator resonance, but is critical in determining the amount of power a material can absorb during heating as shown by Equation 2.3. A high loss factor material will absorb more microwave power than a material with a low loss factor.

Mixture equations have been derived to predict the dielectric properties of two part systems based on the ratio of its components. Six of these equations are listed in Appendix 3.1. The dielectric properties of each component must be measured individually before the equations can be applied. Since the dielectric properties of calcium carbonate were not readily available, a comparison between the measured and predicted dielectric properties of the filled resin system was not performed.

The consequence of changing the resin dielectric constant on the applicator heating efficiency for an arbitrary high Q system is illustrated in Figure 8.2a. Tuning and coupling the applicator to resonate at the magnetron output frequency (2.46 GHz) with a VSWR of unity would result in an applicator heating efficiency of 100%. Altering the resin system could change its dielectric constant and shift the resonant frequency (2.45 GHz) so that the VSWR is reduced (2.64) along with the applicator heating efficiency (80%). Figure 8.2b shows a similar example for an arbitrary low Q system. Altering the dielectric constant so that applicator resonance is focused at 2.45 GHz causes less of a reduction in the VSWR (1.34), resulting in an efficiency of 96%. A low Q system is desirable for microwave

heating applications since applicator sensitivity is reduced enabling a wider range of dielectric materials to be heated.

### **8.3 Applicator Heating Efficiency Trials**

The microwave resin preheating system was set up as shown in Figure 4.6 to perform resin preheating trials. Calcium carbonate filler was added to a base polyester resin (Synolac 6345) in quantities of 25 phr, 50 phr, 75 phr, and 100 phr. The resin mass flow rate was adjusted to provide an average preheat temperature of 75°C for each of resin system so that temperature derived changes in dielectric properties would be consistent. Figure 8.3 shows the average applicator heating efficiency for each filled resin system during preheating. Pure Synolac 6345 resin (0 phr CaCO<sub>3</sub>) was heated as a benchmark measurement resulting in an efficiency of 98%. Successive heating trials on the filled resin systems were performed without retuning of the applicator. A steady decrease in efficiency was measured down to 66% for the highly filled resin system (100 phr). A summary of the results is listed in Table 8.1.

The series of preheating experiments was repeated using a filled, low profile resin system as shown in Figure 8.3. Synolite 1080-M-1 low profile additive (1% of the resin mass), termed LPA, was added to the base polyester resin (Synolac 6345) as described in Section 4.10. Calcium carbonate was added to the low profile resin in quantities of 50 phr and 100 phr. The resin was preheated to an average of 76°C without retuning the applicator and the efficiency was measured. A summary of results is given in Table 8.2. Applicator heating efficiency values were similar to those measured for the standard, filled resin system suggesting that the low profiling agent had a minimal effect on the dielectric constant. A prediction of the average applicator efficiency as a function of calcium carbonate filler loading was obtained by a curve fit procedure for the resin systems with and without the low profile additive (Figure 8.3).

#### 8.4 Sensitivity Analysis of the Cylindrical Applicator

A sensitivity analysis of the cylindrical applicator was performed to relate changes in the resin dielectric constant to the applicator heating efficiency. Figure 8.4 is a graph of the efficiency compared to the dielectric constant (at 25°C), including the curve fit. The efficiency was reduced by 8% (from 98% to 90%) as the dielectric constant increased from 2.61 to 3.21, and decreased an additional 24% when the dielectric constant reached 3.67. This suggested that the resin filled with 50 phr of calcium carbonate (dielectric constant of 3.21) could be heated effectively using the microwave resin preheating system. However, addition of the extender beyond 50 phr would lead to an undesirable reduction in applicator heating performance below 90%. The dielectric mixture equations (Appendix 3.1) provide a simple means of estimating the dielectric constant of a filled resin system. Using Figure 8.4, this predicted dielectric constant could be related to the applicator heating efficiency. The suitability of the filled resin system with regard to preheating using the cylindrical applicator could be determined in this way.

Preheating resin systems with a filler content greater than 50 phr by mass could be achieved by altering the applicator diameter. Hill developed a numerical model to specify applicator geometry based on the properties of the internal dielectrics (air, PTFE, and resin) [22]. The model performed an iterative solution to the conditional equation controlling resonance within the cylindrical applicator. Hill assumed a magnetron output frequency of 2.46 GHz, a PTFE pipe wall thickness of 8 mm, and a dielectric constant of 3.12 for pure Synolac 6345, resulting in an applicator bore of 172 mm with a resin diameter of 52.8 mm. The applicator heating efficiency for this geometry was greater than 98% as shown in Figure 8.5. Using the same model, an applicator bore of 167 mm and a resin diameter of 48.7 mm would be necessary to preheat the highly filled resin (dielectric constant of 3.67) with an equivalent efficiency. Preheating trials with the 172 mm diameter applicator resulted in an efficiency of 66% for the highly filled resin system. Applying a linear analysis to these results indicates that a 6.4% drop in efficiency occurs for every 1 mm increase in the applicator diameter. It is expected that a compromised applicator geometry could be employed to heat both the pure and highly filled resin systems with reasonable efficiency. For

example, selecting an applicator diameter of 169.5 mm should allow both resin systems to be heated at 84% efficiency. Additional on-line tuning for the individual resins could raise the efficiency to a higher level.

## **8.5 Conclusion**

The cylindrical applicator was designed to preheat a polyester resin (Synolac 6345) with a dielectric constant of 3.12 at a frequency of 2.46 GHz. A sensitivity analysis of the applicator was performed with regard to dielectric constant of the resin load. A range of dielectric properties were measured for polyester resin (Synolac 6345) filled with varying amounts of calcium carbonate extender. These resin systems were preheated using the cylindrical applicator with the efficiency being monitored during the trial. Increasing the dielectric constant by 0.98 (from 2.69 to 3.67) led to a 32% reduction in the applicator heating efficiency. Efficient preheating of resins with a high dielectric constant could be accomplished by reducing the applicator and resin diameters. However, a more flexible system might be obtained by selecting a median applicator diameter for preheating at a lower, yet acceptable, efficiency. These results stress the importance of accurate dielectric property information in order to assess the ability of a microwave resin preheating system to operate efficiently.

## **List of Tables**

- Table 8.1 Summary of the resin preheating trials to determine the sensitivity of the cylindrical applicator to CaCO<sub>3</sub> filler
- Table 8.2 Summary of the resin preheating trials to determine the sensitivity of the cylindrical applicator to a LPA and CaCO<sub>3</sub> filler

## **List of Figures**

- Figure 8.1a Dielectric constant for Synolac 6345 polyester resin with various concentrations of calcium carbonate filler
- Figure 8.1b Dielectric loss factor for Synolac 6345 polyester resin with various concentrations of calcium carbonate filler
- Figure 8.2a Effect of changing the dielectric constant on applicator heating efficiency for a high Q system
- Figure 8.2b Effect of changing the dielectric constant on applicator heating efficiency for a low Q system
- Figure 8.3 Relationship between the amount of calcium carbonate filler and applicator heating efficiency for Synolac 6345 resin, with and without a low profile additive
- Figure 8.4 Reduction in applicator heating efficiency as a function of increasing dielectric constant
- Figure 8.5 Relationship between applicator diameter and efficiency

**Table 8.1 Summary of the Resin Preheating Trials to Determine the Sensitivity of the Cylindrical Applicator to CaCO<sub>3</sub> Filler**

Reference Number	Resin	Filler (phr) <sup>1</sup>	C <sub>p</sub> (J/kg °C) <sup>2</sup>	Efficiency (%) <sup>3</sup>
msj126	Synolac 6345	0	1900	98
msj129	Synolac 6345	25	1692	93
msj125	Synolac 6345	50	1553	90
msj128	Synolac 6345	75	1454	72
msj124	Synolac 6345	100	1380	66

**Table 8.2 Summary of the Resin Preheating Trials to Determine the Sensitivity of the Cylindrical Applicator to a LPA and CaCO<sub>3</sub> Filler**

Reference Number	Resin	Filler (phr) <sup>1</sup>	LPA (% of resin mass)	C <sub>p</sub> (J/kg °C) <sup>2</sup>	Efficiency (%) <sup>3</sup>
msj135	Synolac 6345	0	1	1900	99
msj137	Synolac 6345	50	1	1553	86
msj136	Synolac 6345	100	1	1380	65

**Notes**

1. phr = parts per hundred resin
2. Specific heat capacity, C<sub>p</sub>, calculated by a rule of mixtures assuming C<sub>p</sub> = 1900 J/kg°C for Synolac 6345 resin, and C<sub>p</sub> = 860 J/kg°C for CaCO<sub>3</sub> filler
3. Average efficiency measurements recorded during preheating trial

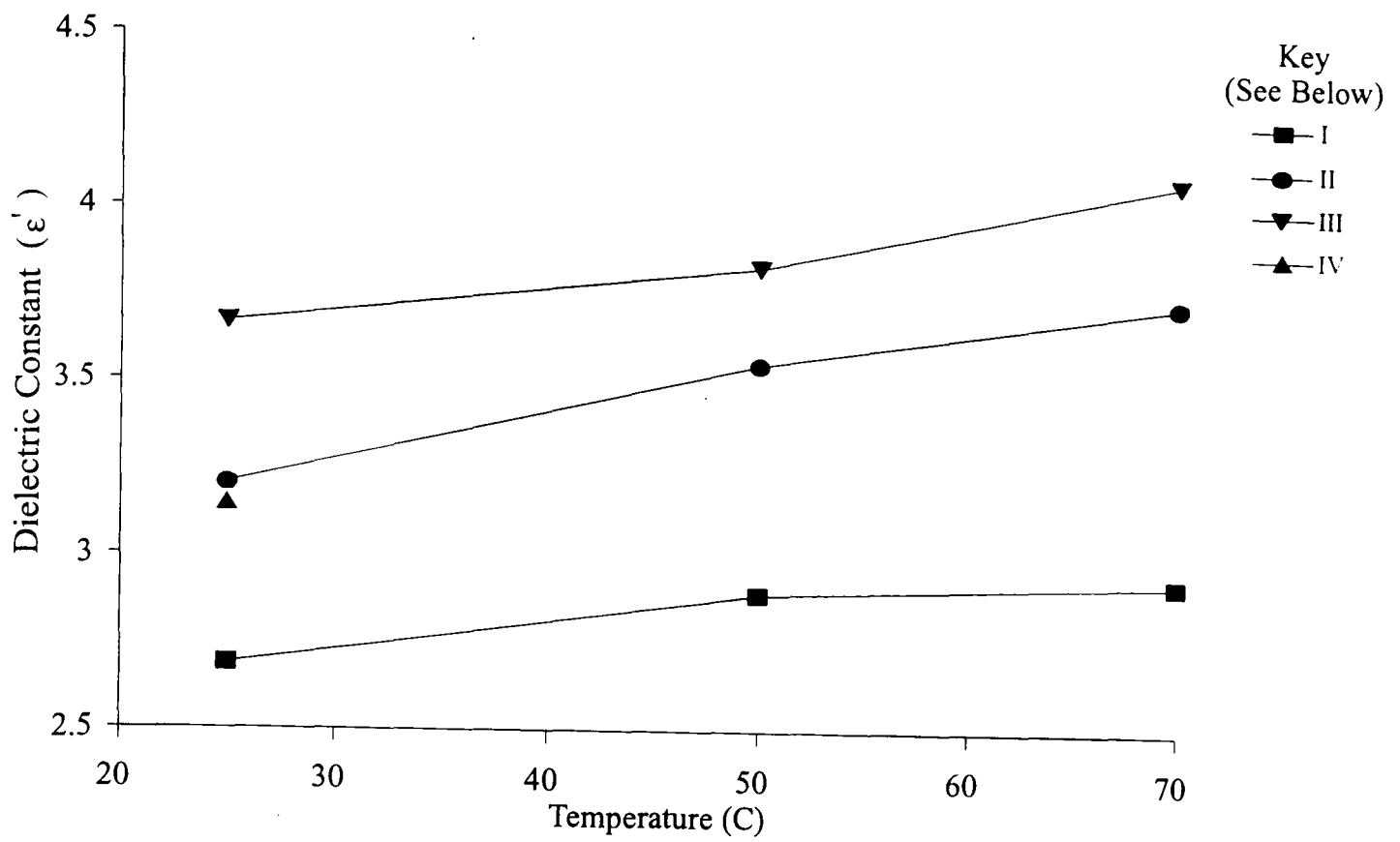


Figure 8.1a Dielectric constant of Synolac 6345 polyester resin with various concentrations of calcium carbonate filler

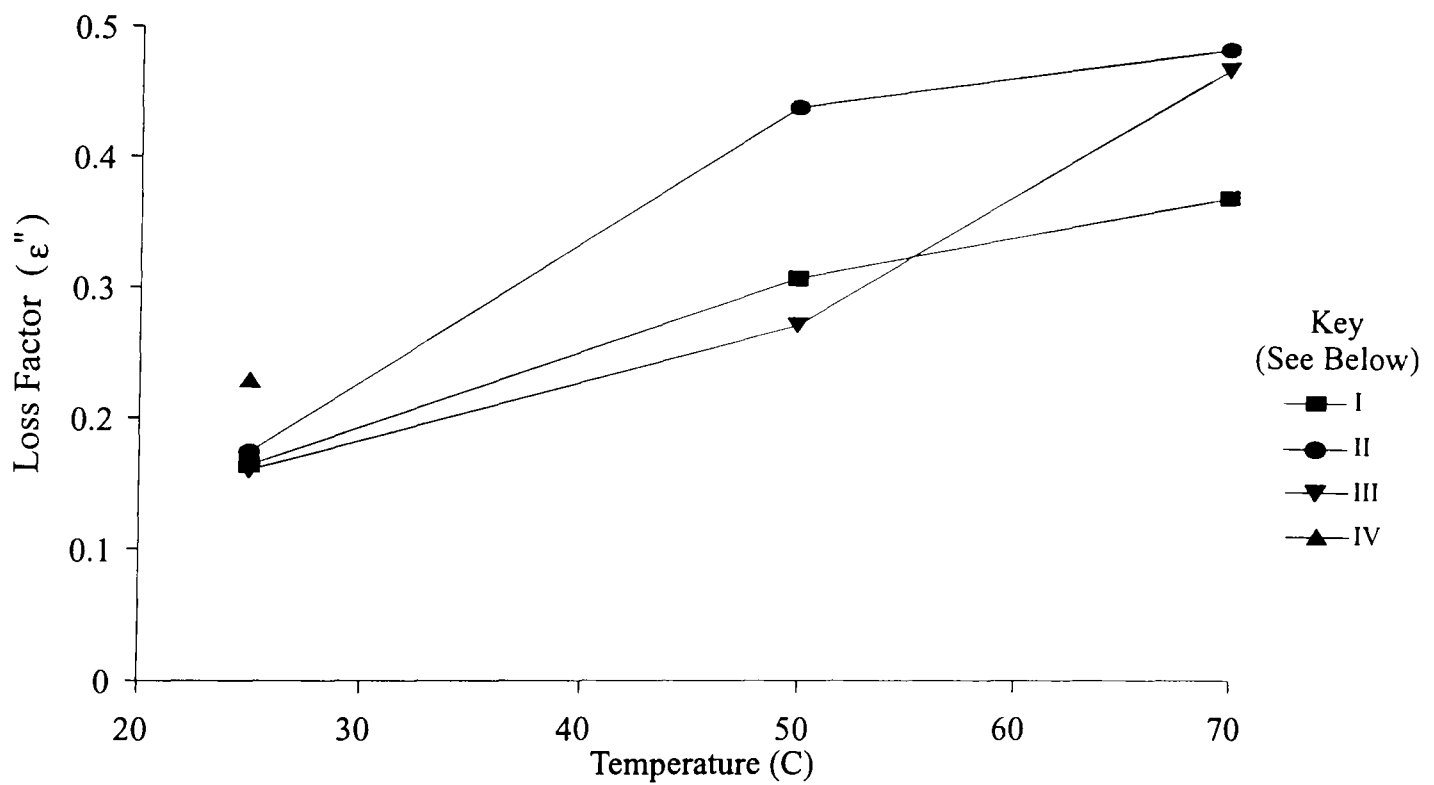


Figure 8.1b Dielectric loss factor of Synolac 6345 polyester resin with various concentrations of calcium carbonate filler

Key to Resin Formulations:

- I Synolac 6345 (Pure)
- II Synolac 6345 + CaCO<sub>3</sub> ( 50 phr)
- III Synolac 6345 + CaCO<sub>3</sub> (100 phr)
- IV Synolac 6345 (Pure - As measured by Hill [22])

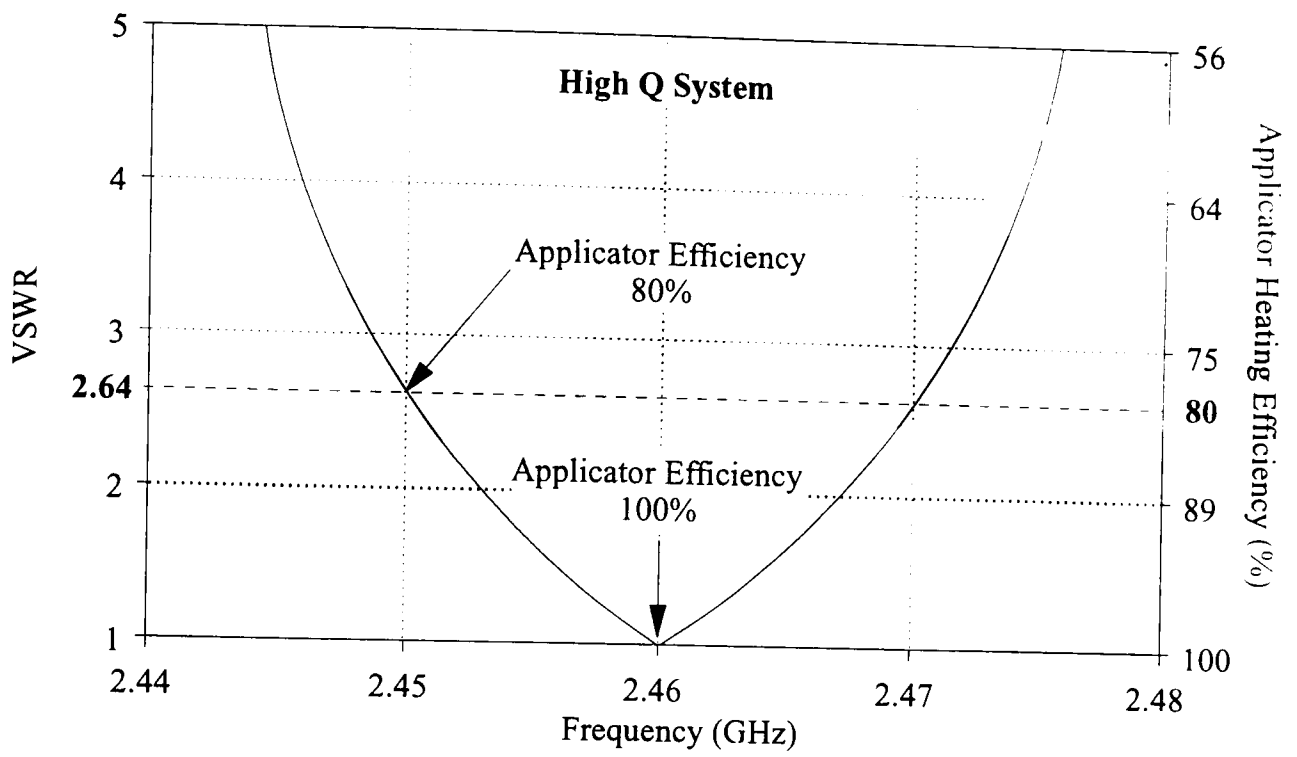


Figure 8.2a Effect of changing the dielectric constant on applicator heating efficiency for a high Q system

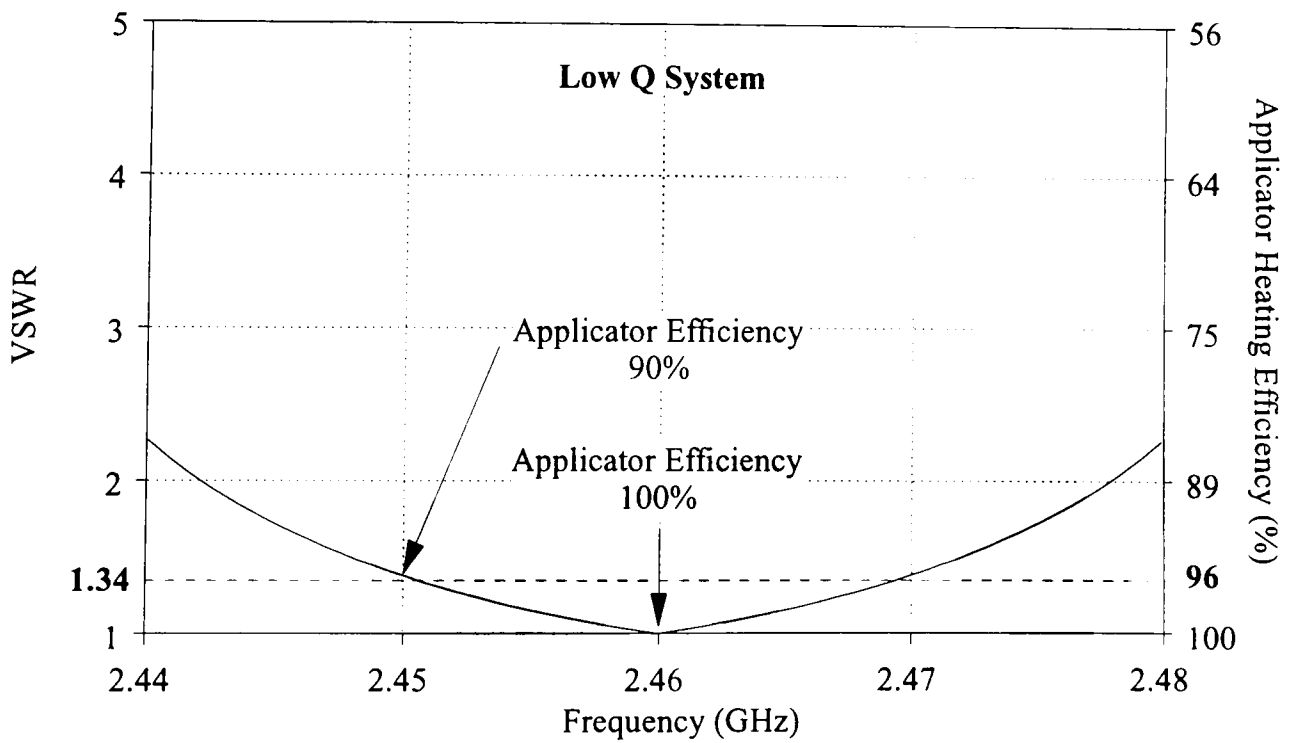


Figure 8.2b Effect of changing dielectric constant on applicator heating efficiency for a low Q system

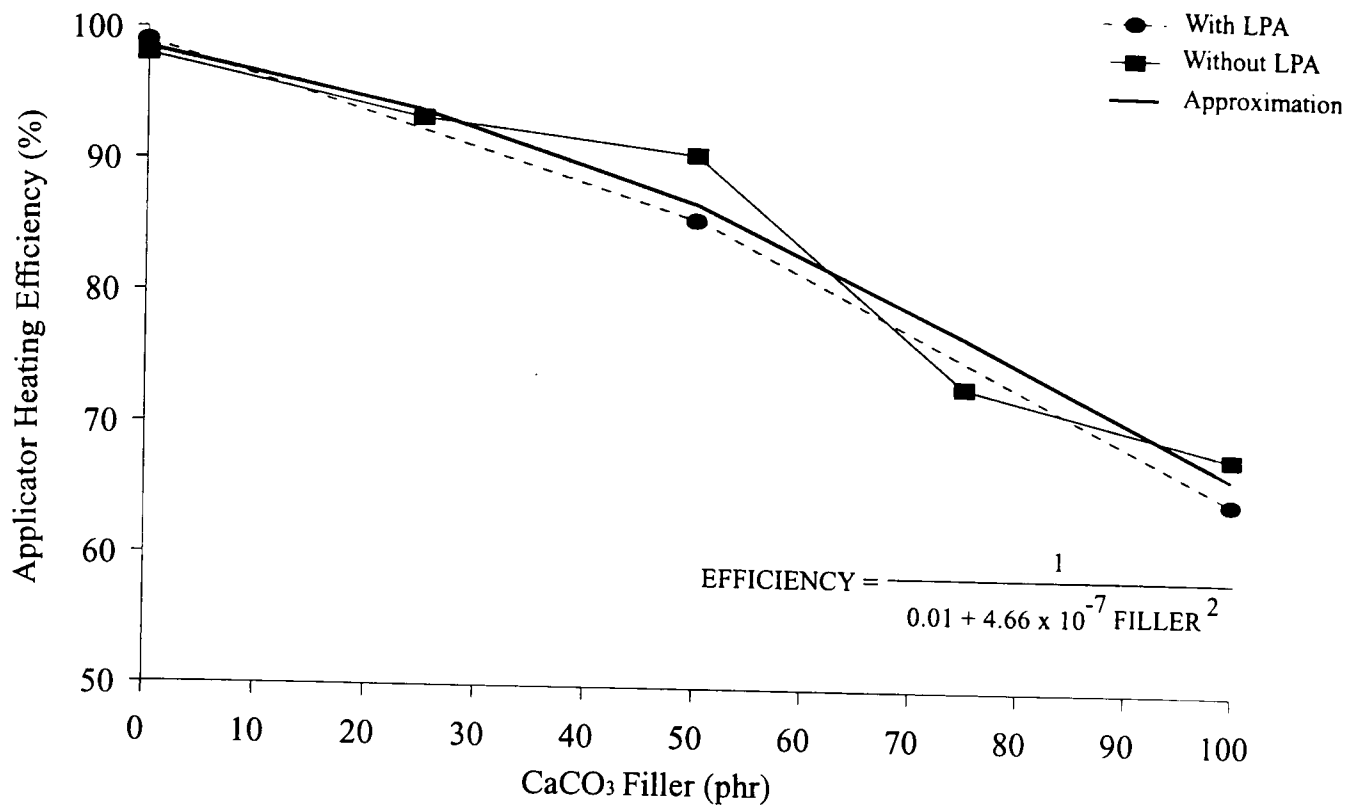


Figure 8.3 Relationship between the amount of calcium carbonate filler and applicator heating efficiency for Synolac 6345 resin, with and without a low profile additive

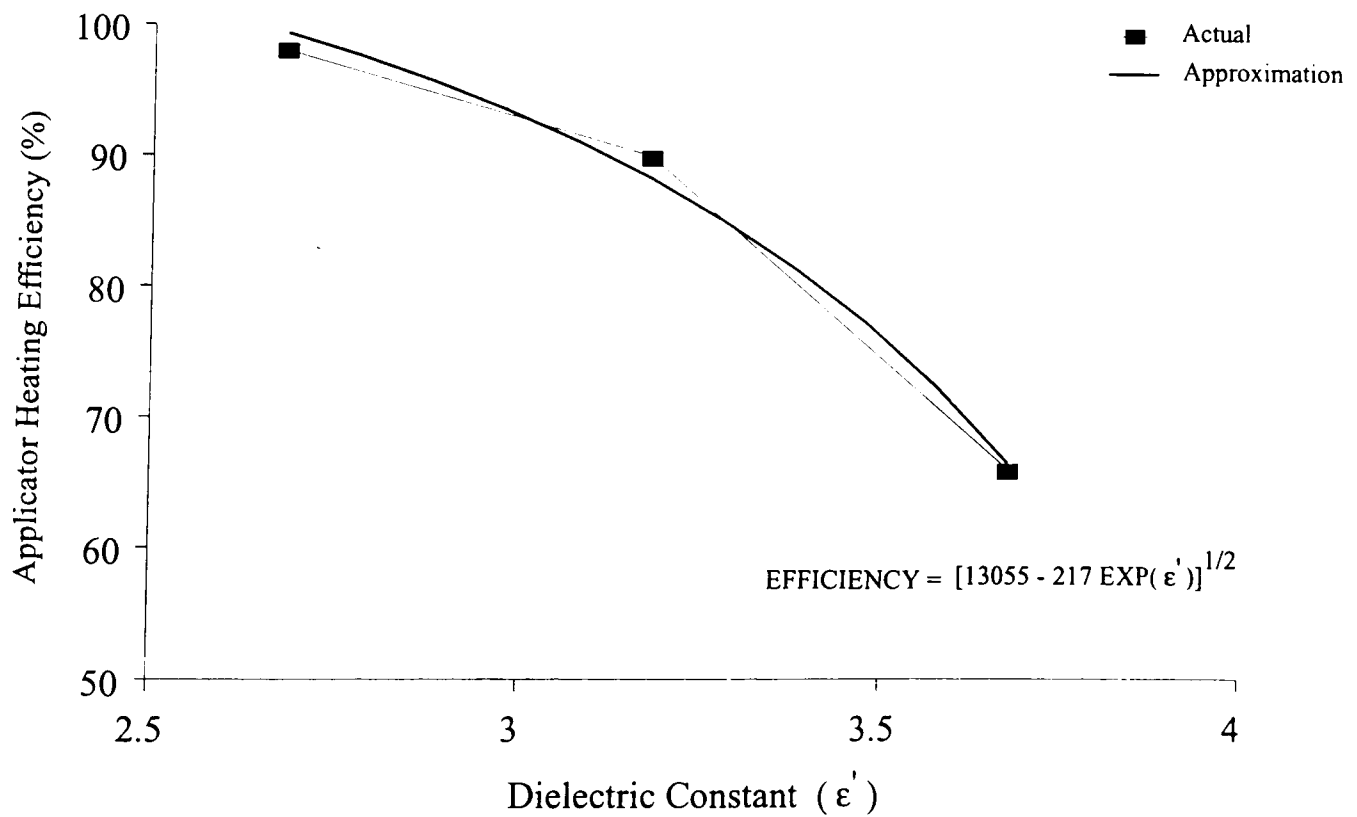


Figure 8.4 Reduction in applicator heating efficiency as a function of increasing dielectric constant

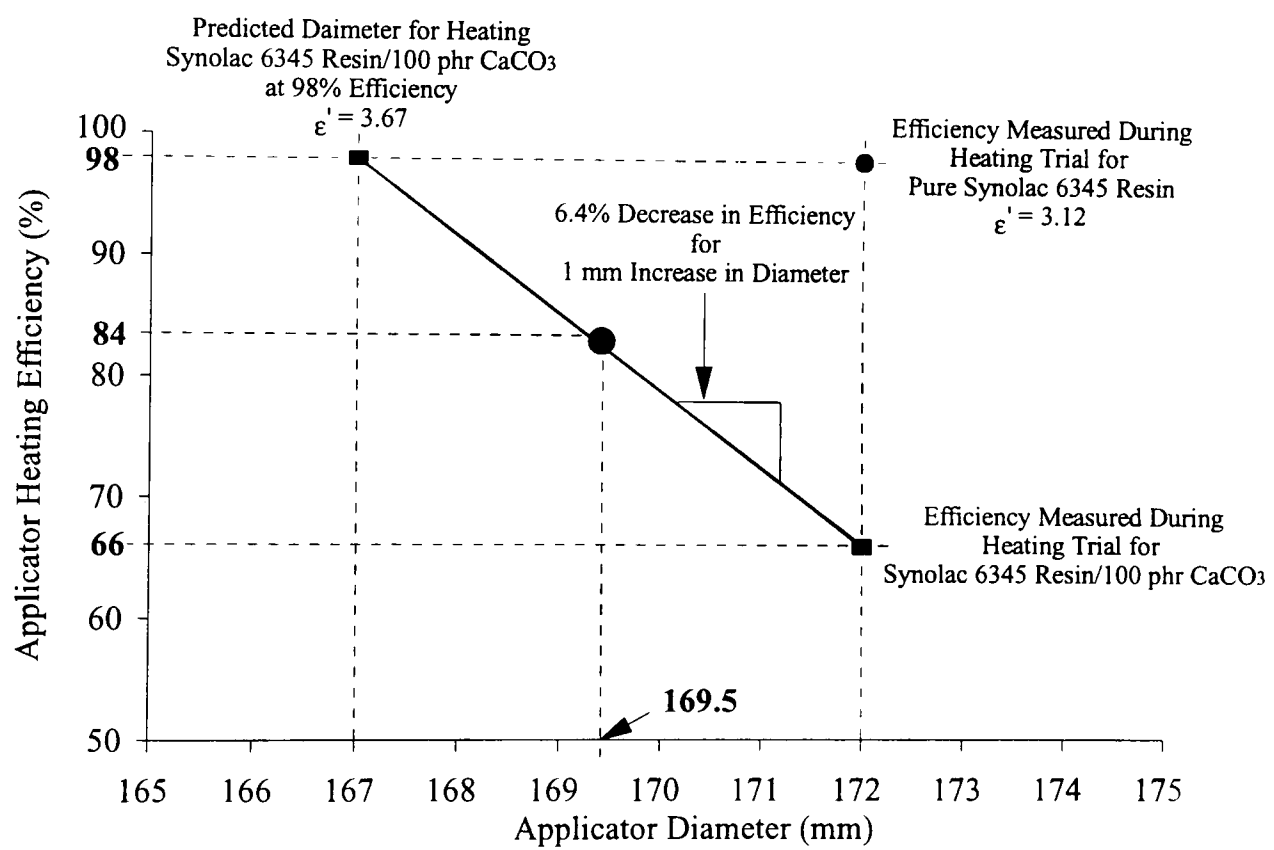


Figure 8.5 Relationship between applicator diameter and efficiency

# Performance Aspects of the Cylindrical Applicator

---

### 9.1 Introduction

Adaptation of the microwave resin preheating system for use in RTM was described in Chapter 5. A low power density approach was adopted to minimise the heating influence of parasitic modes in close proximity to the desired  $TM_{020}$  mode (Section 5.3). Excessive power directed into the parasitic modes caused resin to cure within the applicator, obstructing the injection system. Implementation of the low power density system necessitated a reduction in the resin mass flow rate. Ideally, resin would not cure within the applicator so that modifications to RTM process parameters would not be necessary in order to implement the preheating system. If resonance could be maintained within a pure  $TM_{020}$  mode, the injection rate would not have to be restricted and the resin preheat temperature would be limited only by the amount of power available from a single magnetron source. This chapter identifies the causes of premature resin cure within the cylindrical applicator and suggests improvements to the microwave resin preheating system for unrestricted use in RTM.

### 9.2 Mode Superposition within the Cylindrical Applicator

Figure 9.1a shows the VSWR response trace for the cylindrical applicator used in this thesis. The applicator was configured as a low Q system ( $Q=12$ ) with the critical dimensions defined in Figure 9.1b. The complexity of the trace suggested that a pure  $TM_{020}$  mode had not been isolated at the nominal magnetron output frequency of 2.46 GHz as was desired. Hill [22] proposed that the  $TM_{020}$  mode and a pseudo  $TM_{21n}$  mode were being excited within the applicator. He also claimed that superposition of these modes prompted a heating contribution by the parasitic mode. As a result, the three cured resin lobes shown in Figure 5.3 formed within the applicator after preheating for 94 seconds at 5000 W. Hill

reasoned that a limited portion of the total power was being directed into the parasitic mode due to the small size of the lobes (63 mm × 15 mm). This suggested that the  $TM_{020}$  mode was the dominant heating profile within the applicator. Separation of the  $TM_{020}$  mode from the parasitic mode was expected to eliminate premature resin cure during operation.

### 9.3 Single Mode Isolation within the Cylindrical Applicator

Figure 9.1b shows the dimensions of the applicator used in this thesis. Geometry dictated the heating profile that would resonate within the applicator. The diameters of the metallic cylinder, PTFE pipe, and resin were critical for establishing the desired  $TM_{020}$  mode. Hill [22] determined these diameters analytically by modelling the conditional equation controlling resonance in the  $TM_{020}$  mode. His numerical model calculated the diameters based upon the magnetron output frequency (2.46 GHz), and the three internal dielectrics: air, PTFE and resin (Synolac 6345). The resulting applicator resonated above 2.46 GHz for the reasons discussed in Section 9.8. However, the magnetron output frequency was fixed nominally at 2.46 GHz, so a reduction in the applicator resonant frequency was necessary for resin preheating in the  $TM_{020}$  mode. It was determined empirically that increasing the length of the PTFE pipe reduced the resonant frequency. A PTFE pipe length of 150 mm was adopted as a result. In addition, PTFE tapers were added to provide a smooth transition in resin flow from the 19 mm bore injection line to the 54.45 mm bore PTFE pipe. These changes represented differences to the numerical model and were expected to promote resonance of parasitic modes within the applicator.

The applicator was reconfigured to approximate Hill's numerical model comprising three uniform coaxial dielectrics as shown in Figure 9.2b. Capping the cylindrical applicator and fitting PTFE tapers introduced a slight deviation from the numerical model that assumed an infinite length for the three dielectrics. The VSWR response trace for this configuration is shown in Figure 9.2a indicating a strong resonance at 2.56 GHz. The resonance appeared to be singular with a quality factor of 47 compared to a value of 12 for the original system shown in Figure 9.1a.

The resonant frequency of the loaded applicator must match the magnetron output frequency (2.46 GHz) to minimise reflected power. Instead of increasing the length of the PTFE pipe (from 63 mm to 150 mm), the applicator diameter was enlarged from 172 mm to 176 mm, decreasing the resonant frequency from 2.56 GHz to 2.52 GHz. The quality factor was reduced from 47 to 38 as shown in Figure 9.3, and an impurity in the trace became evident at 2.55 GHz. Figure 9.4 shows that increasing the applicator diameter further to 179.5 mm, decreased resonance from 2.52 GHz to 2.495 GHz, with the impurity separating to form a secondary peak at 2.55 GHz. Enlargement of the diameter beyond 179.5 mm was restricted by the applicator wall thickness, so a tuning device was used to shift the resonance from 2.50 GHz to 2.46 GHz with a secondary peak at 2.52 GHz as shown in Figure 9.5a. Results presented in Section 9.7 will indicate that the dominant mode corresponded to the pseudo  $TM_{21n}$  mode while the secondary mode was related to the desired  $TM_{020}$  mode. This suggests a reversal of the mode orientation shown Figure 9.1a that was proposed by Hill [22]. The quality factor for the system increased from 87 to 161 as illustrated in Figure 9.5b, resulting in high Q system that was sensitive to frequency changes during operation as explained in Section 8.2.

Figures 9.6a through 9.6c demonstrate that the quality factor decreases with increasing pipe length. The effective pipe length in Figure 9.6a is 63 mm with a quality factor of 47. Increasing the pipe length to 130 mm (Figure 9.6b) decreased the quality factor to 25, then to a value of 12 at a pipe length of 150 mm (Figure 9.6c). Reduction in the quality factor resulting from a longer pipe length can be related to the volumetric increase of resin within the applicator.

The quality factor is defined as a ratio of the stored to dissipated energy in the applicator. The amount of energy stored in the applicator is proportional to its volume. Principally, energy is dissipated in the dielectrics (PTFE pipe and resin) within the applicator. PTFE absorbs a negligible amount of microwave energy with a loss factor of 0.0003 compared to Synolac 6345 resin having a loss factor of 0.1648 as indicated by Equation 2.3. Extending the PTFE pipe length expands the applicator volume, increasing its energy storage capacity. However, this additional volume comprises mainly high loss resin so that its energy

dissipation capability of the applicator is raised in greater proportion to the energy storage capacity. As a result, the overall quality factor of the system is reduced by extending the PTFE pipe length.

Similarities were evident between the resonant peaks of the high Q system (Figure 9.5a) and those of the low Q system (Figure 9.1a). Both featured a dominant peak at a tuned resonance of 2.46 GHz. Secondary peaks were established in close proximity to the dominant mode for both systems: 2.50 GHz for the low Q system, and 2.52 GHz for the high Q system. The principal difference between the high and low Q systems was the length of the PTFE pipe. Decreasing the pipe length of low Q system from 150 mm to 63 mm resulted in the high Q system. This suggested that the same modes were established in each applicator. The modes were superimposed in the low Q system as shown in Figure 9.1a allowing both to contribute to the heating profile. The influence of the secondary mode was expected to generate the resin lobes shown in Figure 5.3. Figure 9.5a shows that the modes were separated in the high Q system, enabling resin to be heated in a pure mode at 2.46 GHz. However, the heating profile associated with the mode isolated at 2.46 GHz could not be determined by viewing the VSWR response trace. The results of a resin preheating trial using this high Q applicator are presented in Section 9.7.

#### **9.4 Stability of the High Q Cylindrical Applicator**

The sensitivity of the cylindrical applicator to variations in the dielectric constant ( $\epsilon'$ ) was presented in Chapter 8. Altering the resin system can change the dielectric constant, shifting the resonant frequency so that the applicator heating efficiency decreases. A change in the magnetron output frequency has the same effect since it is no longer coincident with the applicator resonant frequency. Resonance for a high Q system is restricted to a narrower bandwidth making it particularly sensitive to shifts in the resonant frequency of either the magnetron or cylindrical applicator.

A series of resin preheating trials were performed to determine the heating stability of the high Q applicator as described in Section 4.9.2. The microwave resin preheating system was set up as in Figure 4.14 with a directional coupler and

a Hewlett Packard spectrum analyser situated in-line to measure the magnetron output frequency during the trials. Results of the preheating trial at 1000 W are shown in Figures 9.7a-9.7d. An average resin outlet temperature of 42.7°C was measured with a 0.9°C rise in the water load temperature (Figure 9.7a), resulting in an applicator efficiency of 92% (Figure 9.7b). A magnetron output frequency of 2.437 GHz (Figure 9.7c) was recorded by the spectrum analyser. The results are summarised in Figure 9.7d. A second preheating trial was conducted by preheating resin using 3000 W of power. The resin flow rate was adjusted prior to the heating trial for a resin outlet temperature of 43.9°C, comparable with the previous experiment at 1000 W. Figure 9.8a shows that the water load temperature rose by 7.8°C during preheating. Increasing the power to 3000 W decreased the efficiency to 75% as shown in Figure 9.8b. During the preheating trial the magnetron output frequency, shown in Figure 9.8c, increased by 16 MHz to 2.453 GHz. Losses in efficiency at 3000 W can be attributed directly to a shift in the magnetron frequency since temperature related dielectric variations were equivalent at both power levels.

## **9.5 Calibration of the YJ1600 Magnetron**

Frequency shift is an inherent characteristic of magnetrons [87]. Reflected power from an imperfectly matched system is one cause of magnetron output frequency variations, termed pulling. However, a circulator positioned upstream of the magnetron diverts the reflected power to a water load to remove this effect. Two other sources of frequency shift are fundamental to the magnetron design. Microwaves are generated by the transferral of energy to an induced microwave field as electrons accelerate from cathode to anode under the influence of a magnetic field. Chambers within the anode determine the resonant frequency of the magnetron. The size of these chambers alter as power is increased and the anode expands as it heats up. As a result, the magnetron output frequency changes. Secondly, the hardware used to extract microwave power from the magnetron to the waveguide loads the anode chambers and pulls the magnetron frequency. Increasing the power produces higher loading, and a greater amount of frequency shift results.

A calibration of the YJ1600 magnetron was performed to establish the relationship between output frequency and microwave power as described in Section 4.9.1. Positioning the directional coupler and spectrum analyser between the magnetron and circulator isolated this unit from the load so that the true output frequency could be measured. The calibration curve is presented in Figure 9.9 showing an minimum output frequency of 2.435 GHz at 500 W, increasing by 17 MHz to 2.452 GHz at 5000 W. Thus, the magnetron operates within the 2.400 GHz to 2.500 GHz bandwidth specified in the UK for microwave heating, however, the output frequency is beneath the tolerance band specified by the manufacturer (2.45 GHz to 2.47 GHz) at power levels less than 3000 W [77].

A shift in the magnetron output frequency for a high Q system could effect adversely the applicator heating efficiency. A 17 MHz increase in frequency for the system shown in Figures 9.5a and 9.5b would result in a drop in VSWR from unity (at 2.460 GHz) to 18 (at 2.477 GHz) with a corresponding drop in the applicator heating efficiency from 100% to 20%. Large losses in efficiency cause high Q systems to be unstable across the power band. A means of maintaining a high efficiency is necessary for these systems to be useful heating devices.

## **9.6 Methods to Improve Heating Stability for High Q Applicators**

Instability of the applicator heating efficiency for a high Q system results from a mismatch between the magnetron output frequency and the applicator resonant frequency. It has been shown that this variation can occur by either changes in the dielectric constant of the resin (Chapter 8), or by shifting of the magnetron output frequency across the power band (Section 9.4). Three solutions to the problem are described below.

### **9.6.1 Active On-Line Tuning**

Active on-line tuning of the applicator is one technique to maintain high applicator heating efficiency over the power band. A schematic of the proposed system is shown in Figure 9.10. Feedback control based on the reflected power level could be used to tune the system during operation. Calibration of the reflected power

to the tuning stub position for maximum efficiency would be necessary so that servo control of the stub tuner could be utilised for automatic control.

A change in the resin outlet temperature would cause the power level to change via the PID controller. A frequency mismatch between the magnetron and applicator would result from the power variation. Reflected power would then increase necessitating retuning of the system. The tuning stub would be adjusted with reference to a calibration function so that the efficiency was maximised.

Active on-line tuning could be used if power fluctuations during heating were minimal. Since the tuning phase is indirect, a substantial lag between temperature variations and corrective tuning could develop. Control instability may result for this system if rapid temperature changes occurred at the resin outlet. A direct relationship between magnetron power and the tuning stub position would provide better response to temperature variations.

### **9.6.2 Power Modulation Using a Constant Magnetron Output Frequency**

Gerling Laboratories have developed a system to provide a constant magnetron output frequency with variable power delivery to the load [88]. A schematic of the system is shown in Figure 9.11. Two circulators and water loads are required to operate the system. Circulator 1 operates in the standard fashion with a water load (number 1) to isolate the magnetron from the circuit. A second circulator with a tuning stub and a water load (number 2) is attached to the first circulator, acting as a valve. The third port of circulator 2 is coupled to the applicator. The magnetron is set to full power with the tuning stub fully retracted so that all the power is delivered to water load 2. Extending the tuning stub into the waveguide directs a portion of the power to the applicator with the remaining power being absorbed by water load 2. Any reflected power in the system would be directed to water load 1 so that the magnetron remained isolated.

The advantage of this technique is that the power delivered by the magnetron is always constant keeping the magnetron frequency constant. The tuning stub position could be related to a power level and adjusted using servo control. A change in the resin outlet temperature would result in modulation of power level by the PID controller. This power level could be implemented

directly by adjusting the stub. The disadvantage of this system is that constant operation at full power would result in a waste of energy when low power was required for heating. However, the efficiency of energy conversion by magnetrons from mains to microwave power is greatest at high power levels. Consequently, constant maximum power operation could waste less energy than an equivalent system with modulated power control.

### **9.6.3 Frequency Tracking Magnetrons**

Frequency tracking is a sophisticated means of matching the magnetron and applicator frequencies [89]. Independent feedback control of the magnetron voltage and power allows a constant magnetron frequency to be generated. In addition, this technique is used to align the magnetron output frequency with the applicator resonant frequency in reaction to changes in the dielectric properties of the load. Such a magnetron, manufactured by Applied Science and Technology Incorporated, was shown to track the applicator resonance over a 2 MHz range. These magnetrons are expected to provide the best performance with regard to frequency control, though reliability and cost could be a disadvantage.

## **9.7 Preheating Trials Using the High Q Cylindrical Applicator**

The high Q cylindrical applicator shown in Figure 9.5a was tuned on-line at 2500 W for an average efficiency of 94% and stable resin outlet temperature (Synolac 6345) of 43°C. A preheating trial was carried out under these conditions using catalysed Synolac 6345 resin. Results for the experiment are shown in Figures 9.12a-9.12d. Efficiency and resin mass flow rate (Figures 9.12b and 9.12c, respectively) stabilised after approximately 10 seconds of heating. The resin outlet temperature remained unstable after the same period and rose progressively after 13 seconds (Figure 9.12a). The applicator heating efficiency and the resin mass flow rate steadily declined after 20 seconds of heating. Since the microwave power was constant, decreasing efficiency suggested a change in the dielectric properties of the resin, rather than a shift in the magnetron frequency. Furthermore, slowing of the resin mass flow rate indicated a blockage

in the flow path. The microwave was turned off after 30 seconds of heating. A summary of the heating trial is shown in Figure 9.12d.

The applicator was disassembled after the trial and the block of cured resin shown in Figure 9.13 was found within. The lobes on the resin block were analogous to those generated in the low Q system shown in Figure 5.3, although they were joined together and significantly larger.

The heating profile within the low Q system was expected to comprise the  $TM_{020}$  and the  $TM_{21n}$  modes as shown in Figure 9.1a. Heating contributed by the  $TM_{21n}$  mode was predicted to generate the small cured lobes shown in Figure 5.3. The same heating modes were assumed to resonate in the high Q system shown in Figure 9.5a. Separation of the two modes ensured pure heating in either the  $TM_{020}$  mode or the  $TM_{21n}$  mode. Compared to the low Q system (Figure 9.1a), the block of resin shown in Figure 9.13 developed in the applicator under lower power conditions (2500 W compared to 5000 W), and over a shorter heating period (30 seconds as opposed to 94 seconds). This implied that the  $TM_{21n}$  mode had been isolated within the high Q (Figure 9.5a) system at 2.46 GHz, not the desired  $TM_{020}$  mode. Furthermore, the results suggested that the resonant peak at 2.52 GHz shown in Figure 9.5a was the  $TM_{020}$  mode. This contradicts the conclusion by Hill who indicated the opposite frequency orientation of the  $TM_{020}$  mode and the parasitic  $TM_{21n}$  mode defined in Figure 9.1a.

## 9.8 Reconciliation of the Numerical Model by Hill

The model developed by Hill predicted an applicator bore of 172 mm and a resin diameter 54.54 mm for resonance in the  $TM_{020}$  mode. These values were generated assuming a magnetron output frequency of 2.46 GHz and a resin dielectric constant of 3.12. However, calibration of the magnetron revealed that the output frequency varied between 2.435 GHz and 2.452 GHz over the power range (500-5000 W) as shown in Figure 9.9. Furthermore, measurement of the dielectric constant by the cavity perturbation technique resulted in a lower value for the resin dielectric constant (2.69) as demonstrated in Chapter 8. Rerunning Hill's model with a magnetron frequency of 2.452 GHz and a dielectric constant of 2.69 resulted in a 176 mm applicator bore and a resin diameter of 57.06 mm.

Based on the applicator diameter, the response trace for this system was expected to resemble that shown in Figure 9.3. This system had a higher resonant frequency than the 172 mm bore applicator (Figure 9.2a), and was expected to include the undesirable  $TM_{21n}$  mode. Therefore, using more accurate values for the magnetron output frequency and the resin dielectric constant was not anticipated to eliminate premature cure within the cylindrical applicator.

The principal shortcoming of Hill's numerical model was that resonant modes with circumferential ( $l$ ) and longitudinal ( $n$ ) variations, such as the  $TM_{21n}$  mode, could not be predicted. Since the  $TM_{020}$  mode had no electric field component along these coordinate directions, the simplifying assumption was made that variations in these directions did not exist. Implementation of these conditions into the model would add complexity and increase computational time. Software packages to predict the electromagnetic field distributions within complex geometries are commercially available. The Transmission Line Modelling (TLM) technique was chosen to model the cylindrical applicator for its low cost and accessibility. Modelling work was carried out by the Department of Electrical and Electronic Engineering at the University of Nottingham.

### **9.9 Transmission Line Modelling of the Cylindrical Applicator**

The cylindrical applicator configured as a low  $Q$  system as left by Hill was analysed using TLM with a representative geometry of the modelled system shown in Figure 9.14. Table 9.1 shows model dimensions in relation to the actual applicator dimensions. The applicator boundary, PTFE pipe, and resin were modelled using cubic elements with a nodal spacing of 5 mm. Rectangular, rather than cylindrical coordinates were employed to model the rectangular waveguide feed, and to decrease simulation time as the number of elements was reduced. A disadvantage of rectangular coordinates was that approximations for the applicator dimensions were made. Duffy [75] indicated that the dimensional inaccuracy of the model could cause a shift in the resonant frequency, but would not alter the mode structure. It was assumed that the PTFE transitions would have a negligible effect on applicator resonance, and consequently, were not modelled. The

waveguide feed had a length of approximately 50 cm and excitation was by propagation of a plane wave from the source end of the waveguide.

Figure 9.15 shows the frequency response of the simulated applicator. Resonance for the system occurred at 2.338 GHz and 2.485 GHz with the respective applicator mode profiles shown in Figures 9.16a and 9.16b. The mode shape at 2.485 GHz (Figures 9.16b) is representative of the pure  $TM_{020}$  mode with a centrally positioned electric field maximum where the resin mass flow rate would be greatest and decaying to zero along the bore of the PTFE pipe. A mode profile with four electric field maximums and a slight central peak is shown in Figure 9.16a. This profile is similar to the heating profile established within the high Q cylindrical applicator (Section 9.7), based upon the orientation of the lobes shown in Figure 9.13. The profile could be described as the  $TM_{21n}$  mode with suppression of the fourth lobe at the waveguide feed resulting from a perturbation of the electric field caused by the aperture.

It was suggested that the mode profiles in Figures 9.16a and 9.16b represent the two extremes of heating within the applicator. The  $TM_{21n}$  mode (Figure 9.16a) is analogous to the isolated parasitic mode at 2.46 GHz in Figure 9.5a. The pure  $TM_{020}$  mode (Figure 9.16b) is expected to be the resonant peak at 2.52 GHz in Figure 9.5a. Separation between modes for the actual system was 60 MHz (2.460 GHz to 2.520 GHz) compared to 148 MHz (2.338 GHz to 2.485 GHz) for the TLM simulation. This difference could have resulted from dimensional inaccuracies, imprecise specification of the resin dielectric constant, and an inexact value for the magnetron output frequency used for the TLM simulation. Unlike Hill's model, the TLM simulation predicted excitation of a parasitic  $TM_{21n}$  mode in close proximity to the pure  $TM_{020}$  mode.

Simultaneous excitation of the  $TM_{020}$  and the  $TM_{21n}$  modes has been proposed for the low Q cylindrical applicator shown in Figure 9.1a. This proposal is supported by the typical thermal profile measured within the low Q cylindrical applicator at 500 W shown in Figure 4.13. The plot shows a temperature maximum at the centre of the PTFE pipe analogous to the electric field maximum in Figure 9.16b ( $TM_{020}$ ). Three high temperature regions are evident near the periphery of the pipe that coincide with the lobes of cured resin formed in the

applicator (Figures 5.3 and 9.13) and the electric field profile shown in Figure 9.16a ( $TM_{21n}$ ). Superimposing the TLM electric field profiles (Figures 9.16a and 9.16b) results in a mode distribution shown in Figure 9.17 that is similar to the thermal profile (Figure 4.13), and the cured resin lobes (Figures 5.3 and 9.13). Suppression of the electric field maximum at the waveguide feed was not predicted by the TLM simulation.

Shifts in the magnetron output frequency during heating support the proposal of mode superposition within the low Q cylindrical applicator (Figure 9.1a). Hill suggested that the  $TM_{020}$  mode resonated at 2.46 GHz and the  $TM_{21n}$  mode was excited at 2.50 GHz. However, results using the high Q system, and the TLM simulation indicated these modes were excited in the opposite orientation: the  $TM_{21n}$  mode resonated at 2.46 GHz and the  $TM_{020}$  mode at 2.50 GHz. The magnetron output frequency was shown to increase in proportion to the microwave power. This suggested that at maximum power (5000 W), the heating profile would shift closer to the pure  $TM_{020}$  mode, and away from the  $TM_{21n}$  mode. Consequently, heating at 5000 W for 94 seconds produced only small resin lobes (Figure 5.3) as a result of this bias towards the pure  $TM_{020}$  mode.

### 9.10 Performance Improvements to the Cylindrical Applicator

Characterisation of the cylindrical applicator suggested that a parasitic  $TM_{21n}$  mode was excited within the applicator in conjunction with the  $TM_{020}$  mode. Since separation between these modes was minimal (40-60 MHz), superposition of the heating profiles occurred when the applicator was operated as a low Q system. Influence of the  $TM_{21n}$  mode caused lobes of cured resin to form within the applicator during heating.

A pure  $TM_{020}$  mode could be excited within the cylindrical applicator by enlarging its diameter. Figure 9.4 shows the response trace for the untuned cylindrical applicator with a bore of 179.5 mm. The resonant mode at 2.55 GHz was expected to be a pure  $TM_{020}$  mode. This mode would have to be shifted to approximately 2.45 GHz in accordance with the magnetron output frequency (Figure 9.9) to enable resin preheating. Furthermore, the quality factor of the mode would have to be reduced for stable heating.

Heating efficiency is difficult to maintain for a high Q applicator since it is sensitive to variations in the magnetron output frequency and the resin dielectric constant (Section 9.4). A low Q system is desirable for heating applications as applicator sensitivity is de-emphasised. The quality factor could be reduced by lengthening the PTFE pipe so that microwave energy would be dissipated in a greater volume of resin as described in Section 9.3. A disadvantage of minimising the quality factor would be superposition of the  $TM_{21n}$  and the  $TM_{020}$  modes.

Comparison of Figures 9.2a and 9.1a demonstrates that lengthening the PTFE pipe 87 mm (from 63 mm to 150 mm) reduces the resonant frequency by 100 MHz (from 2.56 GHz to 2.46 GHz) as shown in Figure 9.18. This suggests that extending the PTFE pipe from 63 mm to 111 mm, would reduce resonance by 55 MHz.

Examination of Figures 9.2a and 9.4 illustrates that enlarging the applicator bore 7.5 mm (from 172 mm to 179.5 mm) decreases resonance of the  $TM_{21n}$  mode by 65 MHz (from 2.56 GHz to 2.495 GHz) as shown graphically in Figure 9.19. Extrapolation of this result suggests that increasing the applicator bore to 185 mm would reduce the resonant frequency an additional 45 GHz (from 2.495 GHz to 2.450 GHz).

The effects of increased pipe length and applicator bore could be applied to the  $TM_{020}$  mode in Figure 9.4. Increasing the pipe length from 63 mm to 111 mm would reduce the resonant frequency to 2.495 GHz (Figure 9.18). In addition, increasing the applicator bore from 179.5 mm to 185 mm would further reduce the resonant frequency of the  $TM_{020}$  mode from 2.495 GHz to 2.450 GHz (Figure 9.19) for a matched resonance with the magnetron. Figure 9.20 shows the applicator geometry for operation in a pure  $TM_{020}$  mode as determined by this simplified linear approximation.

Empirical determination of applicator characteristics would not be practical for additional applicator design. Simulation methods, such as TLM, provide a more efficient means of determining applicator geometry. Prediction of the mode profile for a complex applicator geometry prior to manufacture is the primary advantage of an electric field simulation. As a result, the applicator could be

produced with the confidence that the resonant frequency and heating profile would conform with the design specification.

### **9.11 Conclusion**

The cylindrical applicator was operated as a low power density system for the characterisation of the RTM process (Chapter 6). Use of the applicator in this manner imposed a restriction on the resin flow rate, but avoided premature cure of the resin in the system during operation. Superposition of a parasitic mode and the  $TM_{020}$  mode within the applicator resulted in premature resin cure. The model developed by Hill used to design the applicator assumed no excitation of circumferential or longitudinal modes so that the parasitic mode was not predicted. Identification of the parasitic mode as a form of a  $TM_{21n}$  mode was established by empirical techniques and an alternate applicator geometry was proposed to allow a pure  $TM_{020}$  mode operation. A TLM simulation supported the experimental findings, and was suggested as a basis for future applicator designs.

## List of Tables

Table 9.1 Summary of the cylindrical applicator geometry used for the TLM simulation

## List of Figures

Figure 9.1a Tuned response trace for the cylindrical applicator used during RTM characterisation showing mode superposition proposed by Hill

Figure 9.1b Cross section of the cylindrical applicator configured as a low Q system as shown in Figure 9.1a and used during the RTM characterisation

Figure 9.2a Untuned response trace for the cylindrical applicator used to approximate the model by Hill

Figure 9.2b Cross section of the cylindrical applicator used to approximate the model by Hill

Figure 9.3 Untuned response of the cylindrical applicator with a diameter of 176 mm

Figure 9.4 Untuned response of the cylindrical applicator with a diameter of 179.5 mm

Figure 9.5a Tuned response of the cylindrical applicator with a diameter of 179.5 mm

Figure 9.5b Tuned response for the dominant mode of the cylindrical applicator with a diameter of 179.5 mm

Figure 9.6a Quality factor for the cylindrical applicator with a PTFE pipe length of 63 mm

Figure 9.6b Quality factor for the cylindrical applicator with a PTFE pipe length of 130 mm

Figure 9.6c Quality factor for the cylindrical applicator with a PTFE pipe length of 150 mm

Figure 9.7a Thermal history of the resin preheating trial at 1000 W power

Figure 9.7b Efficiency of the applicator during the resin preheating trial at 1000 W

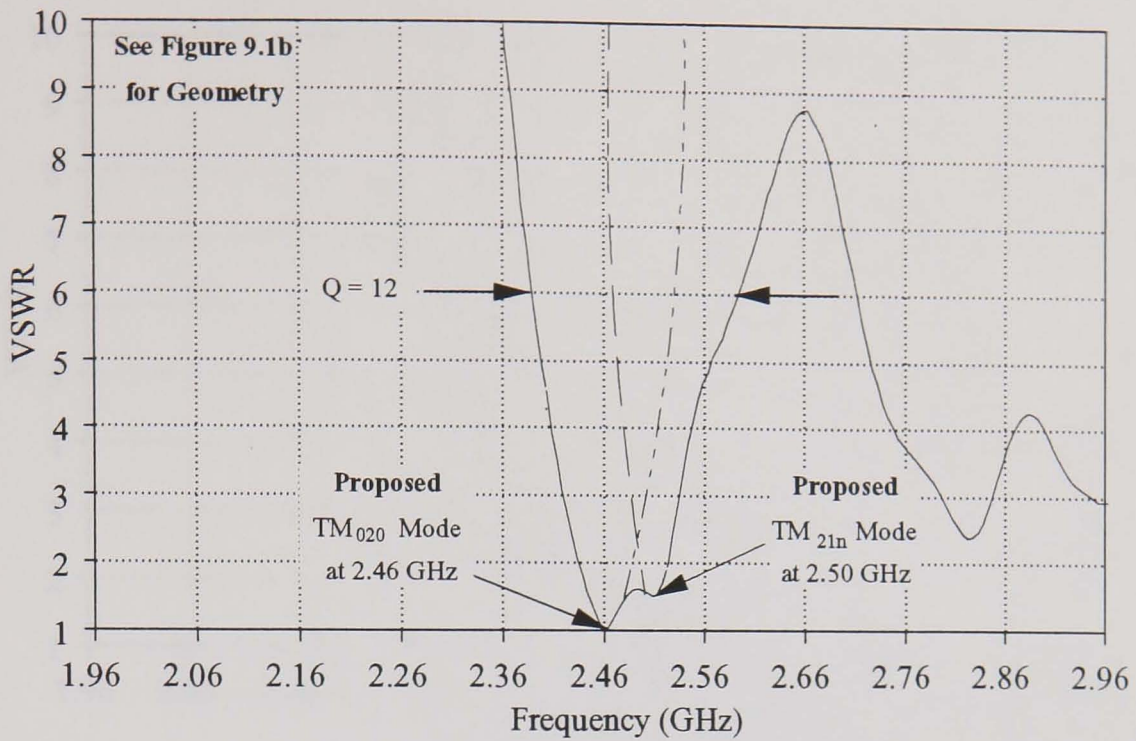
Figure 9.7c Magnetron frequency response during the resin preheating trial at 1000 W power

- Figure 9.7d Summary of the resin preheating trial at 1000 W power for the high Q cylindrical applicator
- Figure 9.8a Thermal history of the resin preheating trial at 3000 W power
- Figure 9.8b Efficiency of the applicator during the resin preheating trial at 3000 W
- Figure 9.8c Magnetron frequency response during the resin preheating trial at 3000 W power
- Figure 9.8d Summary of the resin preheating trial at 3000 W power for the high Q cylindrical applicator
- Figure 9.9 Output frequency of the YJ1600 magnetron as a function of microwave power
- Figure 9.10 Schematic of an active tuning system for use with the high Q cylindrical applicator
- Figure 9.11 Schematic of the Gerling power control system that operates at a constant magnetron frequency
- Figure 9.12a Temperature history of catalysed Synolac 6345 resin heated in the high Q cylindrical applicator
- Figure 9.12b Efficiency for catalysed Synolac 6345 resin in the high Q cylindrical applicator
- Figure 9.12c Mass flow rate of catalysed Synolac 6345 resin heated in the high Q cylindrical applicator
- Figure 9.12d Summary of the resin preheating trial for the high Q cylindrical applicator
- Figure 9.13 Cured resin lobes found within the high Q cylindrical applicator after preheating catalysed Synolac 6345 resin
- Figure 9.14 Critical dimensions for modelling of the cylindrical applicator (See Table 9.1 for values)
- Figure 9.15 Response characteristics of the cylindrical applicator generated by the TLM simulation
- Figure 9.16a Electric field profile for the cylindrical applicator at 2.338 GHz as predicted by the TLM simulation

- Figure 9.16b Electric field profile for cylindrical applicator at 2.485 GHz as predicted by the TLM simulation
- Figure 9.17 Superposition of the  $TM_{020}$  and the  $TM_{21n}$  modes indicating a typical heating profile within the applicator
- Figure 9.18 Relationship between PTFE pipe length and applicator resonant frequency
- Figure 9.19 Relationship between the applicator diameter and applicator resonant frequency
- Figure 9.20 Cross section of the proposed cylindrical applicator for operation in a pure  $TM_{020}$  mode

**Table 9.1 Summary of the Cylindrical Applicator Geometry Used for the TLM Simulation**

<b>DIMENSION</b>	<b>ACTUAL VALUE (mm)</b>	<b>MODELLED VALUE (mm)</b>
<b>a<sub>1</sub></b>	47	45
<b>a<sub>2</sub></b>	13.5	15
<b>b<sub>1</sub></b>	86	85
<b>b<sub>2</sub></b>	43	45
<b>h<sub>1</sub></b>	62	60
<b>h<sub>2</sub></b>	150	150
<b>h<sub>3</sub></b>	194	195
<b>d<sub>1</sub></b>	54.5	55
<b>d<sub>2</sub></b>	69.4	75
<b>d<sub>3</sub></b>	172	175



Reference No.	DJH100	PTFE Pipe Bore (mm)	54.45
Resin	Synolac 6345	PTFE Pipe Height (mm)	<b>150</b>
Applicator Bore (mm)	<b>172</b>	Effective Height (mm)	194
Applicator Height (mm)	62	Aperture Size (mm)	43 x 53

Figure 9.1a Tuned response trace for the cylindrical applicator used during RTM characterisation showing mode superposition proposed by Hill [22]

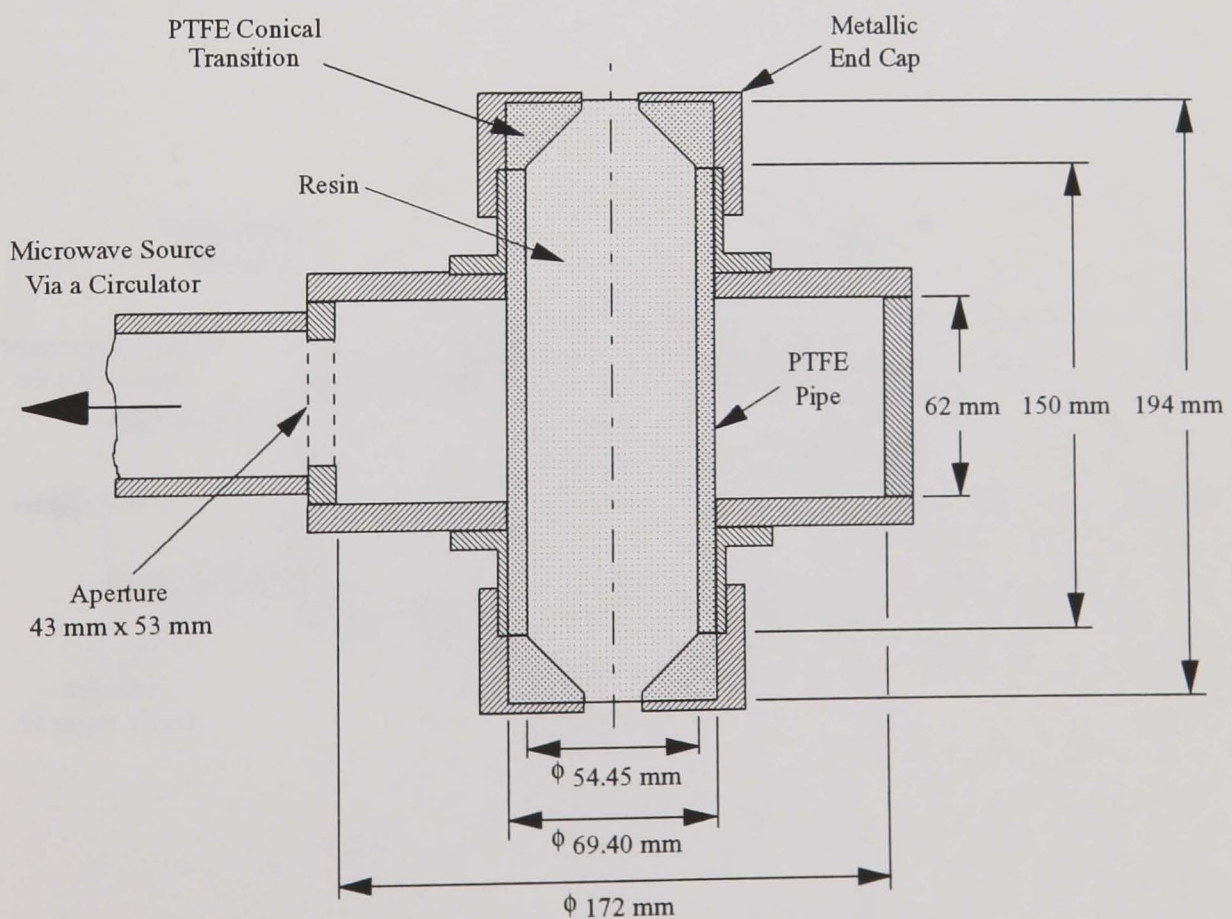
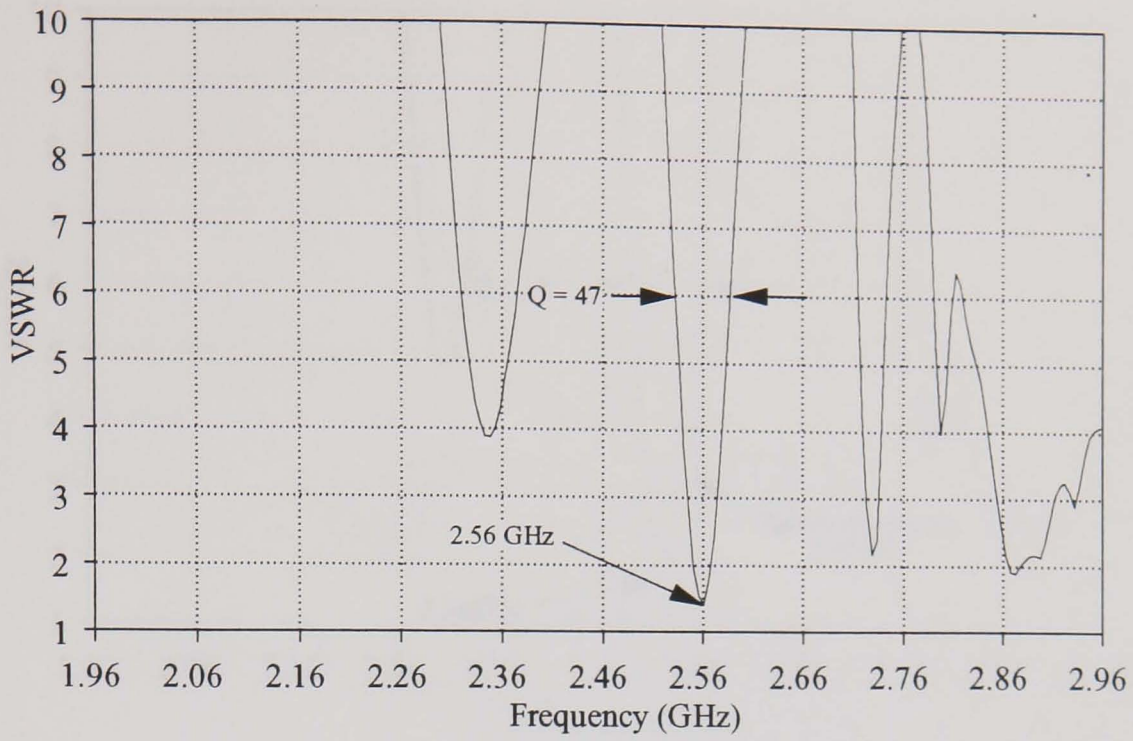


Figure 9.1b Cross section of the cylindrical applicator configured as a low Q system as shown in Figure 9.1a and used during RTM characterisation



Reference No.	MSJ003A	PTFE Pipe Bore (mm)	53.20
Resin	Synolac 6345	PTFE Pipe Height (mm)	<b>63</b>
Applicator Bore (mm)	<b>172</b>	Effective Height (mm)	107
Applicator Height (mm)	62	Aperture Size (mm)	18 x 47

Figure 9.2a Untuned response trace for the cylindrical applicator used to approximate the model by Hill

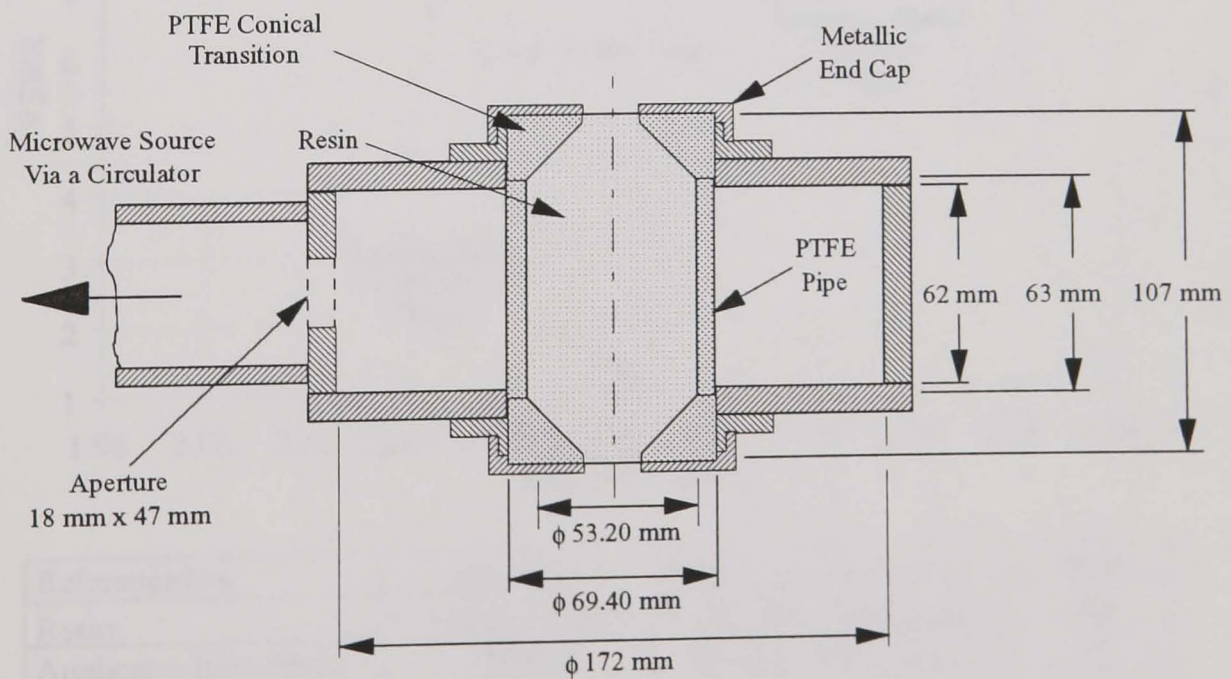
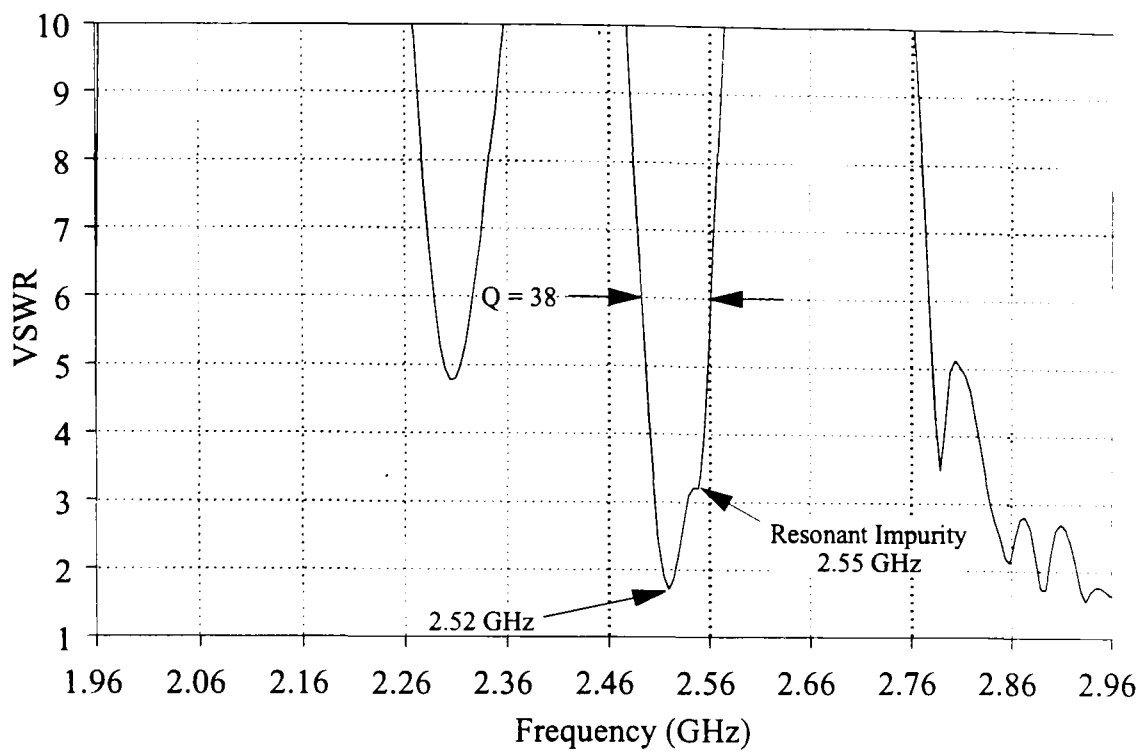
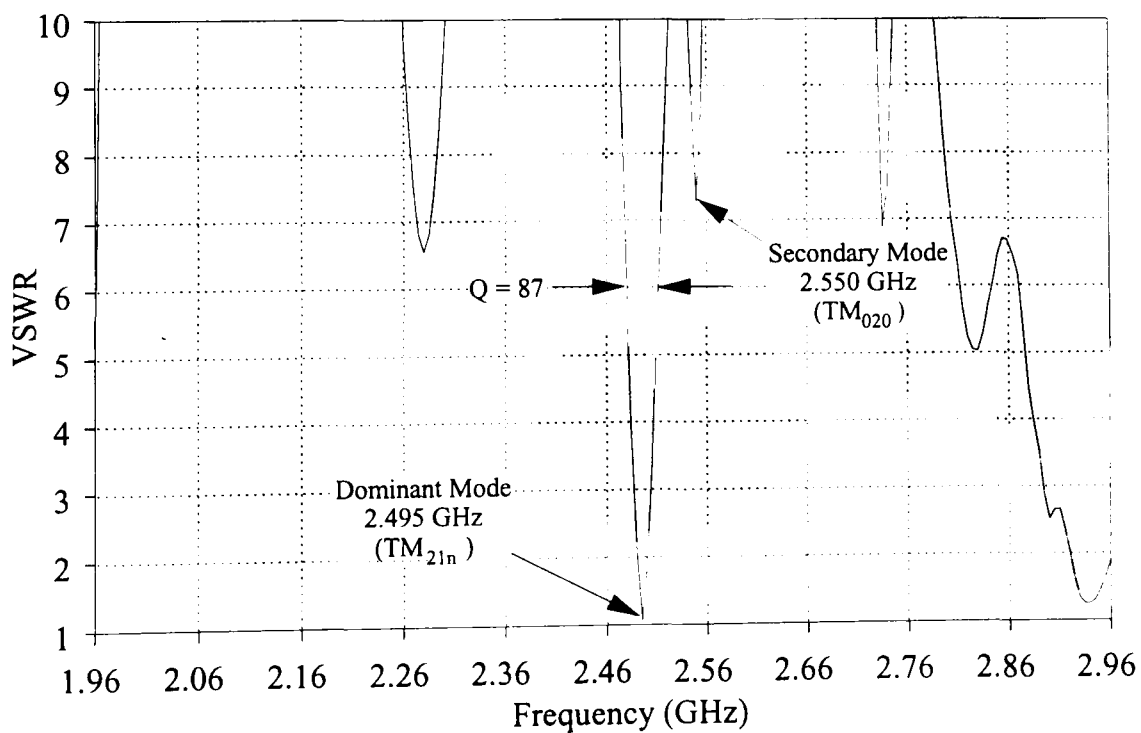


Figure 9.2b Cross section of the cylindrical applicator used to approximate the model by Hill



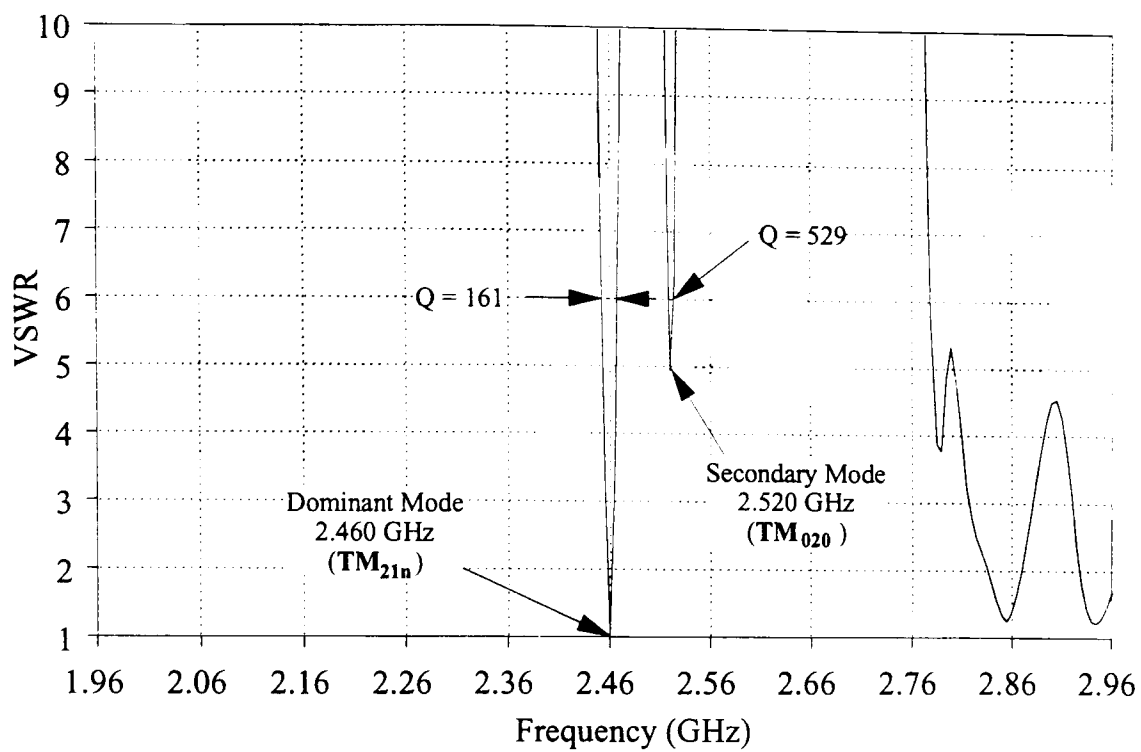
Reference No.	MSJ009A	PTFE Pipe Bore (mm)	53.20
Resin	Synolac 6345	PTFE Pipe Height (mm)	<b>63</b>
Applicator Bore (mm)	<b>176</b>	Effective Height (mm)	107
Applicator Height (mm)	62	Aperture Size (mm)	18 x 47

Figure 9.3 Untuned response of the cylindrical applicator with a diameter of 176 mm



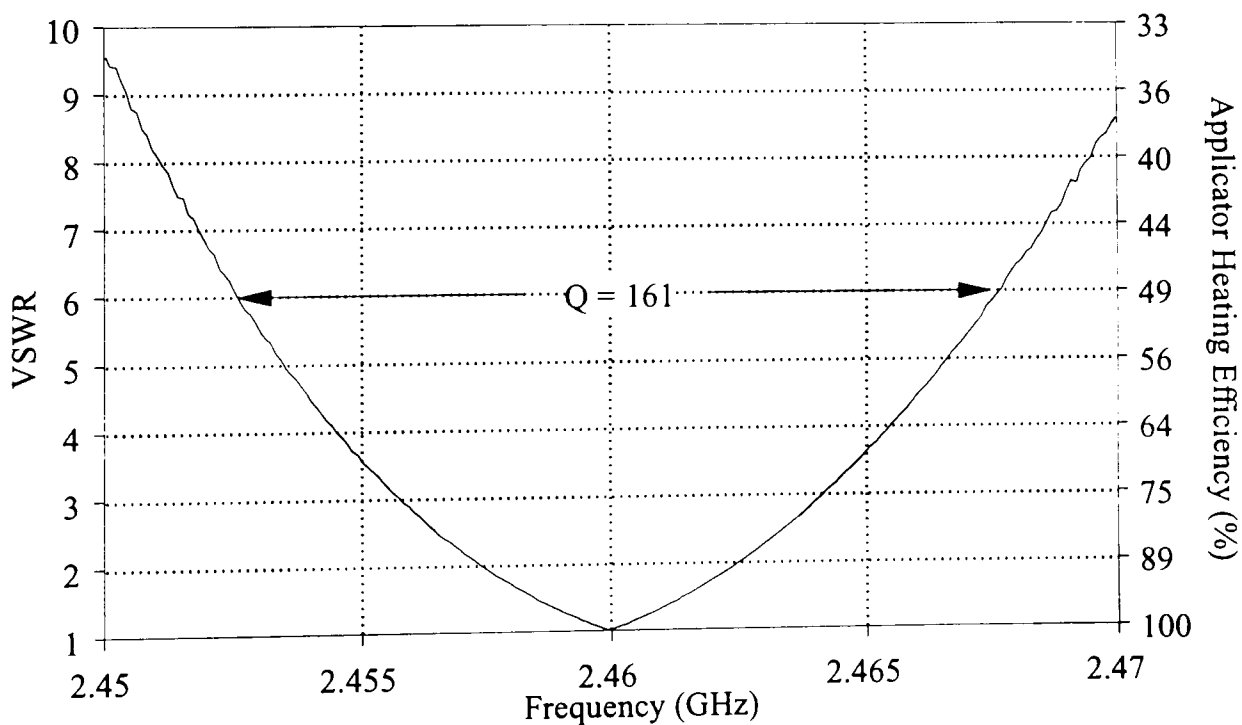
Reference No.	MSJ023A	PTFE Pipe Bore (mm)	53.20
Resin	Synolac 6345	PTFE Pipe Height (mm)	<b>63</b>
Applicator Bore (mm)	<b>179.5</b>	Effective Height (mm)	107
Applicator Height (mm)	62	Aperture Size (mm)	18 x 43

Figure 9.4 Untuned response of the cylindrical applicator with a diameter of 179.5 mm



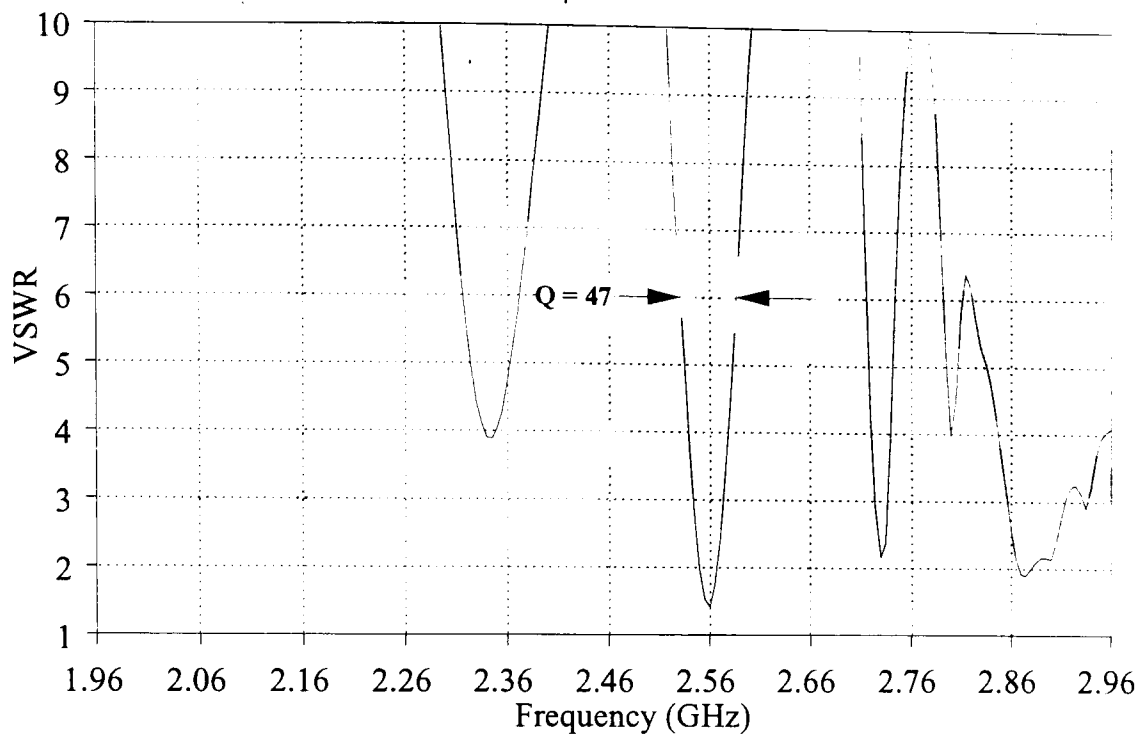
Reference No.	MSJ023B	PTFE Pipe Bore (mm)	53.20
Resin	Synolac 6345	PTFE Pipe Height (mm)	<b>63</b>
Applicator Bore (mm)	<b>179.5</b>	Effective Height (mm)	107
Applicator Height (mm)	62	Aperture Size (mm)	18 x 43

Figure 9.5a Tuned response cylindrical applicator with a diameter of 179.5 mm



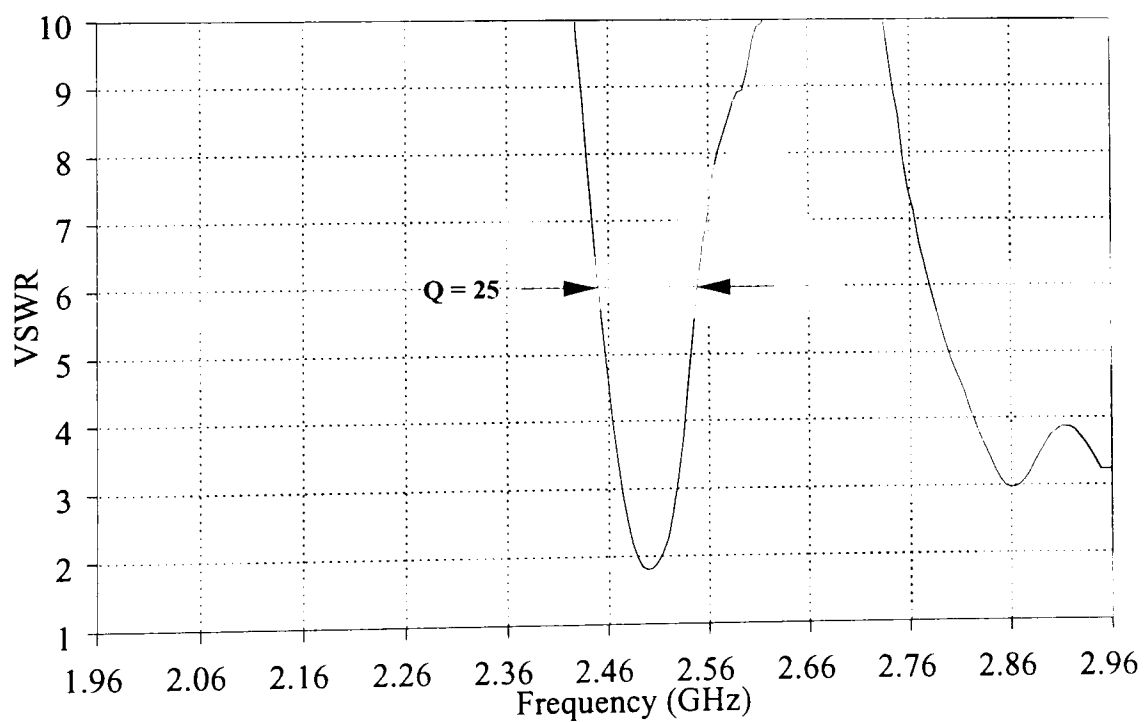
Reference No.	MSJ023C	PTFE Pipe Bore (mm)	53.20
Resin	Synolac 6345	PTFE Pipe Height (mm)	<b>63</b>
Applicator Bore (mm)	<b>179.5</b>	Effective Height (mm)	107
Applicator Height (mm)	62	Aperture Size (mm)	18 x 43

Figure 9.5b Tuned response for the dominant mode of the cylindrical applicator with a diameter of 179.5 mm



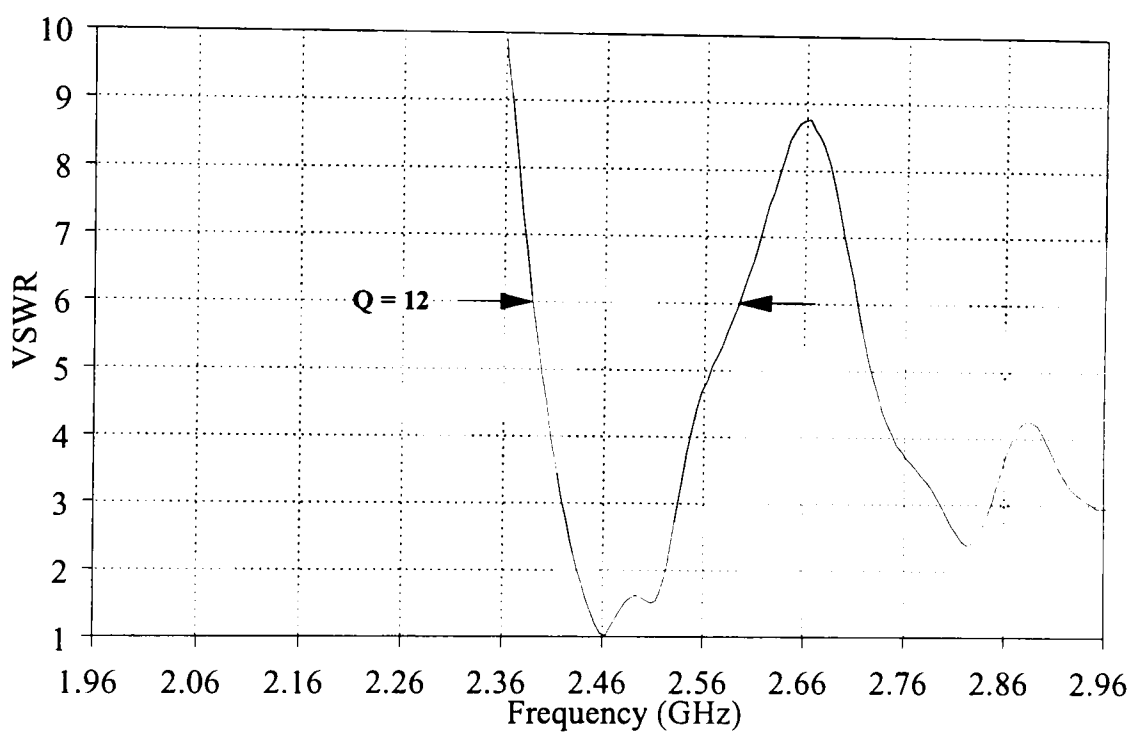
Reference No.	MSJ003A	PTFE Pipe Bore (mm)	53.20
Resin	Synolac 6345	PTFE Pipe Height (mm)	<b>63</b>
Applicator Bore (mm)	172	Effective Height (mm)	107
Applicator Height (mm)	62	Aperture Size (mm)	18 x 47

Figure 9.6a Quality factor for the cylindrical applicator with a PTFE pipe length of 63 mm



Reference No.	MSJ007A	PTFE Pipe Bore (mm)	53.20
Resin	Synolac 6345	PTFE Pipe Height (mm)	<b>130</b>
Applicator Bore (mm)	172	Effective Height (mm)	174
Applicator Height (mm)	62	Aperture Size (mm)	14 x 47

Figure 9.6b Quality factor for the cylindrical applicator with a PTFE pipe length of 130 mm



Reference No.	DJH100	PTFE Pipe Bore (mm)	54.45
Resin	Synolac 6345	PTFE Pipe Height (mm)	<b>150</b>
Applicator Bore (mm)	172	Effective Height (mm)	194
Applicator Height (mm)	62	Aperture Size (mm)	43 x 53

Figure 9.6c Quality factor for the cylindrical applicator with a PTFE pipe length of 150 mm

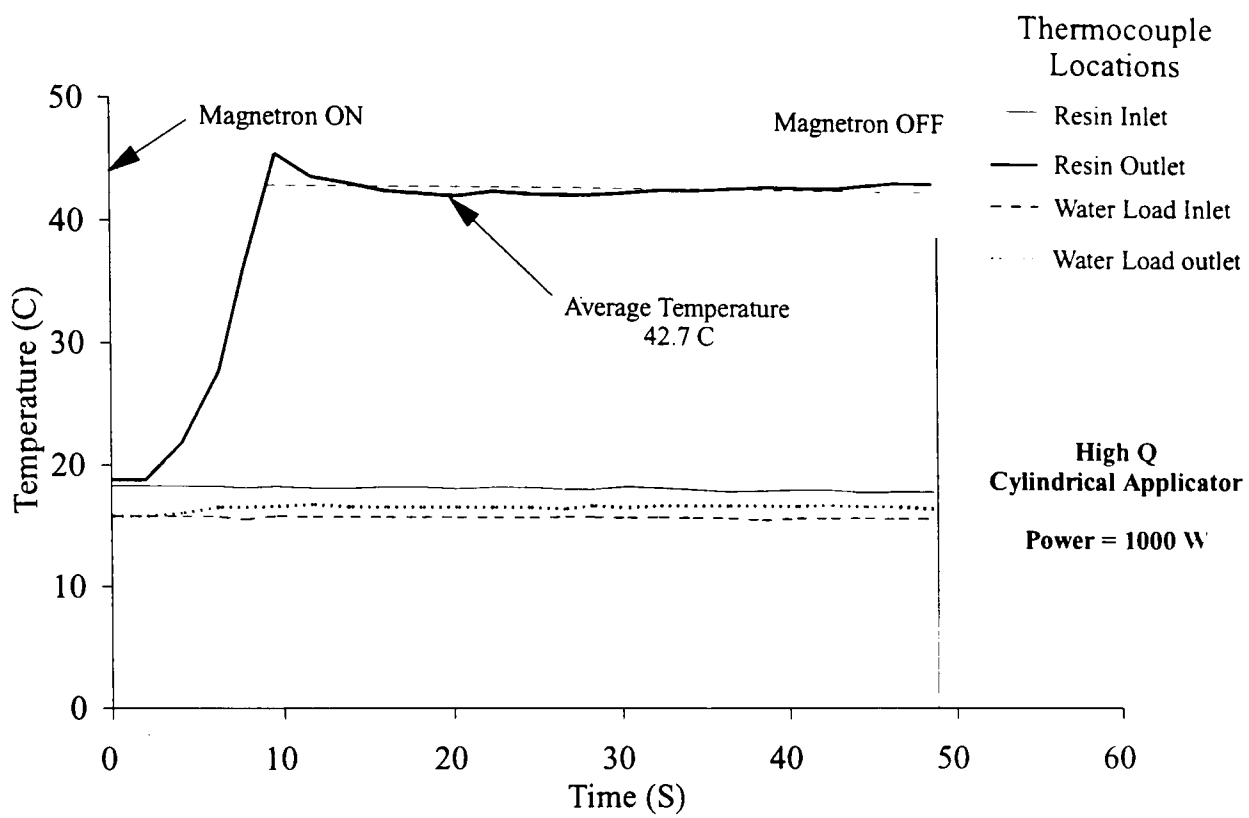


Figure 9.7a Thermal history of the resin preheating trial at 1000 W power

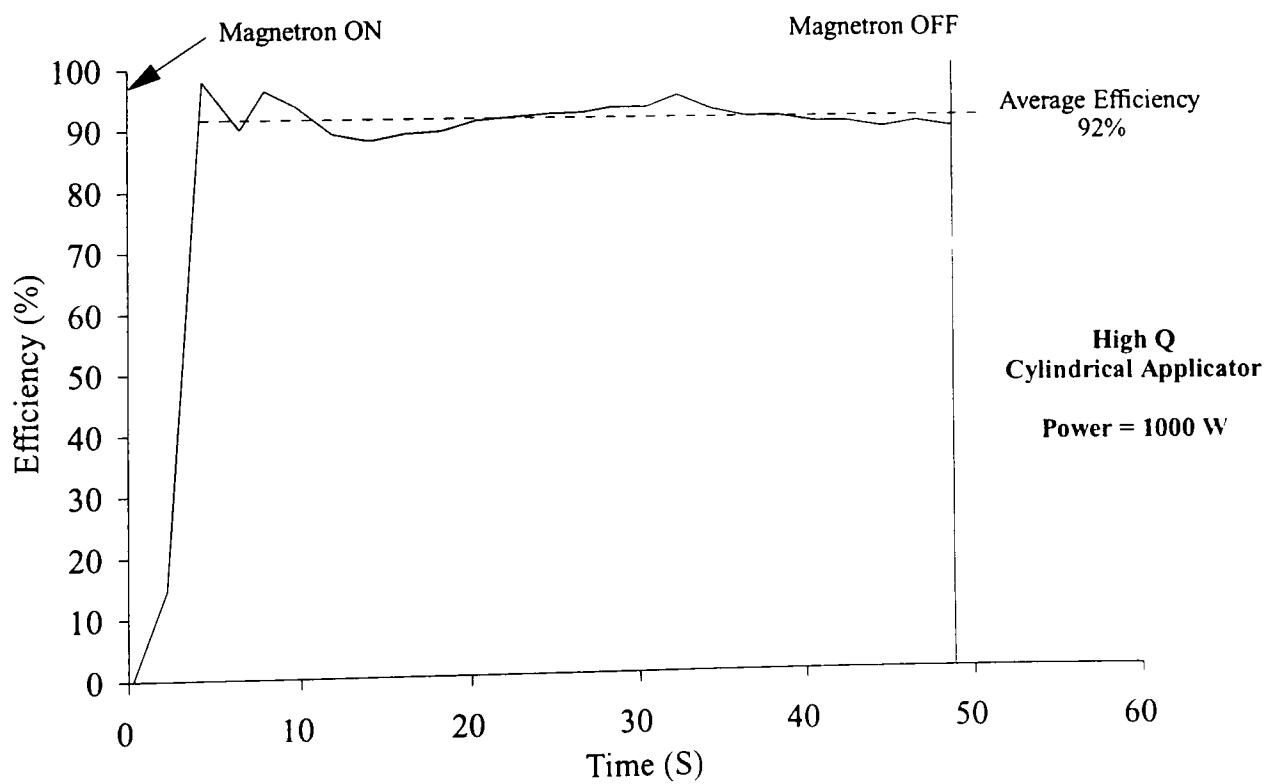


Figure 9.7b Efficiency of the applicator during the resin preheating trial at 1000 W power

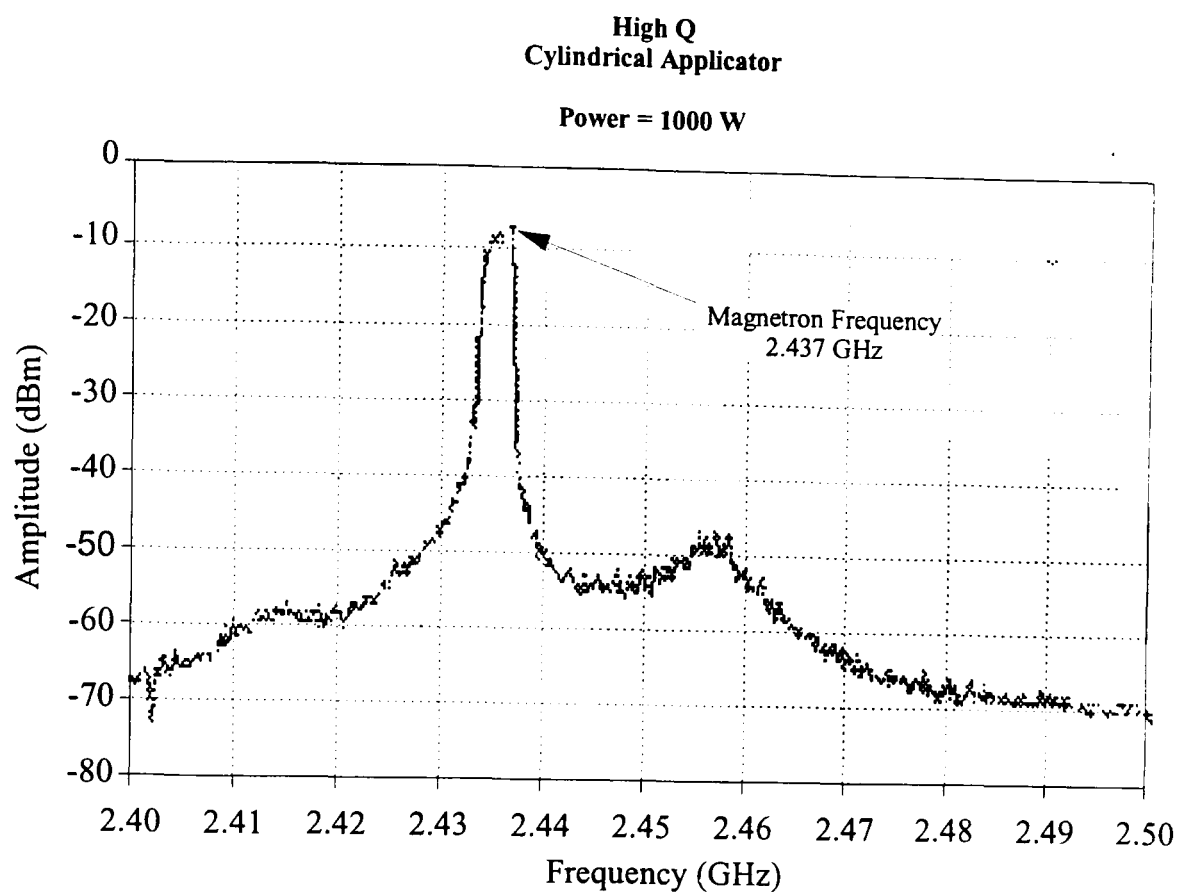


Figure 9.7c Magnetron frequency response during the resin preheating trial at 1000 W power

Reference No.	MSJ130	Magnetron Power (W)	<b>1000</b>
Resin	Synolac 6345	Magnetron Freq. (GHz)	<b>2.437</b>
Applicator Bore (mm)	172	Resin Inlet Temp. (C)	18.2
Applicator Height (mm)	62	Resin Outlet Temp. (C)	42.7
PTFE Pipe Bore (mm)	53.20	Resin Flow Rate (g/min)	966
PTFE Pipe Height (mm)	63	Water Temp. Rise (C)	0.9
Effective Height (mm)	107	Water Flow Rate (g/min)	750
Aperture Size (mm)	18 x 47	Applicator Efficiency (%)	<b>92</b>

Figure 9.7d Summary of the resin preheating trial at 1000 W power for the high Q cylindrical applicator

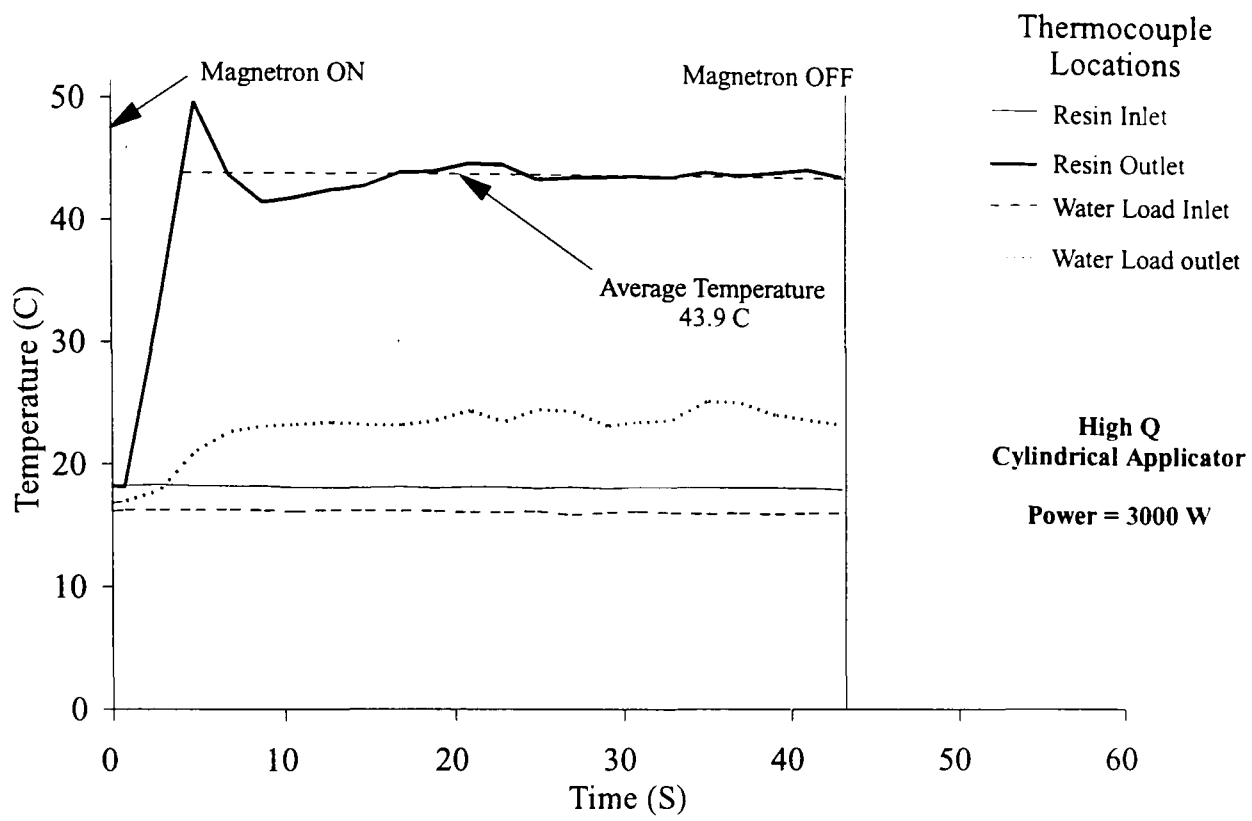


Figure 9.8a Thermal history of the resin preheating trial at 3000 W power

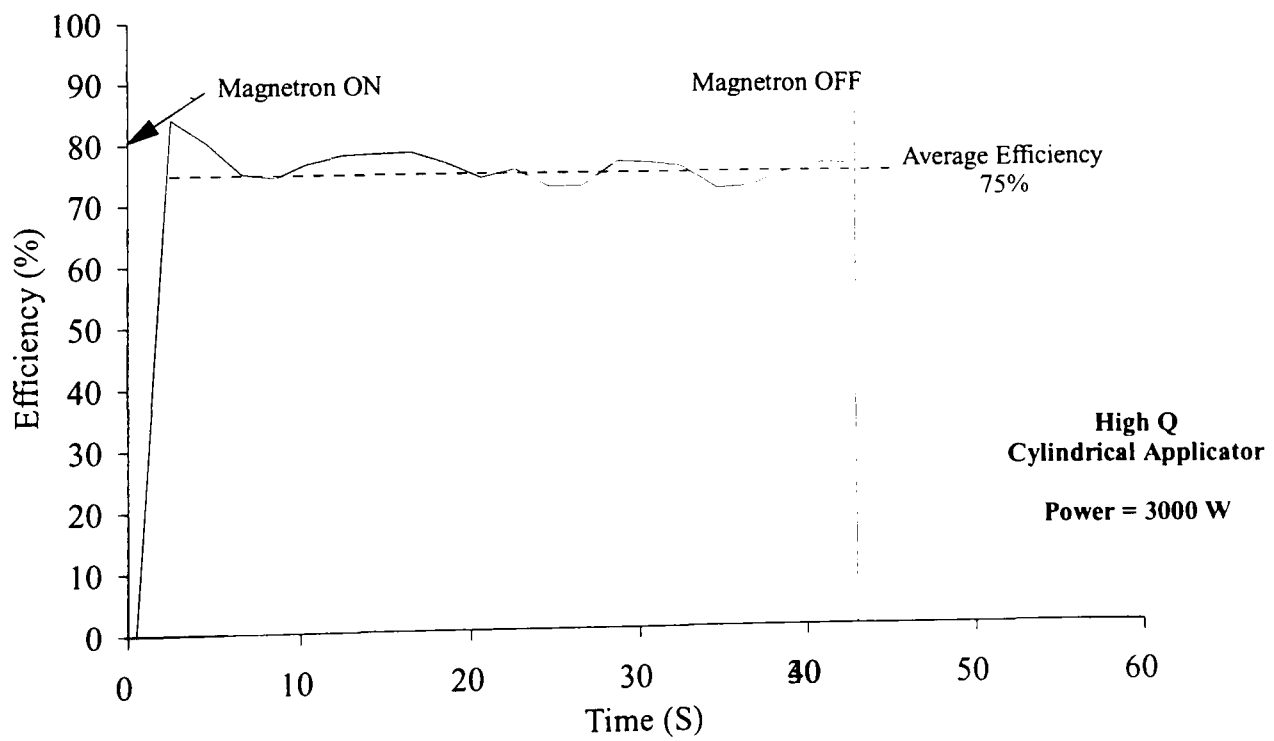


Figure 9.8b Efficiency of the applicator during the resin preheating trial at 3000 W power

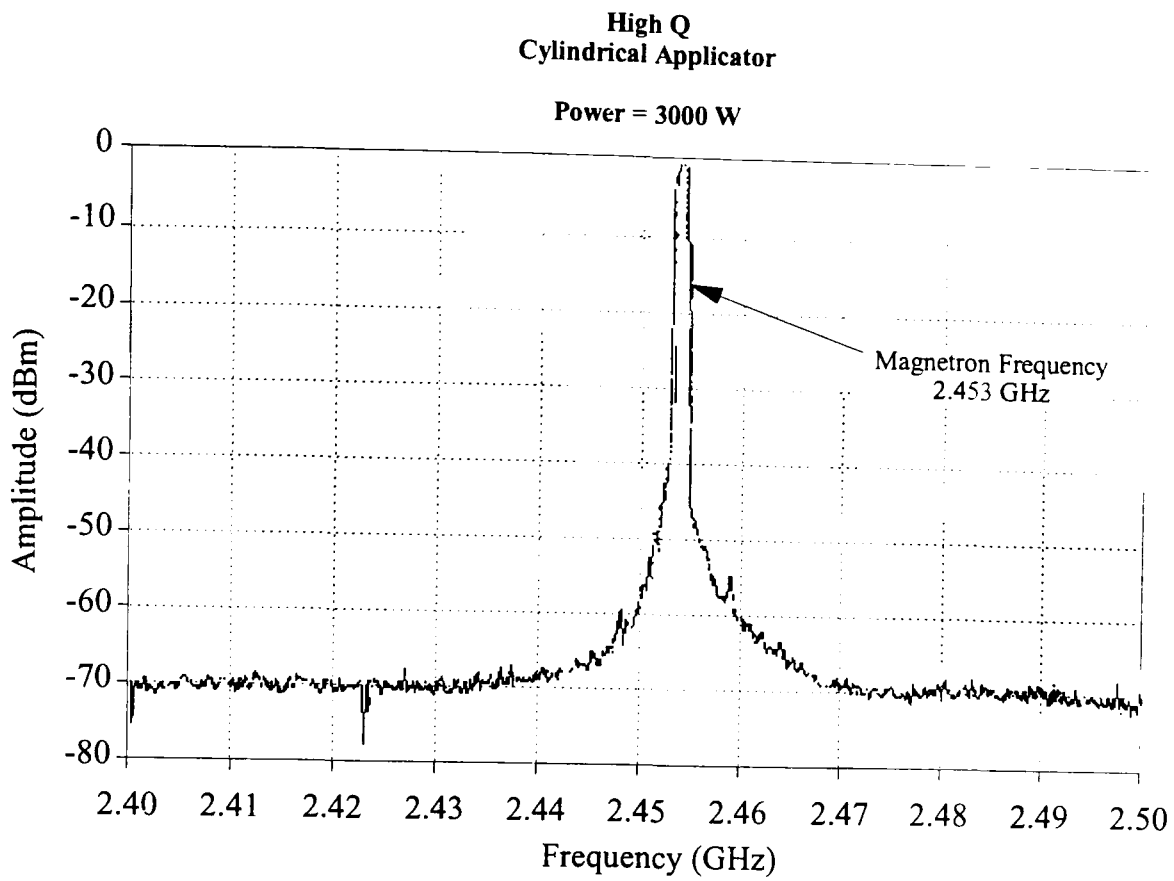


Figure 9.8c Magnetron frequency response during the resin preheating trial at 3000 W power

Reference No.	MSJ131	Magnetron Power (W)	<b>3000</b>
Resin	Synolac 6345	Magnetron Freq. (GHz)	<b>2.453</b>
Applicator Bore (mm)	172	Resin Inlet Temp. (C)	18.3
Applicator Height (mm)	62	Resin Outlet Temp. (C)	43.9
PTFE Pipe Bore (mm)	53.20	Resin Flow Rate (g/min)	2053
PTFE Pipe Height (mm)	63	Water Temp. Rise (C)	7.8
Effective Height (mm)	107	Water Flow Rate (g/min)	750
Aperture Size (mm)	18 x 47	Applicator Efficiency (%)	<b>75</b>

Figure 9.8d Summary of the resin preheating trial at 3000 W power for the high Q cylindrical applicator

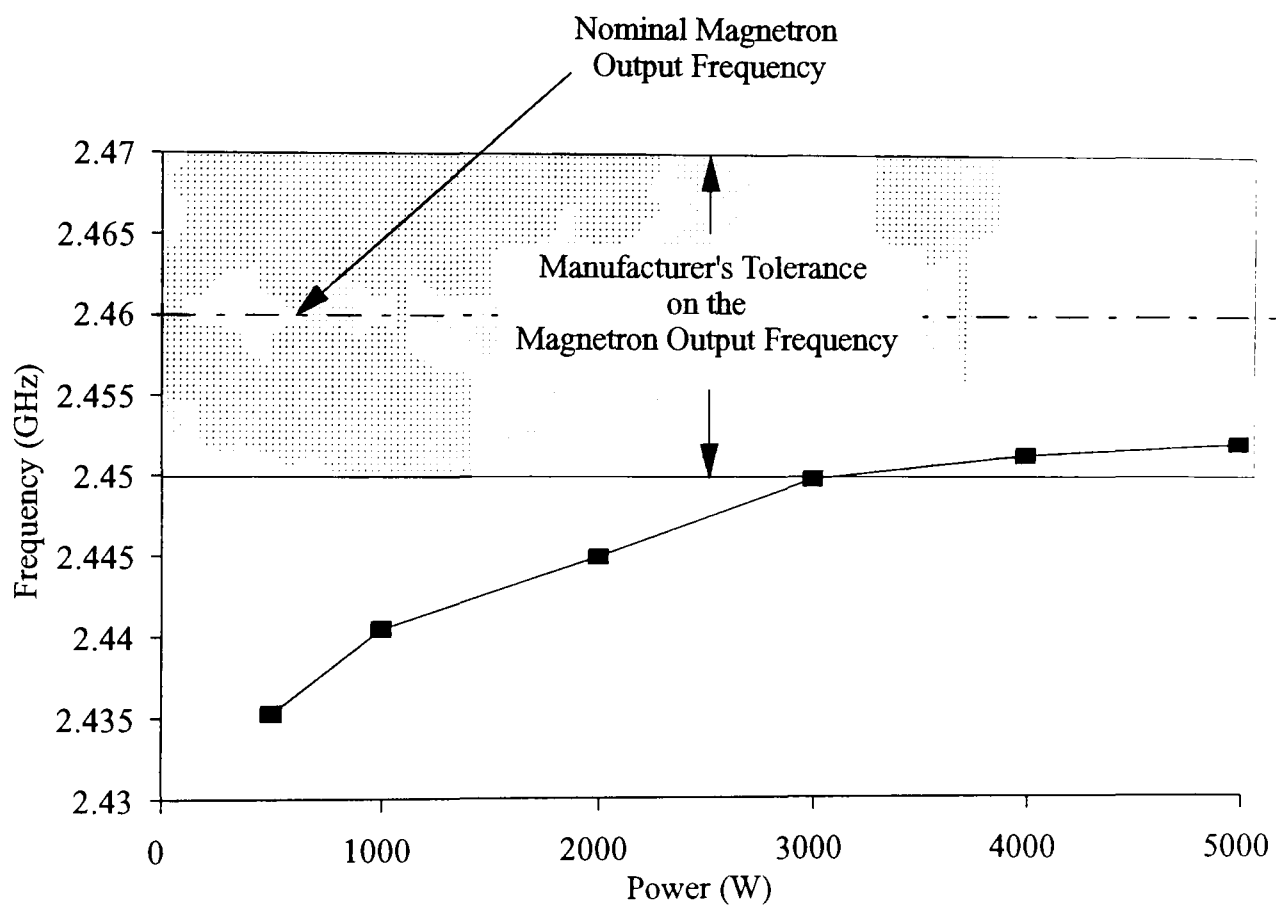
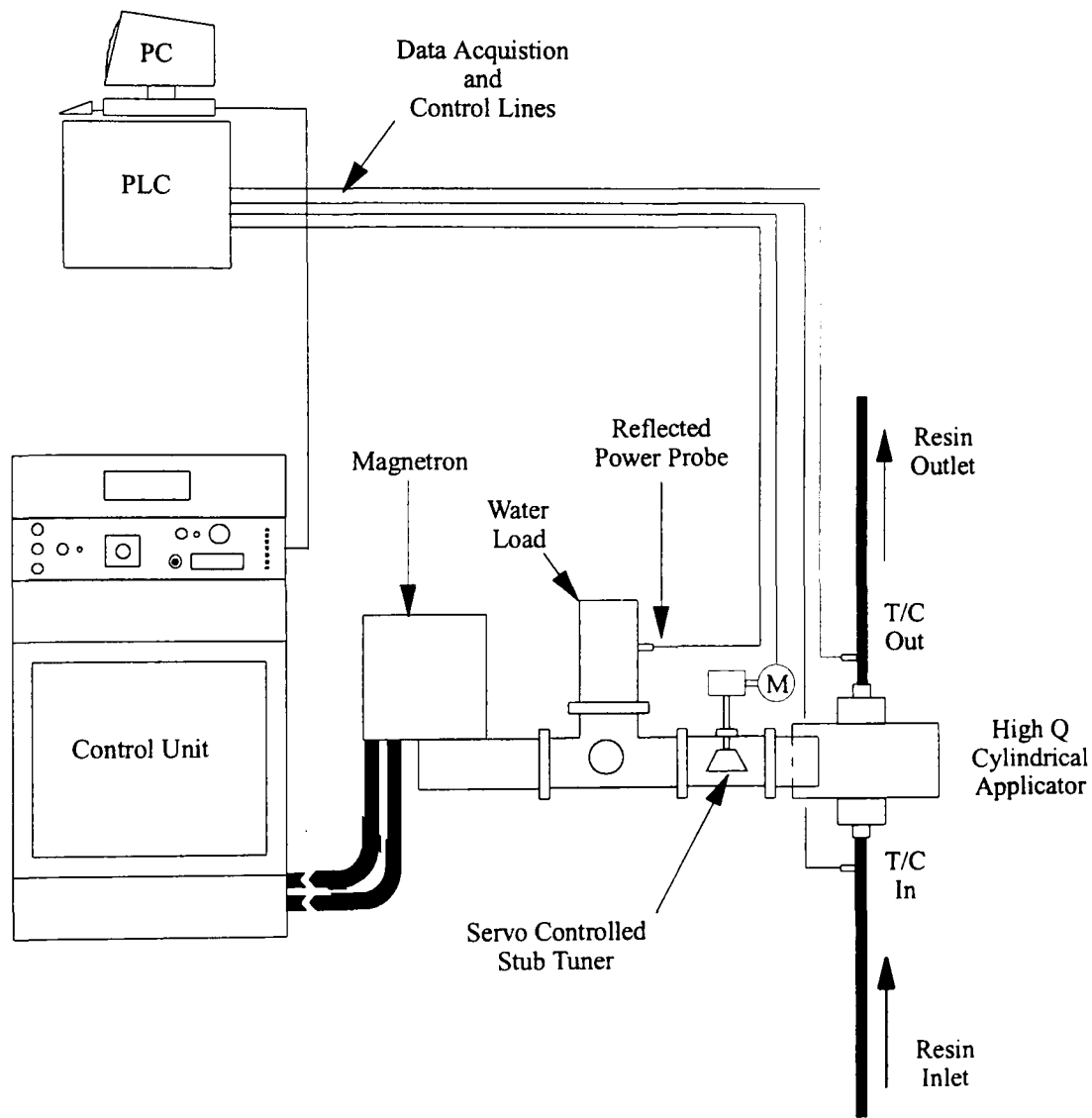


Figure 9.9 Output frequency of the YJ1600 magnetron as a function of microwave power



T/C = Thermocouple

Figure 9.10 Schematic of an active tuning system for use with the high Q cylindrical applicator

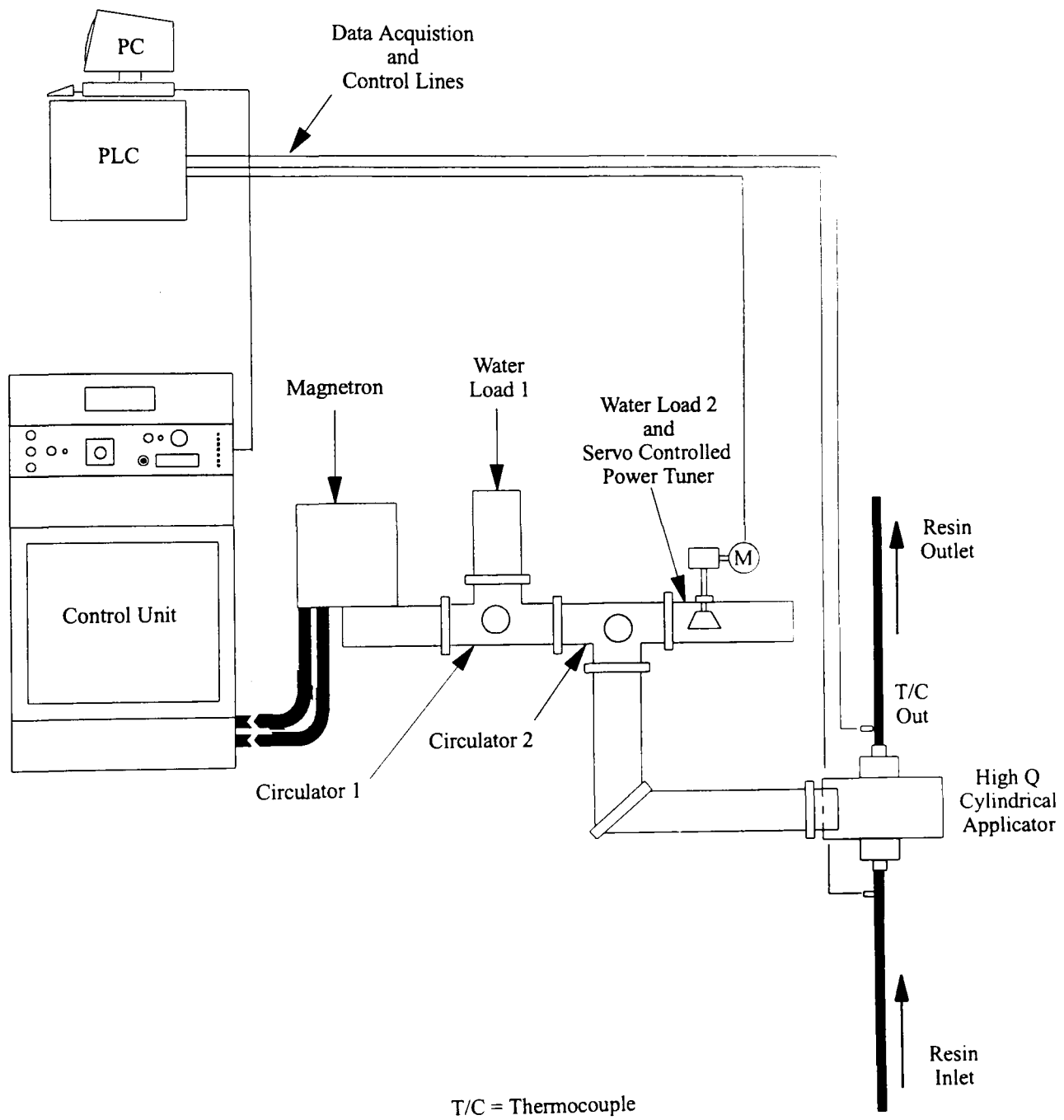


Figure 9.11 Schematic of Gerling power control system that operates at a constant magnetron frequency

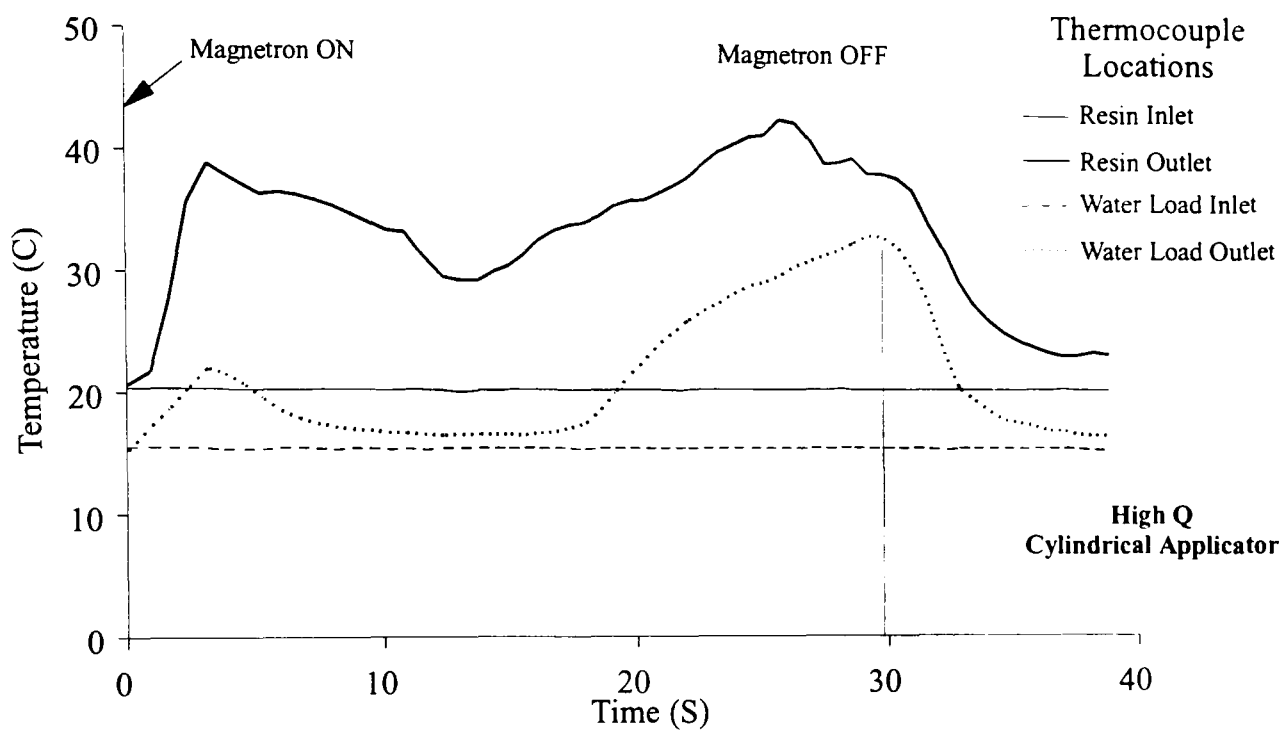


Figure 9.12a Temperature history of catalysed Synolac 6345 resin heated in the high Q cylindrical applicator

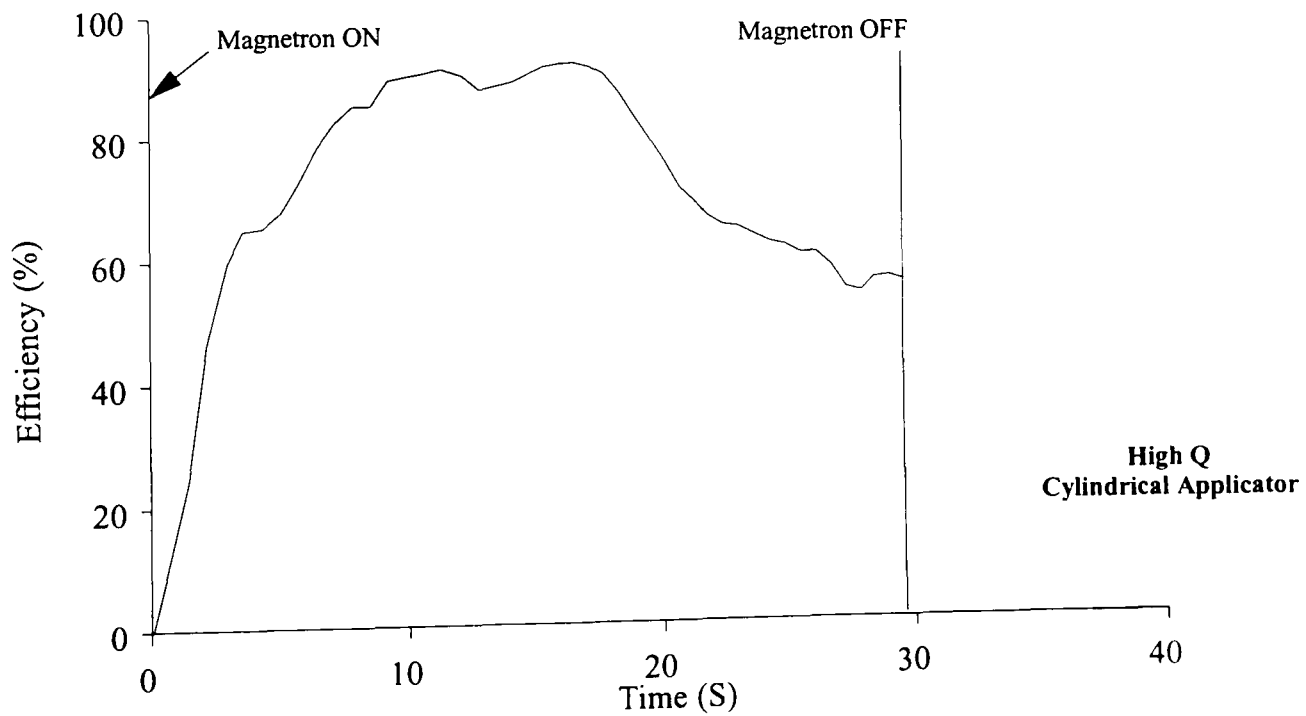


Figure 9.12b Efficiency for catalysed Synolac 6345 resin in the high Q cylindrical applicator

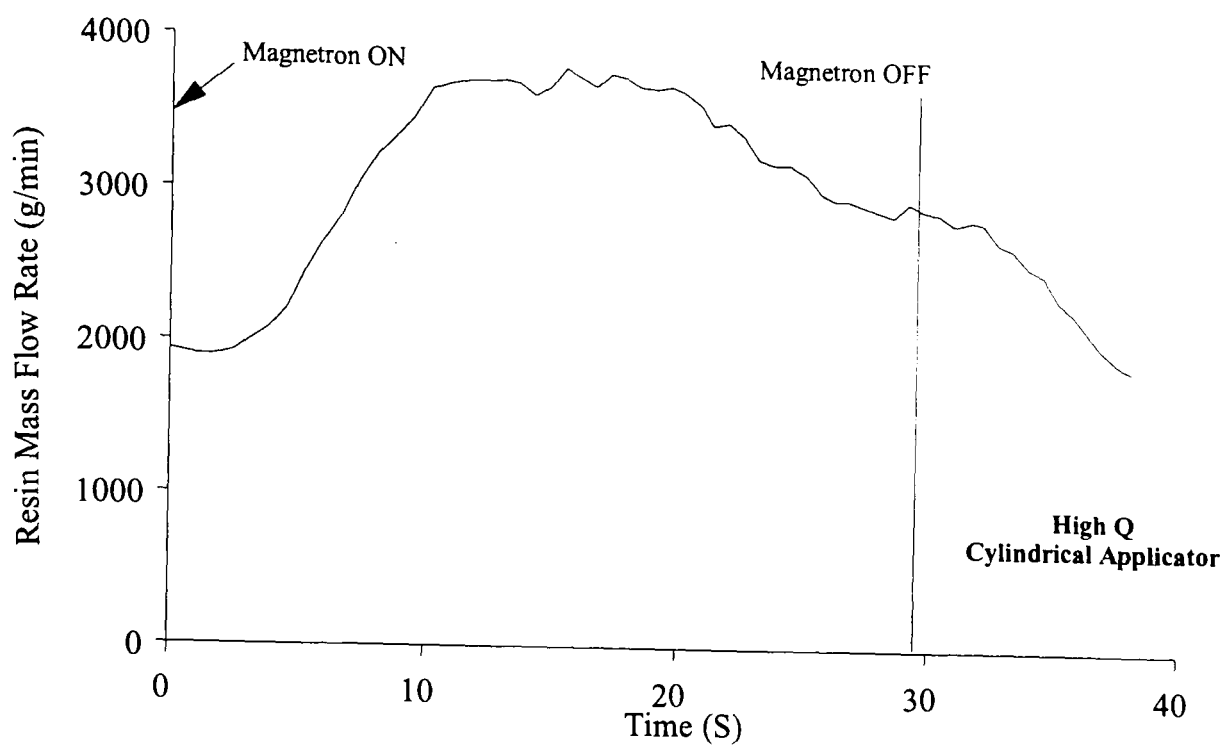


Figure 9.12c Mass flow rate of catalysed Synolac 6345 resin heated in the high Q cylindrical applicator

Reference No.	MSJ073	Applicator Bore (mm)	179.5
Resin	Synolac 6345	Applicator Height (mm)	62
Catalyst	1% TBPEH	PTFE Pipe Bore (mm)	53.20
Magnetron Power (W)	2500	PTFE Pipe Height (mm)	63
Aperture Size (mm)	18 x 43	Effective Height (mm)	107

Figure 9.12d Summary of the resin preheating trial for the high Q cylindrical applicator

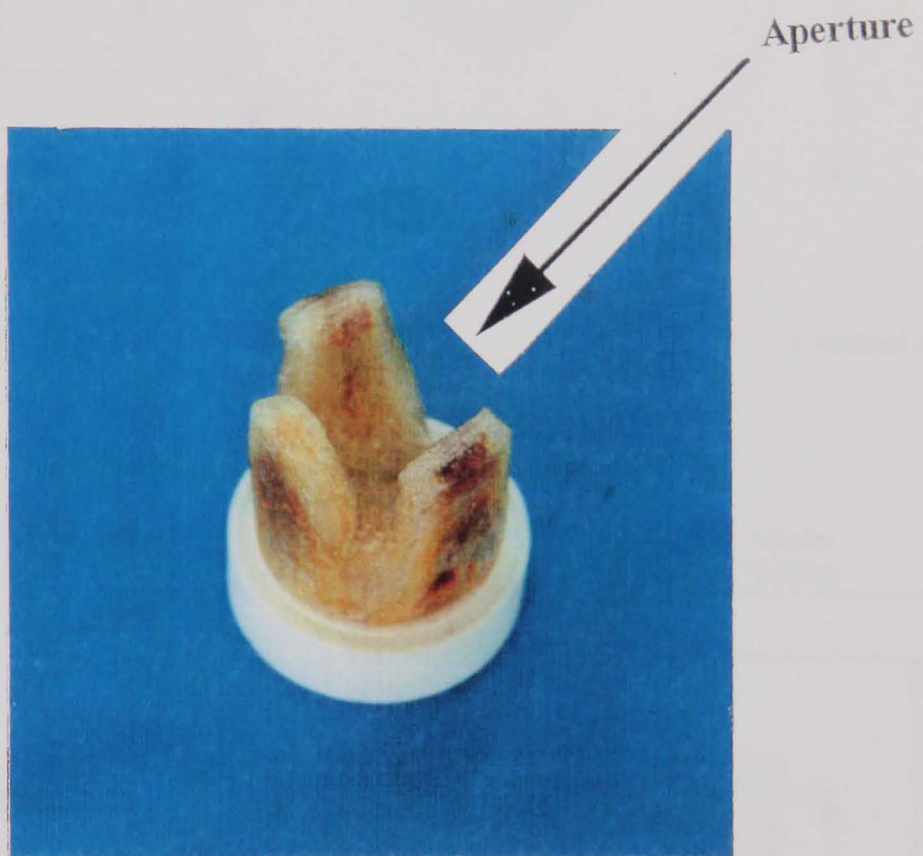


Figure 9.13

Cured resin lobes found within the high Q cylindrical applicator after preheating catalysed Synolac 6345 resin

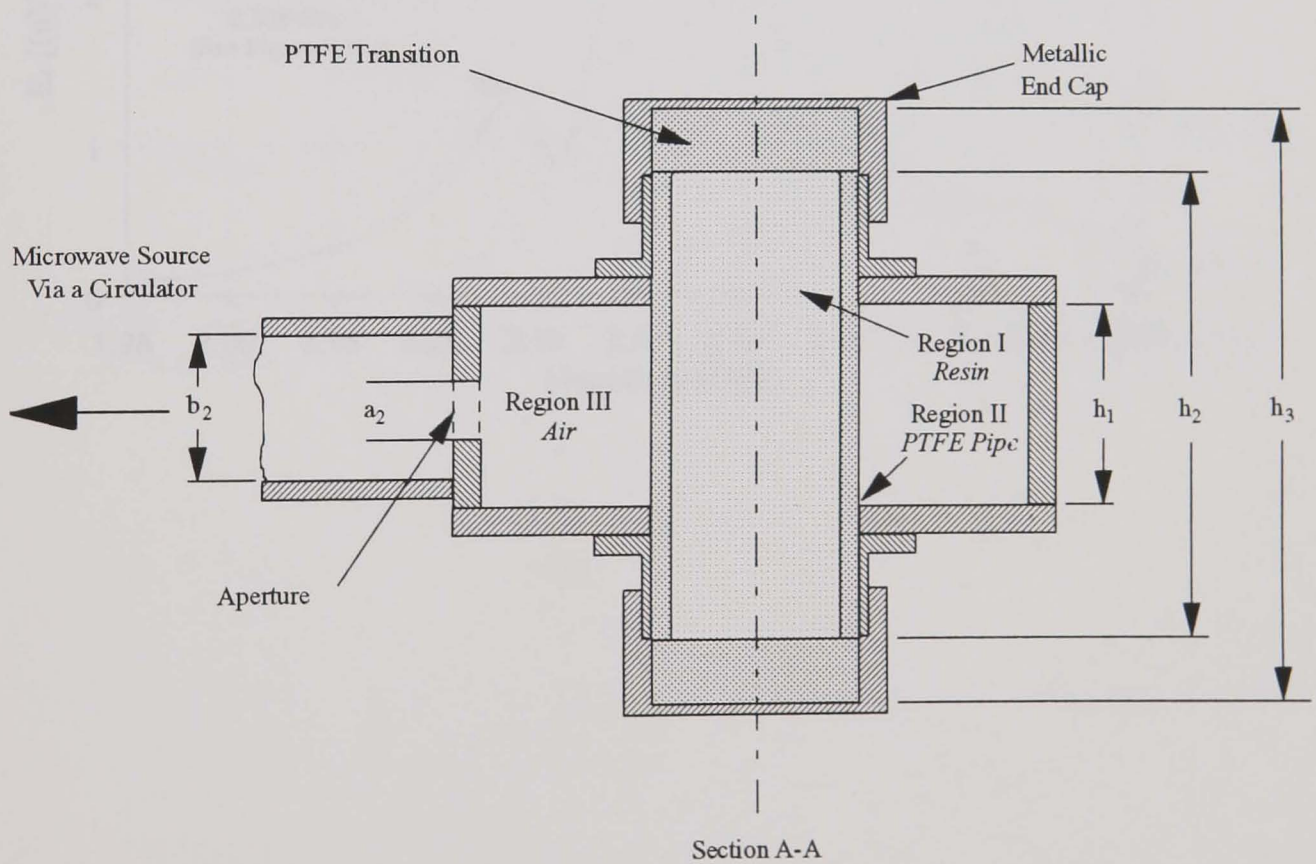
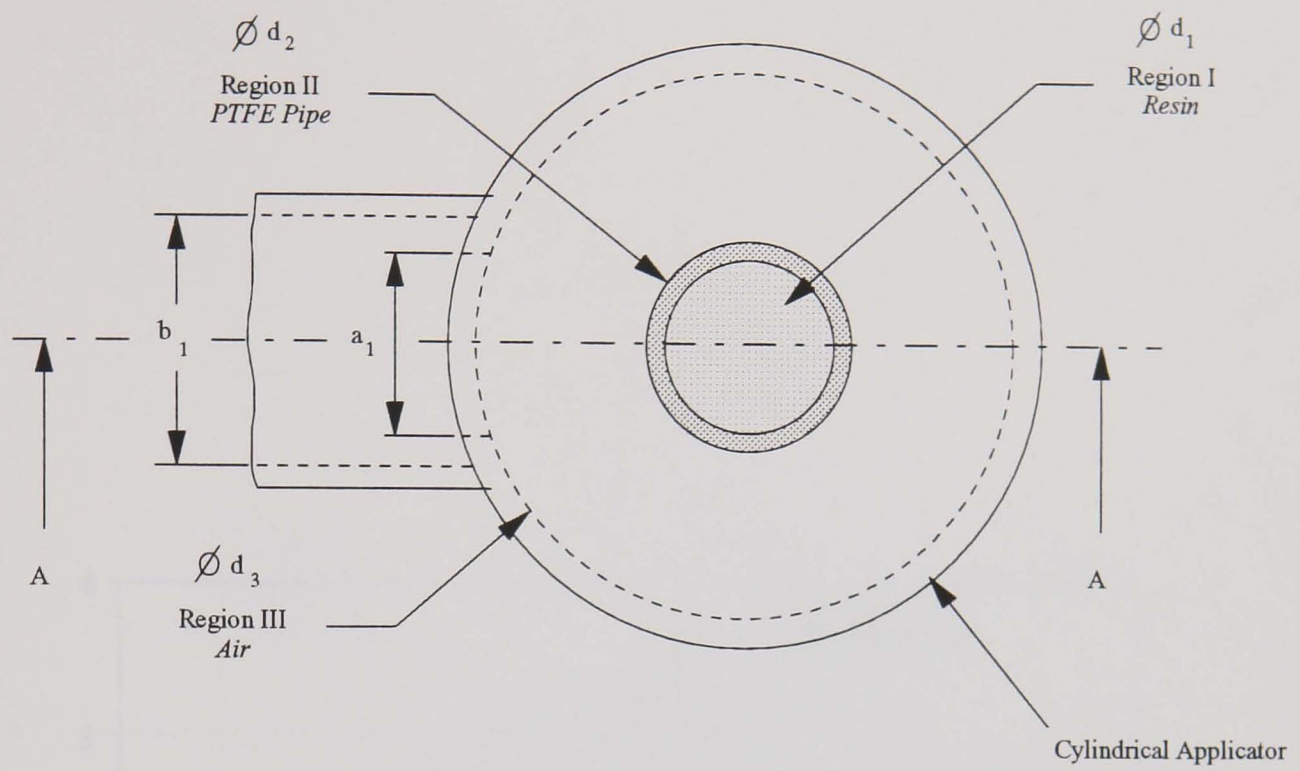


Figure 9.14

Critical dimensions for modelling of the cylindrical applicator (See Table 9.1 for values)

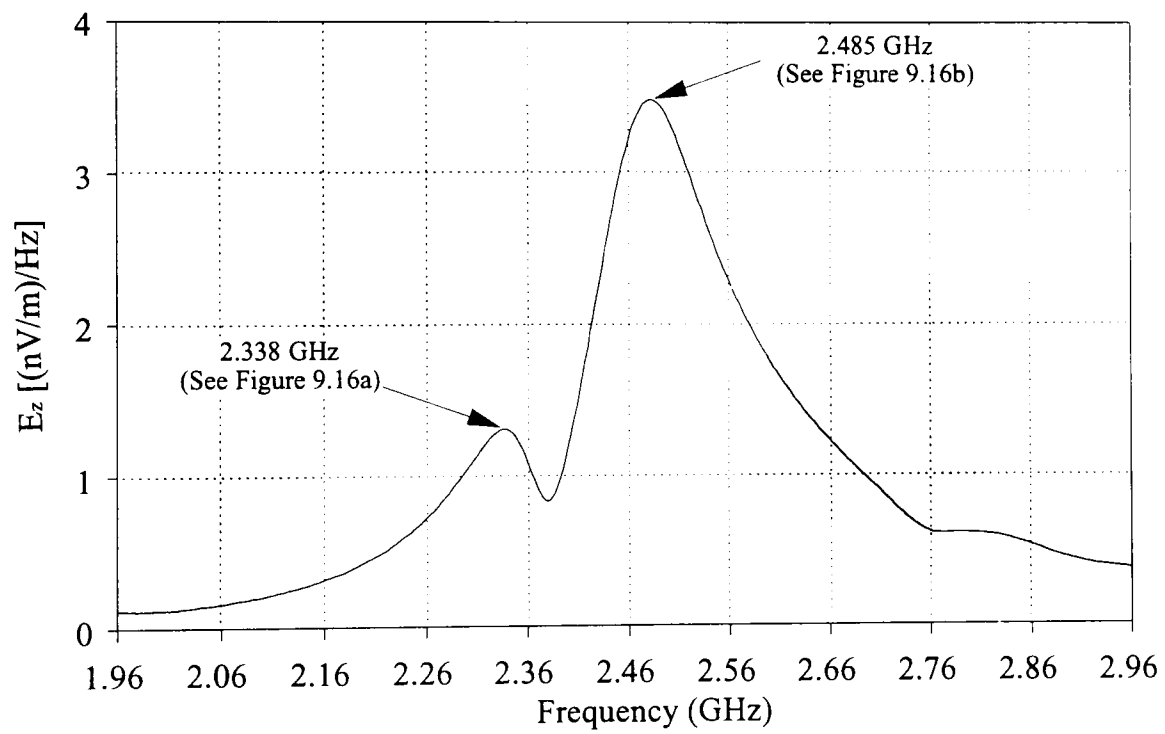


Figure 9.15 Response characteristics of the cylindrical applicator generated by the TLM simulation

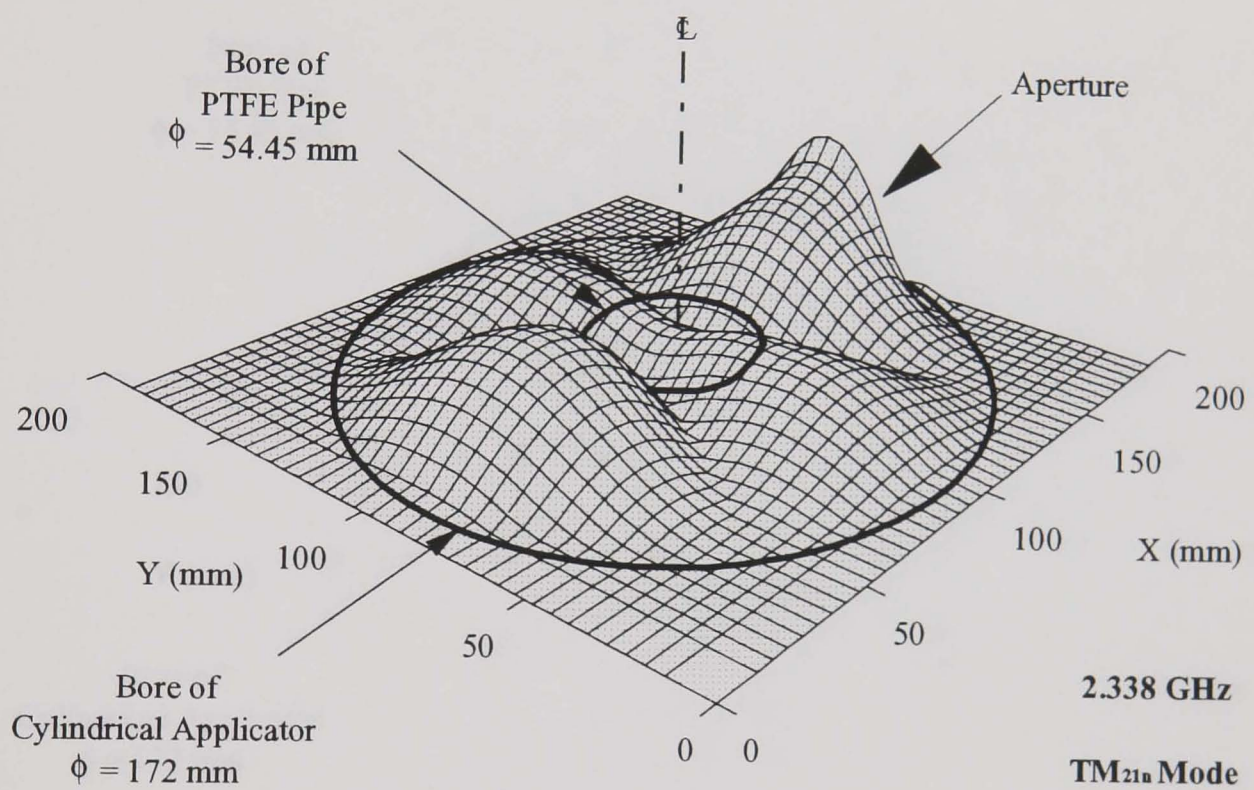


Figure 9.16a Electric field profile for the cylindrical applicator at 2.338 GHz as predicted by the TLM simulation

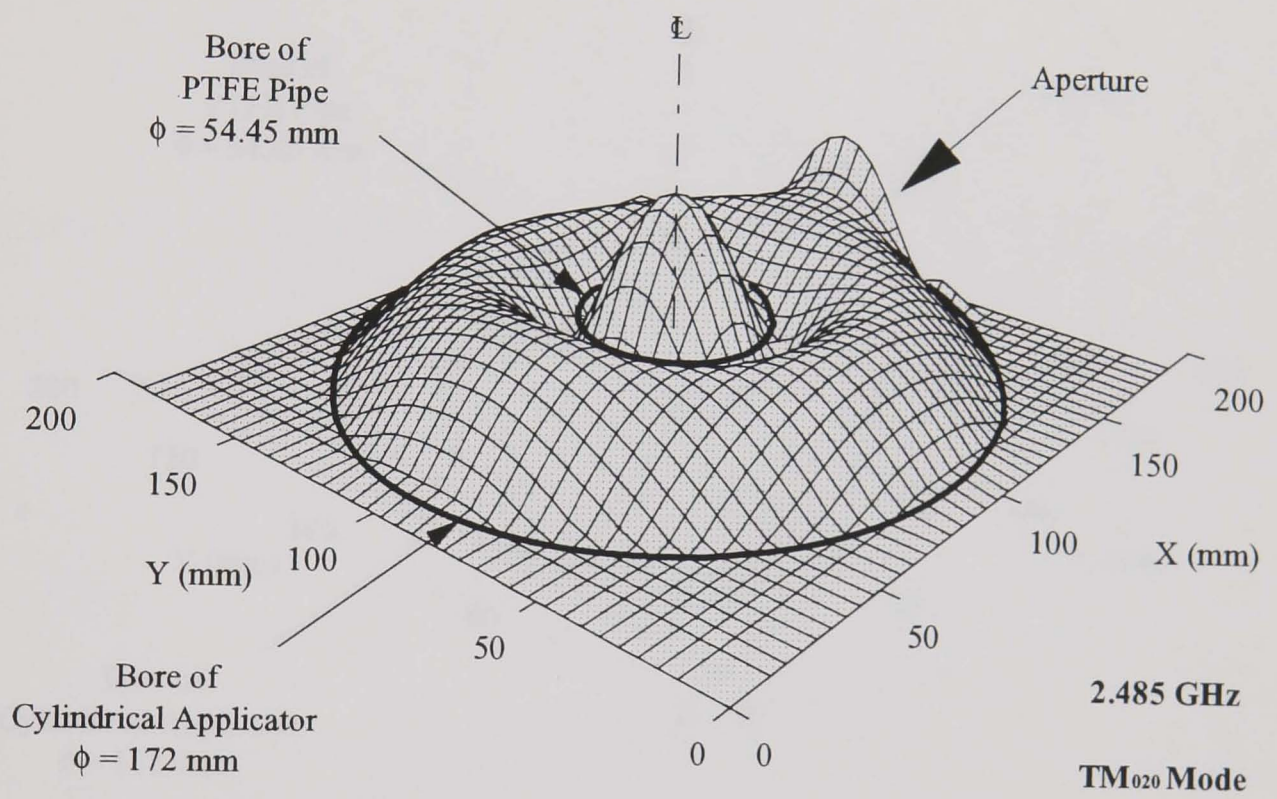


Figure 9.16b Electric field profile for the cylindrical applicator at 2.485 GHz as predicted by the TLM simulation

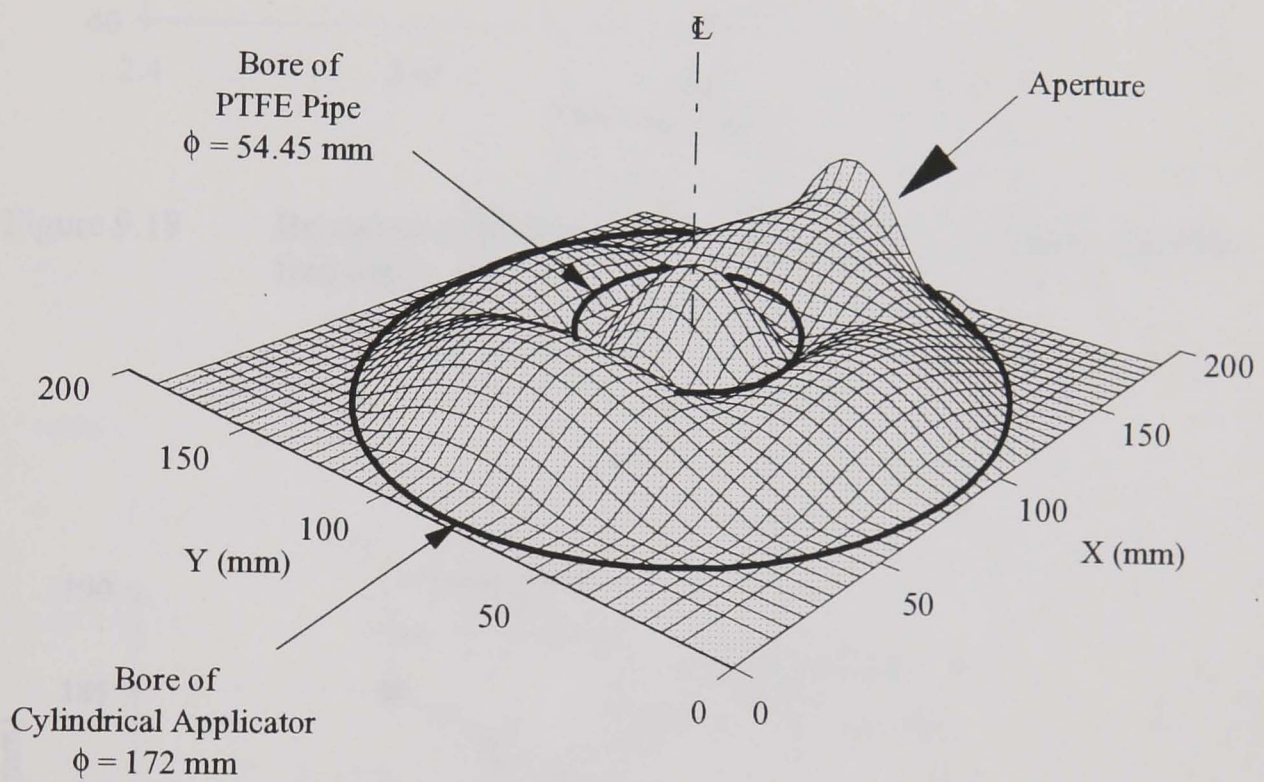


Figure 9.17 Superposition of the  $TM_{020}$  and the  $TM_{21n}$  modes indicating a typical heating profile within the applicator

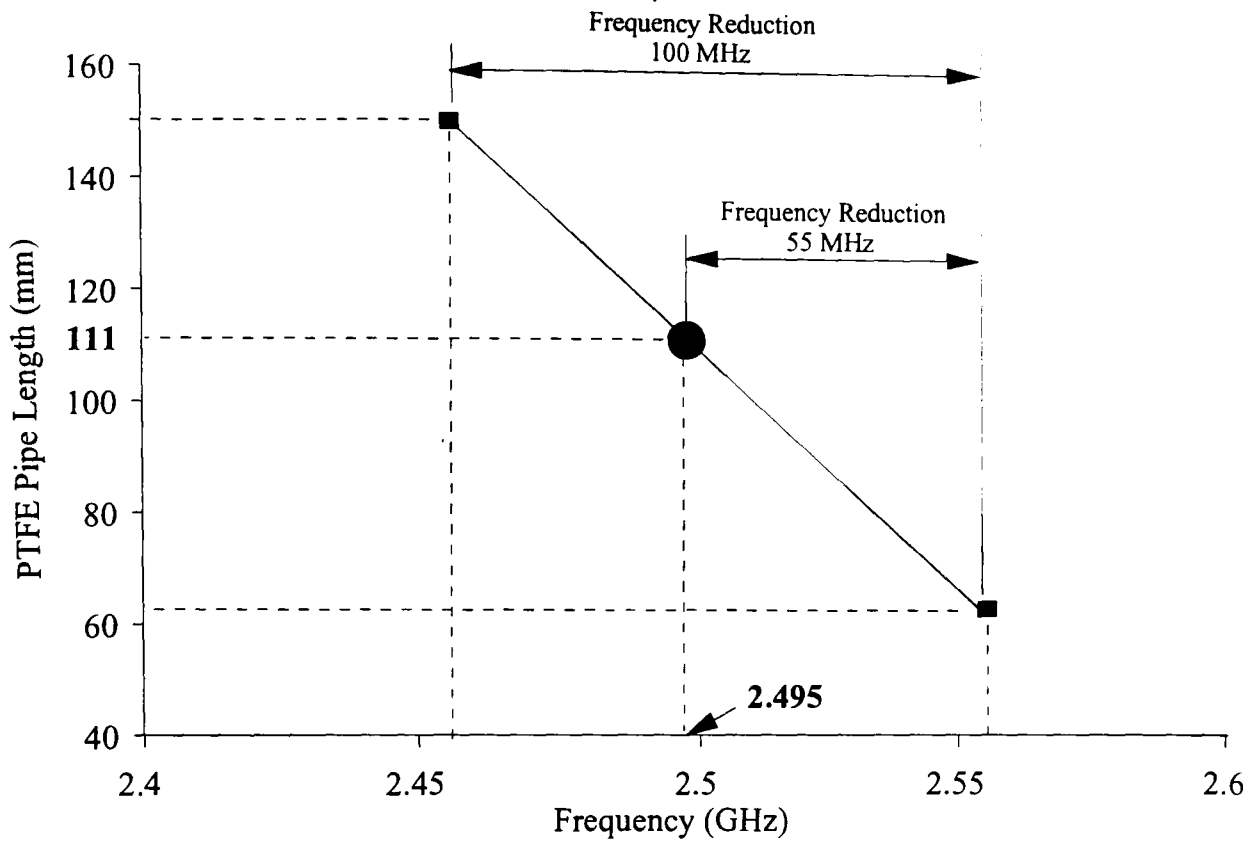


Figure 9.18 Relationship between PTFE pipe length and applicator resonant frequency

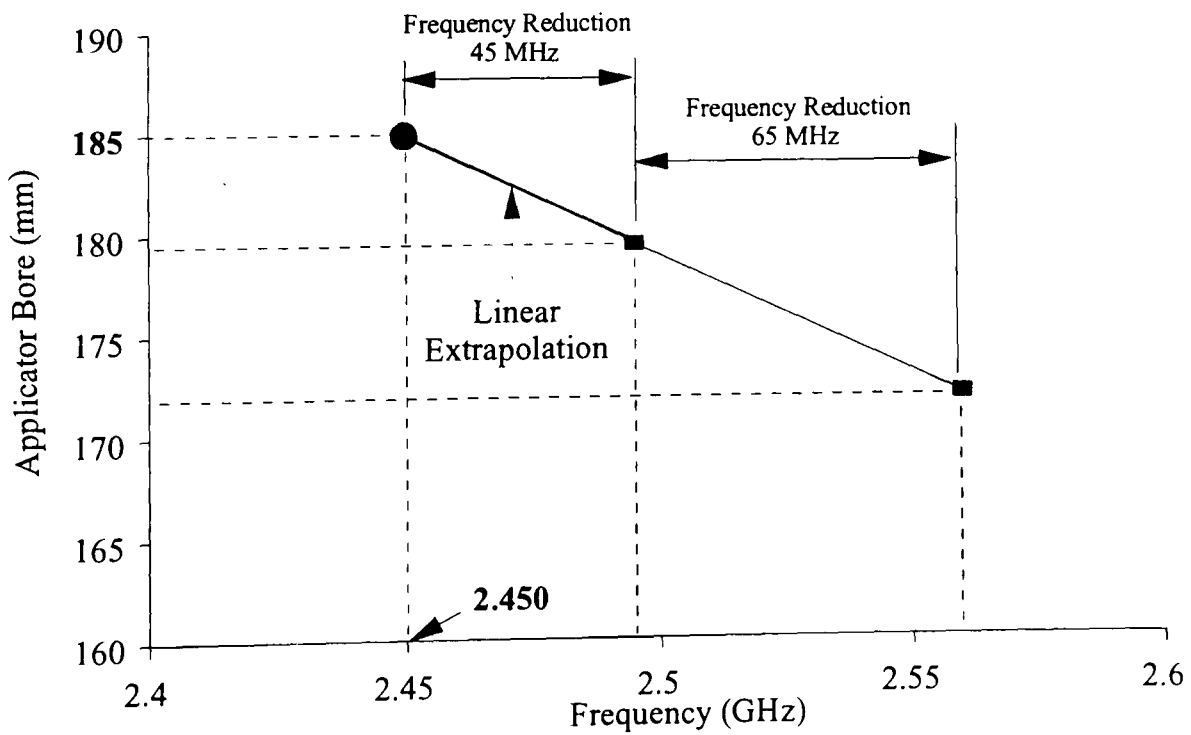


Figure 9.19 Relationship between applicator diameter and applicator resonant frequency

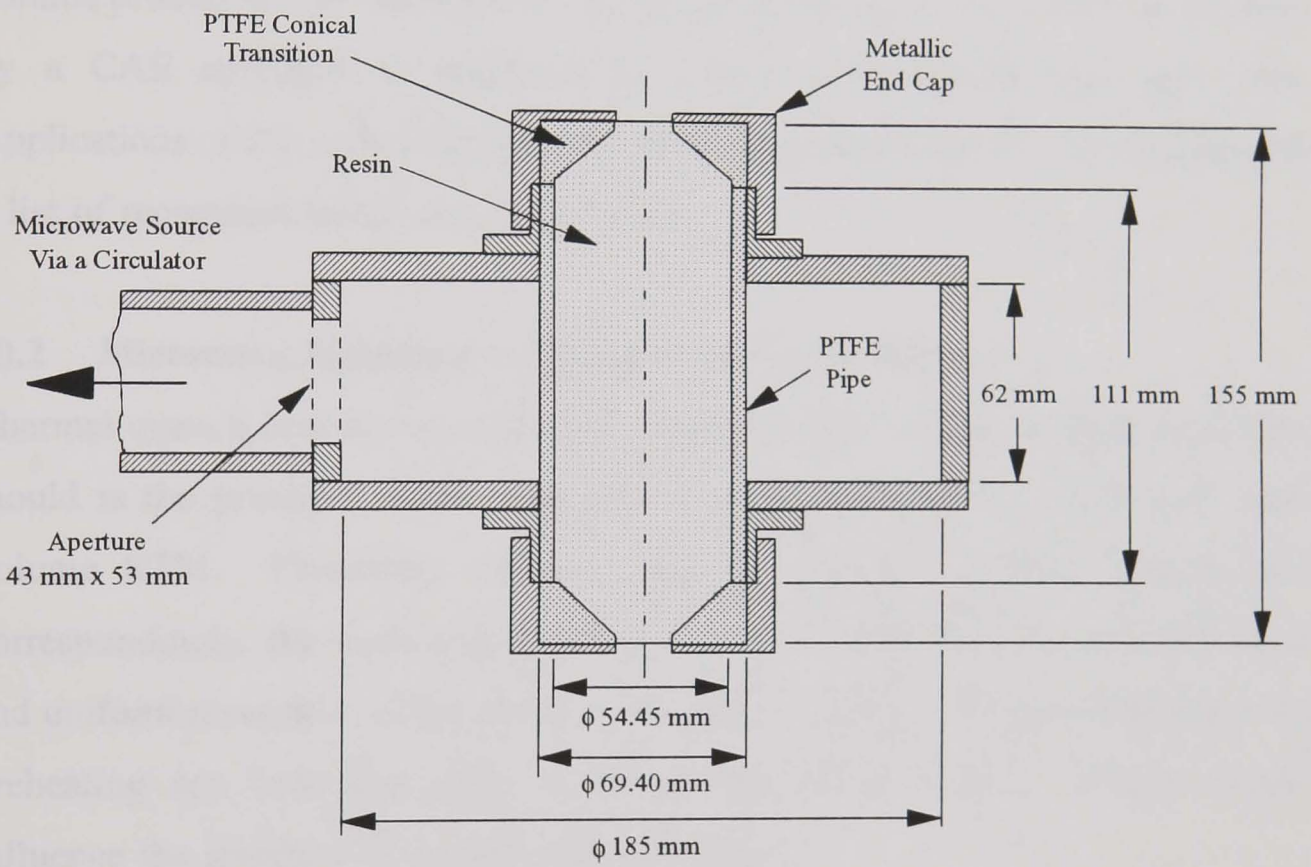


Figure 9.20 Cross section of the proposed cylindrical applicator for operation in a pure  $TM_{020}$  mode

# Discussion

---

### **10.1 Introduction**

This chapter reviews the major findings of this thesis. The use of microwave resin preheating in RTM for low and high volume production is addressed. Twin stream and single stream injection strategies are compared with regard to in-line resin preheating. The benefits of microwave assisted RTM over SRIM for high volume production are established. The design of complex microwave applicators by a CAE approach is suggested to reduce development time and costs. Applications of this technology to other fields is discussed briefly, concluding with a list of recommendations for future work.

### **10.2 Microwave Preheating for Resin Transfer Moulding**

Thermal quench near the injection gate resulting from cold resin entering the hot mould is the principal cause of extended cycle times, and an obstacle to high volume RTM. Preheating the resin prior to injection reduces quench, and correspondingly, the cycle time. Microwave resin preheating can provide rapid and uniform processing of low thermal conductivity resins. Batch and in-line resin preheating are both applicable to RTM although production volumes could influence the selection of a particular technique.

#### **10.2.1 Batch Preheating for Low Volume Resin Transfer Moulding**

Hill [22] demonstrated a 41% reduction in cycle time by batch preheating polyester resin in a multimode oven to 60°C. This cycle time reduction was a result of a lower resin viscosity for improved flow and less thermal quench, shortening the cure phase.

Batch preheating may be applicable to low volume production of FRP components. Capital investment would be minimal. A domestic microwave oven

could be used with minor modifications, including an extraction system. A wide variety of resins can be heated in a multimode oven without regard to dielectric properties. Preheating the resin lowers its viscosity and consequently reduces the impregnation time could for large components having long flow paths. This time savings could compensate for the penalty imposed by off-line batch preheating. Time penalties could be eliminated in a continuous process by preheating the resin in parallel with the moulding operation. The conventional method of lowering resin viscosity is to add styrene to the system. However, saturation of the resin can result in high levels of uncured styrene in the final component that could later diffuse from the part and affect coating operations, such as painting. In such a situation, microwave preheating may be a preferable means of lowering resin viscosity, for improved flow and reduced impregnation times.

Batch preheating is not applicable to high volume RTM. Preheating the resin reduces its storage life, making routine flushing of the entire injection system necessary. This adds to the overall cycle time while generating significant resin and solvent waste. Furthermore, batch preheating does not permit precise resin temperature control, and ramping the resin temperature during injection is not possible. In-line resin preheating is a more efficient means of reducing RTM cycle times.

### **10.2.2 In-Line Resin Preheating for High Volume Resin Transfer Moulding**

In-line microwave resin preheating offers rapid heat up rates, accurate temperature control, fast cool down rates, and a resin temperature ramping capability during injection. The resonant characteristic of single mode applicators provides high power densities compared to multimode ovens for more efficient energy use. Small volumes of resin can be heated as necessary, so that bulk storage of high temperature resin is not an issue. Turning the microwave off just before the end of injection ensures that the stationary resin between the applicator outlet and the injection gate is not preheated so that flushing is unnecessary, minimising resin and solvent waste. True cycle time reductions are possible with in-line resin preheating, making this technique applicable to high volume RTM production of FRP components.

### 10.2.3 Cycle Time Reductions Using In-Line Resin Preheating

The potential of in-line microwave resin preheating to reduce cycle times for high volume RTM has been demonstrated within this thesis. Microwave power modulation was automated using a PID controller. This system was integrated into the automatic RTM cycle to allow continuous production while contributing to process repeatability. Constant and ramped resin temperature injection were considered. Both techniques produced cycle time reductions.

Constant temperature resin injection was constrained by cure at the injection gate, resulting from a shorter resin residence time at that location. The cure sequence for this technique was the same as for conventional RTM with initial cure at the mould periphery, progressing towards the injection gate. Inward cure resulted in the development of a high in-mould pre-exotherm pressure that could damage the tool or degrade component quality. This limitation was overcome using ramped resin temperature injection to control the cure sequence. Coincident cure across the mould was demonstrated, resulting in a minimum cycle time with a reduction of the pre-exotherm pressure to the hydrostatic level.

No adverse effects on the RTM process or laminates were caused by microwave resin preheating. Exotherm temperatures did not increase, and pre-exotherm pressures were less than, or equal to conventional RTM values. Changes in the tensile modulus, tensile strength, and degree of cure were insignificant. These results suggested that in-line microwave resin preheating could be implemented in an existing RTM facility to provide cycle time reductions without risk of mould damage or component quality degradation.

The robustness of the microwave resin preheating system was hindered by two factors. A limited range of resins could be heated within the cylindrical applicator due to its fixed geometry. Adding 100 phr of calcium carbonate filler to polyester resin increased its dielectric constant by 36%, and reduced the applicator heating efficiency from 98% to 66%. However, the principal disadvantage of the system was premature resin cure within the applicator during continuous heating at high power levels. Cured resin lobes could block the injection line, damaging the system. Decreasing the flow rate permitted resin preheating using less power, eliminating premature cure so that cycle time

reductions could be demonstrated. Ideally, the microwave resin preheating system could be used in RTM without dictating the processing parameters.

### **10.3 CAE Design Approach for Microwave Heating Systems**

An explanation was presented in Chapter 9 for the cause of premature resin cure within the cylindrical applicator. Superposition of a  $TM_{020}$  mode and a pseudo  $TM_{21n}$  mode formed a hybrid mode whose heating profile prompted hot spots near the resin flow boundary layer. This conclusion resulted from extensive experimental work with high cost and time implications. This suggested that the applicator design process was flawed.

Altering the geometry of an applicator enables distinct heating profiles to be generated, some of which can be predicted analytically. An idealised system is represented by a rectangular or cylindrical applicator filled with a single material, usually air, whose dielectric properties are fixed and the magnetron output frequency is constant. Additional dielectric materials within the applicator, such as PTFE and resin, complicate the analytical solution. Modifications to the applicator geometry to assist flow, and for waveguide feeds can make the analytical solution unworkable. Interactions between the complex applicator geometry, dielectric property changes, and variations in the magnetron output frequency can excite hybrid modes. These modes consist of a distorted single mode or superimposed modes. Simulation by numerical methods can be used to define a practical applicator geometry while maintaining resonance of a desired heating profile.

A robust simulation tool for the design of microwave heating systems would incorporate several elements. Visualisation of the heating profile within the applicator would be necessary. Based upon a range of dielectric properties, and magnetron frequencies, an applicator geometry that provided a stable heating profile could be determined. This heating profile could be loaded into a computational fluid dynamics package to produce the temperature distribution within the resin as it flowed through the applicator. Ideally, these two solvers would be compatible, accounting for temperature dependent changes in viscosity

and the dielectric properties of the product, as both would affect the overall heating performance.

Presently, simulation software is available. TLM was used to model the heating profile within the applicator (Chapter 9). In addition, Hill [22] used FLUENT, a computational fluid dynamics package, to model the temperature distribution and resin flow for a given heating profile. However, these packages were not integrated to model changes in the temperature distribution as a function of resin viscosity and dielectric properties. It is evident that accurate modelling would require representative viscosity and dielectric property data. While resin viscosity information is readily available, dielectric property data is less accessible, and additional development costs would be incurred obtaining these measurements. However, simulation techniques could reduce overall applicator development time and costs. As a result, the most effective means of designing complex microwave heating systems is through a CAE approach.

#### **10.4 Injection Strategies for In-Line Microwave Resin Preheating**

Resin transfer moulding can accommodate single stream and twin stream injection strategies for high volume production. The applicability of each injection technique to in-line microwave resin preheating is discussed below.

##### **10.4.1 Single Stream Injection**

Accurate resin formulation makes single stream injection attractive for RTM. Since the resin is reactive at elevated temperature, low temperature storage for several hours is possible without the risk of premature cure. In addition, constant pressure, single stream injection systems are simple, relatively inexpensive, and deliver a low pressure, non-pulsed resin stream.

The reactivity of the catalysed resin makes single stream preheating difficult. A heating profile analogous to the parabolic velocity flow profile is required to prevent premature cure within the applicator. Cylindrical applicators in the  $TM_{0m0}$  mode family can supply maximum heating along the axis of flow with zero heating at the flow boundary. This thesis has demonstrated that a pure  $TM_{020}$  mode is difficult, although theoretically possible, to isolate within an

applicator designed for in-line resin preheating. Excitation of the fundamental mode ( $TM_{010}$ ) could be simpler. The fundamental mode is the lowest excitable mode within an applicator. The benefit of heating in the fundamental mode is that superposition cannot occur. Overall, the complexities associated with in-line preheating of catalysed resin suggest that the shape of the heating profile should be established using a CAE design approach. This would provide the most time and cost effective development route.

#### **10.4.2 Twin Stream Injection**

Typically, twin stream injection systems are driven by a reciprocating pump. Resin and catalyst converge in a static mixer just before entering the mould. Catalyst metering is difficult to control. Resin delivery is pulsed resulting in higher cavity pressures than for a single stream, constant pressure injection.

Twin stream injection is desirable for in-line preheating since both streams are non-reactive, making premature cure impossible. A  $TE_{10n}$  mode rectangular applicator could be used for this application with the resin stream positioned along the heating profile maximum, as shown for the  $TE_{101}$  applicator in Figure 2.4. Preheating temperatures would be limited only by the output power of the magnetron source. One advantage of rectangular applicators compared to cylindrical types is the ability to alter their length, compensating for changes in the dielectric constant as a result of temperature variations or alterations to the resin formulation. However, pulsed delivery of the resin stream could complicate temperature control. In the absence of a CAE design capability, in-line resin preheating for a non-pulsed, twin stream injection system could be the simplest, most versatile configuration for high volume production in RTM.

### **10.5 The Scope of Microwave Assisted RTM for High Volume Production**

The manufacture of 100,000 parts per annum has been established as the lower bound of high volume production, requiring a cycle time of approximately three minutes [3]. Based upon the findings of this thesis it is anticipated that these production levels could be reached using microwave assisted RTM. Ramping the resin temperature during injection enabled a coincident cure sequence to be

established across the mould. This suggests that cycle times could be reduced virtually to the impregnation time by using a rapid curing resin system. Furthermore, impregnation times are reduced as a result of a lower resin viscosity at preheated temperatures. In this context, RTM impregnation times, and consequently cycle times, of approximately three minutes are feasible for the production of medium sized FRP components, such as semi-structural panels or structural cross car beams.

SRIM is another technique for producing structural FRP components in high volumes (100,000 parts per annum). However, microwave assisted RTM has a distinct cost and processing advantage at this production level. Unlike SRIM, a low pressure strategy can be adopted. Low cost, lightweight shell tools can be used. Light duty manipulating equipment, without the need for a high tonnage press would further reduce capital cost. Compared to steel tools, lead times for shell tools are shorter, permitting more rapid response to market fluctuations and consumer demands. Processing could also benefit from the use of shell tools that have a low thermal inertia for accurate temperature control. High peak pressures that develop within the mould during cure can be decreased significantly using microwave assisted RTM. As a result, the stiffness, and thermal mass of shell tools could be reduced further. Finally, low cost resin systems such as polyester are applicable to RTM. These overall savings could compensate for the capital investment in microwave preheating equipment. In this way, microwave assisted RTM could provide production volumes equivalent to SRIM at a lower cost.

SRIM is a more obvious choice at production levels in excess of 300,000 parts per annum. More robust tooling at these volumes would be desirable for reduced wear, and long term reliability. The additional cost of a SRIM system could be justified by the greater volumes yielding a cost benefit after a proportionally short production period.

## **10.6 Alternative Applications for the Microwave Preheating System**

Use of the microwave preheating system in this thesis was restricted to processing thermosetting resins. Microwave heating exhibits rapid heat up rates, stable temperature control, and fast cool down rates for processing low thermal

conductivity, dielectric materials. The system can be automated, and ramped heating techniques provide a processing advantage over single temperature, continuous heating systems. As a result, in-line microwave heating could be adapted to other fields, particularly to those processes that require intermittent rather than steady state heating.

Thermally sensitive materials, particularly pumpable foods, could benefit from this technology. Food could be cooked gradually by passing the product through the applicator several times while ramping its temperature. In addition to cooking, high temperatures could be used eliminate bacteria within the food prior to packaging.

Processing of high viscosity materials, such as oil based slurries in the chemical industry, or clay products used for building supplies could benefit from microwave preheating. The viscosity of these materials would be reduced at elevated temperatures, facilitating transport, while enabling secondary products to be mixed with the material before resolidifying at ambient temperature.

### **10.7 Recommendations for Future Work**

The following issues require further investigation so that the full potential of in-line microwave resin preheating can be realised for high volume resin transfer moulding.

1. Improvements to the PID power controller are necessary for more rapid stabilisation at the initial set point temperature. Approximately 20 seconds was necessary for the microwave preheating system to turn on, and reach the set point temperature. Fluctuations in the power source at start up were expected to contribute to erratic control behaviour during this period.
2. A predictive technique to specify the resin temperature ramping function is necessary. A linear function was used successfully in this work to produce coincident resin cure across the undershield component. However, the temperature profile function may be component dependent. Laminates

of varying thickness, or moulds with multi-port injection may require a more sophisticated temperature profiling algorithm.

3. Widening the bore of the existing cylindrical applicator and reducing the PTFE pipe length is expected to provide resonance in a pure  $TM_{020}$  mode. These changes need to be made so that RTM process parameters are not dictated by the microwave resin preheating system.
4. Twin stream injection systems are used widely in industry and offer the potential to preheat non-reactive resin. A microwave preheating system incorporating a  $TE_{10n}$  rectangular applicator should be developed for use with such an injection system. The tuning capability of this applicator would enable a wide variety of resins to be heated without regard to dielectric properties.
5. A CAE approach to the design of microwave resin preheating systems needs to be established. This would provide a time and cost efficient means of developing applicators with complex geometries. Numerical simulations are expected to be the simplest way of designing a microwave preheating system for single stream injection in RTM.

# Conclusions

---

The following is a summary of the major conclusions derived from this thesis.

1. A fully automated microwave resin preheating system has been installed within a prototype RTM production facility. This system has been integrated into the automatic RTM cycle to allow continuous FRP component production.
2. The resin preheat temperature can be controlled precisely using the microwave resin preheating system. Feedback of the resin temperature at the microwave outlet to a PID power controller enables a specific resin temperature to be maintained. The resin can be preheated to a constant temperature during injection or ramped according to a user defined function.
3. Ramping the resin temperature during injection to produce coincident cure across the mould minimises the cycle time. Reductions in cycle time of 36% were achieved by ramping the resin temperature during injection for the given moulding parameters. Greater cycle time reductions could be expected by operating the cylindrical applicator in a pure  $TM_{020}$  mode. Higher power levels could then be used without the formation of cured resin within the applicator, and therefore the resin flow rate could be increased to reduce the cycle times.
4. Preheating the resin to a constant temperature during injection is an effective method of reducing the cycle time. A maximum cycle time reduction of 29% was demonstrated using this preheating technique. The

principal reasons for the cycle time reduction is improved resin flow through the mould, and less thermal quench near the injection gate. The resin preheat temperature is optimised when increases in this temperature do not produce a corresponding cycle time reduction.

5. Ramping the resin temperature during injection to produce coincident resin cure eliminates localised pre-exotherm pressures within the mould. As a result, mould distortion is reduced and less variations in the laminate thickness occurs for improved component quality. Furthermore, less stiff, lighter weight shell moulds could be used as a consequence of lower mould pressures. These moulds would be more responsive thermally, in turn contributing to cycle time reductions.
6. Laminate material properties are not diminished by using microwave resin preheating. The tensile modulus, tensile strength, and degree of resin cure for laminates made with preheated resin were equivalent to conventional RTM laminates.
7. Microwave resin preheating does not increase in-mould exotherm temperatures or pre-exotherm pressures when compared to conventional RTM. This suggests that the microwave resin preheating system could be retrofitted on an existing RTM system without causing temperature, or pressure related mould damage.
8. Adding filler to the resin system reduces the heating efficiency of the cylindrical applicator. Calcium carbonate filler increases the dielectric constant of the resin, shifting the applicator resonance. As a result, retuning of the applicator, or altering its geometry is necessary to improve the applicator heating performance.
9. Increasing the microwave power reduces the heating efficiency of the cylindrical applicator. The magnetron output frequency varies with

microwave power resulting in a mismatch with the applicator resonant frequency. This suggests that a low Q applicator is desirable for microwave resin preheating since it would be less sensitive to frequency variations during heating.

10. A TLM simulation can predict the heating profile within a loaded cylindrical applicator. Integration of this solution with a commercially available computational fluid dynamics package would provide the resin temperature distribution within the applicator during heating. This CAE approach could reduce development time and costs for future microwave heating systems.

## References

---

- [1] **M. Glaskin.** "The Clean Machine." *Engineering* pages 26-27, November 1991.
  
- [2] **P. A. Toensmeier.** "Electric Cars Stage a Comeback; Lightweighting Makes them Practical." *Modern Plastics International* pages 44-45, September 1989.
  
- [3] **M. J. Owen, E. V. Rice, C. D. Rudd, and V. Middleton.** "Resin Transfer Moulding for Automobile Manufacture: Reality and Simulation," pages 121-142. Computational Mechanics Publications, Elsevier Applied Science. *Computer Aided Design in Composite Material Technology III, Newark, DE USA, May 1992.*
  
- [4] **Anonymous.** "30 Years' Experience of Composite Cars at Lotus." *Reinforced Plastics* pages 34-37, February 1991.
  
- [5] **Anonymous.** "RTM Body Panels-Craftsmanlike Quality, but without the High Costs." *Modern Plastics International* page 10, August 1989.
  
- [6] **C. V. Folonari and A. Bruno.** "New Applications for Plastics in Fiat Motor Cars," pages 1-10. Rubber and Plastic Research Association (RAPRA). *New Material for Automotive Applications, Paris, France, October 1990.*
  
- [7] **K. Noakes.** "Successful Composite Techniques." London, Osprey Publishing Ltd., pages 40-48, 1989.
  
- [8] **Anonymous.** "McLaren F1 GTR Set for Le Mans." *Racecar Engineering* 4(5) pages 7-8, 1995.

- [9] **W. Hoffmann.** "Fibre Composite in the Driveline." *Plastics and Rubber International* 14(5) pages 46-49, 1989.
- [10] **N. G. Chavka and C. F. Johnson.** "The Taming of Liquid Composite Molding for Automotive Applications," pages 115-122. *Advanced Composite Materials: New Developments and Application Proceedings, Detroit, MI USA, September 1991.*
- [11] **C. F. Johnson.** "Resin Transfer Molding." In *Composite Materials Technology*, edited by P.K. Mallick and S. Newman. Hanser Publishing Ltd., pages 150-154, 1992.
- [12] **F. Scott.** "Processing Characteristics of Polyester Resins for the Resin Transfer Moulding Process." PhD thesis, University of Nottingham, 1988.
- [13] **I. D. Revill.** "Interfacial Bond Formation During Resin Transfer Moulding of Polymer Composites." PhD thesis, University of Nottingham, 1992.
- [14] **K. A. Lindsey.** "Interfacial Properties of Composites Produced by Resin Transfer Moulding." PhD thesis, University of Nottingham, 1994.
- [15] **J. R. Lowe.** "Void Formation During Resin Transfer Moulding." PhD thesis, University of Nottingham, 1994.
- [16] **C. D. Rudd.** "Preform Processing for High Volume Resin Transfer Moulding (RTM)." PhD thesis, University of Nottingham, 1989.
- [17] **L. J. Bulmer.** "In-Plane Permeability of Reinforcements for Liquid Moulding Processes." PhD thesis, University of Nottingham, 1994.
- [18] **P. McGeehin.** "Preform Manufacture for Liquid Moulding Processes." PhD thesis, University of Nottingham, 1995.

- [19] **K. F. Hutcheon.** "The Application of Resin Transfer Moulding to the Motor Industry." M. Phil thesis, University of Nottingham, 1989.
- [20] **K. N. Kendall.** "Mould Design for High Volume Resin Transfer Moulding." PhD thesis, University of Nottingham, 1991.
- [21] **P. J. Blanchard.** "High Speed Resin Transfer Moulding of Composite Structures." PhD thesis, University of Nottingham, 1995.
- [22] **D. J. Hill.** "Microwave Preheating of Thermosetting Resin for Resin Transfer Moulding." PhD thesis, University of Nottingham, 1993.
- [23] **E. V. Rice.** "Computer Aided Engineering Techniques for Resin Transfer Moulding." PhD thesis, University of Nottingham, 1993.
- [24] **A. C. Long.** "Preform Design for Liquid Moulding Processes." PhD thesis, University of Nottingham, 1994.
- [25] **G. Kaye and T. Laby.** "Tables of Physical and Chemical Constants and Some Mathematical Functions." 15th edition, Longman Group Ltd., pages 287-290, 1986.
- [26] **R. C. Metaxas and R. J. Meredith.** "Industrial Microwave Heating." Peter Peregrinus Ltd., 1983.
- [27] **Richard M. Walker.** "Materials and Construction Techniques." In *Microwave Transmission Circuits*, edited by G.L. Ragan. McGraw-Hill Book Company Inc., pages 133-137, 1948.
- [28] **W. R. Tinga and S. O. Nelson.** "Dielectric Properties of Materials for Microwave Processing-Tabulated." *Journal of Microwave Power* 8(1) pages 23-27, 1973.

- [29] **Anonymous.** "Industrial Applications of Dielectric Heating." *The Electricity Council, Technical Information (EC3464)*, October 1987.
- [30] **Anonymous.** "Magnetrons." In *Electrical and Electronic Trades Training Notes-Fundamental Electronics (AP 3302 Part 1)*, edited by C. Whitmore. Ministry of Defense, pages 1-13, September 1984.
- [31] **P. F. Mariner.** "Introduction to Microwave Practice." Heywood & Company, pages 18-20, 1961.
- [32] **Hewlett Packard.** "HP 8753C Network Analyser Operating Manual." 2nd edition, 1990.
- [33] **M. J. Owen, V. Middleton, K. F. Hutcheon, F. N. Scott, and C. D. Rudd.** "Resin Transfer Moulding (RTM) for Volume Car Production," Paper 28 pages 127-130. The British Plastics Federation. *The 16th Annual Reinforced Plastics Congress, 1988.*
- [34] **G. P. Ehnet.** "Beefed Up SMC Meets Automotive Demands." *Reinforced Plastics* pages 24-28, September 1993.
- [35] **C. F. Johnson, N. G. Chavka, and R. A. Jeryan.** "Resin Transfer Molding of Complex Automotive Structures," Session 12-A pages 1-7. The Society of the Plastics Industry. *The 41st Annual Conference, Reinforced Plastics/Composites Institute, January 1986.*
- [36] **K. N. Kendall.** "Real Time Process Monitoring & Control in Liquid Composite Moulding," pages 355-360. *Proceedings of the 8th Advanced Composites Conference, Chicago, IL USA, November 1992.*

- [37] **L. M. Hufnagel.** "Advances in Structural RIM Equipment Technology." pages 63-67. *Advanced Composite Materials: New Developments and Applications Conference Proceedings, Detroit, MI USA, September 1991.*
- [38] **V. M. Karbhari, S. G. Slotte, D. A. Steenkamer, and D. J. Wilkins.** "Effect of Material, Process, and Equipment Variables on the Performance of Resin Transfer Moulded Parts." *Composites Manufacturing* 3(3) pages 143-152, 1992.
- [39] **M. Parmar, P. Shepard, and G. S. Boyce.** "Development of a High Speed Resin Transfer Moulding Process for the Mass Production of Structural Composite Components," Paper 32 pages 1-8. *Proceedings of the 3rd International Conference on Automated Composites, The Hague, Netherlands, October 1991.*
- [40] **M. Jander.** "Industrial RTM-New Developments in Molding and Preforming Technologies," pages 29-33. *Advanced Composite Materials: New Developments and Applications Conference Proceedings, Detroit, MI USA, 1991.*
- [41] **K. N. Kendall, C. D. Rudd, M. J. Owen, and V. Middleton.** "Characterisation of the Resin Transfer Moulding Process." *Composites Manufacturing* 3(4) pages 235-249, 1992.
- [42] **C. D. Rudd, M. J. Owen, K. N. Kendall, and I. D. Reville.** "Developments in Resin Transfer Moulding for High Volume Manufacture," pages 301-314. *American Society of Materials/Engineering Society of Detroit, Advanced Composites Conference, Detroit, MI USA, October 1990.*

- [43] **C. D. Rudd and K. N. Kendall.** "Modelling Non-Isothermal Liquid Moulding Processes," Paper 30 pages 1-5. *Proceedings of the 3rd International Conference on Automated Composites, The Hague, Netherlands, October 1991.*
- [44] **M. R. Kamal and S. Sourour.** "Kinetics and Thermal Characterisation of Thermoset Cure." *Polymer Engineering and Science* **13**(1) pages 59-64, 1973.
- [45] **B. R. Gebart, P. Gudmundson, and C. Y. Lundemo.** "An Evaluation of Alternative Injection Strategies in RTM," Session 16-D pages 1-8. The Society of Plastics Industry. *The 47th Annual Conference, Composites Institute, February 1992.*
- [46] **C. D. Rudd and K. N. Kendall.** "Towards a High Volume Manufacturing Technology for Composite Components." *Proceedings of the Institution of Mechanical Engineers Journal of Engineering Manufacture* **Volume 206** pages 77-91, 1991.
- [47] **C. D. Rudd, M. J. Owen, and V. Middleton.** "Effects of Process Variables on Cycle Time During Resin Transfer Moulding for High Volume Manufacture." *Materials Science and Technology* **Volume 6** pages 656-665, July 1990.
- [48] **Wen-Bin Young and Chaw-Wu Tseng.** "Study on the Pre-Heated Temperatures and Injection Pressures of the RTM Process." *Journal of Reinforced Plastics and Composites* **Volume 13** pages 467-482, May 1994.
- [49] **R. C. Peterson and R. E. Robertson.** "Flow Characteristics of Polymer Resin Through Glass Fiber Preforms in Resin Transfer Molding," pages 203-208. *Advanced Composite Materials: New Developments and Applications Conference Proceedings, Detroit, MI USA, September 1991.*

- [50] **M. J. Owen, V. Middleton, and C. D. Rudd.** "Fibre Reinforcement for High Volume Resin Transfer Moulding (RTM)." *Composites Manufacturing* 1(2) pages 74-78, 1990.
- [51] **M. J. Perry, J. Xu, Y. Ma, T. J. Wang, L. J. Lee, R. Lin, and M. J. Liou.** "Monitoring and Simulation of Resin Transfer Molding," Session 16-E pages 1-13. The Society of the Plastics Industry. *Proceedings of the 7th Annual Conference of the Composites Institute, February 1992.*
- [52] **F. N. Scott and M. J. Owen.** "Polyester Resin System Processing for High Volume Resin Transfer Moulding (RTM)," Paper 31 pages 1-8. The Plastics and Rubber Institute. *The 3rd International Conference on Automated Composites, The Hague, Netherlands, October 1991.*
- [53] **C. D. Rudd, M. J. Owen, and I. D. Revill.** "Processing and Mechanical Properties of Calcium Carbonate Filled Glassfibre/Polyester Composites," pages 69-80. Institution of Mechanical Engineers. *Eurotech Direct, 1991.*
- [54] **T. S. Lundstrom and B. R. Gebart.** "Influence from Process Parameters on Void Formation in Resin Transfer Molding." 15(1) pages 25-33, 1994.
- [55] **J. S. Hayward and B. Harris.** "Effect of Process Variables on the Quality of RTM Mouldings." *SAMPE Journal* 26(3) pages 39-46, 1990.
- [56] **N. Patel, M. J. Perry, and L. J. Lee.** "Influence of RTM and SRIM Processing Parameters on Molding and Mechanical Properties," pages 105-113. *Advanced Composite Materials: New Developments and Applications Conference Proceedings, Detroit, MI USA, September 1991.*
- [57] **N.S. Strand.** "Fast Microwave Curing of Thermoset Parts." *Modern Plastics* pages 64-67, October 1980.

- [58] **F. Y. C. Boey, I. Gosling, and S. W. Lye.** "Processing Problems and Solutions for an Industrial Automated Microwave Curing System for a Thermoset Composite," pages 651-656. *The 9th International Conference on Composite Materials, Madrid, Spain, July 1993.*
- [59] **D. A. Lewis and J. M. Shaw.** "Recent Developments in the Microwave Processing of Polymers." *MRS Bulletin* pages 37-40, November 1993.
- [60] **W. I. Lee and G. Springer.** "Microwave Curing of Composites." *Journal of Composite Materials* **Volume 18** pages 387-409, July 1984.
- [61] **L. T. Drzal, K. J. Hook, and R. K. Agrawal.** "Enhanced Chemical Bonding at the Fiber-Matrix Interphase in Microwave Processed Composites." *Microwave Processing of Materials II, Materials Research Society Symposium Proceedings* **Volume 189** pages 449-454, 1991.
- [62] **C. Y. Yue and F. Y. Boey.** "The Effect of Microwave and Thermal Curing on the Interfacial Properties of an Epoxy-Glass Composite," Paper 12 pages 1-8. *Proceedings of the Deformation and Fracture of Composites Conference, Manchester, England, March 1993.*
- [63] **M. C. Hawley and J. Wei.** "Processing of Polymers and Polymer Composites in a Microwave Applicator." *Microwave Processing of Materials II, Materials Research Society Symposium Proceedings* **Volume 189** pages 413-420, 1991.
- [64] **E. Marand, K. R. Baker, and J. D. Graybeal.** "Comparison of Reaction Mechanisms of Epoxy Resins Undergoing Thermal and Microwave Cure from In Situ Measurements of Microwave Dielectric Properties and Infrared Spectroscopy." *Macromolecules* **25(8)** pages 2243-2252, 1992.

- [65] **M. T. De Meuse and C. L. Ryan.** "The Microwave Processing of Polymeric Materials." *Advances in Polymer Technology* **12**(2) pages 197-203, 1993.
- [66] **P. J. Costigan and A. W. Birley.** "Microwave Preheating of Sheet Moulding Compound." *Plastics and Rubber Processing and Applications* **9**(4) pages 233-240, 1988.
- [67] **P. Cassagnau and A. Michel.** "Continuous Crosslinking of Ethylene Vinyl Acetate and Ethylene Methyl Acrylate Copolymer Blends by On-Line Microwave Heating." *Polymer Engineering and Science* **34**(12) pages 1011-1015, 1994.
- [68] **J. M. Methven and S. R. Ghaffariyan.** "A Preliminary Assessment of the Microwave Assisted Pulwinding of Composite Re-Bars," Paper 8 pages 1-4. The Plastics and Rubber Institute. *The 5th International Conference on Fibre Reinforced Composites, March 1992.*
- [69] **P. O. G. Risman.** "Method of Preparing Foodstuffs Containing Coagulated Proteins and a Device for Performing the Method." *US Patent 4,237,145*, 1980.
- [70] **T. Ohlsson.** "In-Flow Microwave Heating of Pumpable Foods," pages 1-7. *International Congress on Food and Engineering, Chiba, Japan, May 1993.*
- [71] **A. Singh, V. J. Lopata, W. Kremers, T. McDougall, M. Tateishi, and C. Sanders.** "Electron-Cured Fibre-Reinforced Advanced Composites," pages 277-289. Canadian Association for Composite Structures and Materials. *The 2nd Canadian International Composites Conference and Exhibition, CANCOM, 1993.*

- [72] **X. Jia and P. Jolly.** "Simulation of Microwave Field and Power Distribution in a Cavity by a Three-Dimensional Finite Element Method." *Journal of Microwave Power and Electromagnetic Energy* **27**(1) pages 11-22, 1992.
- [73] **D. C. Dibben and R. C. Metaxas.** "Finite Element Time Domain Analysis of Multimode Applicators Using Edge Elements." *Journal of Microwave Power* **29**(4) pages 242-251, 1995.
- [74] **M. F. Iskander.** "Computer Modeling and Numerical Techniques for Quantifying Microwave Interactions with Materials." *Microwave Processing of Materials II, Materials Research Society Symposium Proceedings Volume 189* pages 149-171, 1991.
- [75] **A. P. Duffy.** "Coupling of Electromagnetic Waves into Wires-Experiments and Simulations." PhD thesis, University of Nottingham, 1993.
- [76] **S. O. Nelson and T. S. You.** "Relationships between Microwave Permittivities of Solid and Pulverised Plastics." *Journal of Physics and Applied Physics Volume 23* pages 346-353, 1990.
- [77] **Philips Export.** "Magnetrons for Microwave Heating." Book T4 pages 99-108, 1989.
- [78] **L. Roskott and A. A. M. Groenendaal.** "Residual Styrene Content-What Does This Mean to the Polyester Processor," Section 5-B pages 1-5. The Society of Plastics Industry. *The 33rd Annual Conference, Reinforced Plastics/Composites Institute, 1978.*
- [79] **O. E. Schupp III.** "Gas Chromatography." John Wiley and Sons, pages 5-10, 1968.

- [80] **A. K. Kochhar and N. D. Burns.** "Microprocessors and their Manufacturing Applications." Edward Arnold Publishers, pages 205-236, 1983.
- [81] **G. F. Franklin, J. D. Powell, and A. Emami-Naeini.** "Feedback Control Dynamic Systems." 2nd edition, Addison-Wesley Publishing Company, pages 116-125, 1991.
- [82] **C. D. Rudd and I. D. Revill.** "Effects of Wetting Times on the Tensile Properties of Glass Fibre/Polyester Laminates," pages 20-24. *Composites 1990, University of Patras, Greece, August 1990.*
- [83] **J. S. Hayward and B. Harris.** "Processing Factors Affecting the Quality of Resin Transfer Moulded Composites." *Plastics and Rubber Processing and Applications* 11(4) pages 191-198, 1989.
- [84] **H. Krenchal.** "Fibre Reinforcement." PhD thesis, Akadenisk Vorlag, Copenhagen, 1964.
- [85] **J. Methven.** Correspondence with D. J. Hill [22]. *UMIST*, March 1991.
- [86] **B. G. M. Helme.** "Measurement of Microwave Properties of Materials." In *Industrial Uses of Microwaves*, edited by J. Sharp. The Institute of Electrical Engineers, Electronics Division colloquia organised by Professional Group E12 (Microwave Devices and Techniques), June 1990.
- [87] **John E. Gerling.** "Microwave Equipment for Plasma Process Research Systems." *Gerling Laboratories, USA* pages 1-13, 1987.
- [88] **John E. Gerling.** "Constant Frequency Operation." *Technical Notes, Gerling Laboratories, USA* pages 1-2, 1986.

- [89] **Anonymous.** "Application of the ASTEX A-5000 to High Q Cavity Loads." *FAX Correspondence from Gerling Laboratories, USA* pages 1-2. August 5, 1994.
- [90] **S. Li, C. Adyed, and R. G. Bosisio.** "Precise Calculations and Measurements on the Complex Dielectric Constant of Lossy Materials Using  $TM_{010}$  Cavity Perturbation Techniques." *Transactions on Microwave Theory and Techniques* **Volume 29**, 1981.

## Appendix 3.1

# Dielectric Property Relationships for Two Part Mixtures

---

The dielectric properties of a two part material, such as resin loaded with filler, can be calculated using the following mixture equations:

### Refractive Index Equation

$$\epsilon_m^* = \left( v_1 \sqrt{\epsilon_1^*} + v_2 \sqrt{\epsilon_2^*} \right)^2 \quad \text{Equation A3.1}$$

### Landau and Lifshitz, Looyenga Equation

$$\epsilon_m^* = \left( v_1 \epsilon_1^{*1/3} + v_2 \epsilon_2^{*1/3} \right)^3 \quad \text{Equation A3.2}$$

### Bottcher Equation

$$\frac{\epsilon_m^* - \epsilon_1^*}{3\epsilon_m^*} = v_2 \frac{\epsilon_2^* - \epsilon_1^*}{\epsilon_2^* + 2\epsilon_m^*} \quad \text{Equation A3.3}$$

### Bruggeman-Hanai Equation

$$\frac{\epsilon_m^* - \epsilon_2^*}{\epsilon_1^* - \epsilon_2^*} \left( \frac{\epsilon_1^*}{\epsilon_m^*} \right)^{1/3} = 1 - v_2 \quad \text{Equation A3.4}$$

### Rayleigh Equation

$$\frac{\epsilon_m^* - \epsilon_1^*}{\epsilon_m^* + 2\epsilon_1^*} = v_2 \frac{\epsilon_2^* - \epsilon_1^*}{2\epsilon_1^* + \epsilon_2^*} \quad \text{Equation A3.5}$$

### Lichtenecker Equation

$$\ln \epsilon_m^* = v_1 \ln \epsilon_1^* + v_2 \ln \epsilon_2^* \quad \text{Equation A3.6}$$

and

$$v_1 + v_2 = 1 \quad \text{Equation A3.7}$$

where

$\epsilon_m^*$  = complex dielectric constant of the mixture

$\epsilon_1^*$  = complex dielectric constant of the resin

$\epsilon_2^*$  = complex dielectric constant of the filler

$v_1$  = volume fraction of the resin

$v_2$  = volume fraction of the filler

The complex dielectric constant is expressed as:

$$\epsilon^* = \epsilon' - j\epsilon'' \quad \text{Equation A3.8}$$

where

$\epsilon'$  = dielectric constant

$\epsilon''$  = loss factor

Calculation of dielectric constant and the loss factor for the mixture can be performed by resolving the complex dielectric constants in Equations A3.1-A3.6 into real and imaginary components as shown in Equation A3.8. For example, Equation A3.1 would become:

$$\epsilon'_m + j\epsilon''_m = \left[ v_1 \sqrt{(\epsilon'_1 + j\epsilon''_1)} + v_2 \sqrt{(\epsilon'_2 + j\epsilon''_2)} \right]^2 \quad \text{Equation A3.9}$$

Equations A3.1 and A3.2 were determined by Nelson and You [76] to yield the most accurate predictions for the dielectric property values.

## Appendix 4.1

### Motorsport Lay-Up

---

Vinyl-ester resin (Derakane 8084) catalysed with Perkadox 16 (2% by mass) was used during the development of the PID power controller for the microwave resin preheating system (Chapter 5). The fibre reinforcement used in conjunction with this resin system was termed the Motorsport lay-up. This balanced reinforcement was made up of the following components:

#### **TOP SURFACE OF UNDERSHIELD**

- i. Glass veil by Vetrotex (UK) Ltd.
- ii.  $\pm 45^\circ$  stitch-bonded glass mat EBXHD 936 by Tech Textiles International Ltd.
- iii. CFRM Unifilo U750-225 or U720-225 by Vetrotex (UK) Ltd.
- iv. Firet Coremat XF2 by Lantor (UK) Ltd.
- v. Coremat XF2 in the outer two swages and two layers of CFRM Unifilo U750-450 in the central three swages
- vi. Two layers of Coremat XF2 or one layer of Coremat XF4
- vii. CFRM Unifilo U750-225 or U720-225
- viii. Coremat XF2 in the inner three swages
- ix.  $\pm 45^\circ$  stitch-bonded glass mat EBXHD 936
- x. Glass veil

#### **BOTTOM SURFACE OF UNDERSHIELD**

The nominal thickness of the undershield component was 6 mm, increasing to 8 mm in the five swage areas. Additional material was placed in the swages to maintain a uniform reinforcement fraction throughout, thus avoiding regions of resin richness.

## Appendix 4.2

### Dielectric Property Calculations

---

The following equations were used to calculate the complex dielectric constant ( $\epsilon^*$ ) using the cavity perturbation technique [90].

#### Dielectric Constant:

$$\epsilon' - 1 = 2 J_1^2(x_{01}) \frac{R_0^2}{R_1^2} \frac{\Delta f}{f_0^{tube}} \quad \text{Equation A4.1}$$

where:

$$J_1^2(x_{01}) = 0.0074$$

$f_0^{tube}$  = resonant frequency with empty tube inserted

$f_0^{sample}$  = resonant frequency with sample inserted

$$\Delta f = f_0^{tube} - f_0^{sample}$$

$R_0$  = applicator radius (373 mm)

$R_1$  = sample radius (5 mm)

#### Loss Factor:

$$\epsilon'' = J_1^2(x_{01}) \frac{R_0^2}{R_1^2} \left( \frac{1}{Q^{sample}} - \frac{1}{Q^{empty}} \right) \quad \text{Equation A4.2}$$

where:

$Q^{sample}$  = Q factor with the sample inserted

$Q^{empty}$  = Q factor of the empty applicator

and:

$$Q = \frac{f_0}{\Delta f} \quad \text{Equation A4.3}$$

## Appendix 5.1

### Ziegler-Nichols Tuning Equations

---

The following Ziegler-Nichols tuning equations were used to determine the PID controller constants based on a marginally stable system :

$$K_p = 0.600 K_u \quad \text{Equation A5.1}$$

$$T_I = 0.500 P_u \quad \text{Equation A5.2}$$

$$T_D = 0.125 P_u \quad \text{Equation A5.3}$$

The gain at which the temperature response became marginally unstable under proportional control is termed the critical gain ( $K_u$ ). The period of oscillation for the marginally unstable system is known as the critical response period ( $P_u$ ) and can be determined graphically as shown in Figure 5.5a. Table 5.1 lists the critical gain, critical period and the PID controller constants determined by applying these equations at 40°C, 50°C, and 60°C.

## Appendix 5.2

# Determination of the PID Controller Constants Over a Temperature Range

---

The PID controller constants were determined at set point temperatures of 40°C, 50°C, and 60°C using the Ziegler-Nichols tuning equations based on a marginally unstable system (Appendix 5.1), and are listed in Table 5.1. A curve fit was performed for each parameter at the three set point temperatures resulting in the following expressions:

$$K_p = 138 - \frac{3600}{T} \quad \text{Equation A5.4}$$

$$T_I = \frac{1}{0.38 - \frac{154.71}{T^2}} \quad \text{Equation A5.5}$$

$$T_D = \frac{1}{1.53 - \frac{622.69}{T^2}} \quad \text{Equation A5.6}$$

These equations could be used to specify the PID controller constants at any temperature between 40°C and 60°C.

## Appendix 7.1

# Estimation of Tensile Modulus Using the Model by Krenchel

---

A modified rule of mixtures expression, established by Krenchal [84], was used to produce the modulus values listed in Table 7.1 corresponding with those measured by Lindsey (30% volume fraction) [14] shown in Figure 7.2. According to Krenchel:

$$E_c = \eta v_f E_f + (1 - v_f) E_m \quad \text{Equation A7.1}$$

where

$E_c$	laminar modulus
$\eta$	efficiency factor (0.375 for CFRM)
$v_f$	volume fraction
$E_f$	fibre modulus
$E_m$	matrix modulus

Rearranging Equation A7.1 yields the following ratio:

$$\frac{E_c - E_m}{v_f} = (\eta E_f - E_m) = \text{Constant} \quad \text{Equation A7.2}$$

The value of this ratio is a constant allowing equivalent materials with differing volume fractions to be compared. Scaling the modulus values for the specimens produced under constant resin temperature injection with a 16% fibre volume fraction (Figure 7.1a) to an equivalent specimen with a 30% fibre volume fraction can be expressed as follows:

$$\frac{E_c^{16\%} - E_m}{v_f^{16\%}} = \frac{E_c^{30\%} - E_m}{v_f^{30\%}} \quad \text{Equation A7.3}$$

Which can be written as:

$$E_c^{30\%} = \frac{E_c^{16\%} - E_m}{v_f^{16\%}} v_f^{30\%} + E_m \quad \text{Equation A7.4}$$

A matrix modulus ( $E_m$ ) of 3.19 GPa was used in the analysis, representing a 97% conversion of the resin [14].